TRIESKOVÉ A BEZTRIESKOVÉ OBRÁBANIE DREVA 2018

CHIP AND CHIPLESS WOODWORKING PROCESSES 2018

Vedecký časopis // Scientific journal

TRIESKOVÉ A BEZTRIESKOVÉ OBRÁBANIE DREVA 2018

CHIP AND CHIPLESS WOODWORKING PROCESSES 2018

Vedecký časopis // Scientific journal

OBSAH / CONTENTS

Sekcia / Section   Delenie a obrábanie dreva / Mechanical Woodworking

Sekcia / Section   Termická úprava dreva / Thermal Treatment of Wood

SEKCIA / SECTION

DELENIE A OBRÁBANIE DREVA

MECHANICAL WOODWORKING

INFLUENCE OF SOME FACTORS ON THE CUTTING FORCE IN MILLING OF SOLID WOOD

Valentin Atanasov – **Zhivko Gochev** – **Georgi Vukov** – **Pavlin Vitchev** – **Georgi Kovatchev**

Abstract

The paper examines the impact of factors cutting speed V, feed speed U and milling area A over the cutting force P when operating with a universal woodworking milling machine with a lower spindle position. For this purpose, a planned three-factor regression analysis was carried out. Modern testing equipment and relevant software products were used to process the obtained values. The selected wood is beech (Fagus sylvatica L.). A regression equation was obtained. It can be used to calculate the cutting force P at different levels of considered factors. The results are analyzed and practical recommendations are proposed.

Key words: *milling machine, beech, cutting force, power-energetic indicators*

INTRODUCTION

The power-energetic indicators of a machine include power and cutting forces, specific cutting force and specific electricity consumption. These are important parameters that need to be defined even before designing some type of machine or its components. For example, when calculating the spindle of a milling machine, it is necessary to determine the forces and moments resulting from the cutting, centrifugal forces due to imbalance, forces from the mechanical gear, etc (Filipov 1979, Sokolovski 2016). Thus, it is possible to correctly design the machines and their components, as well as the determination of their reliability even at the design stage (Kamberov 2015, Ivanova et al. 2017, Madzhov 2017). Another important point is to increase the energy efficiency of the woodworking process– especially with the tendencies to increase the cost of electricity and the desire of companies to reduce production costs (Kubš et al. 2016).

From the point of view of the *Wood Cutting Theory*, a number of empirical correlations for the determination of the cutting force are derived. Generally, in the literature it is defined as the force of the interaction between the cutting tool and the wood and decomposes sequentially on radial and tangential components, which in fact represents an idealization of the actual cutting process. Gradually, forces decompose into radial (R_i) and tangential (P_i) components. The total radial (R) and tangential force (P) are the sums of forces acting normally on the tangent to the cutting path and in the direction of the cutting speed vector, which act on the edge of the tooth, the rear and front side of the cutting edge (Grigorov 1992). For further simplification, with sufficient accuracy for practice, the following equation for determining the cutting force is used in the literature

Department of Woodworking Machines, University of Forestry, 10 Kliment Ohridski Blvd., 1797 Sofia
e-mail: vatanasov_2000@ltu.bg, zhivkog@ltu.bg, givukov@ltu.bg, p_vichev@ltu.bg, g_kovachev@ltu.bg

$$P = \frac{N_c}{v} = \frac{K.b.h.u}{v} \tag{1}$$

where N_c is cutting power, W;

v – cutting speed, m.s^{-1}.

K – specific work of cutting, J.m^{-3};

b – cutting width, m;

h – cutting height, m;

u – feed speed, m.s^{-1}.

The factors that affect the cutting power can be divided into several groups: related to the material: wood species and its physical and mechanical properties; concerning the cutting tool - linear and angular parameters, their material; the conditions of the process; kinematics etc.

There are a number of scientific publications related to the determination of the impact of various factors on the power-energetic indicators of a part of the woodworking machines which are used in furniture production. They are related to the influence of the cutting tool parameters, the effect of heat treatment and type of wood, cutting modes, etc. and refer to milling, circular and sanding machines (Krauss et al. 2016, Barcík et al. 2008, Kováč and Mikleš 2010, Kopecky et al. 2014, Javorek et al. 2015, Samolej and Barcík 2006). The purpose of this study is to examine the influence of cutting and feeding speeds, as well as the area of milling, over the cutting force in processing widespread in furniture production beech wood.

METHODOLOGY

The experimental studies were conducted in the laboratory *Woodworking Machines* at the *University of Forestry* – Sofia, Bulgaria. The experimental unit is a universal milling machine with a lower spindle position. Some of the technical parameters of the machine are: diameter of the spindle in the coupling zone d_c = 30 mm, power of the motor which drives the cutting mechanism N_m = 3 kW and revolutions per minute of the motor n_m= 3000 min^{-1}. Figure 1 shows the general view of the machine and Figure 2 graphically shows a kinematic scheme of the cutting mechanism.

Figure 1. General view of the machine
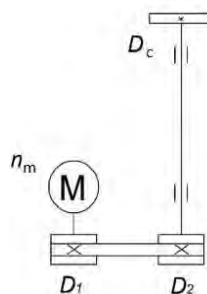
Figure 2. Kinematic scheme of the cutting mechanism

The cutting tool used for experimental studies is a groove cutter with the following basic parameters: thickness of the cutting plates s = 12 mm, diameter of the body Dc = 140 mm,

sharpness angle $\beta = 58°$, front angle of cutting $\gamma = 20°$, number of teeth $z = 6$ pcs., material for hard-alloy plates – HW, weight m = 0,910 kg.

The test specimens are of beech wood and have a square cross-section $a = 50$ mm and length $L = 1520$ mm (Fig. 3). Their average density and moisture are $\rho = 650$ kg.m^{-3} and $W = 13$ %.

For determining the cutting force, a device which allows the determination of the power consumption, the current and voltage, generally and in phases, of the electric motor which drives the cutting mechanism was used – *US301EM* (Fig. 4). Its installation is realized through 3 current (*CNC® CURRENT TRANSFORMER*) and 3 voltage (*UNITRAF AD Ltd 220/100 V*) transformers. Subsequently, a configuration adapted to the connection method of the motor was carried out. The software of the manufacturer is used to report and store reported values. Thus, the mistakes of the human factor are avoided.

Figure 3. Test specimens

Figure 4. Measuring device, model *US301EM* – *Unisyst Engineering Ltd.*

The cutting force is determined by the equation 1. Previously, the efficiency coefficient of the cutting mechanism η and the cutting power N_c were determined

$$\eta = \left(1 - \frac{N_{idle}}{N_{load}}\right).100, \tag{2}$$

where N_{idle} is input power of the cutting mechanism in idle condition, kW;

N_{load}– power of the cutting mechanism in load condition, kW;

$$N_c = \left(\frac{N_{load} - N_{idle}}{100}\right).\eta. \tag{3}$$

The present study was conducted by performing a planned three-factor regression analysis. The factors that are changed are: cutting speed V m.s^{-1} (X_1), feed speed U m.min^{-1} (X_2) and cutting area A mm^2 (X_3). Before starting the main experiments, some preliminary experiments were performed. Their purpose is to determine the range of the considered input parameters.

The cutting speed is determined by the formula

$$V = \pi.D_c.n = \pi.D_c.\frac{n_m}{i}(1 - \varepsilon), \tag{4}$$

where D_c diameter of the cutting tool, m;

n – spindle revolutions, s^{-1};

i – the gear ratio of the belt drive;

ε –sliding coefficient of the belt.

The gear ratio was determined by the diameters of the pulleys $i=D_2/D_1$ (Fig. 2). By changing the diameters of the belt pulleys mounted on the motor ($D_1 = 125$, 190 и 250 mm)

and the diameter of the pulley attached to the spindle D_2 = 90mm, variation levels of the first factor were obtained V = 29, 44 и 59 m.s^{-1}.

The feed speed was changed by a roll feeding mechanism. Accordingly, the variation levels of this factor are U = 2, 6 and 10 m.min^{-1}.

The area of the milling was varied by the depth of the cutting. For this factor, the following levels are selected A = 48; 96 and 144 mm^2.

Table 1 presents the experimental matrix with factor variance levels in an explicit and coded form.

Table 1. Experimental matrix

№	V, m.s^{-1}	X_1	U,m.min^{-1}	X_2	A, mm^2	X_3
1.	29	-1	2	-1	48	-1
2.	29	-1	2	-1	144	+1
3.	29	-1	10	+1	48	-1
4.	29	-1	10	+1	144	+1
5.	59	+1	2	-1	48	-1
6.	59	+1	2	-1	144	+1
7.	59	+1	10	+1	48	-1
8.	59	+1	10	+1	144	+1
9.	29	-1	2	0	96	0
10.	59	+1	10	0	96	0
11.	44	0	6	-1	96	0
12.	44	0	6	+1	96	0
13.	44	0	6	0	44	-1
14.	44	0	6	0	144	+1
15.	44	0	6	0	96	0
16.	44	0	6	0	96	0
17.	44	0	6	0	96	0
18.	44	0	6	0	96	0
19.	44	0	6	0	96	0
20.	44	0	6	0	96	0

The specialized software *QstatLab 5* and *Microsoft Excel* were used to process the results.

RESULTS AND DISCUSSION

The obtained regression equation, which shows the influence of the factors on the target function in the longitudinal milling of beech wood is

P = 12,516 - 1,178X_1 + 6,645X_2 + 5,481X_3 - 0,089X_1^2 - 1,867X_2^2 + 1,587X_3^2 - 0,139X_1X_2 + 3,318X_2x_3 - 4,007X_1X_3. (5)

When comparing the calculated value F_{cal}– Fisher's Criterion, with the critical one F_{cr} used for verification, it becomes clear that the obtained equation is adequate. This means that it can be used for analytical determination of cutting force. As it can be seen from it, in the longitudinal milling of beech wood, the greatest impact on the cutting force P has the feed speed U (coefficient of regression 6,645). The value of the coefficient of regression next to the area of the milling factor A (coefficient of regression 5,481) is close in value. It follows that its influence is almost equal. The factor with the lowest impact is the cutting speed – respectively spindle revolutions (coefficient of regression - 1,178).

Figure 5 illustrates the graph of the effect of the most significant factor on the cutting force at a cutting speed of 44 m.s^{-1} and a milling area of 96 mm^2.It can be seen that the relationship between the input parameter and the target function is almost proportionate.

The same can be noted for the cutting speed but with the difference that in the case, increasing the input parameter leads to a reduction in the target function (Fig. 6).

Figure 7 shows the influence of the important factors on the target function – respectively, at the three levels of area of cutting variation – 48, 96 and 144 mm^2 and feed speed changing from 2 to 10 m.min^{-1}. As can be seen in the smallest area, the influence of the feed speed is the least, with the cutting force not reaching 11 N. Moreover, when the feed speed reaches 8 m.min^{-1}, it is noticed that the impact decreases significantly. As the cutting area increases, the change in speed has an increasing impact on the target function. The steepest is the curve with a cutting area of 144 mm^2. Furthermore, it is not noticeable that the influence of feed speed gradually decreases its intensity at its higher value. It can also be seen that at the maximum of the curve, the target function reaches approximately 28 N, but this is the value at a cutting speed of 44 m.s^{-1}. During the experiments it was found that when milling beech, the highest values of the cutting force are obtained when the electric motor is over its rated power – 3 kW. It is not advisable to perform a long time, because of the danger of overloading.
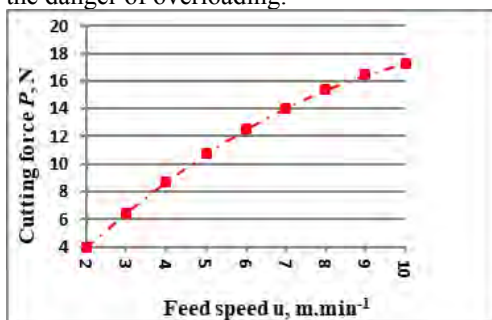
Figure 5. Influence of feed speed on cutting force
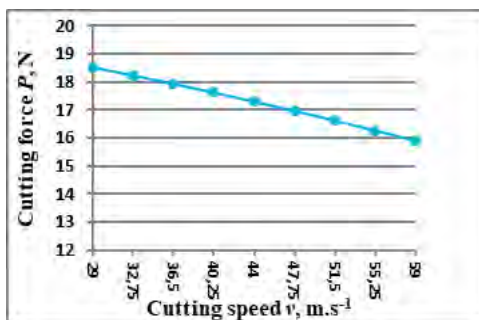
Figure 6. Influence of cutting speed on cutting force
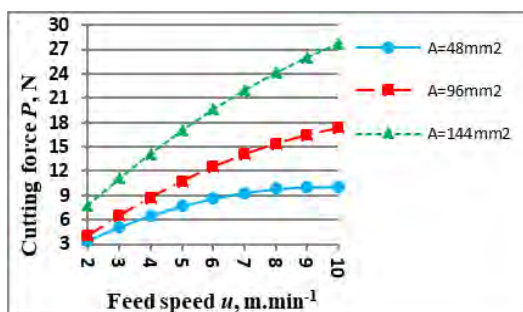
Figure 7. Influence of the feed speed on the cutting force at different areas of milling

The factor with the lowest influence on the force is the cutting speed (Fig. 8). In addition, the "-" sign in the regression equation indicates that its increase leads to a decrease in the target function. The graph also shows that all curves have approximately the same shape, i.e. the difference between the start and end values ranges from 2 to approximately 2,6 N– 2,36; 2,08 и 2,63. It is also noted that the mean value of the feed speed is significantly closer to the curve for 10 m.min^{-1}.
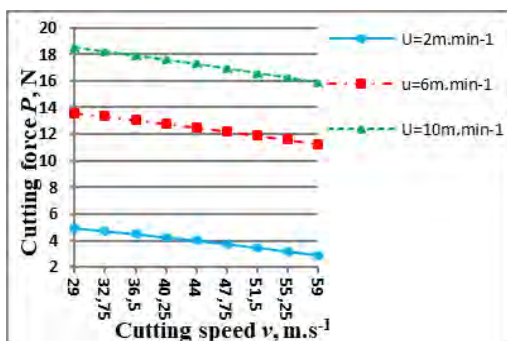
Figure 8. Influence of cutting speed on cutting force at different feed speeds

CONCLUSION

Based on the conducted experimental studies on the influence of cutting speed, feed speed and the area of cutting, the following more important conclusions and recommendations can be made:

1. An adequate regression equation, which can be used to analyze the influence of factors on the cutting force in longitudinal milling of beech wood, has been obtained.

2. From the point of view of the electric motor used to drive the cutting mechanism, it is not advisable for the milling to be longer at the highest feed speeds and the cutting area – $U = 10$ m.min^{-1} and $A = 144$ mm^2. The reason for this is the load on the electric motor over its rated power. It follows that in more difficult operating modes than those mentioned above, it is advisable to use more powerful motors to drive the cutting mechanism.

3. Experimental research has shown that the feed speed (coefficient of regression 6,645) has the greatest impact on cutting force and the cutting speed has the lowest (coefficient of regression - 1,178). The factor area of cutting (coefficient of regression 5,481) has a significant impact on the investigated target function as well.

REFERENCES

1. Barcík, St., E. Pivolusková, K. Richard, 2008, Effect of Technological Parameters and Wood Properties on Cutting Power in Plane Milling of Juvenile Poplar Wood, DRVNA INDUSTRIJA 59 (3) 107-112.

2. Filipov, G., 1979, Machines for Production of Furniture and Furnishing, Sofia, p. 462 (in Bulgarian).

3. Grigorov, P., 1992, Wood Cutting, Zemizdat, Sofia, p. 319 (in Bulgarian).

4. Ivanova, N., Sv. Madzhov, D. Mudev, 2017, Failure Modes and Effects Analysis (FMEA), Collection of Scientific Papers XXVI International Scientific Conference "Management and Quality" – Yambol 2017, pp. 42 – 48 ISSN 1314-4669.

5. Javorek, L., J. Kúdela, J. Svoreň, M. Krajčovičová, 2015, The Influence of Some Factors on Cutting Force and Surface Roughness of Wood After Sanding, PRO LIGNO, Vol. 11 N 4 2015, pp. 516-524.

6. Kamberov, K., 2015, Reliability Analysis Types Based on Virtual Prototyping of Mechanical Product, International Scientific Conference "70 Years of MTF", September 11-13, 2015, Sozopol, (in Bulgarian).

7. Kopecky, Z., L. Hlaskova, K. Orłowski, 2014, An Innovative Approach to Prediction Energetic Effects of Wood Cutting Process with Circular-Saw Blades, WOOD RESEARCH 59(5): 2014, 827-834.

8. Kováč, J., M. Mikleš, 2010, Research on Individual Parameters for Cutting Power of Woodcutting Process by Circular Saws, JOURNAL OF FOREST SCIENCE, 56, 2010 (6): 271–277.

9. Krauss, A., M. Piernik, G. Pinkowski, 2016, Cutting Power During Milling of Thermally Modified Pine Wood, DRVNA INDUSTRIJA 67 (3) 215-222.

10. Kubš, J., M. Gaff, Št. Barcík, 2016, Factors Affecting the Consumption of Energy during the Milling of Thermally Modified and Unmodified Beech Wood, Bio Resources 11(1), 736-747.

11. Madzhov, Sv., 2017, Development of Structure of Methodology for Experimental Investigation of the Reliability of Mechanical Systems, Collection of Scientific Papers, The International Scientific Conference "Technique, Technology and Education" – Yambol, pp. 74 - 83 ISSN 1314-9474 (in Bulgarian).

12. Samolej, A. St. Barcík, 2006, Influence of Specific Pressure on Cutting Power and Wood Removal by Disc Sander, DRVNA INDUSTRIJA 57 (1) 5-11.

13. Sokolovski, S., 2016, Exercise Manual of Machine Elements, Sofia, p. 218 (in Bulgarian).

THE YIELD OF BEECH RAW MATERIAL (Fagus Sylvatica L.) FOR STRUCTURAL TIMBER IN THE PROCESSING PROCESS

Ondrej Bajza – Alena Rohanová

Abstract

Beech wood (Fagus sylvatica, L.) has a wide range of uses. Because of its specific properties, areas of woodworking industry for its application are limited. Is necessary to evaluate the beech structural timber for application in timber constructions not only according to mechanical properties, but also according to the technological processing. Grading parameters, mainly edgewise and flatwise shrinkage affect its qualitative yield. Paper analyse qualitative and quantitative yield of beech wood in timber conversion and processing process. Tested material consist of 15 tree trunks (21 m^{-3}), each was cut into two logs (total 30 logs) further 247 boards (7,4 m^{-3}). After processing by planning was boards adjusted to dimension of 50/150 x 3100 mm. Quantitative yield of trunks/boards was 35%. In next step was boards qualitatively graded according to STN 49 1531/Z1, 2006. Of the total number of boards n = 247, 118 boards was proved as construction timber, (3,5 m^{-3}). Qualitative yield of boards/structural timber was 48%. Total yield of trunks/structural timber was 17%.

Key words: *Beech structural timber, processing process, visual grading, quantitative yield, qualitative yield*

INTRODUCTION

Beech wood (*Fagus sylvatica* L.) is and going to be the most widespread wood in Slovakia as well as throughout Central Europe. Beech wood has a high density and excellent mechanical properties, but it has a volatile nature and is less resistant to wood decay factors as fungi or insect. The great potential of beech wood can be the use of structural timber in wooden constructions. In order to be able to use the beech safely and efficiently, it is necessary to know its properties set on the real size specimens commonly used in wooden constructions. Qualitative grading of structural timber into strength classes is required. Yield of the beech raw material in the processing process is an important factor. Qualitative and quantitative yield of raw material from tree trunks, logs and structural timber boards represents effectiveness of beech wood usage in wooden constructions.

Technical University in Zvolen, T. G. Masaryka 24, 960 53 Zvolen
e-mail: bajza.ondrej@gmail.com, rohanova@tuzvo.sk

MATERIAL AND METHODS

As a tested material was chosen beech wood (*Fagus sylvatica* L.) from cadastral area of Ostrá Lúka, district Zvolen (Slovakia). Average height of beech stands in the locality is 30 m, thickness 38 cm, bonita 28, volume of tree trunks 1,57, phenotype category is rated as valuable. The selection of 15 trees was done individually on an area about 200 x 200 m. Two logs in the length 3300 -3500 ware cut of each tree trunks, and identified by number of log and tree (1/1 – 1/2). Crosscuts of logs were secured against checks cracks by MPC plates. Before main cutting operation were logs trimmed into length of 3100 mm. Some logs contain false heartwood. Wood was healthy, without any damages and possibilities of visual identification of insect or fungi wood decay. Quality of log was rate as very valuable. The quality class of logs was determined according to STN 48 0056, 2007 standard as quality level III.A or II.
Segmental log-sawing pattern (Fig.1) was used for sawing. Logs were saw by the MEBOR 900 horizontal belt band sawmill. Two segments with thickness of 160 mm were cut out from each log. These were then cut on single board with a thickness of 60 mm.

The hatch refers to the side and centre timber as well as the cutting edge
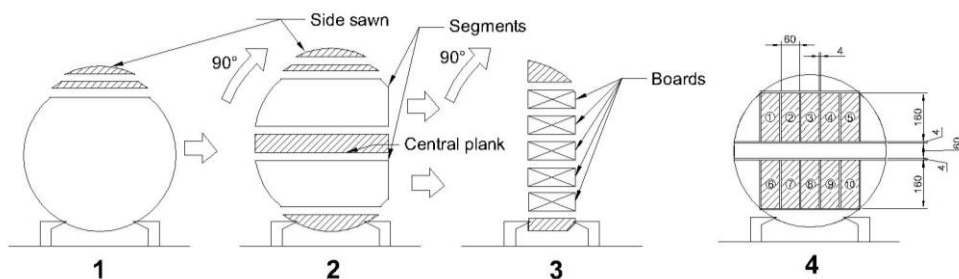
Fig. 1   Method and procedure of segment cut on a belt band saw (Bajza 2018)
1-align of surface, 2 –90° rotation and cut-out of two segments, centre and side timber 3 – 90° rotation of segments and its cutting to single board 4 – cutting schema

The total number of boards is n = 247 pcs. Identifies species and number of individual assortments is set in Table 1.

Table 1 Labeling, frequency and cubature of cutting assortments (Bajza 2018)

Material (*Fagus sylvatica L.*)		Labelling			(n)	Volume (m³)
		Tree trunk	Log	Board		
Tree trunks			N/A	N/A	15	
Logs				N/A	30	
Boards	Structural timber	1 to 15	1 to 2	1 to 12	118	3,51
	Unsuable boards				129	3,84
Overall					247	7,35
Side sawn and dust		N/A				

N/A : not avaliable

Boards were stored into stacks in the exteriors protected timber storage site during 24 months' period. Unplaned boards were visually graded after natural seasoning (drying to w = 15 % ± 2%) according to STN 49 1531 /Z1, 2006 standard.

Grading parameters for visual grading of structural timber:
1. Longitudinal edgewise and flatwise shrinkage (deflection in mm from the plane in the middle of the board)
2. Number and diameter of the knots (right / left side of boards)
3. False heartwood presence: yes / no (right / left side of boards)
4. Presence of bark: yes / no (right / left side of boards)
5. Presence of front or middle clacks: yes / no (right / left side of boards)
6. Other parameters (rot, incest bites, other damage or decay)

The material preparation range that has been used in this research makes possible to track the whole process of timber conversion and processing of beech raw material up to the final product, what mean planned structural timber. This simple yield analysis followed:

- Quantitative yield:
$$K_m[\%] = \frac{volume\ of\ products\ [m^3]}{volume\ of\ raw\ material\ [m^3]} \times 100$$

- Qualitative yield:
$$K_{q,type} = \frac{V_{type}}{V_{board}} \times 100\ (\%)$$

(DETVAJ, 2003, KRAJČOVIČOVÁ, 2012)

RESULTS

In whole process of beech structural timber processing have been observed few parameters: type, number and volume of individual assortments, as well as the factors directly affecting the yield. Of the total number of boards n = 247 was used after the visual grading for structural purposes n = 118. The final size of the boards drying and planing was 150×50×3100 mm.

Table 2 describes the quantitative yield. It defines the percentages of valuable and non-valuable assortments of the total volume of the input log. Total boards yield was 75.3 %. The yield of boards utilized for structural timber was 35.3%. The reach of quantitative yield in the chosen quality focused log-sawing pattern corresponds to the real conditions of processing of the raw beech materials.

Table 2 Quantitative yield of cutting assortments (Bajza 2018)

Quantitative yield analysis								
Assortments			Thickness (mm)	Width (mm)	Volume (m³)	%	Volume (m³)	%
Valuable products	Boards	Timber	**60**	**160**	**7,35**	**35,3**	15,67	**75,3**
		central planks	60	≈	4,33	20,8		
	Side boards		32	≈	3,99	19,2		
Non valuable products	Sawn waste		≈	≈	1,64	7,9	5,13	**24,7**
	Length allowance		≈	≈	1,11	5,3		
	Wood dust and chips		4	≈	2,38	11,5		
Tree trunks			≈	≈	20,8	100	20,8	100

≈ symbolizes different parameters values, each piece was measured separately

Qualitative yield analyses of cutting products as tree trunks / logs / structural timber (Table 2.). Of the total number of boards (n = 247), only 118 qualitatively suited to structural timber purposes what mean 47.8%. Unusable assortments accounted of 52.2%. Final qualitative yield of structural timber in relation to the volume of the input tree trunks is

16.88%, while in the unusable boards it is slightly higher (18.5%). The qualitative yield of structural timber from tree trunks was negatively affected mainly by drying deformations – shrinkage caused by reaction wood. Altogether, up to 107 boards (43.3%) were excluded.

Table 3 Quantitaive yield of cutting assortments (tree trunks/boards/structural timber) (Bajza 2018)

Qualitative yield analysis							
Assortments			(n)	Volume V (m^3)	V_{type} / V_{board} (%)		V_{board} / $V_{trunks.}$ (%)
Name	Dimension	Type					
Boards	160 x 60 x 3100 (mm)	Structural timber	**118**	**3,5**	**47,8**		**16,88**
		Unusuable / Couse of exclusion / Deformation	107	3,2	43,3	52,2	15,3	18,5
		Unusuable / Couse of exclusion / Knots	2	0,1	0,8		0,3
		Unusuable / Couse of exclusion / Splits & shakes	9	0,3	3,6		1,3
		Unusuable / Couse of exclusion / Other	11	0,3	4,5		1,6
		Overall	**247**	**7,4**	**100,0**		**35,34**
Tree trunks volume				**20,80**			

DISCUSSION

Analysis of yield affected factors:
- Dimensions of tree trunks / logs. Average diameter of logs was ø 516 mm, length 3100mm. Yield increase directly with the logs diameter, on the contrary indirectly decreases with the length of the log.
- Conversion of timber technology (band saws MEBOR 900 with sawing belt thick 4mm). Hydraulic drive fixing and centralization mechanism provide efficient alignment of log in band saw. What reduce the effect of the deviation of the parallelism ot the tear surface ot the stem with sawing gap. Technology of timber conversion used in research affect yield positively.
- Dimension and assortment of timber conversion product set optimal log-sawing pattern and number of single cut. That affect volume of chips and wood dust productions. The segment log-sawing pattern was chosen efficiently to considering yield.
- Operator of technology was hig qualified. Volume capacity per work shift was below average, but the operator could focus on the qualitative aspect of the cut. (positive affect on yield)
- Natural seasoning process and its impact on the qualitative yield: Natural seasoning (drying) is a slow drying process, which in a properly chosen process eliminates the deformation sufficiently (TREBULA, 1997). The procedure and the method of natural beech drying were carried out according to recommendations (TREBULA, 1997). Excessive deformations were not caused by improper drying but was probably caused by presence of tensile reaction wood and large internal stresses. (VILKOVSKA et. al. 2018). Unusable boards with excessive deformations reach 43,3 % (n = 107) of total number of boards (n = 247). In the case of effective diagnostics of reaction wood in logs, we could expect increasing of yield.
- Quality of the beech structural timber (strength class). STN 49 1531 / Z1 standard is applied for visual grading of structural timber used in timber construction. Grading parameters defined by this standard fit more to coniferous wood species. This standard is almost unusable for beech wood. For example, character of knots what the main grading parameters in coniferous wood species is very different in deciduous wood species. Grading methodology ignore existence of ring-porous and diffuse-porous woods.

CONCLUSIONS

Requirement of beech wood applications in timber constructions such as building is not only knowledge of its properties but also the economic evaluation of the processing and timber conversion process. Analysis of the quantitative and qualitative yield of structural timber from logs and tree trunks predicts the efficiency of the use of pillar raw material in the products. Yield of timber various with every single wood species. Beech wood is characterized by unpredictable deformations, low resistance to wood decay factors, which affects the yield. Quantitative yield of boards made of logs were 35,3% (n = 247). The qualitative yield of the structural timber from boards was 47.8% (n = 118), from logs only 16.88%. Determining the causes of low quantitative yield of structural timber from logs requires further research and verification.

AKNOWLEDGMETS

REFERENCES

BAJZA, O. 2018: *Verifikácia parametrov kvalit bukového konštrukčného dreva rôznymi metódami triedenia*. Dizertačná práca. DF Technická univerzita vo Zvolene, 2018, 125 s.

DETVAJ, J. 2003. *Technológia piliarskej výroby.* Zvolen: Vydavateľstvo Technickej univerzity vo Zvolene, 2003. ISBN 80-228-1248-X.

KÚDELA, J.; ČUNDERLÍK, I. 2012. *Bukové drevo štruktúra, vlastnosti, použitie*. Zvolen: Vydavateľstvo Technickej univerzity vo Zvolene, 2012. ISBN 978-80-228-2318-0.

KRAJČOVIČOVÁ, M. 2012. *Triedenie guľatiny ovplyvňuje výťaž v procese pílenia.* ACTA FACULTATIS TECHNICAE, XVII ZVOLEN 2012, – SLOVAKIA, s. 45- 54.

TREBULA, P. 1997. *Sušenie a hydrotermická úprava dreva.* Zvolen: Vydavateľstvo Technickej univerzity vo Zvolene, 1997. ISBN 80-228-0574-2.

VILKOVSKA, T., KLEMENT, I., VÝBOHOVÁ, E. 2018. *Effect of tension wood on the selected physical properties and chemical composition of beech wood (Fagus sylvatica L.).* Zvolen: Acta Facultatis Xylologiae Zvolen: scientific journal of the Faculty of Wood Sciences and Technology, Technical University in Zvolen., 2018. č. no. 1, s. 31-40. ISSN 1336-3824. [Online] https://www.researchgate.net/profile/Tatiana_Vilkovska/publication/323934100.

STN 48 0056. 2007. *Kvalitatívne triedenie listnatej guľatiny.* Bratislava: SÚTN, 2007.
STN 49 1531/Z1. 2006. *Drevo na stavebné konštrukcie. Vizuálne triedenie podľa pevnosti.* Bratislava: SÚTN, 2006

INFLUENCE OF THE THICKNESS OF REMOVED LAYER ON GRANULOMETRIC COMPOSITION OF CHIPS WHEN MILLING OAK BLANKS ON THE CNC MACHINING CENTER

Adrián Banski – Richard Kminiak

Abstract

The paper deals with the production of chips in the process of milling oak blanks on a CNC machining center and their granulometric content. They present the results of the experiment in which was simulated milling process of oak blanks by end mill fitted with a replaceable carbide blade under standard conditions: feed speed $v_f = 1 \div 5$ m.min^{-1} and thickness of the removed layer $e = 1/3/5$ mm.

The granulometric analysis suggests that more than half of the chips formed is a coarse fraction consisting of flat particles larger than 2 mm. Fraction of chips in grain ranges of $0.5 \div 2$ mm are fibrous chips, the chin is significantly extended in one direction. Dust fractions below 500 μm formed isometric beads i.e chips having in all three directions about the same size. Inhalable dust particles below 125 μm are on average $0.92 \div 5.82\%$. It can be stated that there are no respirable dust particles with dimensions less than> 10 μm.

Key words: *milling on a CNC machining center, dustability, granulometric composition of chips, dust fraction, respirable particles.*

INTRODUCTION

CNC technology has become an integral part of the woodworking industry whether it is a piece or large-scale production. The range of used CNC machines is wide and the most commonly used are CNC machining centers.

During milling, the separated chips are formed into a rotating air stream. The mixture of rotating air and chips has so much energy that its significant part is not broken by the exhaust air, it hits the walls of the suction hood and falls into the work area of the concealed CNC machine.

Extruded chip is a polydispersible bulk material consisting of coarse, medium coarse and powder fractions (*Hejma et al., 1981, Horák, 1996, Očkajová a Banski, 2013 Dzurenda et al., 2010*). Wood dust with grain size ranging from $1 \div 500$ μm is hygroscopic, low abrasive, explosive bulk. The proportion of dust particles depends on the properties of the processed raw material, the parameters of the tool as well as the technical and technological parameters of the machining process (*Dzurenda, 2002, Kučerka, 2010, Palmqvist a Gustafsson, 1999, Kopecký a Rousek, 2006*).

From a physiological point of view and according to conventions in the sense of international harmonization (USA - ACGIH, EPA a Európa - ISO, CEN, BMRC) fractions of dust below 100 μm *Tureková* (*2012*) broken down as follows:

- breathable (inhalable) weight fraction <100 μm,

Technical University in Zvolen, T. G. Masaryka 24, 960 53 Zvolen
e-mail: banski@tuzvo.sk, richard.kminiak@tuzvo.sk

- thoracic weight fraction 5 ÷ 10 μm,
- tracheobronchial (respirable) weight fraction 2.5 ÷ 5μm,
- High respirable weight fraction <2.5 μm.

Dust fraction (> 10 μm), as indicated *Buchancova* (*2003*), in the work environment, do not quickly adjust and in case of unprotected respiratory they are inhaled by humans. They are captured in the upper respiratory tract and together with mucus and activity of the rib cage epithelium move up into the nasopharynx, from where they can enter the digestive tract or eliminate them from the body by coughing. Problematic are mainly smaller particles (0 < 5 μm) – called. respirable fraction - remain in the air for a long time. They also penetrate into the lung alveoli, where they are phagocyticated by alveolar macrophages. They can remain deposited and cause local biological effects, or they can penetrate into blood and lymph.

Wood dust from beech and oak, as *Očkajová a Kučerka* (*2017*) states is considered to be toxic and is classified as a carcinogen 1st category. Dust with carcinogenic and mutagenic effects according to NV SR č. 83/2015 Z.z., which amends NV SR č. 356/2006 Z.z. on the protection of the health of workers from the risks related to exposure to carcinogens and mutagens at work, as amended NV SR č. 301/2007 Z.z. and the concentration of the toxic component of the aerosol must not exceed the technical guidelines for the given factor (5 mg/m3) (NV SR č. 301/2007 Z.z.; NV SR č. 471//2011 Z.z).

The aim of the article is to determine the granulometric composition of exhausted chips from the milling process of oak grooves on a CNC machining center in the range of commonly used combinations of technical and technological parameters.

MATERIAL AND METHODS

Characteristics of used material:

In the experiment were used furniture blanks of following parameters:
- wood species: European oak (Quercus robur)
- texture: tangential lumber
- dimensions: thickness h = 25 mm (± 0,5 mm), width w = 80 mm (± 0,5mm), length l = 500 mm (± 1 mm),
- moisture: w = 10% (± 2%).

Characteristics of used machinery:

The experiment was performed on a 5-axis CNC Machining Center SCM Tech Z5 (*Fig.1*) supplied by the company SCM – group, Rimini, Italy. The basic technical and technological parameters reported by the manufacturer are given in Tab. 1.

Characteristics of tool:

In the experiment was used end mill KARNED 4451 of diameter D = 16 mm fitted with a replaceable T10MG carbide blade from the manufacturer Karned Tools Ltd., Prague, Czech Republic (*Fig. 2*). Basic technical and technological parameters provided by the manufacturer are presented in *Tab. 2*.

Fig. 1. CNC machining center SCM Tech Z5 (*SCM Group, 2017*).

Tab. 1. Technical and technological parameters of CNC machining center SCM Tech Z5 (*SCM Group, 2017*).

Technical parameters of CNC machining center SCM Tech Z5	
Useful desktop	x= 3,050 mm , y = 1,300 mm, z =300 mm
Speed X axis	$0 \div 70$ m.min^{-1}
Speed Y axis	$0 \div 40$ m.min^{-1}
Speed Z axis	$0 \div 15$ m.min^{-1}
Vector rate	$0 \div 83$ m.min^{-1}
Parameters of the main spindle	
electric spindle with HSK F63 connection	
Rotation axis C	640°
Rotation axis B	320°
Revolutions	$600 \div 24,000$ ot.min^{-1}
Power	11 kW 24,000 ot.min^{-1}
	7,5kW 10,000 ot.min^{-1}
Maximum tool diameter	D = 160 mm
	L = 180 mm

Fig. 2. End mill KARNED 4451 fitted with one replaceable carbide blade (D – cutting diameter, L – cutting length, d - diameter of the chucking shank)

Tab. 2. Technical and technological parameters of end mill KARNED 4451 fitted with one replaceable carbide blade (Karned Tools Ltd, 2017)

Miller	Working diameter D [mm]	Working length l [mm]	Diameter of the chucking shank d [mm]	Dimensions of used razor blades L x š x h [mm]	Blades material	
KARNED 4451	16	49,5	12	49.5 x 9 x 1.5	T10MG	

Classes of TIGRA	ISO CODE	US CODE	Binder%	Hardness		Bending strength	
				HV10	HRA±0.2	N/mm²	psi
T10MG	K10–K40	C3+	10.0	1,65	92.3	3,6	522.000

Milling process:

A milling cutter was fitted into the hydraulic clamp SOBO. 302680291 GM 300 HSK 63F from Gühring KG, Albstadt, Germany. Oak blanks were placed in a CNC machining center so that the longer side was in the X-axis and the shorter side was in the Y-axis. Oak blanks were clamped during the milling by mechanical clampers VCMC-S4 145x145x50 12-80 from J. Schmalz GmbH, Glatten, Germany. The milling process was carried out at constant operation speed of cutter n = 20,000 min^{-1} and changing thickness of the removed layer e = 1/3/5 mm and changing feeding speed from v_f = 1 m.min^{-1} to v_f = 5 m.min^{-1} (representing a maximum feeding speed recommended by the manufacturer of the tools).

Specimens for granulometric analysis of chips were removed isokinetically from the suction line of the CNC woodworking center in accordance with STN 9096 (83 4610): "Manual determination of the mass concentration of solid pollutants".

The granulometric composition of the chippings was detected by sieving. For this purpose, special sets of stacked sieves (2 mm, 1 mm, 0.5 mm, 0.25 mm, 0.125 mm, 0.063 mm, 0.032 mm, and bottom) were placed on the Retsch AS 200c vibration stand of the Retsch AS 200c screening machine Retsh GmbH, Haan, Germany. The sizing parameters were in accordance with STN 153105 and STN ISO 3310-1, sessile interruption frequency 20 seconds, sieve deflection amplitude 2 mm.g-1, siting time t = 15 minutes, weight 50 g. The granulometric composition was obtained by weighing the percentages remaining on the sieves after sieving on a Radwag 510 / C / 2 electrical laboratory scale from Radwag Balances and Scales, Radom, Poland, with a weighing accuracy of 0.001 g. Sittings were performed on three samples for each wood.

RESULTS AND DISCUSSION

In the experiment were simulated conditions normal production practices. Thickness of the removed layer was set at 1, 3. 5 mm, which is a normal addition for the final machining of furniture blanks. The sliding speed was in the range of 1-5 m.min^{-1}, which is the commonly used sliding speed for machining wood. The results are presented in *Tab. 3* and graphically in *Fig. 3*.

Tab. 3. Granulometric composition of oak chips from the milling process on a CNC machining center.

Thickness of removed layer e [mm]	Dimension of mesh sieves [μm]	Fraction designation	Percentage of the fraction [%]				
			Feed speed v_f [m.min⁻¹]				
			1 m.min⁻¹	2 m.min⁻¹	3 m.min⁻¹	4 m.min⁻¹	5 m.min⁻¹
1mm	2mm	coarse	84,01	77,9	67,88	70,84	64,72
	1mm		6,55	8,78	14,83	14,49	17,17
	500μm	medium coarse	1,72	5,32	7,36	6,53	7,44
	250μm		2,14	3,48	4,55	4,62	6,12
	125μm		3,2	3,36	4,08	2,83	3,24
	63μm	fine	1,96	1,03	1,12	0,62	1,09
	32μm		0,41	0,13	0,18	0,06	0,23
	> 32μm		0	0	0	0	0
3mm	2mm	coarse	64,95	74,1	64,77	51,72	44,83
	1mm		9,9	9,77	15,95	16,84	19,36
	500μm	medium coarse	9,87	7,83	9,12	12,82	15,96
	250μm		7,98	4,68	4,41	12,71	14,51
	125μm		5,1	2,75	4,36	4,75	3,84
	63μm	fine	1,78	0,71	1,13	0,95	1,18
	32μm		0,42	0,15	0,26	0,21	0,32
	> 32μm		0	0	0	0	0
5 mm	2mm	coarse	44,01	30,85	33,03	36,1	41,76
	1mm		14,9	16,36	17,93	15,74	13,75
	500μm	medium coarse	14,49	17,16	16,78	17,32	16,57
	250μm		11,57	16,5	18,59	21,51	22,33
	125μm		9,17	14,42	11,34	7,81	4,67
	63μm	fine	4,78	4,11	1,91	1,2	0,7
	32μm		1,04	0,56	0,4	0,32	0,22
	> 32μm		0	0	0	0	0

Fig. 3. Granulometric composition of chips from the milling process of oak blanks on a CNC machining center.

The majority share of resulting chips are fractions of dimensions greater than 2 mm. These chips belong to the category of flat chips, i.e., the length and width of the chips significantly exceed its thickness. Chip has the shape of trimming layers of milled wood. At lower feed speed, the chips were unbroken. With increasing feed speed, the intensity of break in chips increased.

Fractions of 2 mm to 500 μm belong to so-called " fibrous particles, i. to the particles with a significant extension in one direction.

Fractions below 500 μm can be characterized as isometric chips, i.e., splinters having approximately the same dimensions in all three directions.

The inhalable dust fraction particles with dimensions below 125 microns is formed by a proportion of 0,92÷5,82%, depending on thickness of the removed layer and feed speed.

The CNC machining center does not produce fractions of respirable fraction with dimensions less than 10 μm.

Effect of the thickness of removed layer

By increasing the size of the removed layer, the proportion of the fraction with a size above 2 mm is reduced. For the 1÷2 mm fraction there was no significant change in the percentage of the fraction. Increasing the size of the removed layer will cause an increase in the proportion of the fraction below 1 mm. The rationale for the phenomenon can be found in increasing the size of the trimming chips, which affects the force ratios in the chips, cracks are formed in the chips, and the chips are crushed into smaller pieces. It can be concluded addictionas a result of the larger slender ratio of chips there is a greater fragmentation of the chips.

This argument is supported by the basic literature dealing with the problem of wood processing. As say *Siklienka et al* (*2017*), *Lisičan* (*1996*), či *Nemec et al* (*1985*) cutting speed, feed speed as well as thickness of removed layer participate in the creation of the shape and dimensions of the cut layer. Increasing the size of the chips causes a change of character of chips creations, the particle becomes more fragmented.

In favor of the assumption says the change of fractions in changing the feed speed. Increasing the feed speed means increasing the feed rate on the tooth and increasing the thickness of trimming chips - changing the slender ratio of chips. Increasing the feed speed will result in a reduction in the proportion of the fraction with a size above 2 mm and, on the other hand, an increase in the fraction with a size below 1 mm

CONCLUSION

Based on our experiments, we can draw the following conclusions:
- most of the mixture of chips form chips with a size above 2 mm,
- dust particles (> 500 μm) make up 7.71 - 35.59%,
- inhalable dust particles (> 125 μm) make up 0.92 ÷ 5.82%,
- the occurrence of parts smaller than 32 microns and therefore respirable particles have not been proven.

It was shown dependence of particle size distribution of the chips to the chip slenderness ratio. Is valid, greater thickness of removed layer or feed speed, mean greater slenderness ratio and greater percentage of the smaller fractions of the chips.

REFERENCES

[1] BUCHANCOVÁ, J. a kol. 2003: Pracovné lekárstvo a toxikológia. Martin: Osveta. 2003. ISBN 80-8063-113-1.

[2] DZURENDA, L. 2002. Vzduchotechnická doprava a separácia dezintegrovanej drevnej hmoty. Zvolen: TU vo Zvolene, 2002. ISBN 80-228-1212-9.

[3] DZURENDA, L., ORLOWSKI, K., GRZESKIEWICZ, M. 2010: Effect of thermel modification of oak wood on sawdust granularity. Drvna industrija, 2010, 61(2): 89−94.

[4] HEJMA, J. a kol. (1981): Vzduchotechnika v dřevozpracovávájícím průmyslu. Praha, SNTL, 398s.

[5] Horák, M. 1996: Technika ochrany ovzdušia. Bratislava, vydavatelstvo STU Bratislava, 1996, ISBN 80-227-0830-5

[6] KOPECKÝ, Z., ROUSEK, M. 2006: Simulation possibilities of dust emission in high-speed milling. In. 1st Jubilee Scientific Conference Manufacturing Engineering in Time of Information Society. Gdansk: Gdansk University of Technology, 2006, p. 191−196

[7] KUČERKA, M. 2010: Vplyv technicko-technologických faktorov na tvorbu triesky pri brúsení dreva na ručnej pásovej brúske. In. Acta Universitatis Matthiae Belii, séria Technická výchova No. 10. Banská Bystrica: FPV UMB, 2010, s. 15−29.

[8] LISIČAN, J. 1996. *Teória a technika spracovania dreva*. 1 vyd. Zvolen: Matcentrum, 625 s. ISBN 80-967315-6-4.

[9] NEMEC L., ŠULÁN E., ZEMIAR J. 1985. *Technologia výroby nábytku*. SNTL - nakladatelství technické literatury Praha, 514 s.

[10] OČKAJOVÁ, A., BANSKI, A. 2013: Granulometria drevného brúsneho prachu z úzko-pásovej brúsky Acta Facultatis Xylologiae Zvolen, 55(1): 85−90. ISSN 1336-3824.

[11] OČKAJOVÁ, A., KUČERKA, M. 2017: Granulometrická analýza častíc brúsneho dubového prachu. In Acta facultatis technicae: vedecký časopis Fakulty environmentálnej a výrobnej techniky. 2017, roč. 22, č. 2, s. 93-101. ISSN 1336-4472.

[12] PALMQVIST, J., GUSTAFSSON, S.I. 1999: Emission of dust in planning and milling of wood. Holz als Roh- und Werkstoff , 1999, 57: 164−170.

[13] SIKLIENKA, M., KMINIAK, R., ŠUSTEK, J., JANKECH, A. 2017. Delenie a obrábanie dreva. 1 vyd. Zvolen: TU vo Zvolene, 357 s. ISBN 978-90-228-2845-1.

[14] TUREKOVÁ, I., 2012: Zdravotné riziká a bezpečnostné riziká drevných prachov (Health and Safety Risk of Wood Dust). In: Rusko, M. (ed.): Zborník z XII. Konferencie so zahraničnou účasťou, 19.-20.11. 2012, Bratislava. Žilina: Strix. Edícia ESE 12, prvé vydanie. ISBN 978-80-89281-85- 5.

ACKNOWLEDGMENTS

NUMERICAL ANALYSIS OF CHIP REMOVING SYSTEM OPERATION IN CIRCULAR SAWING MACHINE USING CFD SOFTWARE

Jacek Barański[1] − Marcin Jewartowski[1] − Jan Wajs[1] − Kazimierz A. Orłowski[2]

Abstract

Paper presents the analysis of the results of numerical simulations of the air flow process of wood chips removing system in the circular sawing machine. The attention is focused on the upper cover and bottom shelter of the chip removing system. Within the framework of the work a systematic numerical modeling of the air flow distribution in the cover and shelter during operation of the selected rotational speed of saw blade with a diameter of $\varnothing$300 mm and $\varnothing$ 450 mm was carried out. The analysis of the results obtained from the numerical simulations and from the experimental measurements allowed to predict the areas with improper air movement hindering the organized transport of chips. Also, those results from the numerical modeling were used in the process of optimizing the shape of the casing and the shelter. As a result, a new design of chip removing system was obtained, vastly improving the chips extraction from the tool operation space.

Key words: *numerical simulations, CFD, chip removing system, sliding table saw*

INTRODUCTION

The development of woodworking machines design, the introduction of new technologies, and above of all the machining and feed speed result in the need to provide more effective wood wastes (chips) removing systems. A modern machine, which operates without connection to a properly designed extraction installation loses immediately its performance and service life.

Woodworking machines and cutting parameters as well as wood material properties determine the particle size distribution of chipped wood. In the technological processes of machine wood chipping, a by-product is also formed besides the main product.

Particles of wood substance formed in individual processes of chipping and machining are called "bulk wood substance". Workers' exposure to airborne wood dust particles in the surrounding air of the workplace may cause different occupational health problems in wood industry workers. The nature of the present production and conditions of chips require its continual removal from the place where they are formed. As far as sanding dust is concerned, it is removed by means of an air-technical device - suction. To develop an appropriate suction system, it is important to know the size and shape of bulk substance particles, which are the basic data for characterizing bulk material. The above characteristics affect physical and mechanical properties of bulk substance (bulk density,

Gdansk University of Technology, [1]Department of Energy and Industrial Apparatus, [2]Department of Manufacturing Engineering and Automation, Narutowicza 11/12, 80-233 Gdansk, Poland
e-mail: jbaransk@pg.edu.pl

bulk angle, tilt angle, aerodynamic properties of particles in the piping of the suction system) and conditions of separation or filtration in the separating device [1, 5].

Removal of dust is difficult when working zone is large and when the tool moves during processing at relatively high velocities. The dispersion of chips in different directions in the space of the treatment zone is very unfavorable in this respect. When the movement direction of the chips created during machining does not coincide with that of the air suction created by an extraction system, many of the chips are still not removed and can become dispersed in the air surrounding the machine. This takes places during sawing when the whole tool goes into the work piece. For this reason, there are problems with the direct removal of chips from working zone and working tools. The dispersion of chips in all directions also occurs due to the high-speed rotation of those tools.

The authors carried out systematic experimental investigations in existing circular sawing machine, commercially available on the european market. The special attention was focused on upper casing and bottom shelter in its chips removing system.

During the experimental research, pressure distribution inside the casing was accurately recorded with the selected rotational speeds of 3500 1/min and 6000 1/min of saw blade with the diameter of $\varnothing$ 300 mm and $\varnothing$ 450 mm [2, 3]. The analysis of the results of these experiments helped to identify in the upper cover areas with insufficient vacuum (and even with small overpressure), which caused chip ejection from the casing.

In this paper the chosen numerical modeling results of the air flow process in the wood chips removing system for sliding table saw were presented. The aim of the full research was to optimize the chip extracting system. On the basis of the obtained results, a new design of the casing has been proposed [4].

METHODOLOGY

To create 2D numerical models of the sliding table saw complex geometry an unstructured mesh was used. Thus, it was possible to divide the flow region into finite elements of small size. This approach was very important to achieve convergence and accuracy of the solution. For these models, the number of unstructured elements (cells) was about 1 892 600. In selected cases, the air flow in the dust extraction system was analysed without taking into account the occurrence of the wood chips movement. In the Figure 1 the examples of the circular sawing machine numerical model with separation knife and without separating knife respectively are presented. The saw blade with the diameter of $\varnothing$ 450 mm shown.

a)

b)
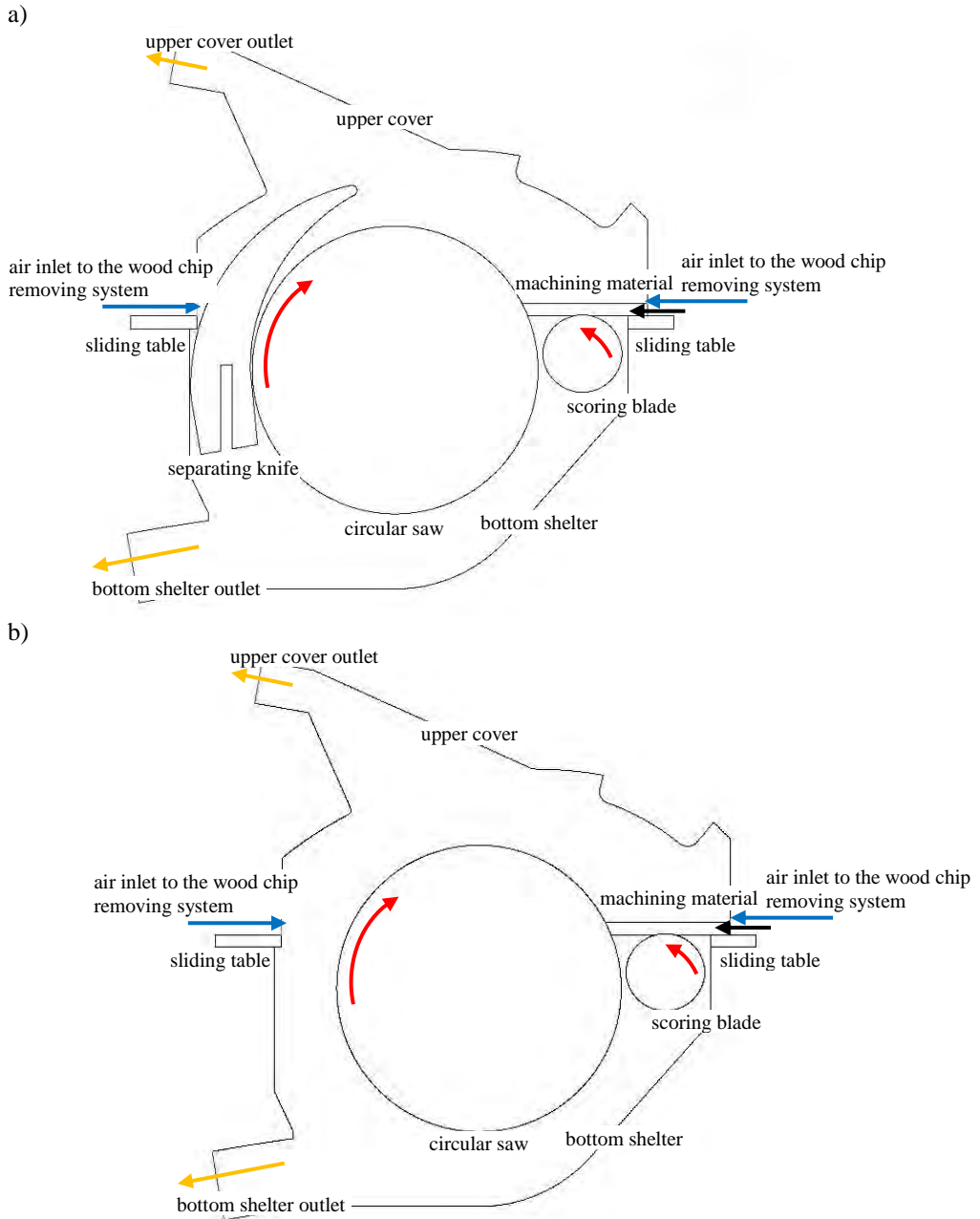
Figure 1. The cross section view of the circular sawing machine numerical model:
a) with separation knife, b) without separating knife.

The numerical simulations were performed for different boundary conditions and circular saw diameter, as presented in Table 1.

Table 1. The boundary conditions assumed for numerical simulations of the chip removal system.

	Ambient pressure	Vacuum pressure at bottom shelter outlet	Vacuum pressure at upper cover outlet	Circular saw rotational speed	Scoring blade rotational speed
	[Pa]	[Pa]	[Pa]	[1/min]	[1/min]
circular saw ⌀ 300 mm					
1.	101 130	- 400	- 200	3 500	8 500
2.	101 130	- 400	- 400	3 500	8 500
3.	101 130	- 1 500	- 1 500	3 500	8 500
4.	101 130	- 400	- 200	6 000	8 500
5.	101 130	- 400	- 400	6 000	8 500
6.	101 130	- 1 500	- 1 500	6 000	8 500
circular saw ⌀ 450 mm					
7.	101 130	- 400	- 200	3 500	8 500
8.	101 130	- 400	- 400	3 500	8 500
9.	101 130	- 1 500	- 1 500	3 500	8 500

A series of computer simulations were performed. Each simulation was performed at various boundary conditions. The differences concerned the rotational speed of the saw, the vacuum pressure in the both outlet and the diameter of the saw, which were presented earlier.

The vacuum pressure values at the outlets from the upper cover and lower shelter were assumed on the base of the results of experimental measurements (200 Pa in the upper cover outlet and 400 Pa in the lower shelter outlet). The maximum value of the vacuum pressure in both outlets, i.e. 1500 Pa, was adopted in accordance with the information provided by the Panel saw manufacturer and the data available in the literature. Simulations of air flow process for vacuum pressure in both outlets with value of 400 Pa were also performed.

For the turbulent flow modeling, a standard model of turbulence k-ε (k-ε standard) and a mesh of the entire dust extraction system with machining material and with or without a separating knife were used.

The calculations for each case were carried out until the values of the solutions of the equations of behavior (the so-called residuals) were stabilized in a narrow range of variation at the level of 10^{-4}.

For each modeling case, which was carried out, the chosen simulation results in the ANSYS Fluent software will be presented graphically for the velocity vector field and possibly the flow line field.

RESULTS OF EXPERIMENTS

Below, the chosen results from numerical simulations of the circular sawing machine will be presented. Figures 2 and 3 present examples of the numerical calculations results of the

velocity field of the sawing system of the table sawing machine for the following boundary conditions:
- vacuum pressure at the upper cover outlet - 200 Pa,
- vacuum pressure in the lower shelter outlet - 400 Pa,
- circular saw diameter $\varnothing$ 450 mm,
- circular saw speed of 3 500 1/min,
- rotational speed of the scoring blade 8 500 1/min.

Fig. 2 presents the results of numerical calculations of the air flow process through the wood chip removal system for the material cutting for a case where a separating knife is present in the sawing machine system.

The occurrence of the knife affects the less favorable distribution of air flow in the rear part of the dust extraction system, Fig. 2a. In addition, in the front part of the upper cover, it can be seen that the air is pushed into the environment with greater intensity compared to the further case (marked with a blue circle). The speed value is higher here, Fig. 2b. There is no air turbulence zone in the upper part of the upper cover, near the handle. This is the effect of the smaller impact of the rotating saw on the flowing medium. The separating knife is an obstacle to the air flow process at the outlet of the lower shelter.
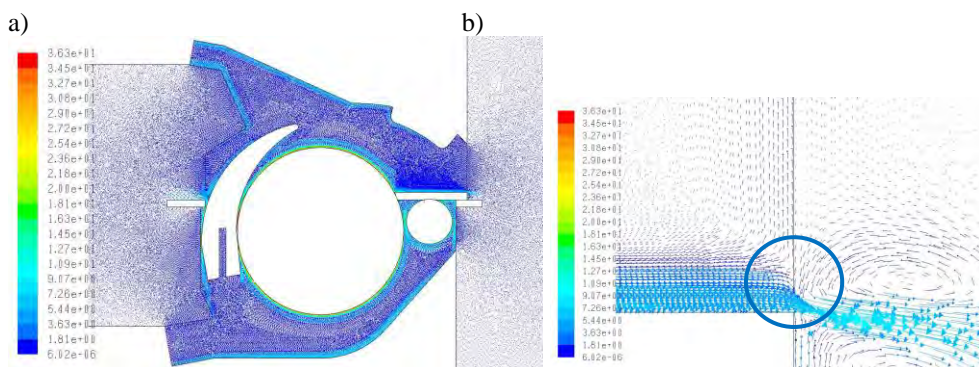
Figure 2. The air flow velocity vectors through the saw and chip removal system with a saw diameter $\varnothing$ 450 mm: a) in the sliding table saw, b) in the front of the upper cover.

In addition, it reduces the impact of the saw on the air flow. In the rear part of the casing, the inflowing air is separated into two streams and flows to the outlets of the lower shelter and the upper cover. It can be seen that the air in the upper cover, in addition to pushing into the environment, is directed towards its upper wall. In addition, there is an area where the air flow values are small

Fig. 3 shows the air flow through the wood chip removal system for the material cutting event without taking into account the presence of a separating knife at the back of the saw. We can see the behavior of the air flow process, which after entering the dust collection system is directed to the outlets of the lower shelter and the upper cover.
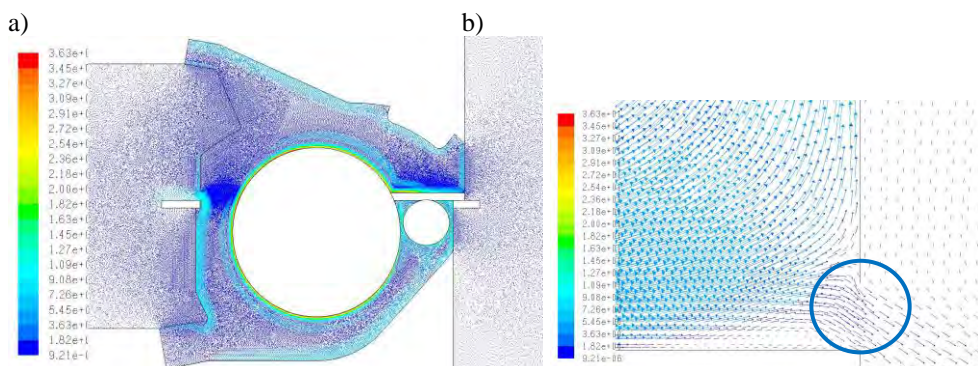
Figure 3. The air flow velocity vectors through the saw and chip removal system with a saw diameter ⌀ 450 mm: a) in the sliding table saw b) in the front of the upper cover.

We can see here the large impact of the rotating saw on the flowing medium and the intensive mixing process with incoming air. This is due to the high value of the linear speed of the saw and the shape of the upper cover, which has got the so-called the dead space from which the air is unable to get out. In addition, we can clearly see the effect of the saw on pushing the air out of the upper cover in its front part (Fig.3b). This is the total effect of the linear speed of the saw and the occurrence of a small vacuum pressure (200 kPa) at the upper cover outlet (marked with a blue circle).

CONCLUSIONS

Existing chip removing system in the analyzed woodworking machine did not provide satisfactory chip extraction from the working area. After numerical simulations and experiments it was proved, that in the area around the tool the insufficient vacuum pressure can occur hindering the organized transport of wood wastes. After several changes in the system, especially in the upper casing, all parts of suction system were optimized and modified, except for the structure of the fan, which allowed to achieve efficient performance. Eventually, a new design of the chip removing system was obtained.

REFERENCES

1. Dzurenda, L. (2007) *Sypká drevná hmota, vzduchotechnická doprava a odlučovanie (Bulk wood mass, air transport and separation)*. 1st ed., 182 p. Technical University in Zvolen, Slovak Republic.
2. Barański J., Jewartowski M., Wajs J., Pikała T. (2016) *Experimental analysis of chip removing system in circular sawing machine*. Chip and Chipless Woodworking Processes (Trieskove a Beztrieskove Obrabanie Dreva), vol. 10, no. 1, pp. 25-29;
3. Barański J., Jewartowski M., Wajs J., Pikała T. (2018) *Experimental examination and modification of chip suction system in circular sawing machine*. Drvna Industria, Vol. 69 (2018), No. 3 (in print)
4. Wajs J., Barański J., Jewartowski M., Orłowski K., Pikała T., Dudek P. *Method of chips upper removal for working space of the circular sawing machine, particularly panel saw*

and upper cover of dust extraction system of circular sawing machine, particularly panel saw. (in Polish) Patent pending No. P.421584.

5. Kohler, B. (1995) *Wood dust and cancer*. National Report - Health, Safety and Environment, IARC, France.

6. ANSYS Fluent User's Guide, 2012.

DEVELOPMENT OF A COLLABORATIVE PLATFORM FOR THE EXECUTION OF TECHNOLOGY WATCH AND COMPETITIVE INTELLIGENCE ACTIVITIES IN FURNITURE AND WOOD SECTOR COMPANIES

Josefina Garrido – Jesús Sanz – Guadalupe Santa – Blanca Puche

Abstract

The aim of this article is to prove that Technology Watch and Competitive Intelligence (TW/CI), when related to information management, can have a positive impact on the different processes linked to innovation management, the development of new products and decision-making in the furniture sector companies. For this purpose, the results of the HABIWATCHING Project will be described. Through this project, the collaborative platform for the execution of Technology Watch and Competitive Intelligence (TW/CI) activities for the Habitat Cluster in Murcia has been implemented.

Key words: *Technology Watch; Competitive Intelligence; Innovation; Knowledge, VINCI*

1. INTRODUCTION

The high competitiveness of the current market forces organisations to be constantly informed of everything that happens around, not exclusively of technological or sector-related news. Being able to know the intentions of competitors in the market framework gives a company the knowledge about a large number of data related to the products and services of these competitors. Under these circumstances, the company informed is allowed to develop a competitive strategy from a very advantageous position.

To obtain this information, Technology Watch (TW) is the organised, selective and permanent process that allows us to gather information from outside and from the organisation itself, and select, analyse, disseminate and communicate this data, to make decisions with less risk and to be able to anticipate changes. According to the research carried out in the thesis on which this article is based, and the bibliographic study accomplished, we can affirm that technology watch is closely related to the management of innovation and the company's strategy (Aguirre, 2015; Rey Vázquez, 2006).

Moreover, according to Leonard Fuld, the fact that the business executive has a high "Competitive Intelligence" about their direct competitors when making decisions will be an added value and will be very advantageous to the organization: "Knowing how, where and why the competitor uses their money is a shortcut in the race to improve the competitive strategy. The costs state how much can be invested in research and development, marketing, advertising campaigns, incentives, etc." (Fuld, 2006).

Technological Centre of Furniture and Wood, Perales s/n, Yecla, 30510, Spain
e-mail: Josefina.garrido@cetem.es

Although accessing information about competitors may seem easy for an organisation nowadays, the reality is that getting the necessary and correct information is becoming increasingly complicated, diffuse, delicate and even overwhelming. That is why performing a correct Competitive Intelligence activity is essential for companies: "Knowing how to find that information, use it for one's own benefit and in time to get ahead of the competitors' practices is the key to success for every forward-looking company." (Fuld, 2006)

On the basis of the above, we can affirm that Technology Watch is an indispensable tool for competitiveness in any kind of organisation whether it is public or private, industrial or service company, or a research organisation.

1.1 USE OF TECHNOLOGY WATCH IN FURNITURE SECTOR COMPANIES.

Traditionally, the furniture sector has been a sector that has followed the trends of fashion, particularly in the case of the subsector of upholstered furniture (sofas, chairs and armchairs), owing to the obvious use of fabrics and leather to cover all or part of the resulting products. Consequently, SMEs are starting to realise **the importance of monitoring the business environment** to learn about the state-of-the-art trends in the months to come.

However, according to the Spanish National Institute of Statistics (INE) statistics, which can be seen in Figure 1, we can say that, from 2008 to 2016, Spanish furniture-related companies reduced their TW/CI activities leading to innovate their creative processes. In order to know current data on the use of Technology Watch tools in the furniture sector at a national level, we have consulted the Survey on Innovation in Spanish Companies, which is carried out biannually by the INE 1. Although the decline is not too significant, we think that this situation has been caused by the global crisis, which has hit Spain in recent years, especially because of its dependence on sectors such as construction or financial institution.
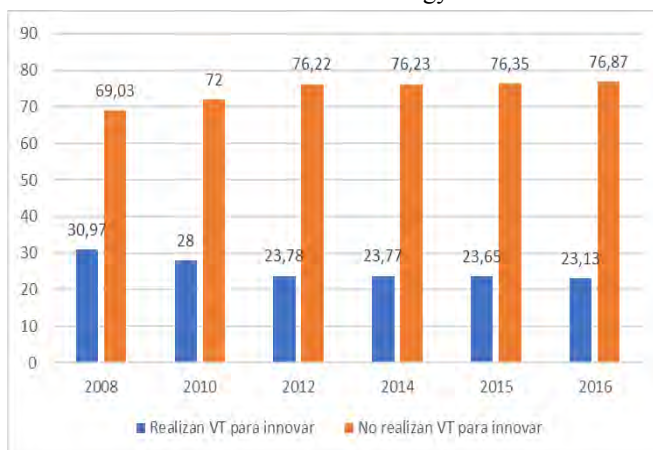
Figure 1 Companies that carried out TW/CI activities (comparative % 2008-2016).

---

[1] www.ine.es In this survey, the INE provides information on the structure of the innovation process (R&D/other innovative activities) and shows the relationships between this process and the companies' technological strategy, the factors that facilitate (or hinder) their ability to innovate and the economic performance of companies. Although the survey does not focus specifically on TW/CI activities carried out by companies, it does include data on the systematic use of information on the environment, products, competitors, etc. within companies' innovation processes.

f we observe the results, it calls our attention that the Technology Watch activities carried out by the companies during 2016 decreased 2.20% in contrast with 2015. However, the expenditure on technology innovation in 2016 increased compared to the previous year. "The technological innovation expenditure reached 13,857,481 million euros in 2016, with an increase of 1.34% compared to the previous year" (INE, 2018).

On the one hand, we remark that in 2016, 52.97% of innovation companies considered that the internal information sources (within the company or group of companies) were the most important ones in order to carry out technological innovation projects. On the other hand, 43.45% of the innovation companies affirmed that the sources of market information (suppliers, customers, competitors, consultants, etc.) were the most relevant ones in the RDI process.

Finally, and according to the data shown in Table 13, we highlight that the tendency of furniture sector companies to consume information from Technology Centres increased until 2014 and decreased again in 2016.

Table 1 Sources used by companies during the last 10 years.

	2016	2014	2012	2010	2008
Number of companies that consult information for their innovative activity	23.13	23.77	23.78	28	30.97
Types of sources used by companies					
Internal Source of the company	33.94	32.38	33.68	32.79	31.28
Sources from the environment: information about competitors, collaborators, suppliers, ICTs, etc.	43.57	43.62	43.90	45.36	46.59
Information prepared by institutional sources (universities, international organisations and reports)	10.24	11.31	10.09	8.92	7.85
Technological Centres	3.38	4.20	3.74	3.21	2.74
Other sources (Conferences, scientific journals, professional associations)	12.24	12.70	12.32	12.93	14.27
Scientific Information	3.54	3.40	3.57	3.46	3.84
Fairs and conferences	5.54	5.60	5.04	5.5	6.23

The interest in attending professional events such as fairs and congresses, as well as in the analysis of scientific and technical information (articles, books, etc.), has been significantly reduced.

2. MATERIALS AND METHODS

As above mentioned, when it comes to watching tendencies (trends, materials, etc.), the furniture sector is always in movement, which has favoured SMEs with a special sensibility SMEs towards **the importance of monitoring the environment**. This is done in order to pick up new trends, technology and design wise, which are going to be important in the following months.

On the other hand, the technological centre CETEM and Murcia's furniture cluster AMUEBLA, have **pioneered the implementation of RDI management systems**, certifying their own system on April 2008, under the then experimental UNE 166.002 standard. Within this management system, Technology Watch and Competitive Intelligence stand out as sources of information for processes such as External Analysis and Idea Generation for RDI projects.

These two facts enabled an important watch culture growth thanks to which a collaborative Technology Watch tool called VINCI has been developed. Using the advantages of **digitalisation of information** through the internet, this tool has introduced technological contents in companies, which has provided them with: (1) the development of innovation projects according to its needs and (2) the creation of economies of scale in the production of valuable information for SMEs.

VINCI was developed freely for Yecla's furniture cluster companies thanks to the HabiWatching[2] project, based on a Cloud environment. The result has been a **collaborative platform** that enables the exchange of knowledge and information between SMEs, knowledge providers and, ultimately, all agents related to the cluster. Its objective is to generate more and better innovation projects more in line with the current state of technology.

2.1. METHODS FOR INCORPORATING COMPANIES TO VINCI

Those companies that had not systematised their watch tasks before were given specific advice by the cluster in order to define their own TW systems. For this purpose, the method for technology watch and competitive intelligence management developed by CETEM was taken as a basis. It consists of the following steps:

1. Planning and systematising tasks. Definers of how TW/CI takes place on a day-to-day basis, as well as relevant topics and sources for the watch.
2. Training. To carry out TW/CI activities, training the staff from each organisation that is going to participate will be needed. This step was developed on the staff of the organisations that took part in the pilot experience. Once the platform has been launched and outside the project, the rest of the staff of the cluster organisations has also been trained.
3. Data search and recovery. This step is already part of the TW/CI process and it is continually developed in the VINCI platform. Both CETEM and AMUEBLA play a key role in the data search and recovery process.
4. Data processing - recovering data in the TW/CI system and filing it in an easy-to-recover way. Thanks to VINCI and CETEM technicians' know-how, the process of filtering data can be optimised and adapted to the language of the industry.
5. Data analysis. During this step, data is analysed bearing one's target always in mind. In this case, our target is to identify opportunities regarding new products or improved processes thanks to technological knowledge and to apply them to the cluster's companies.
6. Data spreading - making the analysed data reach its "users", in this case the cluster's companies. As part of an ongoing process, it was tried out once in the pilot experience during the development of the HabiWatching project. Nonetheless, it is being maintained nowadays since it is considered a fundamental part of the process.
7. Evolution, system and results. The last step is a continuous analysis of the TW/CI system to test its effectiveness and efficiency.

2

3. RESULTS

The main result obtained during this research is the implementation of the collaborative platform VINCI to perform Technology Watch and Competitive Intelligence (TW/CI) tasks for the Hábitat Cluster in Murcia. VINCI has been validated as a collaborative platform where the results of TW/CI are shared by the cluster's technological agents. As the main result of this research, the companies within the cluster are now part of VINCI, a platform that is mostly based on the knowledge and technology providers (technological centres, cluster associations, universities, etc.). In this platform, the SMEs also act as "antennae" by including data related to the market and to business reality. VINCI has been validated as a collaborative platform where the results of TW/CI are shared by the cluster's technological agents.

The following results have also been obtained:

- A TW/CI service is now accessible for all the SMEs of the AMUEBLA cluster through the VINCI software.
- The SMEs industries have become more acquainted with technology through a practical and simple method.
- The first IDEAS on collaborative innovation projects for AMUEBLA companies have been developed.
- The amount of SMEs from the habitat cluster in Murcia taking part in innovation projects has increased.
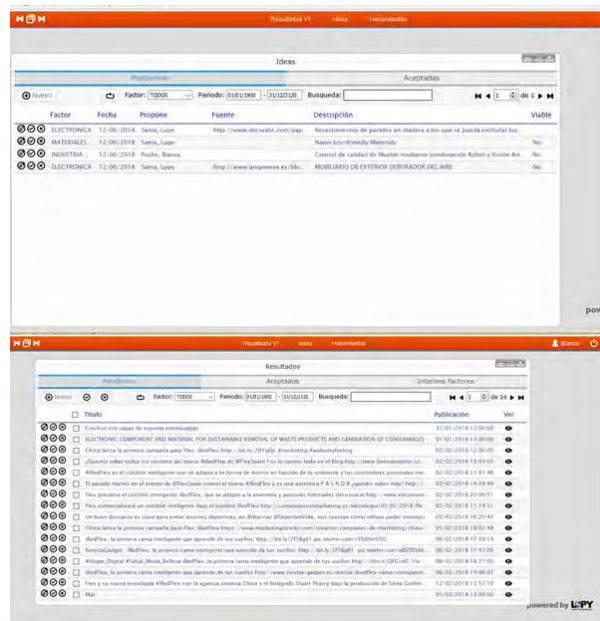
4. CONCLUSION

Thanks to implementing the HabiWatching project we have proven that, taking TW/CI tasks as a basis, companies obtain data that, once analysed, can be converted in valuable information for companies (either for themselves or for technological partners, in this case AMUEBLA or CETEM). The cluster has trained SMEs to **learn and use the data to create innovation projects** to improve their industrial competitiveness.

Moreover, on the research basis of this project, we can confirm that companies use the result of the technology watch and competitive intelligence processes as a strategic input for **decision-making** (basic for preparing a SWOT or other similar methods). We can see that the data gathered through VINCI, especially the data that comes from sectoral information resources, is useful to obtain information on the environment outside the organisation. In other words, information on potential threats and opportunities for which companies must be prepared to act as soon as possible.

REFERENCES

1. AGUIRRE, Joao. Inteligencia estratégica: un sistema para gestionar la innovación. Estudios Gerenciales, 2015, vol. 31, no 134, p. 100-110.
2. BUENO, E et all (2003). Gestión del Conocimiento en Universidades y Organismos Públicos de Investigación. Recuperado de: http://www.madrimasd.org/informacionidi/biblioteca/publicacion/doc/16_Gestion ConocimientoUniversidadesOPIS.pdf
3. CALOF, Jonathan, et al. Foresight, Competitive Intelligence and Business Analytics— Tools for Making Industrial Programmes More Efficient. Foresight-Russia, 2015, vol. 9, no 1, p. 68-81.
4. CHAIN NAVARRO, Celia. Gestión de información en las organizaciones. GUÍA DE LAS TITULACIONES, 1997, p. 71.
5. FULD, Leonard M. The new Competitor Intelligence: the complete resource for finding, analyzing, and using information about your competitors. John Wiley &Sons, Inc. New York, 1995
6. GARCÍA-ALISINA, M., & GÓMEZ-VARGAS, M. Prácti-cas de gestión del conocimiento en los grupos de investigación: estudio de un caso. Revista Interamericana de Bibliotecología, 2015. 38(1), 13-25
7. GARCIA-ALSINA, M. Contribución de la inteligencia competitiva en el proceso de adaptación al EEES: el caso de las universidades españolas. Universitat Oberta de Catalunya, Barcelona, España.2011. Tesis Doctoral
8. GARRIDO LOVA, J. Vigilancia e inteligencia competitiva como herramienta clave en el sistema de gestión de I+D+i de un organismo de investigación. Universidad de Murcia, España. 2016. Tesis Doctoral
9. GONZÁLEZ, J. Modelo para el desarrollo de la gestión del conocimiento en los centros de investigación de las universidades públicas colombianas. Caso aplicativo Universidad Pedagógica y Tecnológica de Colombia (UPTC). Gestión y Estrategia, 2009. (35), 47-62
10. MARTÍN, Rubén Arcos; FERNÁNDEZ, Fernando Velasco. Inteligencia competitiva y márketing: superioridad en la toma de decisiones. Harvard Deusto Márketing y Ventas, 2015, no 129, p. 20-27.
11. MARTÍNEZ, Laura Arribas. Diseño de un sistema de vigilancia tecnológica e implantación en la Fundación ASCAMM. 2008. Tesis Doctoral.
12. OSPINA MONTES, Clemencia; GÓMEZ MEZA, Milena; OSORIO LONDOÑO, Andrés Alberto. Modelo de Vigilancia Tecnológica e Inteligencia Competitiva en Grupos de Investigación de las Universidades de la Ciudad de Manizales. 2014. Tesis Doctoral.
13. REY VÁZQUEZ, L. Ferroatlántica I+D y la vigilancia tecnológica. El profesional de la Información, 15(6), 420-425. http://dx.doi.org/10.3145/epi.2006.nov.03

FUTURE POSSIBILITIES OF SAW LOGS ON MARKET WITH WOOD IN SELECTED COUNTRIES

Miloš Gejdoš – Martin Lieskovský

Abstract

Saw-logs represent the basic commodity of the processing industry, especially for the construction segment. Demand and consumption of this raw material on a global scale every year is growing. Paper analyses the market development for coniferous and non-coniferous sawlogs on central Europe markets. Analyzed Period was from 2011 – 2017 (respectively 2018). Evaluated were supplies volume and prices for spruce, fir and beech sawlogs in this period, for countries: Slovakia, Czech Republic and Austria. In the last ten years, prices of wood assortments increased generally. The fact of the potential risks and opportunities shows, that the timber market could be still dynamically increasing sector, in the future operating on the principle of sustainability. In the future can be expected pressure on prices of coniferous sawlogs.

Key words: *saw-logs, wood prices, market development, wood supplies*

1. INTRODUCTION

The current market for saw logs is mainly influenced by global climate change and by accidental events that directly trigger it. Practically throughout Europe, the intensity and extent of accidental fellings increases. The primary cause is wind storm and subsequent secondary damage to the weakened forest stands by insect attack. Other causes of rising volumes of accidental fellins are often the inappropriate tree species composition of forest stands and their weakness due to drought (especially for spruce stands).
Especially thanks to the high share of accidental fellings, it is possible to maintain the increasing consumption of saw logs and the relative mitigate of the processors' demand for it.
It is already clear that the continuation of this development will not be possible in the next decades. Processors should prepare for a gradual decrease in the market share of coniferous saw logs on the market (as the volume of intention felling will decrease) and adapt their technologies to the processing of other tree species (a gradual change in the tree species composition in forest stands is also expected).
The situation is quite different in the segment of the non-coniferous saw logs. Especially for beech wood, which is dominant in the market share. Demand for beechwood logs is low, especially due to the refusal of the construction and furniture industry. Today, however, there are good modifications of beechwood for its use in wooden constructions, so it is only a matter of time when the demand for this assortment will grow.
The paper evaluate current state and perspectives for the market development in this field. Especially for the coniferous and non-coniferous saw logs.

Technical University in Zvolen, T. G. Masaryka 24, 960 53 Zvolen
e-mail:gejdos@tuzvo.sk, lieskovsky@tuzvo.sk

2. MATERIAL AND METHODS

Development of the supply volumes of sawlogs on the basis of data obtained from the Green Report issued by the Ministry of Agriculture of Slovakia and also in the Czech Republic were evaluated [1,2]. Data for Germany were acquired from the "Holzmarktbericht" [3] and for Austria "Holzeinschlagsmeldung"[4]. Assessment of price developments was focused on sawlogs assortments from spruce, fir and beech trees in selected provinces in Austria, Czech Republic and Slovakia. The analysed period represents the period from 2009 to April 2018. In the case of the Czech Republic the prices were calculated using the exchange rate of the National Bank of the Czech Republic [5]. The prices of assortments for Austria are in the trade parity on forest roads or forest warehouse. Prices in Slovakia and Czech Republic are placed on parity FCO (ex-warehouse vendor, respectively FCA (loaded truck purchaser). In order to provide absolutely correct comparison, it is necessary to add the transport costs to the Austrian prices (eventually parity DAF or CIF). Information on price developments have been drawn from the magazine Holzkurier [6], the Czech Statistical Office [7] and the forestry market information system [8].

3. SUPPLY DEVELOPMENT FOR SAWLOGS

Global production of roundwood confirms the continuous increase in production of this assortment. With the exception of 2009 (Global Economic Crisis), increase global production of sawlogs by almost 156 million m^3 between 1993 and 2016 (+17,2%).
The largest average share (1993-2016) of production of total produced roundwood volume have USA (209 million m^3), Canada (140 million m^3) and Russian Federation (94 million m^3).
If we consider only Europe, the development is similar. An increase in the production of sawlogs from 1993 to 2016 was more than 125 million cubic meters (+55 %). The largest average share (1993-2016) of production of total produced roundwood volume in Europe have Russian Federation (94 mil. m^3), Sweden (34 mil. m^3) and Germany (28 mil. m^3).
In Slovakia, the production of sawlogs has increased almost threefold since 1993 to 5 mil. m^3.

Table 1 *Supplies volumes of sawlogs in selected countries of Central Europe for the period 2011 - 2016*

Country/Year	Coniferous logs III. quality class					
	2011	**2012**	**2013**	**2014**	**2015**	**2016**
Slovakia	3 315 963	2 738 391	2 388 043	3 079 215	2 749 994	2 972 841
Austria	10 064 816	9 358 593	9 052 196	8 585 106	9 193 948	9 236 916
Germany	25 497 000	23 457 000	23 784 000	24 917 000	27 024 000	24 712 000
Czech republic	8 014 152	7 911 000	7 925 000	7 955 000	8 468 081	9 869 000
	Non-Coniferous logs III. quality class					
	2011	**2012**	**2013**	**2014**	**2015**	**2016**
Slovakia	1 352 606	1 392 987	1 501 459	1 498 766	1 427 986	1 410 727
Austria	320 876	295 086	267 120	270 120	296 831	320 625
Germany	3 520 000	3 175 000	3 058 000	3 197 000	3 356 000	3 471 000
Czech republic	823 845	710 000	720 000	593 000	495 728	472 000

Table 1 shows the development of sawlogs supplies in selected countries of central Europe. In coniferous sawlogs can we observed the general decrease in period 2011-2013. In the 2014 was in all countries (except Austria) the slightly increase for the sawlogs volume supplies. In 2015 and 2016, the level of production of sawlogs in individual countries did not change fundamentally. This development reflects the gradual impact of incidental fellings over the past 10 years. In the future, another slight decrease may be expected, especially in the case of coniferous pine logs.

In the supplies of non-coniferous raw wood assortments have the highest share assortments of pulpwood and industrial wood. This is partly related to the settings and preferences of the wood-processing industry. For more valuable purposes of the processing are mainly in tree species oak, maple and ash. The supplies of non-coniferous saw-logs are also affected the tree species composition in the Forest. In the forests of Austria, Germany and Czech Republic are dominant the coniferous tree species. Only in Slovakia is dominant the beech. Generally was the trend for this assortment in last 2 years in Slovakia and Czech Republic slightly decreasing (Table 1). In Germany and Austria was the trend slightly increasing. Also it influences the progressive development of wooden buildings and various support programs in some countries [9].

In the near future, the market for this assortment will continued to be affected by extensive incidental fellings. In the Czech Republic is a particularly unfavorable state of damages in forest stands caused by insects. In 2017, 5.5 million m^3 of wood, damaged by insects, were processed. Another 4 mil. m^3 of predominantly spruce wood was damaged by wind. This year, further grading of this state is foreseen, which will significantly affect the timber market at the regional level. In the short term, we can expect a decline in the prices of coniferous saw-logs. In the long run, however, the volume of this assortment on the market will gradually decrease and the impact will be visible in the gradual increase of prices.

In the case of beech sawlogs, stabilized volumes on the market and gradual recovery in the range of these assortments can be expected, especially as a result of its application in the wooden constructions sector.

The availability of raw materials for sawmills will in the future also affect the development of the energy sector and an increasing demand for timber as an energy renewable resource.

4. DEVELOPMENT OF THE SAWLOGS PRICES

The development of sawlogs prices is affected with a many factors. The most crucial influence had the intensity and extent of incidental felling together with a local and global economic and political situation. In this chapter we focused mainly on the analysis of the sawlogs prices development, mostly traded wood species, spruce, fir and beech in selected provinces in Austria, Slovakia and the Czech Republic for the period 2011 - April 2018. The influence of certain factors on the wood prices in most countries of Central Europe is very similar. We will focus on analyzing the causes of prices, developments in a given period.

4.1 Price Development for the Spruce and Fir sawlogs

Figure 1 represent the price development for the sawlogs, from wood species spruce and fir in Slovakia, Czech Republic and selected regions of Austria. After global economic crisis was the situation on timber market relatively stabilized in years 2011 and 2012. Since that time, practically still continuously increase until the end of the year 2014. In Austria and the Czech Republic a several enterprises got into economic problems in 2014 and decreased its production capacities. For the prices of sawlogs this reality didn´t have any significant

impact. Mainly in Austria was the situation affected by economical restrictions again Russia. The big sawn wood producers in Austria have the frozen capital investments in Russia. That partially influence the timber market in Austria. The market development is continuously affected by big range of incidental fellings in Europe. In near future can we expected the next prices decrease (according to situation in Czech Republic). For the last 5 years was the biggest price level at the end of 2013 in Austria. In Slovakia was the biggest price level at the beginning of 2018.
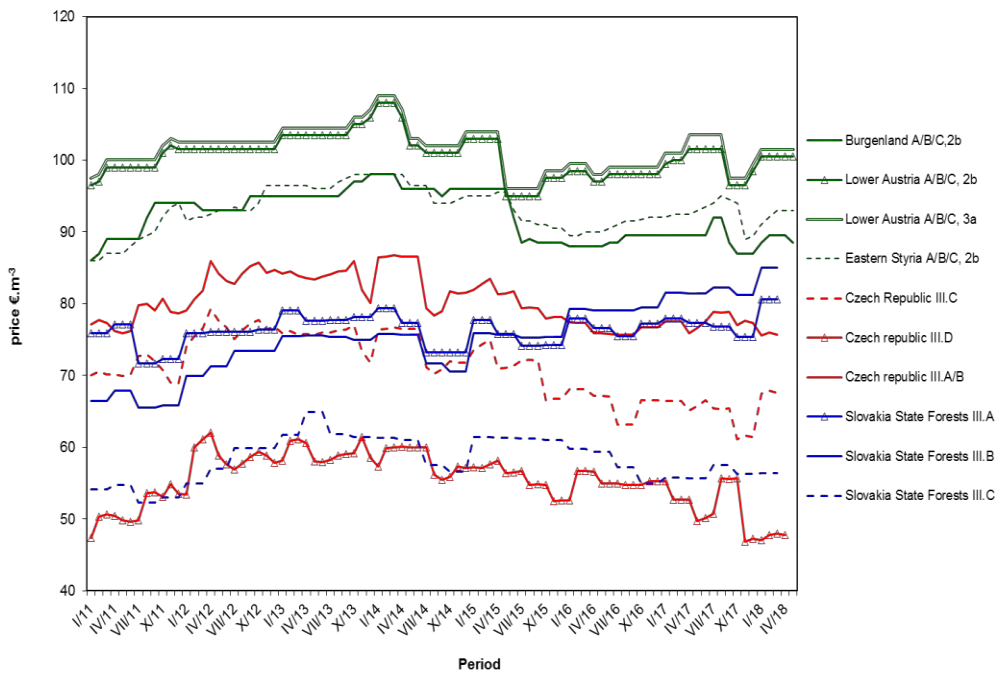
Figure 1 *Development of spruce and fir sawlogs prices in Slovakia, Czech Republic and Austria*

4.2 Price Development for the Beech sawlogs

Figure 2 represents the price development for the sawlogs from wood species beech in Slovakia, Czech Republic and selected regions of Austria. The highest Slovak price levels in the monitored period reached the beech sawlogs just at the beginning of 2018. The minimum was reached in early 2011. At the beginning of 2012, prices have slightly increased and remained at this level basically stable for two years.

In Austria and Czech Republic was the price development similar (despite of other tree species composition in the forests). In the Czech Republic was the price level assortments classes III.C and III.A/B relatively identically in the late 2017.

In Austria the trade with higher quality of broadleaved assortments is seasonal. Since 2013 it has fundamentally changed the methodology of prices information (in Salzburg started to roll out prices for different kind of beech sawlogs assortments), so it was not possible to compare continuously during the entire period. During 2014 it was recorded for a mixed assortment of A/B in different classes of thickness a significant increase of more than 10 € per m^3. Certainly it contributed to various state programs aimed at promoting the beech and products thereof. At the beginning of 2017 was recorded partially decrease in mixed class

A/B, 3b+. In the class III.A/B 4+ was the decrease recorded in the half of year 2017. It indicates the continued stagnation on the market with beech saw-logs.
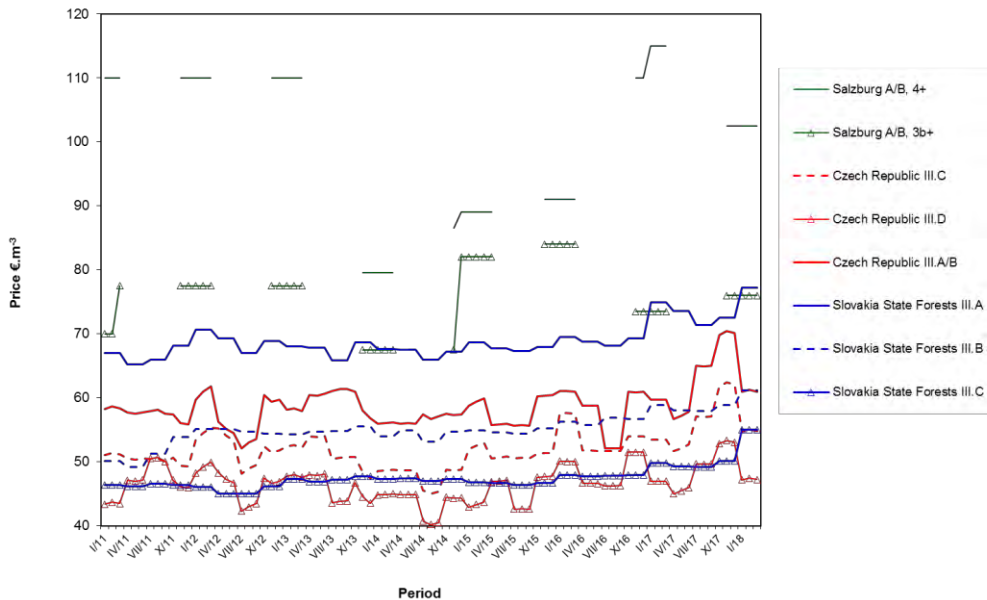
Figure 2 *Development of beech sawlogs prices in Slovakia, Czech Republic and Austria*

5. CONCLUSION

Over the past 5 years, we can mark the situation on the market for sawlogs as stabilized. This is true for both coniferous and non-coniferous logs. The situation was predominantly influenced by the incidental fellings operations which formed the basis for sufficient supply and further growth of the processing industry in this segment. In the near future, there will still be enough wood in the Central European region, mainly due to incidental felling. However, over the several decades, the same continuous increase can´t be expected as after the global economic crisis in 2009. The volume of intentional felling will decrease, the age structure of the forests will change, and the assortment structure will be changed. Another sector, especially in the field of energy and synthetic materials, will play its role. Today's producers should consider alternatives to production programs for spruce and fir raw wood assortments. It can´t be expected that in the long term, enough wood will be available for all processing industries.

REFERENCES

1. Anonymous. 2017. GREEN REPORT 2017. Ministry of Agriculture and rural development, 70 p.
2. Anonymous. 2014. REPORT ABOUT THE FOREST AND FORESTRY MANAGEMENT 2014. Ministry of Agriculture, Czech republic. 136 s., 978-80-7434-153-
3. HOLZMARKTBERICHT 2008 – 2014, Federal Ministry of Food and Agriculture, Bonn, Germany, Ministerium für Ländlichen Raum, Ernährung, Landwirtschaft und Forsten, 25 s.
4. HOLZEINSCHLAGSMELDUNG FÜR JAHRE 2008 – 2014, Federal Ministry of Agriculture, Forestry, Environment and Water Management, Vienna, Austria, 88 p.
5. Information on http://www.cnb.cz
6. HOLZKURIER, years 2008 – 2015
7. Information on http://www.czso.cz
8. Brezinová, M. 2015. Average prices development of assortments and raw-wood supplies for the quarters 2008, 2009, 2010, 2011, 2012, 2013, 2014, 2015 In: Informačný list Národného lesníckeho centra, Zvolen 9 s.
9. Gejdoš, M. 2016. Analysis of market development with saw logs in conditions of Central Europe. In Chip and chipless woodworking processes 2016: 10th international science conference, September 8-10, 2016, Technical University in Zvolen. Zvolen: 2016, p. 31--36.

DUST EMISSIONS DURING SANDING OF THERMALLY MODIFIED BEECH WOOD

Luďka Hlásková[1] **– Zdeněk Kopecký**[1] **– Miroslav Rousek**[1] **– Tomasz Rogoziński**[2] **– Antonín Železný**[1] **– Pavel Haninec**[1]

Abstract

The aim of the paper is determination of dust emission during sanding of native and modified beech. The analysis concerns the characteristics and composition of this dust. The issue of danger for human health exposed to the wood dust is also addressed and impact of dust particles on the working environment hygiene. The experimental part was carried out on a test stand to simulate standard sanding. For our experiment three samples were selected, namely a modified beech at 180 °C, 200 °C and a native beech. In order to evaluate the incidence of wood dust, a methodology was designed to determine the representation of individual fractions of wood particles. Very fine particles (particles smaller than 100 μm) were subjected to microscopic analysis and then mathematical and statistical evaluation.

Key words: *wood dust, sanding, proportion of particles, size of particles, thermally modified wood, beech*

INTRODUCTION

Together with the main product also chips and sawdust are produced during wood machining. Wood dust is an assembly of individual particles which shape and size depends on properties of the worked wood material and working parameters (Prokeš, 1978; Goglia, 1994; Lisičan, 1996; Dzurenda, 2007). The sawdust created during woodworking is dispersed in the air and presents a serious health risk of woodworkers (Hubbard et al., 1996; Beljo-Lučić et al., 2011; Čavlović et al., 2013). Protection against the wood dust should be based on the detailed knowledge on the sources of dustiness of the air around woodworking machines. Thus it is necessary to determine the mass rate of generated dust and its particle-size distribution for evaluation of the health hazard created at working of different wood materials by dust particles dispersed in the air. Different working operations and properties of wood materials are the reason of changeability of total dust created. Beech wood is moreover one of the most hazardous materials worked in wood products and furniture manufacturing. Recently modification technology makes it possible to obtain new materials based on solid wood for manufacturing of such products. The thermal treatment process is aimed at suppression of wood properties that are detrimental for its use, such as water

[1]Mendel University in Brno, Zemědělská 3, 61300, Brno, Czech Republic
e-mail: ludka.hlaskova@mendelu.cz, zdenek.kopecky@mendelu.cz, rousek@mendelu.cz, zelezny66@hotmail.com, xhanine1@node.mendelu.cz
[2]Poznań University of Life Sciences, Wojska Polskiego 38/42, 60-627 Poznań, Poland
e-mail: trogoz@up.poznan.pl

absorption, swelling, shrinkage and resistivity against biologic pest (Gaff et al., 2010; Kopecký et al., 2007). It influences on the working parameters of these materials and on the properties of generated wood dust. Dolný et al. (2011) have found that the smaller dimensions dust particles are generated during the sanding of thermally modified oak wood than of natural oak wood. Similarly conclusion gave Dzurenda and Orłowski (2011) according the sawdust generated during sawing of the thermal treated oak and native oak wood on sash gang saw.

MATERIAL AND METHODS

To obtain samples of wood dust, a stand was used which was manufactured directly for the purpose of this measurement. Samples were cut in the transverse and longitudinal direction. In order to maintain the constant conditions for all samples, a new abrasive belt was used for each individual sample. The cut sample was pressed towards the abrasive belt with a constant compressive force by the lever mechanism - the specific pressure was maintained at 0.40 N·cm^{-2}. The abrasive belt has a length of 610 mm, a width of 100 mm and a grain size of 80. To determine the dust emission during sanding, a method of dust collection has been proposed from the inside of the box with the grinder. Prior to each measurement, there was carried out a precise cleaning of the area around the grinder and of the grinder itself. Subsequently, the box was sealed with a flexible seal. Then, a layer of workpiece was sanded off so that the amount of wood dust was at least 50 g. After the dust had settled (about 30 minutes), the wood dust was manually removed and prepared for granulometric analysis.

Thermall modified beech at 180°C and 200°C was selected as experimental material and native beech. Samples were modified in a laboratory (Katres s.r.o.) for 3 hours in a steamy environment.

Tab. 1: Properties of experimental samples

Wood	Process	Density [kg·m^3]		Weight	Equilibrium
		untreated	treated	loss [%]	moisture [%]
BK native		723.6	-	-	12.9
Thermo – 180 °C	process I = 180 °C	719.0	694.4	3.42	6.8
Thermo – 200 °C	process II = 200 °C	742.3	677.4	8.73	4.9

For the granulometric analysis, a sieving method was chosen to determine the particle size. The granulometric analysis was performed using the Retsch AS 200 digit instrument with the option of continuously amplitude adjusting of the vibrations in the three-axis network. The device is equipped with 5 mm, 1 mm, 500 μm, 250 μm and 100 μm sieves according to ISO 565 (DIN ISO 3310-1), vibration amplitude A = 1 mm, sieving time t = 10 min. At precise digital scales Vibra AJ - 420 - CE with an accuracy of ± 0.001 g, the particles were weighed, which were sieved through individual sieves.

For particles smaller than 100 μm, microscopic analysis was used. Microscopic images were evaluated for a fraction less than 100 μm. Regards to inhalation, the most dangerous dust particles are 0.25 to 5 μm (Koncz, 1970). For each sample, approximately 20000 dust particles were put to the probability analysis. Using an analysis system and a Keyence VHX – 5000 microscope image processing that measures the shape of a subject using Focus

Variation, the particle samples have been examined, which have fallen to the bottom of the sieving device (particle size below 100 μm).

To assess the behaviour of dust from various aspects, such as its ability to separate in different types of separators, its health effects, its settling capability, its explosive capability, its probable occurrence in a given dust emission must be known. For a probability analysis of fine dust up to 100 µm, it is possible to use a two-parameter Weibull model, which complies for most cases of occurrence of a random variable. Weibull model data is obtained from image analysis. Since the Weibull model parameters - the shape parameter and the scale parameter are movable, ie dependent on the statistical distribution of the particles, the Weibull model can pass e.g. in Gauss, log-normal, exponential and other probability models (Kopecký, Mazal, 2005).

RESULTS

The granulometric analysis shows that for the longitudinal sanding model (Figure 1a), the particle size is below 100 µm for native beech (60%) and THERMO beech for 180°C (52%). At THERMO 200°C, the largest representation is in the range of 100-250 μm (60%).
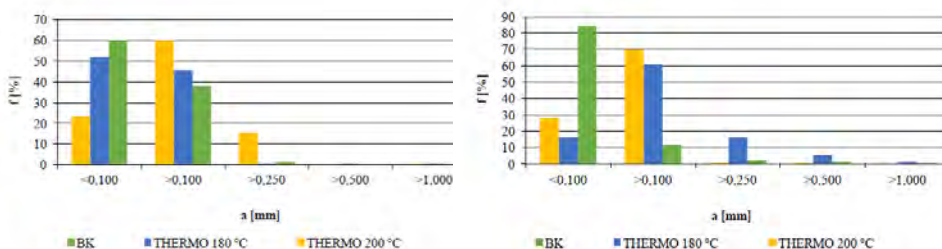
Fig. 1: Histograms of the sawdust particle-size distribution for a) longitudinal direction of sanding, b) transverse direction of sanding

From the fractional representation in the beech dust histogram from the transverse sanding model (Figure 1b), it is clear that the largest representation of particles below 100 μm is for native beech (83%). In the range of 100-250 μm, the largest proportion is for the THERMO 200°C (70%) and THERMO 180°C (62%).

In order to better illustrate and compare the effect of the modification on the fractional composition of wood dust, we created a cumulative particle-size distribution curve (Figures 2a and 2b). A log-normal or log-log coordinate are used to display this chart appropriately. The results show, that with the increasing temperature of the modification, the proportion of dust particles smaller than 100 μm decreases, especially in cross-sanding. In the THERMO200°C longitudinal sanding model (Figure 2a) 38% less fine dust up to 100 μm is produced than for the native beech, for the THERMO 180°C is a 30% difference.

In the transverse sanding model (Figure 2b), the differences are more apparent than in the longitudinal sanding model. THERMO 180°C has a 53% lower proportion of fine dust particles up to 100 μm than the native beech, THERMO 200°C makes this difference even more noticeable, up to 67%. The dropout curve is important when designing separating devices. If the curve is deflected to the left side, there is a higher demand on the filter device.
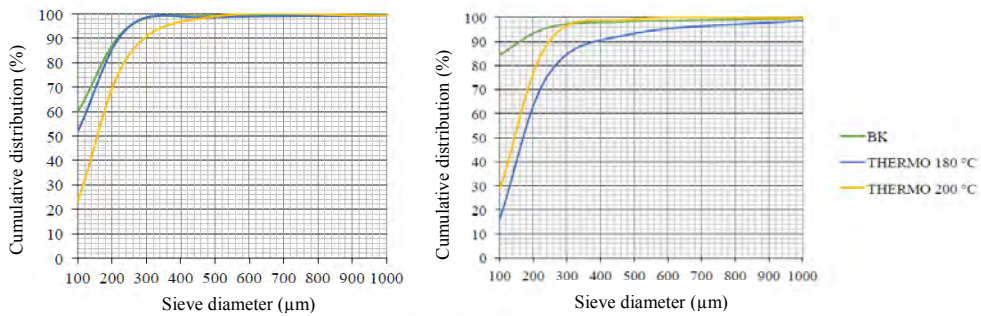
Fig. 2: The cumulative particle-size distribution for a) the longitudinal direction of sanding,
b) transverse direction of sanding

The particle-size distribution probability density graph for the longitudinal sanding model (Figure 3) results in a significant occurrence of dust particles in dimensions smaller than 30 μm. The probability density exponentially increases in the range of x = 2 to 30 μm. With the increasing temperature of the modification, the probability density of occurrence of small dust particles decreases in the range of x = 5 to 40 μm. In the range of x = 2 to 5 μm, the opposite impact occurred, and the THERMO 200°C dust has the highest probability density of occurrence.
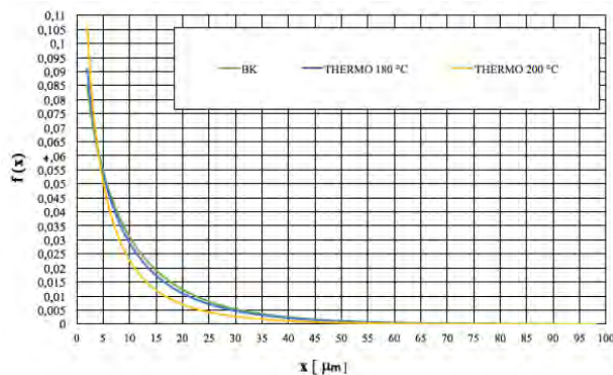
Fig. 3: Particle-size distribution – longitudinal direction of sanding
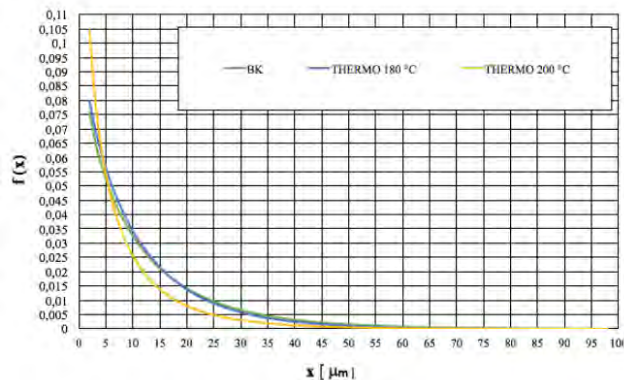
Fig. 4: Particle-size distribution – transverse direction of sanding

The probability density in the transverse sanding model (Figure 4) exponentially increases in the range of x = 2 to 45 μm. From the course of values it is clear that the difference between native beech and THERMO 180°C is negligible. In the range of x = 5 to 40 μm the probability density of THERMO 200°C relative to the native beech and THERMO 180°C decreases. In the range of x = 2 to 5 μm the opposite effect occurred and THERMO 200°C has the highest probability of occurrence probability.

DISCUSSION

Granulometric analysis results for particulates smaller than 100 μm (airborne particles) that with the increasing temperature of the modification in longitudinal sanding, the percentage of finest dust particles decreases by up to 37% at THERMO 200°C compared to native beech. In the transverse sanding model, the smallest percentage of fine particles was for THERMO 180°C, 52% less than the native beech. The measured results clearly showed that the modified beech has a smaller percentage of fine particles than native beech. It is also clear from the results that the temperature of the modification and the sanding model have had a major influence on the granulometric composition of the individual fractions of wood dust in all the samples examined. Jobbágyová (2008) monitored the granulometric composition of wood dust, depending on the type of wood and the sanding model, and recorded a particle size under 0.08 mm in average percentage of 93.34% and in the longitudinal sanding 83.34% in the transverse sanding model of a native beech. These values are comparable with the results of our native beech analysis. Similar results are published by Očkajová, Rončka and Banski (2006).

Longitudinal sanding has larger particles than a transverse sanding, due to the microscopic structure of the wood, because most of the cellular elements are located in the longitudinal direction and have a fibrillar structure, resulting in less cutting of the wood elements. Boonstra et al. (2006b) studied the microscopic structure of heat-treated hardwood and concluded that the treated beech and birch had radial cracks near the wood rays. Broken cell walls perpendicular to the fibre direction can cause transverse cracks creation.

In addition, a microscopic analysis of wood dust with dimensions less than 100 μm was carried out in order to determine the probable occurrence of hazardous inhalable particles which are the most dangerous in terms of hygiene and labour safety. The probability analysis showed that in the fraction up to 100 μm, most of the samples contained particles smaller than 40 μm. For a range of 5-40 μm, it has been found that the modified beech has a smaller percentage of fine particles than native beech. The highest probability density of fine dust was for THERMO 200°C both in the longitudinal and transverse direction, namely 2 μm. From a medical point of view, according to Bean (1996), these particles with dimensions smaller than 10 μm can reach the bronchial system depending on their size in different sections of the tract (bronchoalveolar, tracheobronchial). According to Standfest (2008), the hardness according to Brinell of modified beech increased approximately by 10 N·mm^{-2}. This factor probably affected the total sanding time of the individual samples the most, which was up to three times longer for the modified beech compared to the native beech. Also, Očkajová, Rončka and Banski (2006) examined the dependence of the density of the sanded material on the granulometric composition of wood dust. They came to the conclusion that with increasing density of native wood, the proportion of wood particles below 80 μm increased, by about 10%. The decrease of density for the modified beech was probably one of the main reasons for reducing the number of wood particles to 100 μm.

CONCLUSION

According to the measurement results, we found that thermal modification of wood as well as the sanding model have significant effect on the resulting particle size and on the shape and proportion of particles in individual fractions. In practice, it is preferable to select the model of longitudinal direction of sanding in order to reduce the emission of dust. Today as in the future, it is necessary to focus on reducing or eliminating hazardous substances in the workplace. It is therefore necessary in all industry sectors, including in woodworking to seek out ways how to eliminate pollution. Thanks to the knowledge of the dust properties we are able to influence positively the development of separation techniques and technologies leading to the emission reduction in the working environment.

Acknowledgement

REFERENCES

Bean, T., L., 1996. OSHA'S Wood Dust Exposure Standard. Ohio State University Extension Food, Agricultural and Biological Engineering.

Beljo Lučić R, Čavlović AO, Jug M, 2011: Definitions and relation of airborne wood dust fractions. 14th International Scientific Conference-Woodworking Technique, Prague, 25-32.

Boonstra, M., Rijsdijk, J., Sander, C., Kegel, E., Tjeerdsma, B., Militz, H., Van Acker, J., Stevens, M., 2006b. Physical aspects of heattreated wood. Part 1. Hardwoods. Maderas Ciencia y tecnología. 8, 209-217.

Čavlović AO, Beljo Lučić R, Jug M, Radmanović K, Bešlić I, 2013. Side-by-side determination of workers' exposure to wood dust with IOM and open-faced samplers. Archives of Industrial Hygiene and Toxicology, 64: 379-384.

Dolny, S.,Grocki, W., Rogoziński, T., 2011. Properties of waste from the cutting of thermally modified oak wood. Acta Scientarum Polonorum – Silvarum Colendarum Ratio et Industria Lignaria, 10(1), 11-18.

Dzurenda L. 2007: Sypka drevna hmota, vzduchotechnická doprava a odlučovanie. (Bulk wood mass, air transport and separation). Zvolen: V-TU. 182 p.

Dzurenda L., Orlowski K., 2011: The effect of thermal modification of ash wood on granularity and homogenity of sawdust in the sawing process on a sash gang saw PRW 15-M in view of its technological usefulness. Wood Research. Reports. 54(186), 27-37.

Gaff, M., Gáborík, J., Koristová, E., 2010: Shape and dimensional stability and surface modified wood molding – embossed. (Tvarová a rozmerová stabilita a povrchu dreva modifikovaného lisovaním – reliéfovaním.) Zvolen: Technická univerzita vo Zvolene, 76 pp. ISBN 978-80-228-2107-0 (in Slovak) .

Goglia V. 1994: Strojevi i alati za obradu drva I. Zagreb: GRAFA. 235 p.

Hubbard R, Lewis S, Richards K, Britton J, Johnston I, 1996: Occupational exposure to metal or wood dust and aetiology of cryptogenic fibrosing alveolitis. Lancet. 347, 284-289.

Jobbágyová, A., 2008. Vplyv dreviny na vlastnosti drevného brúsneho prachu. Disertační práce. Technická univerzita vo Zvolene, Fakulta drevárska, Katedra obrábania dreva.

Koncz, I., 1970. Odstraňovanie a odlučovanie prachu. ALFA Bratislava, 1975. 1. vydání.

Kopecký, Z., Mazal, P., 2005. Microscopic and stochastic analysis of wood dust. Warsaw Agricultural university. SGGW Annals. Forestry and Wood Technology. 2005, č. 56, s. 354-357. ISSN 0208-5704.

Kopecký, Z., Rousek M., 2007: Dustiness in high speed milling. Wood Research 52(2): 65-76. ISSN 1336-4561.

Lisičan, J., 1996: Theory and technique of wood processing. (Teória a technika spracovania dreva.) Zvolen: Mat centrum. Pp 102-104, ISBN 80-967315-6-4 (in Slovak).

Očkajová, A., Rončka, J., Banski, A., 2006. The influence of material density on its granularity. In: Trieskové a beztrieskové obrábanie dreva 2006. TU Zvolen. 211-215. ISBN 80-228-1674-4.

Prokeš S. 1978: Obrabeni dreva a novych hmot ze dreva. (Processing of wood and new wood materials). Praha: SNTL. 583 p.

Standfest, G., Zimmer, B., 2008. The surface hardness of thermally treated woods. In: Poster presentation at 62nd International Convention of the Forest Products. p. 22-24.

WEAR OF THE ZrC AND ZrC/Ni-ULTRADISPERSE DIAMONDS COATED EDGES KNIVES OF WOOD-CUTTING TOOL

Vadzim Chayeuski[1] – **Valery Zhylinski**[1] – **Andrey Kuleshov**[2] – **Pavel Rudak**[1] – **Štefan Barcík**[3]

Abstract

In this work, laminated chipboards milled by a tool with knives were coated with ZrC and ZrC/Ni-nanodiamond (ultradisperse diamonds (UDD) layers. ZrC- and combined ZrC/Ni-UDD-coatings were synthesized on the surface of hard alloy tungsten carbide WC – 2 wt.% Co knives by electroplating as well as combined electroplating and cathodic arc physical vapour deposition (Arc-PVD) techniques. The wear of coated knives edges was investigated. Intensive abrasive wear of tool knives occurred. The wear intensity of the knife edges with deposited coatings was reduced. Knife edges with ZrC-coating are more wear resistant than cutter edge coated with combined ZrC/Ni-UDD. The value of wear of knife edges with coatings was calculated. If compared with bare tool, the wear of ZrC-coated edges is 1.3 times less.

Key words: *cutting tool, knives, wear, coating, nanodiamonds*

INTRODUCTION

Durability and reliability of cutting tools of modern equipment in the woodworking industry is one of the main conditions for the effectiveness of its work. The level of resistance and reliability of the cutting tool is determined primarily by the characteristics of the physical and mechanical properties of the tool material. When cutting composite materials on a wood basis (laminated chipboards, laminated plastics, glass fiber, etc.), the action of the abrasive-containing particles included in their composition, having a hardness commensurate with the hardness of the tool material, leads to an increase in the friction forces on the back surface of the cutter and to more intense abrasive wear of the contact surfaces of the tool [1]. Increasing the wear resistance of surfaces using special coatings, including composite electrochemical coating (CEC), which show high physical, mechanical and electrochemical properties [2], is still one of the most effective methods to improve the functional and operational characteristics of products and parts for various purposes. The use of ultradisperse diamonds (UDD), produced by detonation of explosives, as a composite material in electrochemical and chemical metal-diamond coatings also leads to an increase in their wear resistance, significant adhesion, a sharp decrease in the coefficient of friction [3]. It was found that the combined

[1]Belarusian State Technological University, 13a, Sverdlov str., 220006, Minsk, Republic of Belarus
[2]Belarusian State University, 4, Nezavisimosti ave., 220030, Minsk, Republic of Belarus
[3]Technical University in Zvolen, T. G. Masaryka 24, 960 53 Zvolen, Slovak Republic
e-mail: chaevskiv@gmail.com, zhilinski@belstu.by, kuleshak@bsu.by, RudakPV@belstu.by,
    barcik@tuzvo.sk

ZrN-Ni-Co-coatings formed by galvanic method and the method of cathodic arc physical vapour deposition (Arc-PVD) on the blades of steel knives of the tail mills provide an increase in the resistance period of the cutting tool [4] when cutting materials from laminated chipboards and softwood.

In this regard, the aim of this work was to form by Arc-PVD and electroplating methods gradient ion-plasma and galvanic (based on UDD) coatings on the surface of blades of tungsten carbide WC of wood-cutting tool and explore the physical and mechanical properties (phase and elemental composition, wear resistance) of the cutting elements of the tool and formed layers.

MATERIALS AND METHODS

The materials used were substrate and UDD. The substrate was a hard alloy tungsten carbide WC – 2 wt.% Co knife made in Germany (Leitz company) [5]. When preparing samples, UDD nanopowders of the detonation synthesis (nanodiamonds) with a particle size 4-6 nm were used [6].

Ni-UDD composite electrochemical coatings were electroplated on the prepared surface of knives edges at direct current densities of 200–250 A/m^2 using sulphate-chloride electrolyte of nikel plating at the concentration of nanodiamonds in the electrolyte corresponding to 4.5 kg/m^3. The composition of electrolyte was following (kg/m^3): $NiSO_4 \cdot 7H_2O$ – 30; $NiCl_2 \cdot 6H_2O$ – 4; H_3BO_3 – 3. Before the deposition of Ni-nanodiamond coating the surface preparation of sample was carried by chemical degreasing at the temperature 333–353 K for 360–480 s, rinsing in hot (313–333 K) and cold (291–228 K) water, etching in solution H_2SO_4 (5–10 kg/m^3) with inhibitor at the temperature 291–298 K, cold rinsing, activation, and washing.

The ZrC-coating was deposited by the cathodic arc physical vapour deposition (Arc-PVD) method on the samples in two stages [7]. At first, the surface of specimens was treated with zirconium ions for 60 s at a negative bias of 1 kV, the cathode arc burning current of 100 A, and the vacuum in the chamber 10^{-3} Pa. This stage resulted in heating the substrate to 723–773 K prior to deposition. Then, coating was precipitated for 600 s at CH_4 pressure in the chamber was 10^{-1} Pa under a bias of -120 V.

The prepared samples were characterized through X-ray diffraction (XRD) using Cu-K$_\alpha$ characteristic of X-ray radiation. The XRD measurements were performed by the Ultima IV diffraction meter (Japan). The microstructure of the coatings and the knife edges, and the surface morphologies of the coatings were analyzed for wafer surface samples and samples fracture, using scanning electron microscopy (SEM) equipped with energy-dispersive electron probe microanalysis (EPMA) by LEO-1455VP electron microscope (Japan).

The pilot tests of coated knives edges when milling laminated chipboard were carried out with the processing center RANC-330AE, using a mill with a diameter of $21 \cdot 10^{-3}$ m with mechanical fastening of the cutting element. Laminated chipboard with a thickness of $25 \cdot 10^{-3}$ m was milled. The computer numerical control (CNC) processing center is used at the following modes: the frequency of rotation of milling cutters – 200 s^{-1}; feed rate speed – 0.07 m/s; machining allowance – $5.0 \cdot 10^{-3}$ m/pass; average chip thickness at the contact arc – $0.15 \cdot 10^{-3}$ m. Appearance of defects on the treated surface was the criteria of losing the cutting ability of the cutting element.

The volume wear of the knife edge after pilot tests was calculated by the method of determining the transverse dimensions of the knife edge along its entire length with the help of an optical microscope Microvert in 2 stages, taking into account the initial unworn blade

sharpening angle [4]. To assess the wear of the edge of knives, taking into account large areas of destruction of the edge, mathematical processing of optical images of these areas was carried out.

RESULTS AND DISCUSSION

The process of cutting with modified cutters coated knife edges in industrial conditions was accompanied by intense abrasive wear of the milling tool. At the same time on the edges of knives there were numerous different size areas of destruction of the edges in the form of the remaining after tearing the base material (including coatings) recesses, voids, chips (Fig. 1-3), as well as abrasion of the knives edges (Fig. 3).

a)

b)

c)
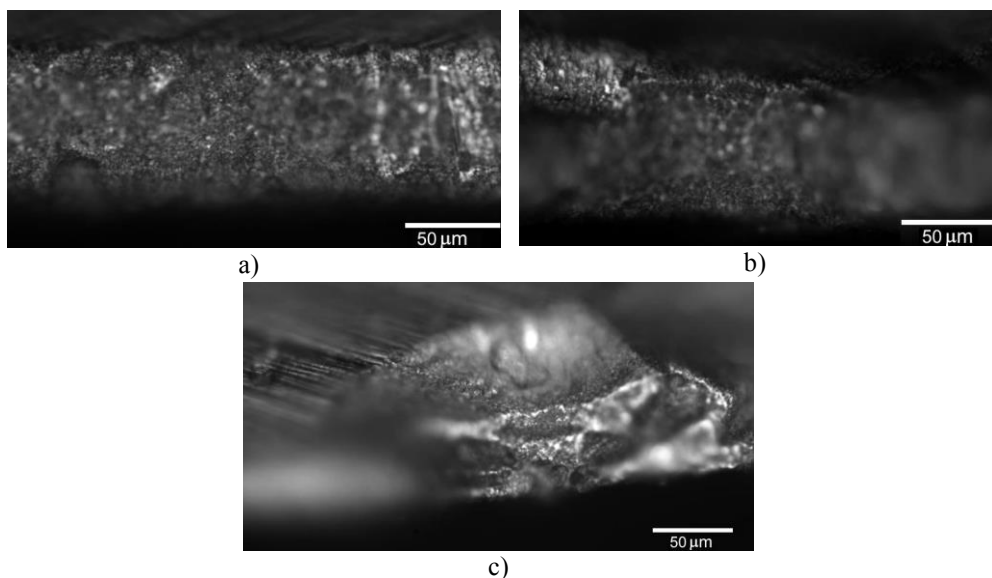
Fig. 1. Optical images of the worn edge of the uncoated knife (a, b) and a large area of destruction of the knife with ZrC-coating (c)

a)

b)
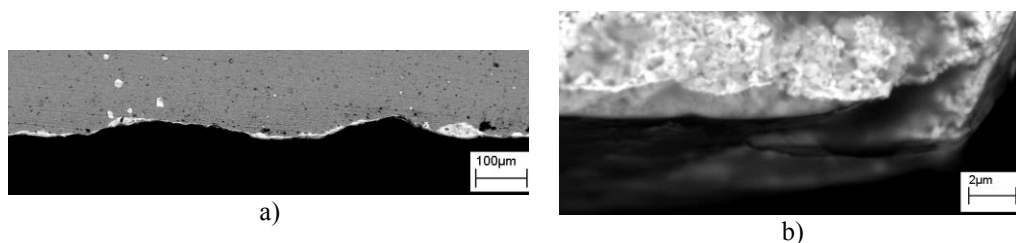
Fig. 2. SEM-images of the destroyed section of the knife edge with coating (a) and cleavage of the edge b)
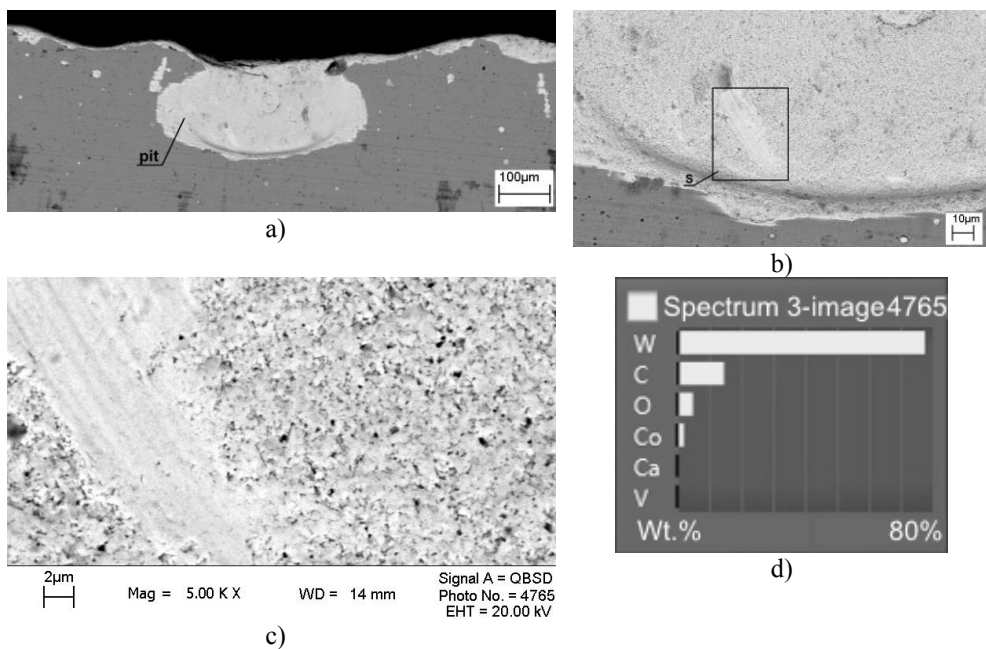
Fig. 3 SEM-images of the destroyed section of the knife edge with tearing of the coating with the base, abrasion of the coating (a) and the selected fragment of the abrasion strip of the coating (b, c) with EPMA-determination of the elements on the strip (d)

For ZrC-coating deposited on a hard alloy knife edge, a fairly clear abrasion boundary is observed at distances up to ~50 µm from the edge tip (Fig. 4).
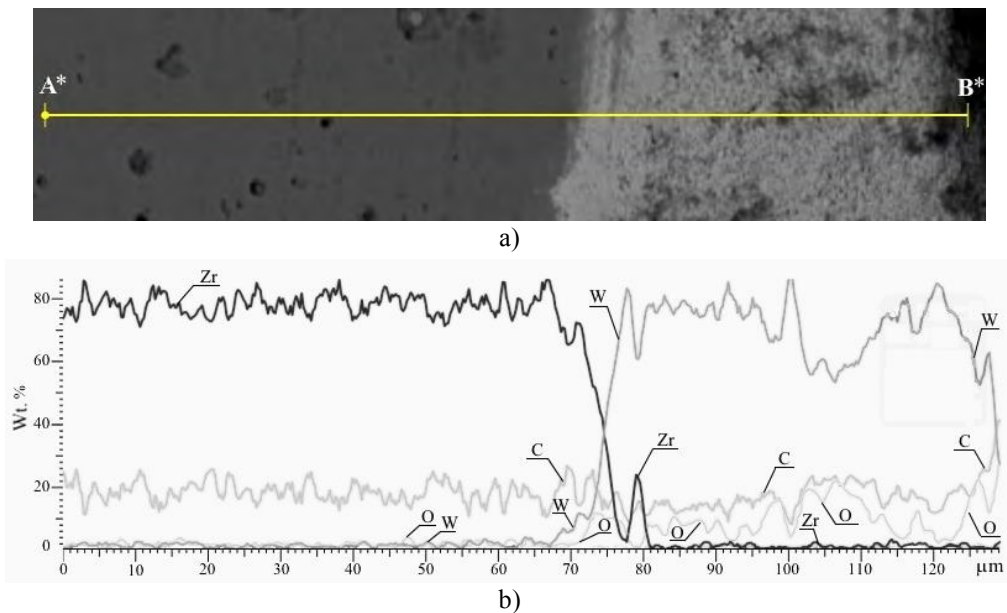
Fig. 4. SEM-image of the worn section of the knife edge with ZrC-coating (a) and the distribution of the concentration of elements along the A*B* line (b)

ZrC/Ni-UDD-coatings are characterized by a transition area of abrasion (up to ~100 µm), associated with the presence of a transition Ni-UDD-layer (Fig. 5).

a)

b)

c)

d)
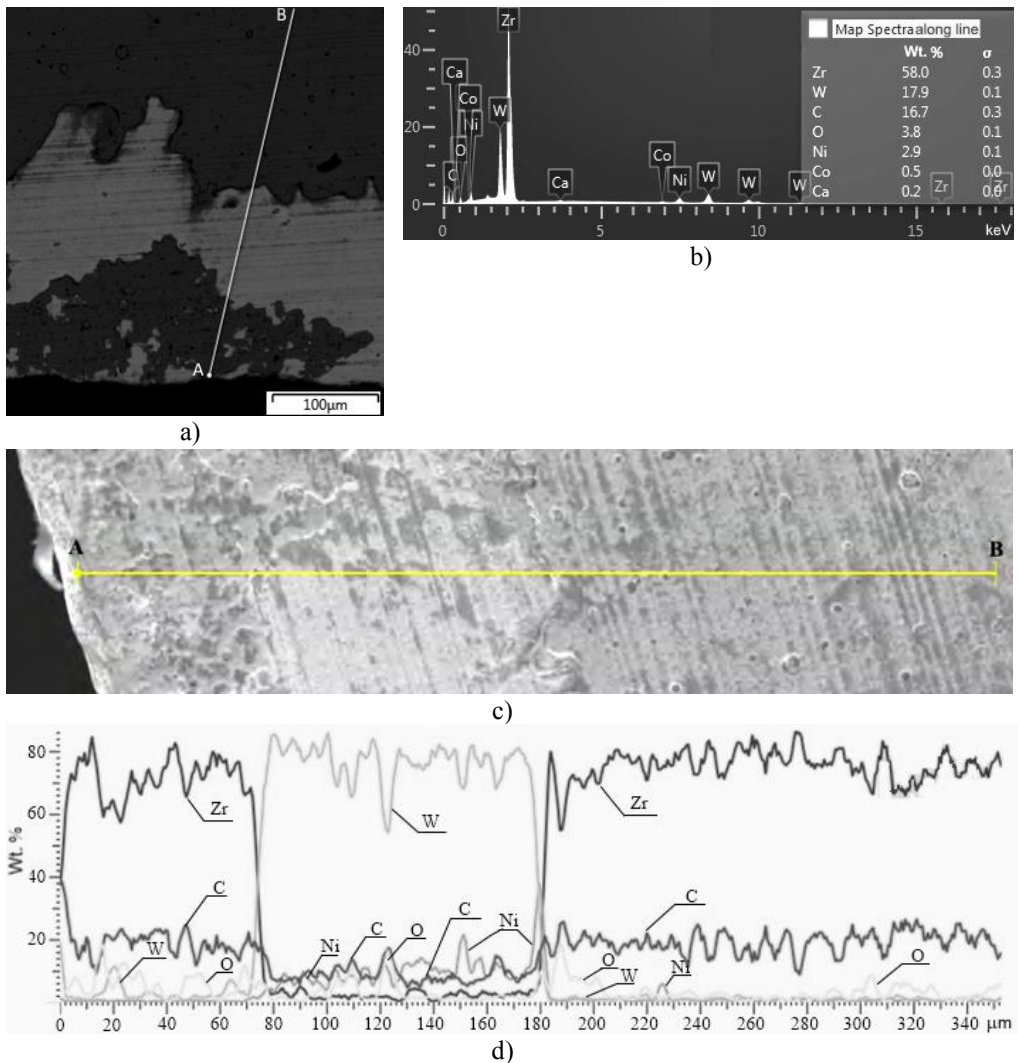
Fig. 5 SEM-images of the morphology of the worn section of the knife edge with ZrC/Ni-UDD-coating (a, c), the total spectrum (b) and the distribution of the concentration of elements along the line AB (d)

The calculated estimates of the volume wear of the knife edges after pilot tests of modified cutters (Table) indicate that the volume wear of the knife edges with ZrC-coating is reduced by more than 1.3 times compared to the bare edge knife. The volume wear of the knife edges with ZrC/Ni-UDD-coating is slightly reduced compared to the untreated tool. Optical images of the worn edge of the knife with ZrC- and ZrC/Ni-UDD-coatings confirm the calculations of volume wear and show that the degree of wear of the knife edges with ZrC-coating is less than in the case of the knife with ZrC/Ni-UDD-coating.

Table. Volume wear of knife edges modified by coatings after pilot tests of cutting laminated boards

Machining type	Volume wear, 10^7, $[\mu m^3]$
Bare edge knife	129.9 ± 0.9
ZrC-coating	93.6 ± 0.6
ZrC/Ni-UDD-coating	115.2 ± 0.8

CONCLUSION

We have selected the deposition modes and obtained Ni-UDD-CEC and combined ZrC/Ni-UDD-coatings on the knife edges of the hard alloy wood-cutting milling tool. It is shown that during the cutting of laminated chipboards in the pilot tests, untreated knife edges and knife edges with coatings experience intense abrasive wear. The wear of the knife edges with a ZrC-coating reduced in 1.3 times in comparison with untreated tool.

REFERENCES

1. Abrazumov V.V., Kotenko V.D., The analusis of the phenomena on contact surfaces of a cutting at cutting board wood composite materials, *Vestnik Moskovskogo gosudarstvennogo universiteta lesa*, *Forestry Bulletin*, 2006, no 6, pp. 138-141, in Russian.
2. Kubrak P.B., Drozdovich V.B., Zharski I.M., Chaevskiy V.V., Electrodeposition of Composite Coatings Containing Carbon-based Nanomaterials and Properties of Coatings Obtained, *Electroplating and Surf. Treat.,* 2012, v. XX, no2, pp. 43-49, in Russian.
3. Burkat G.K., Dolmatov V.Yu., Application of ultrafine-dispersed diamonds in electroplating, *Phys. Solid State,* 2004, v. 46, no 4, pp. 703-710.
4. Chayeuski V., Zhylinskiy V., Grishkevich A., Rudak P., Barcik Š., Influence of high energy treatment on wear of edges knives of wood-cutting tool. *MM Science Journal*, 2016, no. 6, pp. 1519-1523.
5. LEKSIKON Leitts: catalog firmy Leitz (LEKSIKON Leitz: Leitz Co. Catalog), on CD-ROM, Moscow, *Leitts Instrumenty*, 2011, in Russian.
6. Kononov A.G., Sachivko Ya.S., Korzhenevskiy A.P., Shtemplyuk R.G., Thermal stability of chromium coatings modified with nano-sized oxygen-containing additives, *Mechanics of Machines, Mechanisms and Materials*, 2015, no 4, pp. 353-357.
7. Kuleshov A.K., Uglov V.V., Rusalsky D.P., Grishkevich A.A., Chaevski V.V., and Haranin V.N., Effect of ZrN and Mo–N Coatings and Sulfacyanization on Wear of Wood-Cutting Knives, *J. Frict. Wear*, 2014, v. 35, no 3, pp. 201-209.

STUDY ON THE INFLUENCE OF SOME FACTORS ON THE SOUND ABSORPTION CHARACTERISTICS OF WOOD FROM SCOTS PINE

Yonka Ivanova[1, 2] – Pavlin Vitchev[3] – Desislava Hristodorova[3]

Abstract

The aim of the current study was to trace the variations in the frequency-dependent sound absorption coefficient of flooring and wall lining material, made out of Scots pine (Pinus Sylvestris L.) wood, depending on the thickness of the material and the type of the protective coating. The sound absorption has been assessed at the frequency range from 250 Hz to 2 kHz, on details with the following thickness: 20, 30 and 40 mm, and three different surface coatings: water-soluble lacquer (acrylic lacquer), polyurethane lacquer (two components) and hard wax oil for wood. The results obtained would be useful to determine the total equivalent sound absorption area of a room in order to provide the necessary acoustic characteristics. The tests were carried out using an impedance tube, according to the requirements of EN ISO 10534.

Key words: *sound absorption, Scots pine, equivalent sound absorption area, reverberation time.*

INTRODUCTION

Wood is a basic building material used for light frame constructions, beams, columns, etc. Further more solid wood materials and wood-based composites are considered as acoustic materials because of their ability to reduce the noise level and to absorb the sound.

It is well-known that the acoustic parameters of the wooden materials depend on different characteristics, like thickness, density, porosity, airflow resistance, as well as on their situation in the room (Seddeq, 2009; Arenas et al, 2010).

Many studies have been focused on the investigation of the acoustic behavior of wood and wood based bio-materials, aiming to ensure the necessary acoustic requirements along with resolving the problem of sound pollution (Wassilieff, 1996; Martellottaa et al., 2011; Smardzewski et al., 2013; Smardzewski et al., 2015; Amel et al., 2016; Negro et al., 2016; Daeipour et al, 2017). One of the main applications of wood is as an acoustic insulator in floors, ceilings and walls. Another important application is for sound absorbing materials. It is known that wooden-plated panels in front of an air cushion are used for absorbing low frequencies as well as wooden linings lead to a bright sound because of low frequency

[1]Sofia University, Faculty of Physics, 5 James Boucher Blvd., Sofia, Bulgaria
[2]Institute of Mechanics, Bulgarian Academy of Science, bl. 4 Acad. G. Bonchev Str., Sofia, Bulgaria
e-mail: yonka@imbm.bas.bg
[3]University of Forestry, 10 Kliment Ohridski Blvd., Sofia, Bulgaria
e-mail: p_vitchev@ltu.bg; dhristodorova@yahoo.com

absorption (Bucur, 2006). Sound absorption and sound reflection efficiency are related to the type of wooden materials, the internal structure and properties (anisotropy, density, mechanical and elastic properties) as well as to surface treatments.

The aim of the present study was to investigate the changes in the sound absorption coefficient of flooring and wall lining material, made out of Scots pine (*Pinus Sylvestris* L.) wood in dependence of thickness and surface coatings.

The experiments are carried in laboratory conditions in a Kundt's tube.

MATERIALS AND METHODS

The materials used for the research are Scots pine (*Pinus Sylvestris* L.) wood samples with the following characteristics: density $\rho = 490$ kg.m^{-3}, moisture content $W = 12$ % and modulus of elasticity $E_{L(12\%)} = 10520.10^6$ N.m^{-2}. The characteristics of the used material have been determined in accordance with the following standards: BDS ISO 3131, BDS ISO 3130 and EN 310.

The methodology of the experiments included the following steps: (i) assessment of the influence of the thickness of the tested material on its sound absorption properties and (ii) assessment of the sound absorption properties of the tested material depending on the type of the surface coating material.

For the implementation of our first task – evaluation of the influence of the thickness of the tested material, nine specimens with a diameter of $d = 90$ mm and three different thicknesses (T): $T_1 = 20$ mm, $T_2 = 30$ mm and $T_3 = 40$ mm have been used. The data are presented in Table 1. All specimens are cut in the longitudinal direction of the tree. The used specimens with their coding are shown in Figure 1.

Table 1. Characteristics and coding of the specimens used for the evaluation of the influence of the thickness of the tested material on the sound absorption

Number	Thickness (T), mm	Code	Number	Thickness (T), mm	Code
1	$T_1 = 20$	1.20.1	6	$T_2 = 30$	1.30.3
2	$T_1 = 20$	1.20.2	7	$T_3 = 40$	1.40.1
3	$T_1 = 20$	1.20.3	8	$T_3 = 40$	1.40.2
4	$T_2 = 30$	1.30.1	9	$T_3 = 40$	1.40.3
5	$T_2 = 30$	1.30.2			

Figure 1. The tested specimens with different thickness

For our second task – evaluation of the influence of the coating material on the sound absorption coefficient, 12 specimens with diameter of d = 90 mm and thickness T = 30 mm have been prepared (Figure 2).

The samples have been divided into 4 groups: 1 – without coating; 2 – with hard wax oil (Levis, UK); 3 – with polyurethane lacquer (Orgachim, Bulgaria); 3 – with water soluble lacquer (Renner, Italy). The characteristics and coding of the test specimens are presented in Table 2.

Table 2. Characteristics and coding of the specimens used for the evaluation of the influence of the coating material on the sound absorption coefficient

No	Coating type	Code	No	Coating type	Code
1	Natural (no coating)	2.1	7	Polyurethane lacquer	4.1.PL
2	Natural (no coating)	2.2	8	Polyurethane lacquer	4.2.PL
3	Natural (no coating)	2.3	9	Polyurethane lacquer	4.3.PL
4	Hard wax oil	3.1.O	10	Water soluble lacquer	5.1.WSL
5	Hard wax oil	3.2.O	11	Water soluble lacquer	5.2.WSL
6	Hard wax oil	3.3.O	12	Water soluble lacquer	5.3.WSL

Figure 2. Specimens with different protective coatings

Measurements of the sound absorption coefficient

The experiments for the evaluation of the sound absorption levels are carried out in a Kundt's tube, in laboratory conditions at constant temperature and pressure. The experiments have been performed in accordance with EN ISO 10534-1. The experimental design consists of impedance tube, made from Plexiglas, loudspeaker, sound generator Feel Tech FY2300 H, PC based Real Time Analyzer and Sound Level Meter System VT RTA-168, microphone ECM999 and Multi-Instrument Software. The experimental design is schematically presented in Figure 3 and described in details in the papers of Djoumaliisky, Ivanova et al., 2012 and Djoumaliisky, Ivanova et al., 2013.
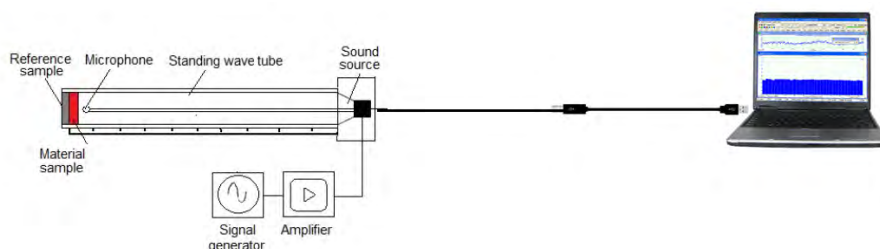
Figure 3. Scheme of the experimental equipment used for assessment
of the absorption coefficient

The loudspeaker, which is located at one end of the tube is induced by signal generator, that generates sine waves in the frequency range from 100 to 2000 Hz. The waves propagate in the tube to the other end and are reflected at the hard termination end cap made from brass material. The wood samples are placed on a rigid end cap. The phase interference between the waves in the pipe which are incident upon and reflected from the test sample results in the formation of standing waves.

The pressure amplitudes at nodes and antinodes are measured with a microphone probe attached to a car which slides along a ruler. The ratio of the pressure maximum (antinode) to the pressure minimum (node) is called the standing wave ratio SWR

$$SWR = \frac{p_{max}}{p_{min}}. \tag{1}$$

This ratio is used to determine the sample's reflection coefficient amplitude R and absorption coefficient α. Sound power reflection coefficient R_p can be expressed by

$$R_P = \left| \frac{SWR - 1}{SWR + 1} \right|^2 \tag{2}$$

The sound absorption coefficient α at a given resonance frequency is calculated by (Fahy, 2005)

$$\alpha = 1 - R_p \tag{3}$$

$$\alpha = \frac{4SWR}{(SWR + 1)^2} \tag{4}$$

Measurements in the frequency range are performed twice on each sample that is glued and hard adhered to the tube wall.

RESULTS AND DISCUSSION

Variation of sound absorption coefficient vs. frequency for different thicknesses of tested wood specimens from Scots pine

The dependence of the sound absorption coefficient on the frequency, measured for the tested specimens with different thicknesses is presented in Figure 4 (a, b, c). The specimens with the tickness of 20 mm, showed absorption in the frequency range from 1400 to 1600 Hz (Fig. 4 a), the one with the thickness of 30 mm, absorb from 1400 to 1800 Hz (Fig. 4 b) and the specimens with the thickness of 40 mm showed the highest values of the absorption coefficient in the frequency range of 1600 – 1700 Hz.
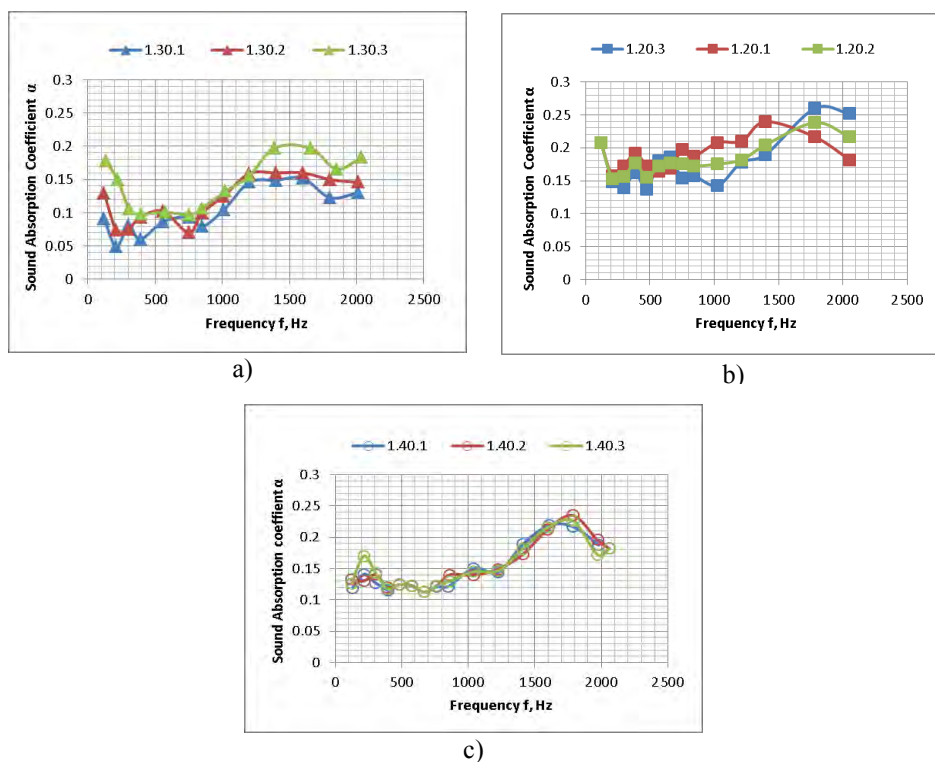
Figure 4. Sound absorption properties of wood specimens from Scots pine with different thickness – 20 mm; b) – 30 mm; c) – 40 mm

The average values of the sound absorption coefficients for the experimental groups 1.20, 1.30 and 1.40 have been compared and presented in Figure 5. It is visible that the wood samples with lower thickness have better sound absorption than the one with higher thickness. It has to be noticed that the absorption curves show amplitude peaks and variable frequency position according to the considered thicknesses.

The specimens with $T_1 = 20$ mm have two absorption peaks: the first, observed at 120 Hz has an absorption coefficient $\alpha = 0.22$; the second is observed around 1581 Hz and reaches a value of $\alpha = 0.25$ (Fig. 5). In the frequency range from 200 to 1400 Hz the averaged value of sound absorption coefficient is $\alpha = 0.177$.

The specimens with $T_2 = 30$ mm have also two peaks of absorption: the first peak is observed at 132 Hz ($\alpha = 0.13$), the second peak - at 1656 Hz with a value $\alpha = 0.17$. In frequency range from 200 to 1400 Hz the value of absorption coefficient slightly varies around $\alpha = 0.09$.

For the specimens with $T_3 = 40$ mm, the value of the absorption coefficient varies around $\alpha = 0.13$ in the frequency range of 100-1000 Hz. At this frequency range also two absorption peaks are observed: the first one is registered between 150 and 250 Hz and reached a low average value $\alpha = 0.15$ and the second – about 1800 Hz and reached a value of $\alpha = 0.23$.
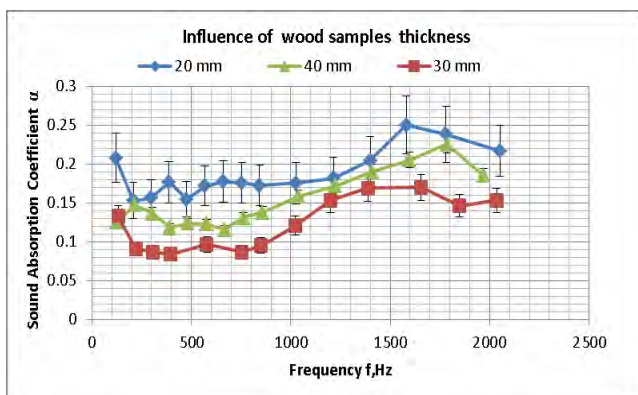
Figure 5. Comparison in the variation of the sound absorption coefficient vs frequency for wood specimens with $T = 20$, 30 and 40 mm

Assessment of the influence of the protective surface coatings on the sound absorption of wooden specimens from Scots pine

The experimental results of the influence of different surface coatings on the acoustic properties of the specimens are presented in Fig. 6, as follow: in Fig. 6a – uncoated (control) specimens; Fig. 6b – specimens with hard wax oil coating; Fig. 6c – specimens with polyurethane lacquer coating; Fig. 6d – specimens with water-soluble lacquer coating. From the results it is visible that the protective coatings decreased the dispersion of the measured sound pressures and sound absorption (Fig.6 b,c,d).
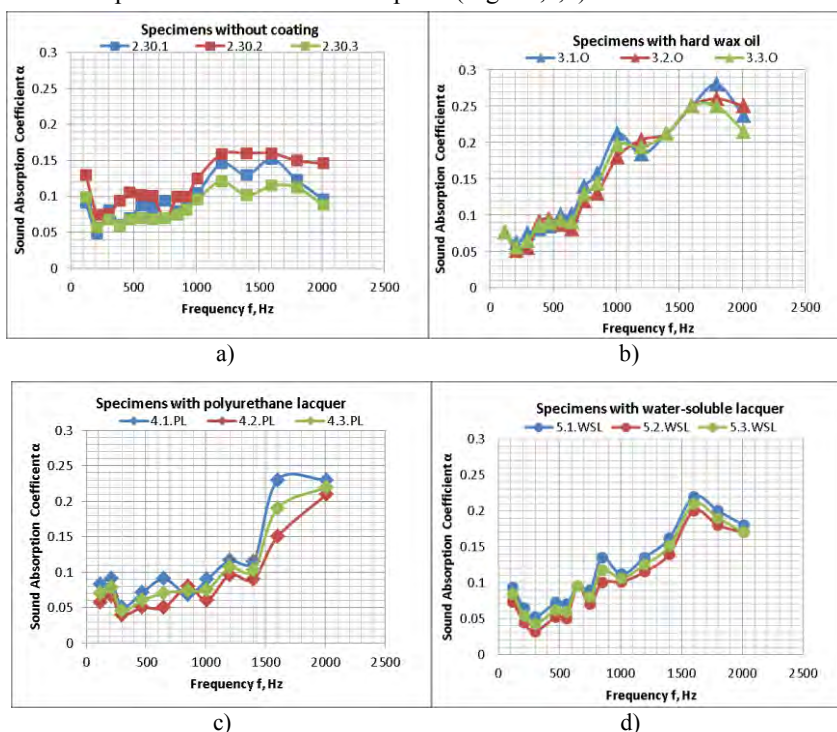
Figure 6. Changes in the sound absorption vs frequency for wood samples with and without protective coatings

The average values of the sound absorption, measured for the different groups, have been compared and the comparison is presented in Figure 7. It is visible that the specimens coating with hard wax oil showed better sound absorption properties – the maximum value is α = 0,25 at 1600 Hz, when compared to the other specimens. The sound absorption behavior of the specimens with lacquer (water-soluble and polyurethane) coatings, slightly differ at higher frequencies. It has to be noated, however, that the samples coated with water-soluble lacquer has better sound absorption in the frequency range of 500-1500 Hz, with a peak value of α = 0.22 at 1600 Hz.
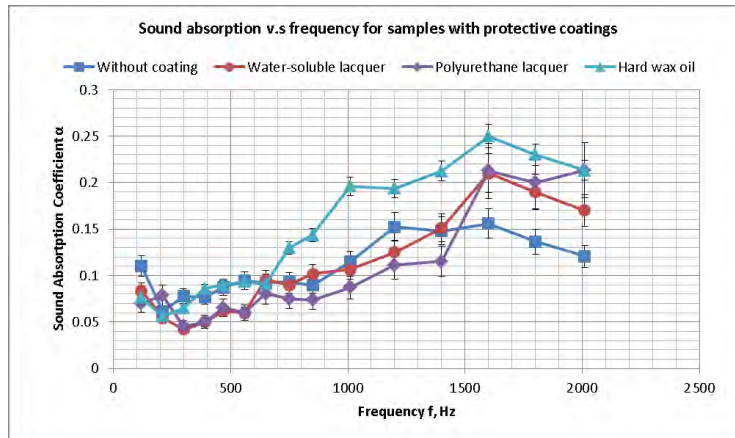
Figure 7. Comparison in the variation of the sound absorption coefficient vs frequency for wood specimens with different protective coatings

CONCLUSIONS

This paper presents results from experimental study, which investigated the influence of the thickness and the coating material on the sound absorption properties of specimens prepared from Scots pine (*Pinus Sylvestris* L.) wood, cut in longitudinal direction. The experiments were carried out in laboratory conditions with constant temperature and air pressure using the impedance tube method at a normal incidence. The moisture content of materials is constant.

Based on the results obtained under the conditions of this study, the following conclusions can be made:

• The sound absorption coefficient is influenced by the thickness of the specimens. When comparing the specimens with different thicknesses (20, 30, 40 mm), the best sound absorption properties are observed for specimens with $T = 20$ mm, for which the average value of sound absorption coefficient is α = 0.177.

• The absorption coefficient is easily influenced by the surface state and the presence of coatings. The coating reduces the dissipation of the results most probably due to the more homogeneous surface it provided. Our results show that the surface protective coatings (hard wax oil, water-soluble lacquer (acrylic lacquer), polyurethane lacquer) used in this study, improved the sound absorption properties of the tested specimens. Among the differently coated specimens, the best sound absorption properties in the frequency range of 600-2000 Hz showed those coated with hard wax oil. The peak value of the absorption coefficient is α = 0.25 at 1600 Hz. The specimens coated with water-soluble lacquer film

showed better sound absorption abilities in the frequency region of 500-1500 Hz, with a peak value of α = 0.22 at 1600 Hz, when compared to the samples coated with polyurethane lacquer.

ACKNOWLEDGEMENTS

REFERENCES

Amel L., Abdellatif Z., Daniel Q. (2016). Determination of acoustic parameters of Bio-based materials distended for building: Application case to Aleppo pine wood cork and their composites, Wood research, 61 (1): 25-34.

BDS ISO 3130 (1999): Wood – Determination of moisture content for physical and mechanical tests.

BDS ISO 3131 (1999): Wood – Determination of density for physical and mechanical tests.

BDS EN ISO 10534-1 (2006): Acoustics – Determination of sound absorption coefficient and impedance in impedances tubes – Part 1: Method using standing wave ratio.

BDS EN 310 (1999): Wood-based panels – Determination of modulus of elasticity in bending and of bending strength.

Bucur V. (2006). Acoustics of Wood, Springer-Verlag Berlin Heidelberg.

Daeipour Z., Safdari V., Nurbakhsh A. (2017). Evaluation of the Acoustic Properties of Wood-Plastic-Chalk Composites, Engineering, Technology & Applied Science Research 7(2): 1540-1545.

Djoumaliisky S., Ivanova Y., Borovanska I., Mihailov M. (2012). Multilayered sound absorbing panels based on secondary plastic materials, Proceedings of 27th International Conference on Non-Destructive Testing (NDTdays'12), 33(1): 391-394 (in Bulgarian).

Djoumaliisky S., Ivanova Y., Kotzev G. Borovanska I., Tsolov T. (2013). Multilayered sound absorbing panels based on waste materials, Proceedings of 23rd International Conference "Technomer 2013", November 14-15, Germany, P2 (1-7), ISBN: 978-3-939382-11-9.

Fahy F. (2005). Foundation of Engineering Acoustics, Elsevier Academic Press, San Diego.

Martellottaa F., Castiglione M. L. (2011). On the use of paintings and tapestries as sound absorbing materials, Conference: Forum Acustica 2011, Aalborg (DK).

Negro F., Cremonini C., Zanuttini R., Fringuellino M. (2016). Development of framed poplar plywood for acoustic improvement, Wood research, 61 (1): 121-128.

Smardzewski J., Kamisiński, T., Dziurka D., Mirski R., Majewski, A., Flach A., Pilch A. (2015). Sound absorption of wood-based materials, Holzforschung 69(4): 431-439.

Smardzewski J., Batko W., Kamisiński T., Flach A., Pilch A., Dziurka D., Mirski R., Roszyk E., Majewski A. (2013). Experimental study of wood acoustic absorption characteristics, Holzforschung 68(4):467-476.

Wassilieff C. (1996). Sound Absorption of Wood-Based Materials, Applied Acoustics, Elsevier Science, 48 (4): 339-356.

MAKING OF TENSION TESTING SAMPLES BY TURNING AND MILLING IN SINGLE PROCESS

Zbigniew Karwat – Grzegorz Koczan

Abstract

In this work the authors present the process of making and testing, using the tension test, wooden cylindrical samples. In general, samples of this type are not in accordance with norms, with the exception of old American and Australian norms. In spite of that, the making of cylindrical samples was validated by two reasons. Firstly, such samples can be made with ease and a high degree of precision using a combination of milling and turning. Secondly, cylindrical samples seemed to give greater chances for obtaining higher tensile strengths, which is desirable in the wood strength theory.

The cylindrical samples were made of beech and ash woods, and their tests were compared with analogous samples with a rectangular section. The results obtained for the cylindrical samples turned out to be as good as for the normative samples.

Key words: *tension strength, cylindrical sample, beech, ash, turning, milling*

INTRODUCTION

Tensile strength tests are some of the most demanding tests wood samples are subject to [8]. It is mostly about the proper alignment of grains in raw wood and then in a prepared sample. Also the shape of the samples is more complex than in case of compression, bending and even shearing strength tests. Thus, such samples are a challenge in terms of their preparation. The most often used method is planing (or milling), carried out in a few stages in order to avoid chipping.

Tensile strength test of wood is characterised by a high coefficient of variation [2, 3]. This is probably why the enormous American wood strength database [5] does not provide this important parameter. Tensile strength and compression strength should determine bending strength. In reality, this implication is not as trivial and it is the subject of research one of the authors of this article. Performed research suggest that tensile strength may be slightly lowered. Thus we decided to test cylindrical samples. The motivation behind this decision came from the fact that a sample with circular section minimises the lateral area at a determined cross-section and height of a sample. Small lateral area reduces the probability of surface defects. Also, a cylindrical sample does not have any sharp edges prone to be damaged. A counterargument is the anatomic structure of mature wood at the macro and microscopic level. Due to annual growth rings, beams and the geometry of the cell walls, paradoxically, wood structure inscribes much better into a rectangular shape. The above issues can only be resolved in the process of experiments.

Faculty of Wood Technology, Warsaw University of Life Sciences - SGGW
e-mail: ztakarwat@gmail.com

At the end of the article is a list of XI norms concerning determining tensile strength of wood along the fibres. All current norms for small laboratory samples and large samples of sawn wood concern rectangular section. In the representative norm [VIII] the base of the sample for tensile strength is 4 x 20 x 90 mm [4]. Very similar samples with base dimensions of 4 x 18 x 90 mm are in the still popular, although abandoned, Polish norm [IX]. Similarly different samples ([VIII] versus [IX]) were tested, in a largely simplified manner, in work [7]. It is also worth to mention the British norm [III] which describes a very thin, 3 x 6 x 50 mm sample base. While the wood tensile strength test at microscopic level is presented in work [10].

The attached list of norms has two old norms of turning cylindrical samples. The American norm [VII] used wooden rods with 1" diameter and 48" length which at their ends were glued into thicker drilled boards at a length of 6" [9]. While the Australian norm from New Wales [XI] was based on a sample fully turning, with the base thickness of 1.25" and length of 10" (Fig. 1).
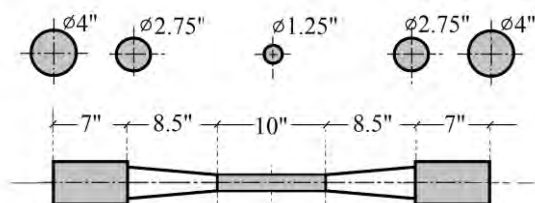
Fig. 1. Design of old tension test used in New South Wales (Australia) [9]

The testing of tensile strength of large construction elements is determined by norms [II, V, X]. Some details for the American norm are described in work [2], while in work [1] sawn exotic wood samples were tested for their tensile strength. The remaining norms [I, IV, VI] concern the testing of small laboratory samples.

MATERIAL AND METHODS

In order to prepare samples, two species of wood - beech[1] and ash (sap-wood and heart-wood) - were used.   Two types of samples were made: with round section (Fig. 2) and reference samples with rectangular section.
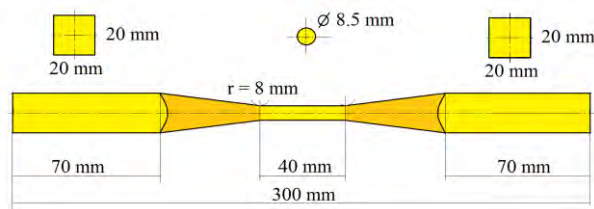
Fig. 2. Dimensions and shapes of the cylindrical samples

The cylindrical samples were made using a precision lathe with installed electrospindle instead of a cutter holder. The lathe was adjusted so that it allowed

---

[1] On the basis of work [6], we can compare tension and compression for beech.

 to precisely make samples using a template. Removing the cross-feed bolt allowed us to obtain an indenting feed of the cutting tool controlled manually with an installed feed control lever.   Material holders (with square section) were seated in a round grip of the lathe's spindle and tail centre.

The process of making samples with cylindrical bases started with placing a 300 x 20 x 20 mm wooden beam in the grips. The material rotated by the spindle was also milled with a cylindrical milling cutter installed in the electrospindle grip. Triple feed of the sample in the milled section with simultaneous in-feed limited by the template allowed us to ideally copy the shape of template.

The use of special grips (Fig. 3) allowed us to stiffen the machined material while retaining the axial alignment. Thanks to this the machined material was under only a slight axial pressure, unlike in case of traditional clamping between the clamp and the tail centre. This type of clamping reduces the risk of the material bucking. It is particularly important in case of samples with small diameter necking (8–9 mm).

The parameters of turning and milling were tested experimentally and the maximum possible speed were used: lathe spindle – 1750, milling electrospindle – 25000 (Fig. 4). The diameter of double-bladed milling cutter was 16 mm and that of the mandrel was 8 mm. The milling cutter length was 20 mm.

Fig. 3. Sample clamping in the grips and in the bushing and the tail centre

Fig. 4. Clamping of the sample in the lathe and the kinematics of the process

Comparative samples with rectangular sections were made using a bottom-milling machine in accordance with the norms described in the introduction.

RESULTS AND DISCUSSION

Parameters of the beech samples for tensile strength test are in table 1 and the strength values are presented in graph (Fig. 5). Of the three sets of rectangular samples, only the third set (20 x 4 mm) was made of twin pieces of wood in relation to the cylindrical samples (Ø 8.5 mm).

Table 1. Values of tension strength of beech wood for rectangular and cylindrical samples

Properties of samples	Rectangular	Rectangular	Rectangular	Cylindrical
Dimension of cross section [mm]	18 x 4	10 x 4	20 x 4	Ø 8.5
Density [kg/m^3]	732	694	694	694
Moisture content	9.3%	6.5%	7.6%	7.1%
Mean tension strength [MPa]	163.8	154.2	140.0	143.1
Standard deviation [MPa]	19.8	30.6	20.8	21.3
Standard error [MPa]	3.8	11.6	7.4	6.4
Minimum value [MPa]	106	135	124	131
Maximum value [MPa]	189	222	176	175
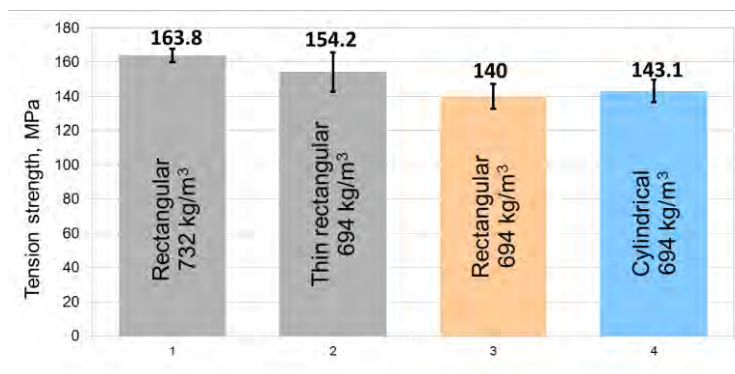
Fig. 5. Mean values of tension strength (with standard errors)
of beech wood for rectangular and cylindrical samples

Table 2. Values of tension strength of ash for sap-wood and heart-wood

Properties of samples	Rectangular	Cylindrical
Dimension of cross section [mm]	10 x 4	Ø 8,5
Density [kg/m^3]	627	742
Moisture content	6.0%	7.5%
Mean tension strength [MPa]	148.5	173.0
Standard deviaton [MPa]	27.9	17.1
Standard Error [MPa]	11.4	5.4
Minimum value [MPa]	134.0	148.4
Maximum value [MPa]	180.7	201.6

Testing of the ash samples proved to be more of a comparison of sap-wood and heart-wood rather than of rectangular and cylindrical samples (table 2, Fig. 6). The result meeting the expectations for such a comparison indirectly shows that the cylindrical samples do not fall behind in strength from the rectangular samples.
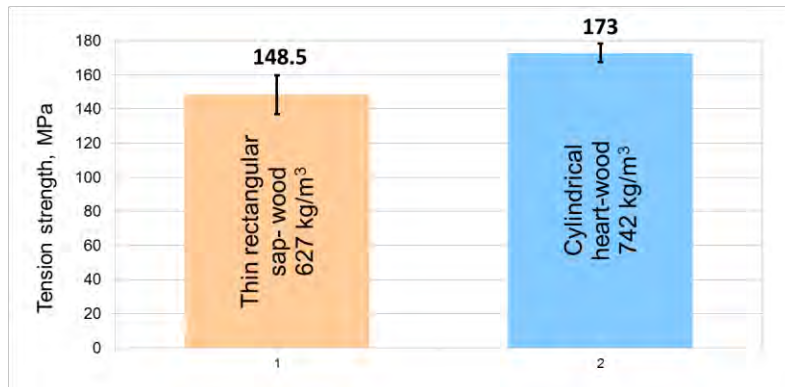
Fig. 6. Mean values of tension strength (with standard errors)
of ash for sap-wood and heart-wood (rectangular and cylindrical samples)

CONCLUSION

The use of turning and milling in a single process and using of stiff clamping of the processed material allowed to obtain precise and repeatable samples with circular section. The results for tensile strength tests for those samples did not differ much from the tests of the samples with rectangular section.

Simultaneous turning and milling allows to simplify the sample making process and allows for a greater tolerance in the material flaws. This manner of material processing allows to prepare a miniaturised versions of cylindrical samples on the basis of the old norms.

REFERENCES

[1] **Ahmad Z., Bon Y. C., Abd Wahab E.S.** [2010]: Tensile strength properties of tropical hardwoods in structural size testing. International Journal of Basic & Applied Sciences IJBAS-IJENS Vol: 10 No: 03: 1-6

[2] **Bohannan B.** [1965]: Exploratory development of tension test method for structural-size lumber. U.S. Forest Service Research Paper, FPL 40

[3] **Cown D. J., Walford B., Kimberley M. O.** [1996]: Cross-grain effect on tensile strength and bending stiffness of *pinus radiata* structural lumber. New Zealand Journal of Forestry Science 25(2): 256-62

[4] **Gašparík M., Gaff M., Babiak M.** [2017]: Tension stress simulations of layered wood using a finite element method. Wood Research 62 (4): 517-528

[5] **Green D. W., Winandy J. E., Kretschmann D. E.** [1999, (2010)]: Wood handbook – wood as engineering material. Chapter 4 (5): Mechanical properties of wood. USDA Gen. Tech. Report 113 (190), FPL, Madison

[6] **Koczan G., Kozakiewicz P. [2016]:** Comparative analysis of compression and buckling of European beech wood (*Fagus sylvatica* L.). Annals of Warsaw University of Life Sciences, Forestry and Wood Technology, No 95, pp. 81-90

[7] **Kohan N., Via B.K., Taylor S.** [2012] : A comparison of geometry effect on tensile testing of wood strands. Forest Products Journal Vol. 62, No. 3: 167-170

[8]   **Markwardt L. J., Youngquist W. G.** [1956]: Tension test methods for wood, wood-base materials, and sandwich constructions. For presentation at the Annual Meeting, American Society for Testing Materials (ASTM), Atlantic City, N. J.

[9]   **Record S. J.** [1914]: The Mechanical Properties of Wood, Including a Discussion of the Factors Affecting the Mechanical Properties and Methods of Timber Testing. Yale University

[10] **Živković V., Turkulin H.** [2014]: Microtensile testing of wood – overview of practical aspects of methodology. Drvna Industrija 65 (1) 59-70

STANDARDS

[I]   **ASTM D 143-94** [1994]: Standard test methods for small clear specimens of timber. 16: Tension parallel to grain (reapproved 2000, current 2014)

[II]   **ASTM D 198-02** [2002]: Standard test methods of static tests of lumber in structural sizes. 28-35: Tension parallel to grain (reapproved 2003, current 2015)

[III] **BS 373:1957** [1957]: Methods of testing small clear specimes of timber. 12. Tensile test. a) Tension parrallel to grain. b) Tension perpendicular to grain (confirmed-current)

[IV]   **DIN 52188** [1979]: Prüfung von Holz. Bestimmung der Zugfestigkeit parallel zur Faser (Testing of wood. Determination of ultimate tensile stress parallel to grain) (current)

[V]   **EN 408:2010** [2010]: Timber structures – Structural timber and glued laminated timber – Determination of some physical and mechanical properties. 13: Determination of tension strength parallel to grain (annexed +A1:2012 - current)

[VI]   **GOST (ГОСТ) 16483.23** [1973]: Древесина. Метод определения предела прочности при растяжении вдоль волокон (Wood. Method for determining tension strength along fibers)

[VII] **Hatt W. K.** [1906]: Instructions to engineers of timber tests (About old cylindrical tension test used in United States), p. 55, Revised edition 1909 p. 56

[VIII] **ISO 13061** [2014]: Physical and mechanical properties of wood. Test methods for small clear wood specimens. 6: Determination of ultimate tensile stress parallel to grain (current)

[IX]   **PN-D-04107** [1981]: Drewno. Oznaczenie wytrzymałości na rozciąganie wzdłuż włókien (Wood. Determination of ultimate strength in tension parallel to grain) (withdrawn 2011)

[X]   **PN- EN 408:2004** [2004]: Konstrukcje drewniane. Drewno konstrukcyjne lite i klejone warstwowo. Oznaczenie niektórych właściwości fizycznych i mechanicznych. 15: Oznaczenie wytrzymałości na rozciąganie wzdłuż włókien (replaced by English 2010, see title of EN-408)

[XI]   **Warren W. H.** [1911]: The strength, elasticity, and other properties of New South Wales hardwood timbers (About old cylindrical tension test used by the Department of Forestry of New South Wales), pp. 58-62

INFLUENCE OF THE THICKNESS OF REMOVED LAYER ON THE QUALITY OF CREATED SURFACE WHEN MILLING OAK BLANKS ON THE CNC MACHINING CENTER

Richard Kminiak – Mikuláš Siklienka – Ján Šustek

Abstract

The article deals with the quality of oak blanks machined on the CNC machining center. It focuses on the effect of the thickness of removed layer on the quality of created surface, namely its indicator arithmetical mean deviation of the roughness profile Ra. The paper presents results of operating experiment, in which the edges of the oak blanks of thickness h = 25 mm were milling with end mill of diameter D = 16 mm fitted with a replaceable T10MG carbide blade. The experiment was performed on a 5 axis CNC machining center at tool speeds n = 20,000 rpm, feed speed v_f = 1 ÷ 5 m.min^{-1} and thickness of removed layer e = 1, 3 and 5 mm.

The article states that, the arithmetical mean deviation of the roughness profile was in the range of Ra = 5.6 ÷ 7.1 µm. The analysis of the results points to the fact that, the impact of the thickness of removed layer and feed speed on the surface roughness was not demonstrated. As an explanation of the phenomenon, the article provides a comparison the thickness of the chips in the layer corresponding to the new surface depending on the technical and technological parameters of the process.

Key words: *CNC machining center, end mill with a replaceable carbide blade, quality of created surface, thickness of removed layer, feed speed, thickness of the chips.*

INTRODUCTION

The workpiece accuracy and the quality of a created surface can be regarded as an objective indicator of the quality of the created product. The workpiece accuracy presents the degree of approaching of the geometric values of the workpiece to the values set in the drawing, as the shape and dimensional accuracy is considered (*Kminiak, Banski and Chakho, 2017*).

An adequate accuracy is solved by CNC machining centers by the machine itself, therefore the quality of the worked out surface seems to be more important issue. The surface quality can be exactly defined by surface roughness parameters (*Siklienka et al. 2017*).

The surface shows some surface roughness during milling as well, such as microscopic changes (roughness) or macroscopic changes (waviness, grooves, elevations, partially drawn fibers). The occurrence of these changes (except waviness) on the workpiece surface is irregular (*Korkut, Diziroglu and Aytin, 2013*). The waviness consists of almost regular

Technical University in Zvolen, T. G. Masaryka 24, 960 53 Zvolen

e-mail: richard. kminiak@tuzvo.sk

repetitive elevations and depressions of approximately the same shape and size (*Gündüz, Korkut and Korkut, 2008, Novák, Rousek and Kopecký, 2011*).

Roughness and waviness are, in fact, very small deviations from the desired shape, but they significantly affect the further processing of the workpiece, in particular its surface treatment (*Aydin and Colakoglu, 2005, Očkajová et al. 2016*).

Roughness and waviness depend on the kinematic conditions of cutting and are mainly influenced by the following factors:

- The way of separating chips, which depends not only on the method of machining, but also on the accuracy of a tool and its geometry.
- Cutting conditions (cutting speed, feed speed, thickness of the removed layer, etc.).
- Microgeometry (dulling the cutting edge of the tool).
- Physical and mechanical characteristics of machined material (its density, hardness and structure) (*Karagoz, Akyildiz and Isleyen, 2011*).

This article aims to analyze the influence of the thickness of removed layer and the feed speed on the quality of created surface when milling the oak blanks.

MATERIAL AND METHODS

Experimental samples:

In the experiment were used European oak (Quercus robur) blanks of dimensions h = 25 x w = 55 x l = 500 mm and the moisture WP 8 ± 1%.

Experimental machine:

Blanks were milled on 5 axes CNC machining center SCM Tech Z5 (*Fig. 1*) supplied by SCM–group, Rimini, Italy. Basic technical and technological parameters provided by the manufacturer are presented in *Tab. 1*.

Experimental tool:

In the experiment was used end mill KARNED 4451 of diameter D = 16 mm fitted with a replaceable T10MG carbide blade from the manufacturer Karned Tools Ltd., Prague, Czech Republic (*Fig. 2*). Basic technical and technological parameters provided by the manufacturer are presented in *Tab. 2*.

Fig. 1. CNC machining center SCM Tech Z5 (*SCM Group, 2017*).

Tab. 1. Technical and technological parameters of CNC machining center SCM Tech Z5 (*SCM Group, 2017*).

Technical parameters of CNC machining center SCM Tech Z5	
Useful desktop	x= 3,050 mm , y = 1,300 mm, z =300 mm
Speed X axis	0 ÷ 70 m.min^{-1}
Speed Y axis	0 ÷ 40 m.min^{-1}
Speed Z axis	0 ÷ 15 m.min^{-1}
Vector rate	0 ÷ 83 m.min^{-1}
Parameters of the main spindle	
electric spindle with HSK F63 connection	
Rotation axis C	640°
Rotation axis B	320°
Revolutions	600 ÷ 24,000 ot.min^{-1}
Power	11 kW 24,000 ot.min^{-1}
	7,5kW 10,000 ot.min^{-1}
Maximum tool diameter	D = 160 mm
	L = 180 mm

Fig. 2. End mill KARNED 4451 fitted with one replaceable carbide blade (D – cutting diameter, L – cutting length, d - diameter of the chucking shank)

Tab. 2. Technical and technological parameters of end mill KARNED 4451 fitted with one replaceable carbide blade (Karned Tools Ltd, 2017)

Miller	Working diameter D [mm]	Working length l [mm]	Diameter of the chucking shank d [mm]	Dimensions of used razor blades L x š x h [mm]	Blades material	
KARNED 4451	16	49,5	12	49.5 x 9 x 1.5	T10MG	
Classes of TIGRA	ISO CODE	US CODE	Binder%	Hardness		Bending strength
				HV10	HRA±0.2	N/mm^2	psi
T10MG	K10–K40	C3+	10.0	1,65	92.3	3,6	522.000

Milling process:

A milling cutter was fitted into the hydraulic clamp SOBO. 302680291 GM 300 HSK 63F from Gühring KG, Albstadt, Germany. Oak blanks were placed in a CNC machining center so that the longer side was in the X-axis and the shorter side was in the Y-axis. Oak blanks were clamped during the milling by mechanical clampers VCMC-S4 145x145x50 12-80 from J. Schmalz GmbH, Glatten, Germany. The milling process was carried out at constant operation speed of cutter $n = 20{,}000$ min^{-1} and changing thickness of the removed layer $e = 1/3/5$ mm and changing feeding speed from $v_f = 1$ m.min^{-1} to $v_f = 5$ m.min^{-1} (representing a maximum feeding speed recommended by the manufacturer of the tools).

Determination of surface roughness:

The surface roughness of the samples was measured with a laser profilometer LPM-4 (*Fig.3*) by the manufacturer Kvant Ltd, Bratislava, Slovak Republic. The profilometer uses a triangulation principle of laser profilometry. The image of the laser line is scanned at an angle by digital camera. Afterwards, an object profile in cross-section is evaluated from scanned image. Obtained data are mathematically filtered and there are set individual indicators of the primary profile, profile of waviness and profile of roughness (*Kminiak and Gaff, 2015*).

There was used a methodology by *Siklenka and Adamcova (2012)* for measuring of the surface roughness that fulfills the standard EN ISO 4287. Within each sample, there were realized measurements in three tracks, located in the middle of the sample, evenly located across the width of the sample (5/12.5/20 mm from the sample edge), track length was 60 mm and the track was oriented in the direction of displacement of the spindle in a milling process. Surface roughness was evaluated by using parameter of arithmetic mean deviation of roughness profile Ra.
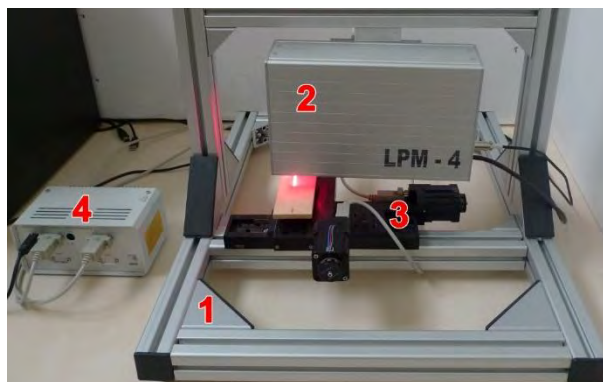
Fig. 3. Laser Profilometer LPM - 4 (1 - supporting structure allowing manual setting of working distance and fitting of profilometric head and trolley system, 2 - profilometric head, 3 - feed system of the XZ axis, 4 - control system of working desk shifts) (*Kminiak and Gaff 2015*)

RESULTS AND DISCUSSION

The roughness of the formed surface was monitored by arithmetical mean deviation of the roughness profile Ra. The obtained data were subjected to statistical analysis for the

purpose to confirm or refute general assumptions about dependence of surface roughness on the parameters of the chopped layer under specific machining conditions on the CNC machining center. Among the arguments the validity of which we had in order to verify in the given conditions are:

- increasing the feed speed decrease the quality of the created surface,
- increasing the thickness of removal layer decrease the quality of the created surface.

Specific machining conditions on a CNC machining center result mainly from the tool diameter. Most of basic research in this area is based on the experiments performed on the vertical single spindle miller with a tool diameter $D = 100 \div 120$ mm. We use tools of a much smaller diameter in the CNC machining center, for example $D = 10 \div 30$ mm. The different tool diameter causes a different direction of the cutting forces in the cutting area, which should be reflected in the topography of the surface, especially at the roughness level.

The statistical evaluation of the data (*Tab. 3*) has shown that the feeding speed or thickness of removal layer not have a statistically significant effect on the quality of the created surface.

Tab.3. Multifactor analysis of the impact of the thickness of removal layer and the feed speed on the arithmetical mean deviation of the roughness profile.

	SS	Degr. of Freedom	MS	F	p
Intercept	10573,15	1	10573,15	4731,331	0,000000
thickness of removal layer	1,47	2	0,74	0,329	0,719803
feed speed	18,46	4	4,62	2,065	0,085805
thickness of removal layer*feed speed]	28,17	8	3,52	1,576	0,132360
Error	569,85	255	2,23		

Graphic representation of dependence of the arithmetical mean deviation of the roughness profile on the thickness of removal layer and the feed speed is shown in the graph in *Fig.4*.
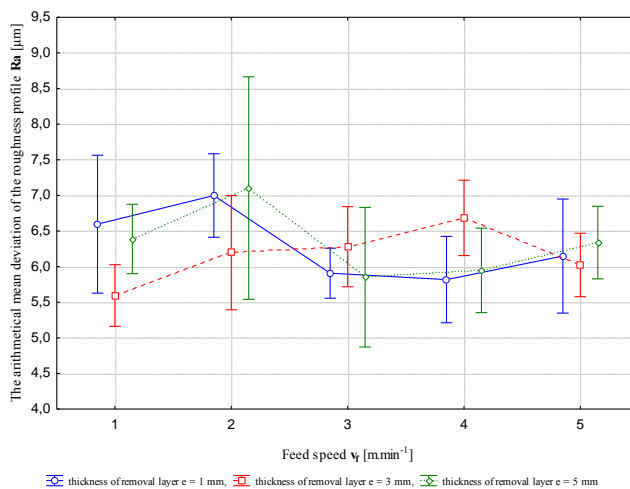
Fig.4. Influence of feed speed and thickness of removal layer on the arithmetical mean deviation of the roughness profile.

In graphical expression cannot be observed a significant trend that would confirm the dependence of roughness on the monitored parameters.

The arguments which we are trying to confirm, have their basis in the assumption that, the increasing nominal thickness of the chips causes the change in the force ratios at the place of separation of the chips and consequently deterioration of roughness as a result of microcracks.

Why this is not in our case, it can be justified as follows. Although the thickness of removal layer is increasing 1/3/5 mm, but the height of the layer in which the final surface is formed remains relatively small. The height of the layer in which the final surface is formed can be identified with the maximum heights of the primary profile. Although the thickness of removal layer increase, the average value of the maximum height of the waviness profile changes only slightly and its values are in the range of $0.21 \div 0.36$ mm (*Fig.5*).
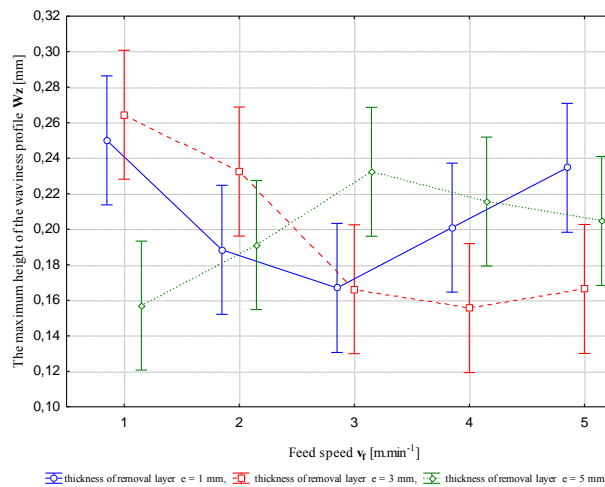
Fig.5. Influence of feed speed and thickness of removal layer on the maximum height of the waviness profile

Subsequently, the maximal chip thickness within the height of forming a final surface is in e range of 0.0084 to 0.047 mm. *Fig. 6* provides a comparison of the maximum thickness of the chips found in the height corresponding thickness of removal layer and height corresponding the layer in which the final surface is formed. As can be seen in the chart, the increase of the thickness of removal layer and feed speed do not cause significant change.
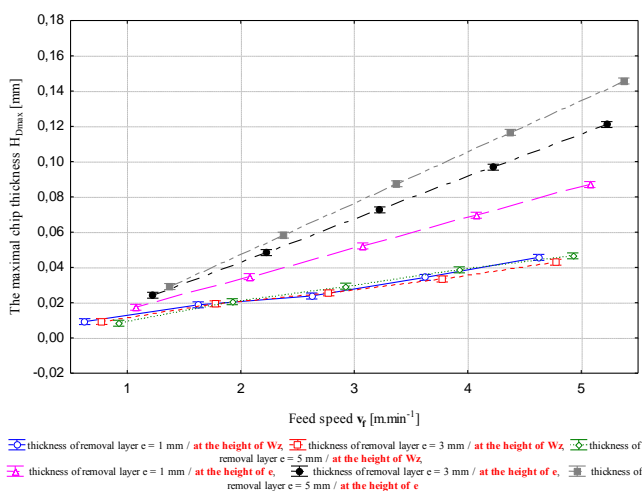
Fig. 6. Influence of feed speed and thickness of removal layer on the maximal chip thickness

CONCLUSION

When milling oak blanks with end mill fitted with one replaceable carbide blade on a CNC machining center, it is possible to achieve surface roughness at the level of 5.6 ÷ 7.1 µm. The influence of the feed speed as well as the thickness of removal layer on the surface roughness was not demonstrated.

REFERENCES

Aydin I., Colakoglu G. 2005. Effects of surface inactivation, high temperature drying and preservative treatment on surface roughness and colour of alder and beech wood. Applied Surface Science, 252, 2: 430–440.

Barcík Š., Pivolusková E., Kminiak R. 2008. Sledovanie drsnosti povrchu pri rovinnom frézovaní topoľového dreva kontaktnou a bezkontaktnou metódou. Trieskové a beztrieskové obrábanie dreva, 9,1: 55–62.

Barcík Š., Pivolusková E., Kminiak R., Wieloch G. 2009. The influence of cutting speed and feed speed on surface quality at plane milling of poplar wood. Wood research, 54, 2: 109–115.

Dzurenda L. 2017. Modification of wood colour of Acer platanoides L. to a brown-red shade caused by thermal treatment. Annals of Warsaw University of Life Sciences, 98: 26–32.

Gündüz G., Korkut S., Korkut D. S. 2008. The effects of heat treatment on physical and technological properties and surface roughness of Camiyani black pine (Pinus nigra Arn. subsp. pallasiana var. pallasiana) wood. Bioresource Technology, 99,7: 2275–2280.

Karagoz U., Akyildiz M. H., Isleyen O. 2011. Effect of heat treatment on surface roughness of thermal wood machined by CNC. Pro Ligno, 7, 4: 50–58.

Kminiak R., Banski A., Chakho D. K. 2017. Influence of the thickness of removed layer on the Quality of created surface during milling the MDF on CNC machining centers. Acta Facultatis Xylologiae Zvolen, 59, 2: 137–146.

Kminiak R., Gaff M. 2015. Roughness of surface created by transversal sawing of spruce, beech,and oak wood. BioResources, 10,2: 2873–2887.

Korkut S. D., Diziroglu S., Aytin A. 2013. Effect of heat treatment on surface characteristics of wild cherry wood. BioResources, 8, 2: 1582–1590.

Kubš J., Kminiak R. 2017. The effect of selected factors on the milled surface quality of thermally modified solid beech. BioResources, 12, 1: 1479–1490.

Kvietková M., Gaff M., Gašparík M., Kaplan L.; Barcík Š. 2015. Surface Quality of Milled Birch Wood after Thermal Treatment at Various Temperatures. BioResources, 10, 4: 6512–6521.

Novák V., Rousek M., Kopecký Z. 2011. Assessment of wood surface quality obtained during high speed milling by use of non-contact method. Drvna Industrija, 62, 2: 105–113.

Očkajová A., Kučerka M., Krišťák Ľ., Ružiak I., Gaff M. 2016. Efficiency of sanding belts for beech and oak sanding. Bioresources. 11, 2: 5242–5254.

Siklienka M., Adamcová E. 2012. Výskum vplyvu materiálu reverzibilných nožov stopkových nástrojov na kvalitu opracovaného povrchu MDF. Chip and chipless woodworking processes 8, 1: 315–323.

Siklienka M., Kminiak R., Sustek J., Jankech A. 2017. Delenie a obrábanie dreva. Zvolen: TU vo Zvolene: 357.

ACKNOWLEDGMENTS

INFLUENCE OF TOOL ANGULAR GEOMETRY ON SURFACE QUALITY AFTER PLAIN MILLING OF THERMALLY MODIFIED OAK WOOD

Michal Korčok – Marek Vančo – Štefan Barcík – Vlado Goglia

Abstract

The article deals with examination of angle geometry of end quality results of natural and temperature modified oak wood during face milling. Experiment part focuses on evaluation of equipment impact (angle geometry - y = 15°, 20°, 30°) of material (of natural and temperature modified oak wood with temperature: 160 °C, 180 °C, 210 °C, 240 °C) and technology factors (such as: cutting velocity - vc = 20 m.s⁻¹, 40 m.s⁻¹, 60 m.s⁻¹) adjustable velocity - vf = 6 m.min⁻¹, 10 m.min⁻¹, 15 m.min⁻¹) on quality processing of surface (Ra - medium aritmetic deviation of surface). We have measured end quality of surface, using contactless method with help of device LPM - 4, which works on a principle of laser profilometry. The best quality of wood, we have gained during wood working with temperature treatment of 210 °C with cutting-edge side rake of 30° and on the contrary, the worst quality of wood, we have gained with the same temperature treatment of 210 °C, but with cutting-edge side rake of 15°.

Key words: *thermowood, angular geometry, surface roughness, thermal modification*

INTRODUCTION

Wood as renewable material is being used in different ways, especially in building industry. During working with natural wood in outdoor conditions, we however have certain restrictions, which are resulting from it's unwanted characteristics, among which we include poor resistance against biological attacks of wood-decaying fungi and wood-destroying insects, dimension instability and changes caused in consideration of atmospheric conditions. Disadvantages caused by these effects were overcome by use of more permanent kinds of hardwood, especially rain forest species, or by the means of wood preservation. To increase resistance of wood against decay are most often being used different chemicals (Kučerová et. al. 2016), but during chemical modification, during process of manufacture, we can get negative impact on environment, life span of wood and as well as during disposal or during recycling of wood. (Kocaefe et. al. 2008).

Because of that, we have to protect the wood against unwanted effects, so that it last's as long as possible. One of most used ways of how to improve it's properties and preservation of wood is temperature treatment. Thermal modification of wood is based on thermal and hydrothermal processing of wood with temperatures ranging from 150 °C to 260 °C. Under high temperatures polymers are degrading and new in water insoluble substances are being formed, in like manner as substances with toxic or repellent effect

Technical University in Zvolen, T. G. Masaryka 24, 960 53 Zvolen
e-mail: korcokmichal@gmail.com

against biological pests, such as fungi and mushrooms (Kaplan et. al. 2018). In basic terms Thermowood requires higher caution during handling like ordinary wood, because during next processing is susceptible to mechanic deterioration due to increased brittleness. Thermo modified wood is more crack susceptible than untreated wood, whereas wooden elements are changing in irreversible way (Kminiak et. al. 2015).

Milling in present age is gaining ground in workmanship. Milling is method of chip formation, during which a layer of material is being removed from workpiece in form of small individual chips with help of multipurpose rotary machine, which we call mill, milling cutter, milling tool, milling machine (Sedlecký et. al. 2018). During milling, milling cutter is turning around it's rotary axis (main process of movement) and it's very teeth are gradually cutting through workpiece material, which at the same time moves in retrograde motion of machine (secondary process of movement), (Prokeš et. al. 1982). Each cutting blade of milling machine gradually removes short chips from workpiece material, at which process of milling is not interrupted (Lisičan et. al. 1996).

Increasing cutting speed results in better surface finish of workpiece from wood (Mithchell et. al. 2002). By end quality of cutting process, we understand operation of machine as a whole (with one or more cutting edges) in overall quality of surface, which are qualified by three kinds of accuracy: shape accuracy, dimensional accuracy and surface accuracy (Vančo et. al. 2017).

As long as we want to achieve high-quality finish of surface, we have to take care of proper sharpness of cutting tool during milling. It is however necessary to remove formation of chips, which are constantly emerging across the grain in a given type of machining on the beginning and on the end of milling, where cutting edge of cutting tool gets out of cut (Lisičan et. al. 2007).

MATERIALS AND METHODS

Sample preparation

For experimental measurements had been used species of oak wood (Ouercus robur L.) from locality Vlčí Jarok (Budča, Slovak Republic), 440 m. n. n.. Average age of round logs after counting annual rings was approximately 96 years. Wood species itself at average of 350 mm – 400 mm, had been in form of sawn timber secured by School's Woodland Enterprise in Zvolen. Experimental samples were made by machining round logs, at which each round log was needed for process of making/machining different series of samples. On log band saw, which is located in campus workshop of Technical University, by cutting round logs, we have gained cut timber with diameter of 25 mm. After cutting, we have fed the cut timber into kiln dryer, where it dried to moisture content of 10 %. During rip sawing, we were left with side tangential timber with width of 110 mm. By following scarfing and by thickness plan sawing the timber had reached exact thickness of 20 mm. On the circular saw, we have shortened the dimension timber on the required length of 500 mm.

Thermal modification of material

The wood samples were thermally modified at Volga State University of Technology, in town Joshkar-Ola, Russia. The development of thermal modification itself is displayed on the Fig. 1. and on the Tab. 1., where are the records of the time intervals of individual phases of thermal modification. During experiment was used one sample in natural state and remaining four were thermally modified by given temperatures.
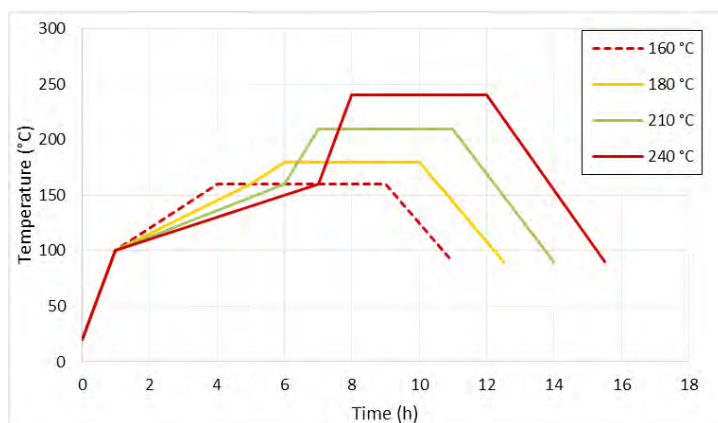
Fig. 1 Graphical progress of thermal modification of samples

Tab. 1 Process of thermal modification – phase of individual heat treatments

Temperature [°C]	Phase 1 [h]	Phase 2 [h]	Phase 3 [h]
160	4	5	2
180	5	5	2.5
210	6	5	3
240	7	5	3.5

Assessing wood density

In accordance to STN 49 0108 norm, for given experiment was being determined density of wood, which was next machined by lower spindle milling machine.

For the sake of wood density determination, 5 samples were made with dimensions of 20 x 20 x 30 mm (width x length x height). Number of individual samples during woodworking of average value was 16 pieces during individual thermal treatments. The samples themselves were measured on a adjustable digital meter with accuracy of 0.01 mm and with laboratory digital scales, weighed with accuracy of 0.01 g. After measuring and weighing were given values recorded in program EXCEL and by certain formula was calculated density of samples.

End measured values were compared with natural and thermally modified oak wood with thermal treatment of (160 °C, 180 °C, 210 °C, 240 °C).

Tab. 2 Measured density values of modified oak wood

Thermal modification [°C]	ρ [kg·m^{-3}]	Percentage change [%]
N	639	-
160	622	2.73
180	619	3.23
210	588	8.67
240	571	11.90

Description and characterization of the machine

For experiment was used Lower Spindle Milling Machine FVS (Limed, Hradec Králové, Czech Republic) with cylinder feeding system FROMMIA. All main parameters are recorded in Tab. 3.

Fig. 2 Lower Spindle Milling Machine with attached Feeder

Tab. 3 Technical parameters

Lower spindle mill FVS		Feeding device Frommia	
Supply voltage	360, 220 (V)	**Type**	ZMD 252 / 137
Cutting speed	20, 40, 60 (m·min^{-1})	**Feed**	2.5;10; 15; 20; 30 (m·min^{-1})
Input power	4 (kW)	**Motor**	360 (V), 2 800 (m·min^{-1})

Characteristics and description of the milling head

For experiment measurements were used 3 milling heads for milling wood, brand STANON made in SZT - machinery Turany with changeable cutting disks with type of marking FH 45, shown on the Fig. 3., with parameters in Tab. 4. Each milling head was equipped with two knives. One knife was attached so, the cut reduction of knife was 1 mm and the second knife was inserted in the milling head whole, so it really has been used to just balance the machine. Used cutting disks were made from steel Maximum Special 55: 1985/5 with hardness of 64 HRC WOOD-B, Nové Zámky, Slovakia).

Fig. 3 Used milling heads

Tab. 4 Milling heads parameters

Parameters of the cutter body	
Diameter of the cutter body with extended knife	130 (mm)
Diameter of the cutter body	125 (mm)
Thickness of the cutter body	45 (mm)
Number of knives	2
Cutting geometry	$\beta = 45°$; $\gamma = 15°, 20°, 30°$

Experimental milling

All samples were cross milled alongside fibers of wood, under given cutting requirements. Used cutting requirements are displayed in the Tab. 5, whereby on the Fig. 4 is stated the principle of experimental milling. Whole development of experimental plain milling happened in premises of development workshop in Zvolen.

Tab. 5 Cutting conditions for experiment

Cutting terms		Value
Feed speed v_f (m·min^{-1})		6, 10 15
Cutting speed v_c (m·s^{-1})		20, 40, 60
Cutting geometry (°)	Face angle	$\beta = 45°$
	Blade angle	$\gamma = 15°, 20°, 30°$
Depth of cut a_P (mm)		1
Thermal modification T (°C)		N
		160
		180
		210
		240
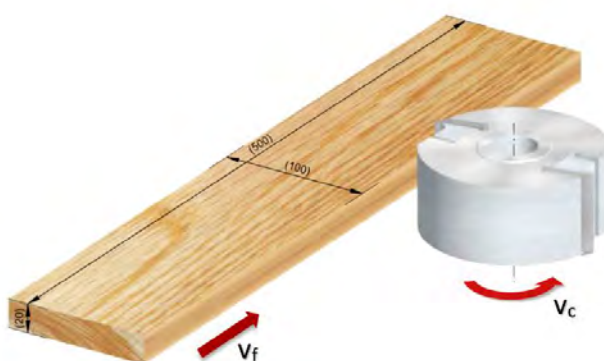
Fig. 4 Graphical representation of principle of machining samples

Measuring roughness of surface

The samples before experimental measuring, which were thermally modified had moisture content of 3 - 6 %. On the machined samples we have next measured roughness of surface with help of contactless laser profilometer LMP - 4 (Fig. 5), which works on a principle of laser profilometry. In Table 6 are displayed technical parameters of laser profilometer.
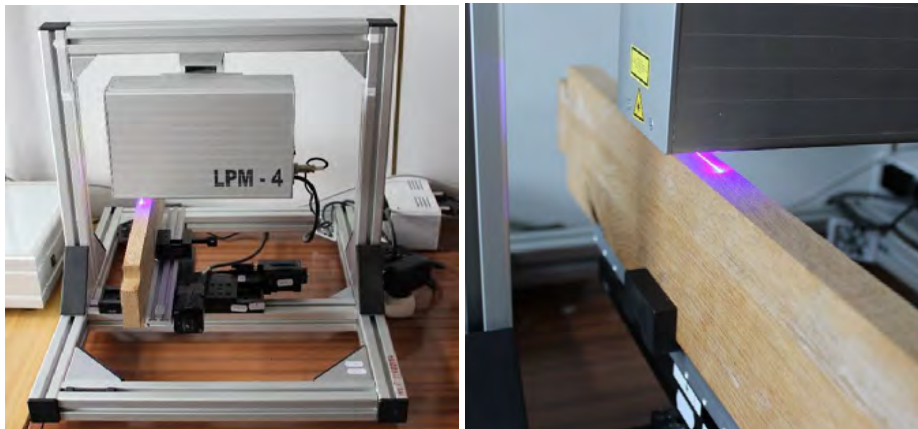
Fig. 5 For experimental measuring was used Laser profilometer LMP – 4

Tab. 6 Technical parameters of laser profilometer LMP – 4

Technical parameters LMP – 4	
Measuring range in axis (vertical)	420 mm to 470 mm
Measuring range in axis z	± 0.15 mm
Measuring range in axis x (transverse)	200 mm
Number of samples in axis x	1350
Processing speed	25 prof./s
Dispered laser angle	30°
Roughness parameters	R_p, R_v, R_z, R_a, R_q, R_c
Waviness parameters	W_p, W_v, W_z, W_a, W_q, W_c

All measurements taken with profilometer were evaluated and displayed on the personal computer, with help of software program LPM-View. The output figures gave us result of quality of surface, as well as it's primary profile and profile of it's roughness. Through the use of program STATISTICA 10 (StatSoft CR s.r.o., Prague, Czech Republic) were next the data taken processed. For the purpose of data evaluation has been used this program for interpretation of a single factor and of a two - factor analysis of dispersion with graphs and it's given relativity.

RESULTS AND DISCUSSION

Influence of angle geometry on surface roughness

Dispersion multifactor analysis in dependence on rake angle geometry from surface coarseness is displayed on the Fig. 6 and analysis of dispersion depending on rake angle

geometry from surface coarseness is displayed on the Fig 7. From multifactor dispersion analysis we can see, that the best end quality finish of surface we have gained with thermal modification of 160 °C. The best values of wood machining of surface we have gained with sample thermally modified at 210 °C with machine rake angle of 30°. By contrast the worst values of surface wood machining were gained with machine rake angle of 15° and thermal modification of 210 °C.
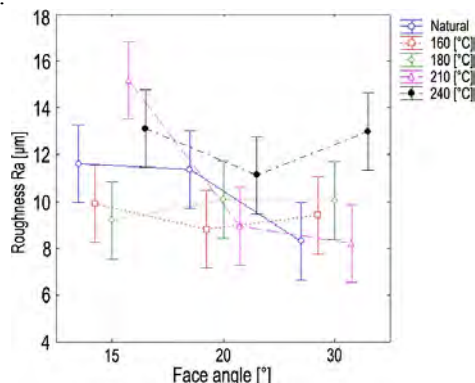
Fig. 6 Multifactor analysis of variance for the dependence of rake angle speed on surface quality

In Table 7 are dispersal the likelihood of dependence of surface roughness on face angle at different variants of feed speed, thermal treatment and cutting speed 20, 40 a 60 [m.s⁻¹]. Via this table we can see, that statistically important result is thermally modified wood treated at 210 °C with cutting speed 60 m.s⁻¹.

Tab. 7 View dispersal and the likelihood of dependence of surface roughness on face angle at different variants of feed speed, thermal treatment and cutting speed 20, 40 a 60 [m.s⁻¹].

Cutting speed v_c [m.s⁻¹]	Effect	SS	Degr. Of Freedom	MS	F	p
	Native	66,053	4	16,513	1,7961	0,158767
	160 °C	23,468	4	5,867	0,4672	0,759202
20	180 °C	34,477	4	8,619	2,645	0,055319
	210 °C	119,424	4	29,856	1,6828	0,183019
	240 °C	19,654	4	4,913	0,4392	0,779148
	Native	20,196	4	5,049	0,6934	0,603003
	160 °C	46,491	4	11,623	0,8065	0,531908
40	180 °C	16,204	4	4,051	1,2696	0,306258
	210 °C	67,367	4	16,842	0,9597	0,445484
	240 °C	23,499	4	5,875	0,7233	0,583666
	Native	69,509	4	17,377	0,9832	0,433247
	160 °C	19,005	4	4,751	0,3023	0,873858
60	180 °C	13,080	4	3,270	0,8571	0,502010
	210 °C	1673,940	4	418,485	6,7363	0,000678
	240 °C	27,040	4	6,760	0,2090	0,931166

From worked out analysis of dispersion it is visible, that with each graph with increasing face angle the quality of machined surface is at the same time decreasing. The best quality of machined surface, we have gained during thermal treatment of 210 °C, with use of face angle of 30°. The worst quality, we have gained during thermal treatment of 210 °C and with tool face angle of 15°. During machining all samples of natural character

and samples with thermal treatment the best results worked out to be with use of tool with face angle of 30°.
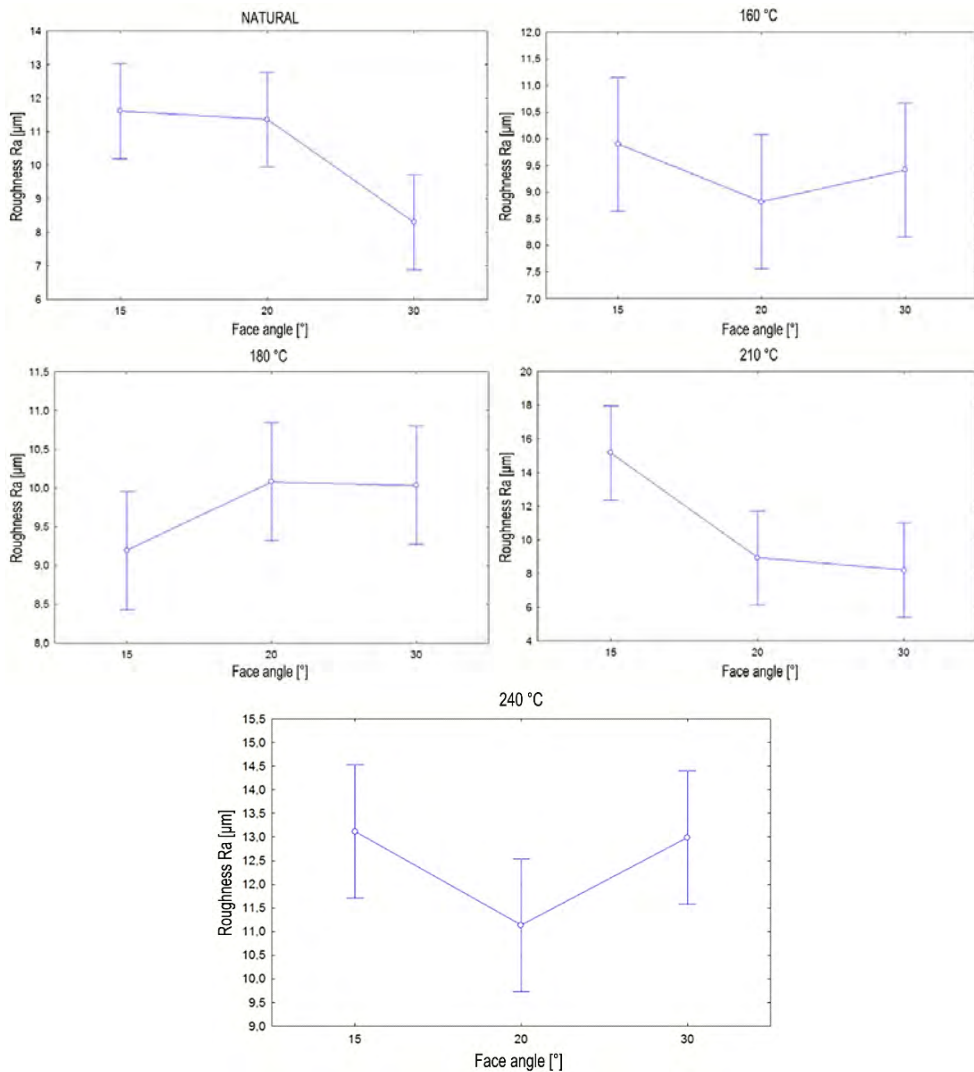
Fig. 7 Analysis of variance for the dependence of surface roughness on the rake angle

CONCLUSIONS

The report has been fixated on reaching most optimal tool face angle during wood machining samples, during which one sample was in natural state and the ones left were thermally modified. During measuring we have realized, that during wood machining of used samples the lowest value of roughness was reached during heat treatment of 210 °C with tool face angle of 30°. With gradual tool face angle increase was found, that roughness of surface of all samples was decreasing. In our experiment it has been proven, that during

the smallest face angle was roughness of surface the worst and with gradual growth of face angle, we have gained the best roughness of wood machined surface. During given experiment wasn't proven the fact, during which with increasing tool face angle, simultaneously worsens the quality of wood machined surface of material. On basis of roughness research of thermally modified wood, we can in present time compare our work with authors, such as Barcík et. al. 2014 and Kvietková 2015. The authors were in their works dealing with pinewood (Barcík) and with beech wood (Kvietková). The surface roughness measurement and it's evaluation in their case was executed with contact method.

ACKNOWLEDGEMENTS

REFERENCES CITED

BARCÍK, Š. ,GAŠPARÍK, M., HOUSKA, A., RAZUMOV, E., JU., SEDLECKÝ, M. 2014. "Vliv technologických faktorů na kvalitu opracování povrchu při frézování termicky modifikovaného borovicového dřeva [Influence of technological factors on the surface quality after milling of thermally modified pine wood]," In: Trieskové a beztrieskové obrábanie dreva 2014: Zborník prednášok [Chip and Chipless Woodworking Processes 2014: Conference Proceedings], Zvolen, Slovakia pp. 11-22.

BOONSTRA, M. J., VAN ACKER, J., PIZZI, A. (2007). "Anatomical and molecular reasons for property changes of wood after full-Scale industrial heat-treatment," Proceedings of the Third European Conference on Wood Modification, Cardiff, UK, pp. 343-358.

GAFF, M., KVIETKOVÁ, M., GAŠPARÍK, M., KAPLAN, L., BARCÍK, Š. (2015) "Effect of selected parameters on the surface waviness in plane milling of thermally modified birch wood," BioResources 10(4), 7618-7626. DOI: 10.15376/biores.10.4.7618-7626

HORÁČEK, P. 1998. Fyzikální a mechanické vlastnosti dřeva 1. vyd. [Physical and Mechanical Properties of Wood, 1st edition], Mendel University, Brno, Czech Republic

KAČÍKOVÁ, D., KAČÍK, F. 2011. Chemické a mechanické zmeny dreva při termickej úprave [Chemical and Mechanical Changes During Thermal Treatment of Wood], Technical University in Zvolen, Zvolen, Slovakia

KAPLAN, L., SEDLECKÝ, M., KVIETKOVÁ, MS., SIKORA, A. (2018). "The Effect of Thermal Modification of Oak Wood on Waviness Values in the Planar Milling Process, Monitored with a Contact Method," BioResources 13(1), 1591-1604. DOI: 10,15376 / biores.13.1.1591-1604

KMINIAK, R., GAFF, M., (2015). "Roughness of Surface Created by Transversal Sawing of Spruce, Beech, and Oak Wood," BioResources 10(2), 2873-2887. DOI: 10.15376/biores.10.2.2873-2887

KOCAEFE, D., PONCSAK, S., BOLUK, Y. (2008). "EFFECT OF THERMAL TREATMENT ON THE CHEMICAL COMPOSITION AND MECHANICAL PROPERTIES OF BIRCH AND ASPEN," BioResources 3(2), 517-537.

KUČEROVÁ, V., LAGANA, R., VYBOHOVA, E., HYROGOVÁ, T. (2016). "Effext of Chemical Changes during Heat Treatment on the Color and Mechanical Properties of Fir Wood," BioResources 11(4), 9079-9094. DOI: 10.15376/biores.11.4.9079-9094

LISIČAN, J. (2007) Teória a technika spracovania dreva [Theories and Techniques of Wood Processing], Mat Centrum, Zvolen. Slovakia, pp. 102-104

MITCHELL, PH., LEMASTER, RL. (2002). "Investigation of machine parameters on the surface quality in routing soft maple," BioResources 52(6), 85-90

PROKEŠ, S. (1982). Obrábění dřeva a nových hmot ze dřeva [Machining of wood and new wood materials], SNZI, Prag, Czech Republic

REINPRECHT, L., VIDHOLDOVÁ, Z. 2008. Termodrevo – Príprava, Vlastnosti a Aplikácie [Thermowood – Preparation, Properties and A

pplications], Technical university in Zvolen, Zvolen, Slovakia

SEDLECKÝ, M., KVIETKOVÁ, MS., KMINIAK, R. (2018). "Medium-density Fiberboard (MDF) and Edge-glued Panels (EGP) after Edge Milling-Surface Roughness after Machining with Different Parameters," BioResources 13(1), 2005-2021. DOI: 10.15376/biores.13.1.2005-2021

VANČO, M., JAMBEROVÁ, Z., BARCÍK, Š., GAFF, M., CEKOVSKÁ, H., KAPLAN, L. (2017). "The Effect of Selected Technical, Technological, and Material Factors on the Size of Juvenile Poplar Wood Chips Generated during Face Milling," BioResources 12(3), 4881-4896.

THE ANALYSE ACTIVITY OF CUTTING FORCES FOR THE CHIPLESS CUTTING WOOD

Ján Kováč – Jozef Krilek – Pavol Harvánek

Abstract

On the score of largeness energic slope and value delimbing (expurgation xylem stuff trunk from limb) is very important analysis cutting forces in process delimbing. The paper shows investigation and influence on chosen technological parameters machine delimbing to improve the process of the cutting of bough and increase of qualities machine delimbing during tree processing. This paper is intent on evalutionof influence on individual aspects at cutting force with keep to the terms of delimbing that are tobe used at machine delimbing. The analyse of the cutting forces in the process of delimbing is important with aspect to energy losses and the quality of delimbing (delimbing of tree trunk).

Key words: *cutting force, cutting speed, chipless cutting*

INTRODUCTION

The part of felling machines is technological or manipulation device, which does main operations like cutting, delimbing, shortening and other manipulation of a tree. The most important task in this area is optimization of technical and technological parameters of cutting mechanisms (KOVÁČ J., 2005). The general requirements for cutting mechanisms are high cutting property, operational reliability, durability of a tool, low requirements for operation and maintenance, weight and suitable quality of work (Kováč J., 2004).

The process of chipless wood cutting looking like operation of tree delimbing, which is used in all sorts of multifunctional machines is characteristic by quantity parameters. There are realized theoretical and experimental works in the area of chipless transverse separation of wood with delimbing and at barked wooden assortments, with analysis of dynamic and kinematic parameters (Marko J., 2008). There is paid attention to the score of most often used technologies at multifunctional machines. A lot of factors deal with main qualitative indicators e.g. cutting force, quality of section, wearing resistance of a cutting edge, etc (Lisičan J., Siklienka M., Zemiarová B., 1994).

Power necessary on transposition tree near breaking down limb in branch chaplet must overcome cut and grinding resistance.. Specification of these forces will permit to determine the power of drive e.i. energetic intensity of delimbing process. It is necessary to do force analysis of forces which works in parallel with an axis of wooden tunk (Marko J., Holík J., 1994). The base for this analysis is investigation of force arangement, which are produced at cutting by the knife with its shape of wedge and with the dorsal angle α = 0° (Fig. 1). At the same time we get a picture about character of sawing, which takes part in

Technical University in Zvolen, T. G. Masaryka 24, 960 53 Zvolen

e-mail: kovac@vsld.tuzvo.sk, jkrilekmail.com, xharvanek@is.tuzvo.sk

the area of non - chips producing process through the medium of knives in the direction which is discordant with the direction of fibres on sawing wood (Mikleš M., 1994).
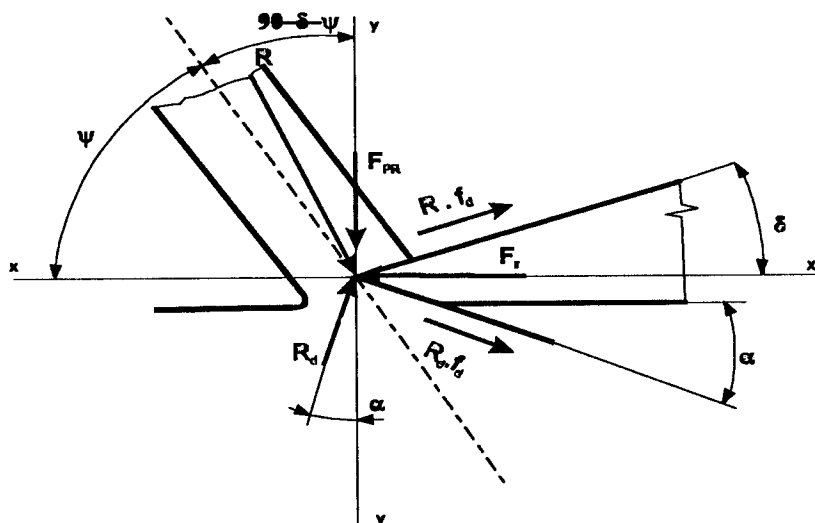
Fig. 1   Application cutting forces in the delimbing

Formation of balance formula of forces in the direction of axis x, y:

$$\sum F_X = 0; \quad -F_{PR} + R_d.(\cos\alpha - f_d\sin\alpha) - R.(\cos\delta - f_d\sin\delta) = 0 \tag{1}$$

$$\sum F_Y = 0; \quad F_R - R_d(f_d\cos\alpha + \sin\alpha) - R(f_d\cos\delta + \sin\delta) = 0 \tag{2}$$

On base of knowledge from theory of elasticity and hardness we form the formula, which defines the violence of limbs at local deformations of combined stress (from the knife) on tension and bend. After the reform we get:

$$R.\sin(\delta+\psi) - \frac{\sigma.S.W}{(W+eS)} = 0 \tag{3}$$

where:
F_{PR} – compressive force of knife toward the trunk, (N)
R_d – reaction of trunk on the back of the knife, (N)
R – reaction of a branch on the forehead of knife, (N)
f_d – coefficient of friction between the surface of knife and wood of a limb, (-)
s – stronghold limit of limbs on the tension along (in the direction of) fibres, (Mpa)
S – area of a part of the branch which is not cut, (mm)
W – three-dimensional modulus in bend, to z-axis, (mm3)
e – elentricity of a branch cross-section, (mm)
δ – cutting angle, (°)
a – dorsal angle of a knife, (°)
ψ – growth angle of the branch, (°)

When we project all forces to axis y, we get:

$$F_{PR} = R.\cos\delta - R.f_d.\sin\delta - R_d$$

(4)

The study of authors (Koceragov, Mensikov) demonstrated and our study has certified (Jandel, Mikles, Koren, Marko) that reaction of forces on a knife from ability of elastic reversibility of fibers we can omit. According to general law of wood sawing, compression of fibers will take a part at constant tension on the dorsal and frontal surface where the wood elasticity is characterized at bending and compression of fibers by numerical data. In that case the general pressure on the surfaces of a knife can be simplified and it is proportional to the perimeter of penetrated part of a knife. Frictional force $R_d.f_d$ at big thickness of a chip (over the 5 mm) generates 1,0 - 1,5 % from the whole cutting force. Collapsing length of limbs, where the creation of chips is turned off, is equal to 40 - 50 mm. It follows that forces R_d and $R_d.f_d$ we can omit like minimal. Then mentioned formula gains pattern:

$$F_{PR} = R.\cos\delta - R.f_d\sin\delta$$

(5)

The fulfilled condition refers for the quality of delimbing that comprehensive force F_{PR} has to be bigger than reaction force of knives, which reacts opposite the force of comprehension.

MATERIAL AND METHODS

At the production of experiments as the main roll is comparison of cutting force with the magnitude of cutting resistance with reference to quality of cutting process according to the changing parameters which limbs cutting defines. The goal of measurements was comparison of cutting speed according to the magnitude of cutting resistance with the reference to the quality of delimbing process. The tests were made on the machine for cutting of wood by high speed with reversible movement of cutting mechanism. The power of cutting mechanism was performed by pneumatic cylinder. It was designed by professor Mikleš and made at VDL TU in Zvolene.

At laboratory experiment of delimbing measurements there was studied maximum cutting force characterized by the rest and by the rip of a limb at the speeds of 1,5 m.s^{-1}, 2,0 m.s^{-1} and 2,5 m.s^{-1}. The technical parameters of tested knives are shown in Tab. 1. The individual speeds of knife movement result from the scale of the pressure magnitude which was justified in a pneumatic engine at the pressure of 0,8 MPa. There was measured 3,12 m.s^{-1} by a sensing device of acceleration a maximum speed of piston motion and it was produced in program NEXT WIEV 2.5, at the speed of 2,48 m.s^{-1}.

Tab. 1   Technical parameters of tested knives

No.	$\delta(°)$	$\alpha(°)$	h(mm)	s(mm)	ρ- radius of a cutting edge
1	20	7	2	15	0,012-0,025
2	15	4	2	15	0,012-0,025
3	20	4	2	15	0,012-0,025

The character of a cutting force depends on works along the movement of a knife in the process of cutting. The cutting force increases linear and the speed of cutting decreases linear at increasing penetration depth by penetration of a knife. The linear dependency of the cutting force (Fig. 3) changes at penetration depth of a tool approximately at $0,5 . d_0$, or something less than the half of a limb diameter.
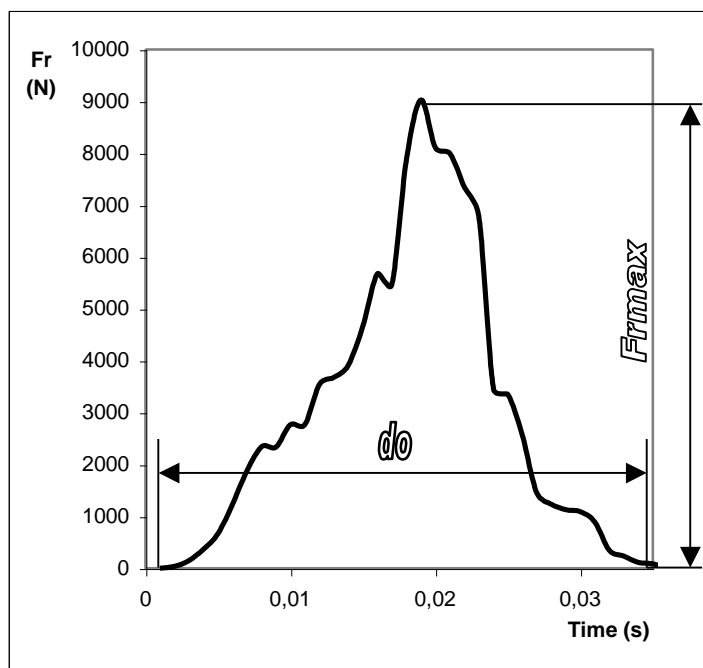
Fig. 2   Course cut force near grained branches

For a spruce the character of dependency changes at cutting by knives with different geometrical parameters and it does not change with increasing limb thickness and also it does not vary with the change of growing angle of a limb in the limits characteristic for given wooden species.

RESULTS AND DISCUSSION

The individual laboratory results of measurements handled in a table form we handled for limpidity in graphical form by MS Excel (e.g. Figures 4,5 and 6). The flows of individual investigated values e.g. the maximum cutting force, the maximum cutting force on $1mm^2$ of the limb surface, the index of low energetic severity and also a qualitative index, at specification of dependent parameters give better scheme at appraisal mentioned parameters from the quality and energetic severity point of view of chipless cutting process.

The course of maximum force at the speed of 2.0 m.s⁻¹
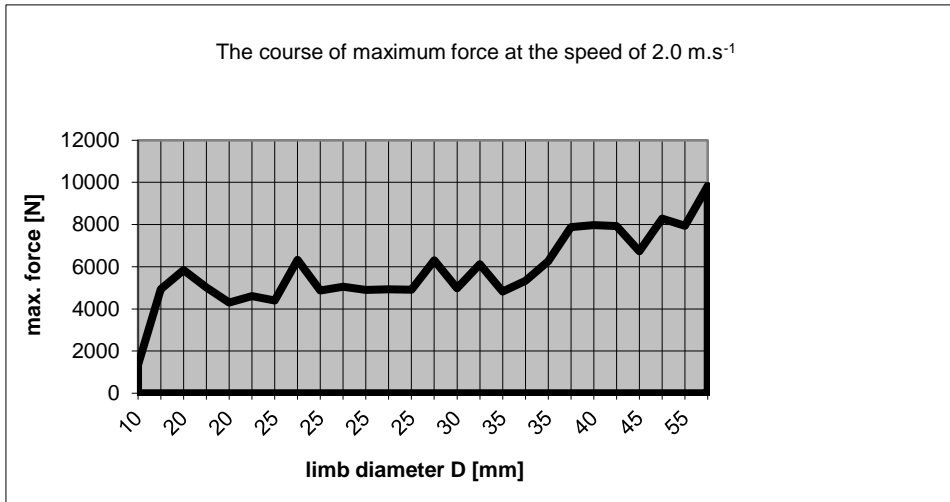
Fig. 4   The course of max. cutting force at the speed of 2.0 m.s^{-1}and knife No.1

The course of maximum force at the speed of 2.0 m.s-1
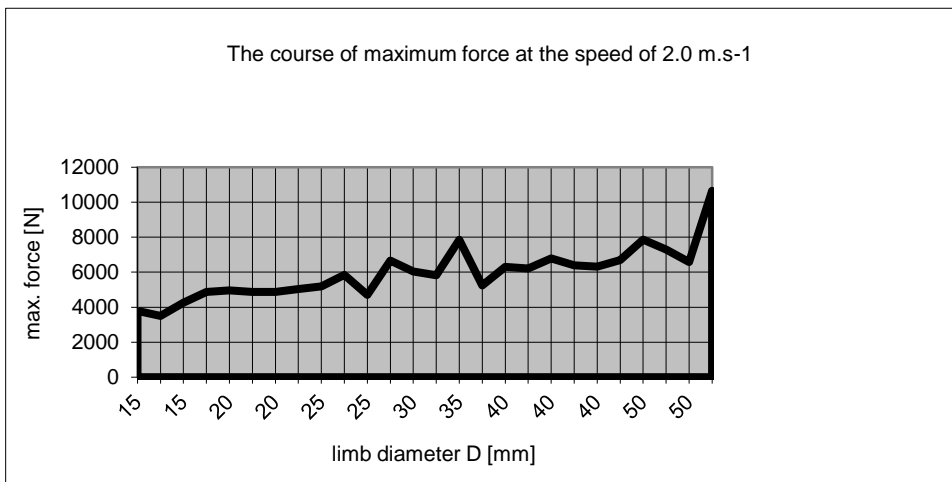
Fig. 5   The course of maximum cutting force at the speed of 2.0 m.s^{-1}and knife No.3
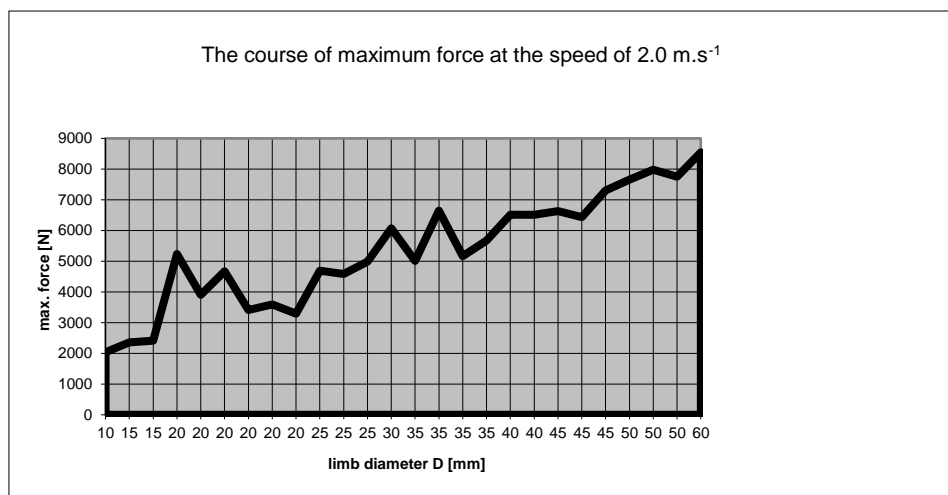
Fig. 6   The course of maximum cutting force at the speed of 2.0 m.s^{-1}and knife No.2

The meaning is in statistical knowledge. The processes have relative comparison with an individual selected pack at studying properties of chosen packs. For investigation of relative dependency on multiple factors in maximum cutting force of delimbing there was used covariance of multi-factorial analysis called ANOVA.

The results of statistical features are shown in Table 2 for the dependency among maximum cutting speed (2), type of a knife (1) and limb diameter (3). There were shared to two classes DP1 – limbs at diameter of 0 to 35 mm; DP2 – limbs at diameter of 35 to 55 mm; the majority of diameters occur in these two classes.

Tab. 2 Attributes statistical characterization dependencies max. cut strength on diameter limb, cut speed, unmarried husband knives, Summary of all Effects; 1-NOZ, 2-VUU, 3-DUP

	df Effect	MS Effect	df Error	MS Error	F	p-level
1	3	21033206	283	1533050,63	13,720	0,000
2	2	5998744,5	283	1533050,63	3,913	0,021
3	1	332425824	283	1533050,63	216,839	0,000
12	6	436176,34	283	1533050,63	0,285	0,944
13	3	468428,94	283	1533050,63	0,306	0,821
23	2	681868,19	283	1533050,63	0,445	0,641
123	6	1639006,4	283	1533050,63	1,069	0,381

df effect - degree of freedom for factor,
MS effect - scatter (average square) for input,
df error - residual degree of freedom for accidental anomalies,
MS error - scatter (average square) for accidental anomalies,
F - Fischerov F-test, share scatter infliction input and scatter infliction adventitious effect,
p-lion - significance level test

From the results it is evident that the biggest statistical effect has the type of a knife and there is a cutting speed of small statistical account, diameter of a limb has also very important statistical effect on maximum cutting force, it confirms assumptions acquired throughout measurements (so the diameter of a limb has the biggest effect on the maximum cutting force, then the type of a knife and the cutting speed has small statistical effect). All three factors work independently without interaction. The differences among knives vary at different speeds and different diameters of limbs.

The smallest maximum cutting force is at the knife No. 3, i.e. verification of correctness of geometry selection of a knife mentioned in methodology of work of the academic dissertation. For more accurate statistical interpretation we made multi-regression, where we got following mathematical model expressed by a pattern of regression in the second grade of dependency between maximum cutting force and mentioned independent parameters (Kováč J., 2004).

When the effect of speed is not significant then formulas for specification of maximum cutting force depend on significant factors (diameter of limbs and type of a knife) as following:

a.) at the cutting speed of 1,5 m.s⁻¹

$$F_{R,max} = -38,125 + 207,487d + 601,91n\hat{o}\check{z}$$
$$-1,388d^2 + 6,573d \cdot n\hat{o}\check{z} - 185,212n\hat{o}\check{z}^2 \qquad (6)$$

b.) at the cutting speed of 2,0 m.s⁻¹

$$F_{R,max} = 693,16 + 173,732d + 545,401n\hat{o}\check{z}$$
$$-0,728d^2 + 0,767d \cdot n\hat{o}\check{z} - 146,447n\hat{o}\check{z}^2 \qquad (7)$$

c.) at the cutting speed of 2,5 m.s⁻¹

$$F_{R,max} = -647,936 + 277,969d + 719,312n\hat{o}\check{z}$$
$$-2,378d^2 + 3,512d \cdot n\hat{o}\check{z} - 199,326n\hat{o}\check{z}^2 \qquad (8)$$

CONCLUSION

The results of experiments always have relationship to exact cutting conditions. The cutting force as one of main parameters establishes material quality, shape dimensions and energetic consumption of a cutting tool (Marko J., 1993).

Discovered values of cutting forces, designed parameters of cutting tools, knowledge about decreasing defected area of wood at delimbing process make exact results for projection of cutting tools, dimensioning operational parts and estimation of asked power consumption of harvesters and processor heads of felling machines. Obtained results and knowledge can be applied at projection of working mechanisms in the harvester heads, respectively also at the development of cutting mechanisms and process parameters of chipless cutting for some working machines in forest depots in the commercial forestry of the Slovak Republic (KOVÁČ J., 2005).

REFERENCES

JandeL R., Koreň J.,1976. Problematika beztiereskového (nožového) prerezávania   dreva v prevádzke lesného hospodárstva. Lesnictví 22 (9): 723 – 746

Koreň J.,1983. Beztrieskové rezanie dreva, Vedecké a pedagogické aktuality. 6: 105

Kováč J., 2005. Vplyv viacerých faktorov na reznú silu pri odvetvovaní stromov. Acta facultatis technicae 2: 85 - 94

Kováč J.,2004. Vplyv vybraných parametrov na kvalitu strojového odvetvovania. Dizertačná práca: 151

Lisičan J., Siklienka M., Zemiarová B.,1994. Teória a technika spracovania dreva. Bratislava Príroda: 468

Marko J., 1993. Výskum adaptérov pre mechanizáciu výchovných zásahov. Kandidácka dizertačná práca:191

Marko J., 2008. Výskum nožového rezného mechanizmu vhodného na prerezávky. In: Kolokvium ku grantovej úlohe č. 1/3534/06: 32-37

Marko J., Holík J.,1994. Teória delenia dreva. TU vo Zvolene: 63

Mikleš M.,1994. Výskum geometrie nožov odvetvovacej hlavice. Acta Facultatis Forestalis, XXXVI: 15

INFLUENCE OF THE BELT TYPE OVER VIBRATIONS OF THE CUTTING MECHANISM IN WOODWORKING SHAPER

Georgi Kovatchev

Abstract

This study presents the influence of the belt type over vibrations of the cutting mechanism in a woodworking shaper. The case of the drive mechanism with the ability to use different gears is investigated. Emphasis is placed on the two widely used belts in contemporary machine building. The study is aimed at improving the reliability and efficiency of wood shaper machine to ensure the accuracy and quality of products.

Key words: *Woodworking shaper, V-belts, ribbed belts, vibration*

INTRODUCTION

Wood shapers are widespread in practice machines. Their universality allows them to be used in diverse industries in the woodworking and furniture industry. Their main use is in the manufacture of furniture, windows, doors, construction products and many other items used in everyday life. Wood shapers allow different devices to be attached to them. This increases their technological capabilities. Contemporary wood shapers should be able to work at different cutting speed. Most often the speed ranges is between 30 m/s – 60 m/s [Gochev.2005], according [Obreshkov.1997] to 90 m/s. This inevitably is associated with the machinery resources to work at different rotational speed. They are a precondition for the emergence of different cutting forces that create conditions for loads in the mechanisms which lead to errors during operation [Atanasov.2015, Vukov.2012]. Dynamic effects are constantly changing, which is a premise for permanent shifting loads in the bearings.

For driving the cutting mechanisms of wood shapers with bottom location of the working shaft most commonly V-belts and ribbed belts are used. This is the most common way to drive cutting, filing and other mechanisms in the woodworking machinery. This, undeniably is due to their advantages over other types of gears. Belt drives operate quietly and smoothly owing to the elasticity of the belt, reduce the shocks of the emerging rapid changes in load during operation of the mechanism, transmitting power over long distances [Sokolovski.2007]. Belt drives do not require special efforts to maintain. They are easy to operate; replacement of the old belt with a new one is faster and cheaper. Their simple construction means reducing costs, increasing security and durability. At the same time they enable the reduction in the level of vibration and noise.

Typical of the woodworking machines is that they operate at high cutting speeds. This requires a machine element carrying the energy of the motor to the executive parts of the machine to be able to run at high speed. Belt drives operate at high speeds – most often

University of Forestry, 10 Kliment Ohridski Blvd., 1797 Sofia
e-mail: g_kovachev@ltu.bg

from 5 m/s to 30 m/s. There are also rapidly-operating ones which can run at speed above 60 m/s [Sokolovski.2007].

The aim of this work is the measurement and analysis of vibration speed at idle and working tread at universal wood shaper with bottom location of the working shaft. The load on the bearings is researched when using different belt drives to drive the cutting mechanism. The study is aimed at improving the reliability and efficiency of wood shaper machine to ensure the accuracy and quality of products.

MATERIAL AND METHODS

To conduct the experimental part, a universal wood shaper with bottom location of the working shaft is selected Fig.1. The cutting mechanism of the selected machine is of relatively simple construction, which helps in the more accurate execution of the experimental part. The cutting mechanism is driven by an asynchronous electric motor with a power of 3 kW and rotation frequency of 2880 min^{-1}. For the purposes of the study were designed and developed belt pulleys for V-belt with Z-section and ribbed belt PK section. During the trials, the cutting mechanism was driven by two V-belt with Z-section and one ribbed belt 3PK section.

Fig.1. *Universal wood shaper with bottom location of the working shaft*

Fig.2. *Electric motor with a pulley*

Before carrying out the practical part, it is necessary to choose the factors in which the research will be conducted. The rotation frequency used for the experiments was 6000 min^{-1}. This is one of the most commonly used frequency in milling machines. The selected rotational speed is realized by pulleys mounted on the electric motor shaft and the machine shaft. The dimensions of the pulleys depend on the technical characteristics of the electric motor Fig.2.

A cutter with diameter D = 125 mm was used Fig 3. The technical data of the cutting tool are shown in Table 1. Cutting speed, calculated to the ability of the machine to operate with rotation frequency n=6000 min^{-1} and cutting tool with diameter D=125 mm are V= 39 m/s. The cutting speed is calculated by the formula 1 [Gochev. 2005].

$$V = \pi.D.n, \text{ m./s,} \tag{1}$$

where:

D – diameter of the cutting tool, *m*;

n – rotation frequency of the cutting tool, s^{-1}.

Fig.3. *Groove cutter*

Fig.4. Roll feeder

Table 1. *Technical data of the cutting tool*

Type of instrument	D mm	d mm	B mm	α °	β °	γ °	z бр	Material of the teeth
Groove cutter	125	30	12	16	55	19	6	HM

For the purpose of the research, a universal roller feeding mechanism is mounted to the shaper, shown in Fig.4. It consists of three feed rollers mounted in a housing. The feed speeds of the treated material, with which the experiments were made are respectively U1 = 4 m/min, U2 = 10 m/min, U3 = 16 m/min. Pine wood (*Pinus Nigra*) with thickness of the remove layer h = 12mm have been treated.

The intensity of the vibrations, whose cutting mechanism is driven by two different types of straps is assessed on the basis of the root mean square value of the vibration speed (v) mm.s^{-1} (r.m.s.) measured at different working modes of the machine. The measurements have been performed at six measuring points, located on two bearing housings of the main shaft of the machine. The measurement points on each bearing housing are located mutually perpendicular radial and one axial to the main shaft of the machine Fig.5 . [BDS ISO 10816 – 2002, Gochev. 2017].
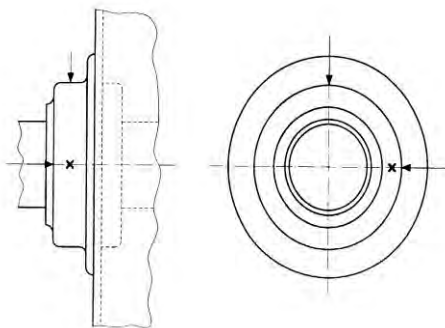
Fig.5. *Measurement points*

Fig.6. *Bruel & Kjaer Vibrotest 60*

Vibration speed is measured using a specialized device model Bruel & Kjaer Vibrotest 60 shown in **Fig.6**. The measurement points are located on the bearing housing of the machine. It significantly responds to the dynamic state. The exact vibration state measurements need to make in three mutually perpendicular directions [ISO 10816 – 2002, Gochev 2017]. Measurements are performed at idle state and during machine operation

RESULTS AND DISCUSSION

The experimental part includes idling trials and work trials in milling of pine wood (*Pinus Nigra*) specimens. The operation of the cutting mechanism was investigated when it was driven by V-belt and ribbed belt. Table.2 shows the average values of vibration speed (r.m.s) at idle state.

For the bearing housing located in proximity to the cutting tool, hereinafter referred to as "upper bearing housing", the measurement points are indicated by A: A_x – in direction parallel to the feed direction, A_y – in direction perpendicular to the feed direction and A_z axial direction.

For the bearing housing located in proximity to the driven belt pulley, hereinafter referred to as "lower bearing housing", the measurement points are indicated by B: B_x – in the direction parallel to the feed direction, B_y – in direction perpendicular to the feed direction and B_z axial direction.

Table 2. *Values of vibration speed (v) measured at idling mode with cutting tools*

Belt type	Vibration speed v, mm.s⁻¹ (r.m.s)					
	Measuring points					
	A_x	A_y	A_z	B_x	B_y	B_z
2Z	2.629	3.407	2.281	1.069	2.588	2.569
3PK	2.354	2.478	2.040	0.904	1.592	2.285

Fig.7 shows the average values of vibration speed (v) mm.s⁻¹ (r.m.s) at idle state close to the upper bearing housing. Fig.8 shows the average values of vibration speed (v) mm.s⁻¹ (r.m.s) at idle state close to the bottom bearing.
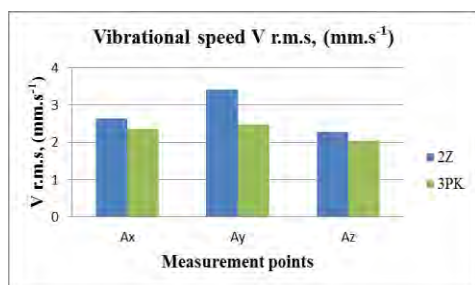
Fig.7. *Upper bearing housing vibration speed (r.m.s) at idle state*
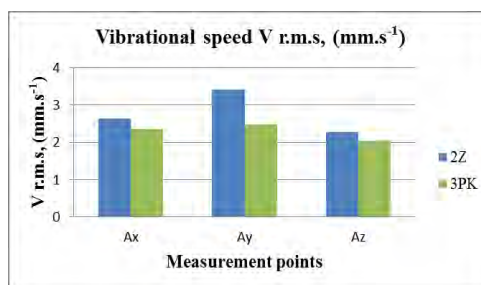
Fig. 8. *Bottom bearing housing vibration speed (r.m.s) at idle state*

Table 3 shows the average values of the measured square vibration speed (v) mm.s⁻¹ (r.m.s) measured near the upper bearing housing at working mode.

Table 3. *Values of vibration speed (v) measured at a working mode close to the upper bearing*

Feed speed U, m/min	Vibration speed v, mm.s^{-1} (r.m.s)					
	Upper bearing housing measuring points					
	Belt type: 2Z			Belt type: 3PK		
	A_x	A_y	A_z	A_x	A_y	A_z
4	1.126	2.61	2.604	1.648	2.058	2.381
10	1.481	3.014	3.003	1.998	2.480	2.780
16	2.583	3.064	3.054	3.100	2.530	2.831

Fig.9 and **Fig.10** shows the average values of vibration speed speed (v) mm.s^{-1} (r.m.s) measured in radial direction (A_x, A_y) at working mode close to the upper bearing.
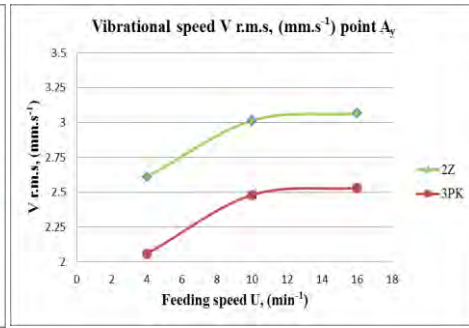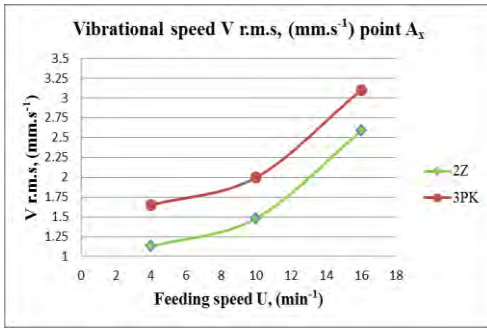
Fig. 9. *Vibration speed measured at a point Ax*   **Fig. 10.** *Vibration speed measured at a point Ay*

Table 4 shows the average values of the measured square vibration speed (v) mm.s^{-1} (r.m.s) measured near the bottom bearing housing at working mode.

Table 4. *Values of vibration speed (v) measured at a working mode close to the bottom bearing*

Feed speed U, m/min	Vibration speed v, mm.s^{-1} (r.m.s)					
	Bottom bearing housing measuring points					
	Belt type: 2Z			Belt type: 3PK		
	B_x	B_y	B_z	B_x	B_y	B_z
4	0.709	1.508	2.951	0.549	1.062	2.705
10	1.011	1.744	3.222	0.851	1.298	2.976
16	1.164	2.368	3.276	1.004	1.922	3.030

Fig.11 and **Fig.12** shows the average values of vibration speed (v) mm.s^{-1} (r.m.s) measured in radial direction (B_x, B_y) at a working mode close to the bottom bearing. The tendency to change the vibrational speed in the axial direction at the points (Az and Bz) is the same as in the radial direction. For this reason, the vibration speed is not represented graphically.
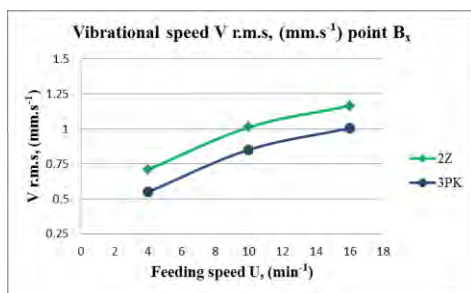
Fig. 11. *Vibration speed measured at a point Bx*   **Fig. 12.** *Vibration speed measured at a point By*
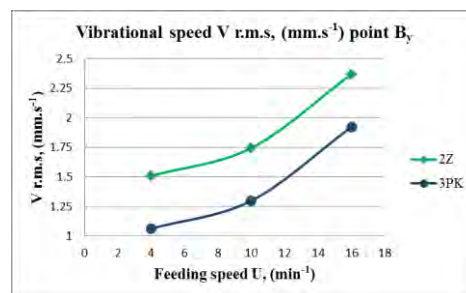
CONCLUSION

As a result of research and analysis of the results, the following conclusions can be made. The vibration speed (v) mm.s^{-1} (r.m.s) measured in idle is lower at the six measured points when the cutting mechanism is driven by a ribbed belt. During the working mode in the radial direction (A$_x$), the measured vibration speed at the three feed rates is lower with V-belts. At the other measuring points, the presented results show that machine worked better with ribbed belt PK independently from feeding speed. This gives reason to conclude that the vibration speed is lower when the cutting mechanism is driven by a ribbed belt with a PK profile. Lower vibration levels have a positive impact over the machine's overall performance, working capacity and reliability. This has a direct influence over the quality of the production.

REFERENCES

1. Atanasov V**.**, (2015), Research of the processing quality in cutting poplar logs with different narrow bandsaw blades, International Scientific and Technical Conference „WOOD TECHNOLOGY AND PRODUCT DESIGN", Ss. Cyril and Methodius University of Skopje, pp. 17 – 25;
2. Gochev, Z., Manual for Wood Cutting and Woodworking Tools, Sofia (2005), 232 p.
3. Gochev, Z., G. Vukov, P. Vitchev, V. Atanasov, G. Kovatchev, (2017), Study on the vibration severity generated by woodworking spindle moulder machine, International Scientific and Technical Conference „WOOD TECHNOLOGY AND PRODUCT DESIGN", Ss. Cyril and Methodius University of Skopje, pp. 55 – 60;
4. Obreshkov P., Woodworking machines, Sofia (1997), 182 p.
5. Sokolovski S., Machine elements, Sofia, (2007) 318 pp.
6. Vukov, G., Zh. Gochev, V. Slavov, Torsional Vibrations in the Saw Unit of a Kind of Circular Saws. Numerical Investigations of the Natural Frequencies and Mode Shapes. Proceedings of Papers, 8th International Science Conference "Chip and Chipless Woodworking Processes", Zvolen, 2012, ISBN 978-80-228-2385-2, pp. 371 – 378.
7. ISO 10816-1:2002, Evaluation of machine vibration by measurement on non – rotating parts – Part 1: General guidelines, 25 p.

BONDING QUALITY AND BENDING STRENGTH OF LAYERED LIGNOCELLULOSIC MATERIALS INFULENCED BY VENEERS MOISTURE CONTENT

Grzegorz Kowaluk – Anita Wronka

Abstract

The aim of the research was to analyze the impact of softwood veneer and hardwood thin boards moisture content, on the bonding quality and on bending strength of layered lignocellulosic materials made from these raw materials. The mentioned materials prior to glue bonding were conditioned in different air moisture content to achieve various equilibrium moisture content. The research showed that in the studied range of variability of the parameters used, no significant influence of the changed factors (in this case wood moisture content) on the bending strength and the bonding quality was found. Nevertheless, it should be added, that the moisture content of wood used to create layered composites, can have a significant impact on the parameters of the bonding process, i.e. overheating of the pressed set of wood layers, as well as on the detailed technological guidelines for pressure control in the press as a function of pressing time.

Key words: *wood moisture content, equilibrium moisture content, conditioning, bonding quality, bending, tensile strength, shear strength*

INTRODUCTION

According to Mukudai and Yata (1986), the fundamental mechanism of viscoelastic behaviour of wood under moisture change is the looseness of the interface between the S1 and S2 cell wall layers. Going from the sub-micro- to macro scale, that looseness can lead to decrease the mechanical strength of wood. Moisture content changes have a significant impact in case of composite materials, like wood mechanically enhanced by fiber – reinforced polymers (FRP) (Zhou *et al.* 2015). The macroscopic tests showed that the mechanical properties and fracture behaviour of such composites notably change under various levels of air humidity. The moisture absorbed by such multi – layer system critically determines the mechanical features of the entire system. Kläusler *et al.* (2013) confirmed, that in case of various ambient moisture conditions (5 – 95% relative humidity), the tensile strength and modulus of elasticity of wood bonded with use one component polyurethane or melamine – urea – formaldehyde resin depends linearly. Both mentioned mechanical parameters decreased remarkably with increased relative humidity. In case of plywood production, the moisture content of veneers is counted as a one of most important factor influencing the bonding strength (Demirkir *et al.* 2013). The significance of wood moisture content and ambient relative humidity was investigated by Bomba *et al.* (2014). In the mentioned research it has been confirmed, that in a humid environment,

Warsaw University of Life Sciences – SGGW, Nowoursynowska Str. 159, 02-776 Warsaw, Poland
e-mail: grzegorz_kowaluk@sggw.pl

the strength of joints created with use PVAc (poly(vinyl acetate)) glue falls below the minimum of the standardized value. The bonding and bond resistance of white oak, sugar maple, aspen, Sitka spruce, southern yellow pine, and ipe have been tested by Frihart *et al.* (2008). The achieved data indicate, that the wood properties greatly influence the internal and/or interfacial stress and thus the durability of the bonded assembly.

The goal of this research was to analyze the impact of softwood veneer and hardwood thin boards moisture content, on the bonding quality and on bending strength of layered lignocellulosic materials made from these raw materials.

MATERIALS AND METHODS

Veneers

The study used pine (*Pinus sylvestris* L.) with a nominal thickness of 3.2 mm, circumferentially cut. The veneers have been obtained from one of the plants, industrially producing the veneers with the thickness as above. The dimensions of the sheets in which it was delivered for testing were approx. 1000 x 1000 mm^2.

The tests were also carried out on samples of oak boards (*Quercus robur* L.) with a nominal thickness of 3 mm and a humidity of approx. 5%. The boards were obtained from the industrial sawing of oak wood on a frame saw.

Glue mass

A glue mass based on an industrial urea – formaldehyde resin was used to bond the composite layers. A hardener was added to the resin in such a way that the curing time of the composite was not longer than 120 seconds at 120°C.

Wood conditioning

In order to prepare the research material to determine the influence of wood moisture on the gluing quality and selected strength properties of lignocellulosic layered composites, the above mentioned raw material, previously formatted to 320 x 320 mm^2 for pine *(Pinus Sylvestris* L.) and 320 x 120 mm^2 for oak *(Quercus* L.), has been conditioned at 20°C in a climatic chamber, which is part of a set of devices for synergistic modification and analysis of the properties of wood materials, in which the air parameters (temperature and humidity) are computer controlled. The set air relative humidity levels were as follow: 10, 35, 64, 75, 92 and 95%. For each of the mentioned humidity levels, sets of pre-samples were prepared, in a number enabling the preparation of not less than 12 samples from each wood species, each humidity variant for each type of test.

The conditioning was conducted to the weight stabilization state, in which the weight difference of a single pre-sample, measured at 24h intervals, was not higher than 1%. For this purpose, 5 sheets of each type of wood were inspected.

The final equilibrium moisture of the conditioned materials was determined by a gravimetric method, using for this purpose 5 samples with dimensions of 50 x 50 mm^2 from each type of wood for each of the applied climates.

Preparation of composites – bonding

After the conditioning process, lignocellulosic composites were made, consisting of 2 layers of coniferous and deciduous wood, respectively, mentioned above, bonded with the mentioned adhesive mass, applied in an amount of 180 g/m^2 per single bonding line, pressed at 120°C for 300 seconds. at a maximum unit pressure of 1.5 MPa.

Bonding quality tests, as well as bending strength during static bending, were carried out in accordance with the methodology described in the following standards: EN 310:1994

and EN 314-1:2007. For each of the above mentioned tests, no less than 12 samples from each wood species variant and a given humidity during the conditioning were used. The glued layered materials were cut into samples according to the above mentioned standards, after which the samples were subjected to conditioning at 20°C / 65% air relative humidity to stabilize the samples weight.

The studies used, among others, an universal testing machine, which is part of a set of devices for synergistic modification and analysis of wood materials properties.

RESULTS AND DISCUSSION

Equilibrium moisture content of conditioned materials

The obtained equilibrium moisture content of conditioned wood materials is shown in fig. 1. As it can be seen from the figure below, in the applied air relative humidity, the equilibrium moisture content of the pine wood varied from 2.2% to 20.4%, and the moisture content of the oak wood varied from 2.6% to 22%. It was found that the moisture content level of oak wood was on average almost 14 percentage points higher than the moisture content of pine wood.
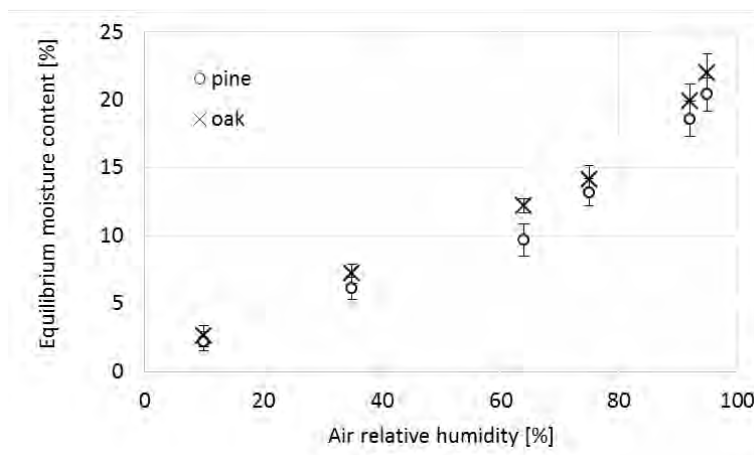
Fig. 1. Equilibrium moisture content of veneers conditioned in variable air relative humidity

Bending strength

The results of the bending test of samples made of wood conditioned before gluing in different humidity conditions are shown in fig. 2. As it can be seen from the data presented, the moisture content of the wood before gluing slightly affects the bending strength of the layered composite made of the mentioned wood. In the case of pine wood, with the increase of its moisture content from 2.2% to 9.7%, there was a slight increase in the bending strength of the layered composites. This increase was from 37 N/mm^2 for moisture content of 2.2% to 44 N/mm^2 for moisture content of 9.7%, and it was the highest value of strength in the tested range of moisture content of wood. With further increase in humidity, the strength slightly decreased to 40 N/mm^2 for 20.4% moisture content. In the case of oak wood, the relationship was similar. However, the hgher values of bending strenght have been obtained for oak wood, in regards to pine wood: maximum, 47 N/mm^2 for moisture content of 12.2% and minimum, 39 N/mm^2 for 2.6% moisture content. It should be added, that in the case of both, pine and oak wood, taking into account

the dispersion of individual results of the bending strength test, around the average values, presented in fig. 2, there is no basis for claiming the statistical significance of the differences of individual average values.
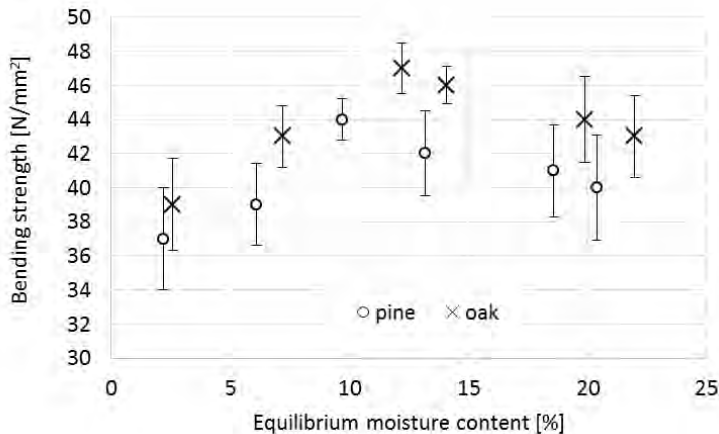
Fig. 2. Bending strength of bonded composites influenced by equilibrium moisture content of veneers

Bonding quality

The results of the tensile shear strength tests of the lignocellulosic composites, made of wood conditioned in different humidity conditions before bonding, are shown in fig. 3. The presented data show that the tensile shear strength of the tested samples increased slightly in the case of samples made of wood with an equilibrium moisture of 9.7% and 12.2% for pine and oak, respectively. The maximum strength values, obtained for these variants, were 4.2 N/mm^2 for pine and 6.9 N/mm^2 for oak. With a further increase in moisture content, a slight decrease in tensile shear strength was noted.

It is worth noting that both, in the case of pine and oak wood, taking into account the dispersion of individual tensile shear strength test results around the mean values presented in fig. 3, there were no statistically significant differences between individual mean values.
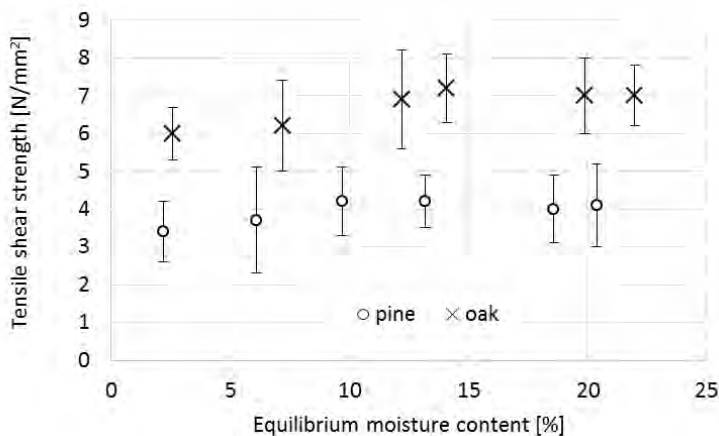
Fig. 3. Tensile shear strength of bonded composites influenced by veneers equilibrium moisture content

When testing the tensile shear strength of the prepared layered composites, the destruction of the samples was also observed. The observation concerned the estimation of the share of the surface of destruction of samples in a wood substance or in bonding line. Based on the observations made, it was found that the destruction of the tested samples occurred generally (over 98% of the total number of samples tested) in the wood substance. It should be added that such a trend is desirable from both producers of composite wood materials, and from the point of view of glue producers. Examples of various forms of destruction of the tested samples are shown in fig. 4.

Fig. 4. An example of bonded sample damaged in wood structure (left) and in bond line (right)

The analysis of the results of the bending strength test as well as the quality of bonding samples of lignocellulosic composites made from various types of wood (pine and oak), conditioned before gluing in different air humidity conditions (from 10% to 95% relative humidity), allows to conclude that there is no significant influence of changed parameters (in this case wood moisture content) on the mentioned strength. Several factors can influence this fact. One of them is the presence of water in the adhesive mass, the amount of which is much higher than in conditioned wood, even with the highest moisture obtained. The second factor is the relatively long pressing time, dictated by the necessity of curing the adhesive mass to achieve a proper joint. During the pressing, heat is transferred through the wood structure, and the temperature of the press shelves used, 120°C, leads to a significant reduction in the humidity of the bonded wood. Hence, the influence of wood moisture content on the mechanical strength of the samples is minimized. For intensive removal of moisture from glued materials, especially when reducing the pressing pressure and opening the press, especially in the case of samples with higher humidity, it was necessary to take special care at this stage to prevent delamination of the glued composite.

CONCLUSIONS

The paper presents the results of research and their analysis in terms of bending strength and bonding quality of lignocellulosic composites made from various types of wood (pine and oak), conditioned before gluing in different air humidity conditions (from 10% to 95% relative humidity).

The research showed that in the studied range of variability of the parameters used, no significant influence of the changed factors (in this case wood moisture content) on the bending strength and the gluing quality was found. Nevertheless, it should be added that the moisture content of wood used to produce the layered composites, can have a significant impact on the parameters of the bonding process, i.e. overheating of the pressed set of wood layers, as well as on the detailed technological guidelines for pressure control in the press as a function of pressing time.

ACKNOWLEDGEMENTS

REFERENCES

Bomba, J., Šedivka, P., Böhm, M., & Devera, M. (2014). Influence of Moisture Content on the Bond Strength and Water Resistance of Bonded Wood Joints. BioResources. https://doi.org/10.15376/biores.9.3.5208-5218

Demirkir, C., Özsahin, Ş., Aydin, I., & Colakoglu, G. (2013). Optimization of some panel manufacturing parameters for the best bonding strength of plywood. International Journal of Adhesion and Adhesives. https://doi.org/10.1016/j.ijadhadh.2013.05.007

EN 310:1994. Wood – based panels. Determination of modulus of elasticity in bending and of bending strength

EN 314-1:2007 Plywood – bonding quality – part 1: Test methods

Frihart, C. R., Yelle, D. J., & Wiedenhoeft, A. C. (2008). What Does Moisture-Related Durability of Wood Bonds Mean? In Proceedings of the Final Conference on COST@34 Bonding of Timber

Kläusler, O., Clauß, S., Lübke, L., Trachsel, J., & Niemz, P. (2013). Influence of moisture on stress-strain behaviour of adhesives used for structural bonding of wood. International Journal of Adhesion and Adhesives.
https://doi.org/10.1016/j.ijadhadh.2013.01.015

Mukudai, J., & Yata, S. (1986). Modeling and simulation of viscoelastic behavior (tensile strain) of wood under moisture change. Wood Science and Technology.
https://doi.org/10.1007/BF00351586

Zhou, A., Tam, L. H., Yu, Z., & Lau, D. (2015). Effect of moisture on the mechanical properties of CFRP-wood composite: An experimental and atomistic investigation. Composites Part B: Engineering. https://doi.org/10.1016/j.compositesb.2014.10.051

DETERMINATION OF THE DEFECTS IN THE PRODUCTION OF FURNITURE BENT PANEL BOARDS

Vladimir Mihailov – Dimitar Angelski – Vasil Merdzhanov

Abstract

The use of vacuum membrane technology makes the manufacturing of bent panel boards in something routine and easy compared to the costly molding technology used up to 10 years ago that were also difficult to manufacture. This article examines the problems with the defects in the production of bent furniture boards and their subsequent lining. The technological possibilities for making such details are compared by using the adhesive dispersions and coating materials used. The resulting defects in the production of curved furniture boards are examined as well as the subsequent lining with synthetic cladding materials. The defects are grouped, analyzed and represented graphically.

Key words: *defects, membrane technologies, vacuum, adhesive dispersions, cladding materials*

INTRODUCTION

The most common lamination processes apply overlay material to the substrate by cold or hot pressing with either flat (platen) or continuous (roll or double belt) laminating presses.

Because each type of overlay material has unique properties and lamination requirements, the choice of laminating material introduces variables that affect the laminating process and influence the performance of the finished product. As with the most lining technologies and the vacuum technology, it is very important to follow the technological regimes for obtaining non-defective production. Defects in bent furniture boards made with vacuum membrane technologies can be grouped into two main groups - those that appear between the individual layers of the boards and those that are on the surface (of the lined material) of the workpiece. This paper describes the defects obtained using the most commonly used adhesive in making such details - PVA dispersion recommended for membrane presses. Wherever the defects are formed in the structure of the parts or their surface, they are highly dependent on the satisfactory adhesion achieved between the details or the individual elements. Adhesion is a complex physico-chemical phenomenon for which, however, there is not a rigorous theoretical definition. Adhesion is difficult to define, and an entirely satisfactory definition has not been found (Landrock A. 2008). The adhesion strength is the bond between the lined material and the substrate, which can be the weakest link of the system. Due to this fact, adhesive systems must be rationally selected to ensure satisfactory adhesion between both the elements forming the bent furniture boards and the coating materials such as PVC foil or veneer (Angelski D., Mihailov V., 2017).

University of Forestry, Kliment Ohridski Bd. 10, 1756 Sofia, Bulgaria
e-mail: vladko86mihailov@gmail

MATERIAL AND METHODS

The test samples are made of high density fiberboard - HDF and poplar plywood The HDF boards are with a thickness of 2,8 mm produced by "Kronospan" and a density of 900 kg/ m^3. The plywood boards are produced by "WELDE Bulgaria" with a thickness of 6 mm and density of 500 kg/ m^3. One pattern with corresponding internal radius of curvature 100 mm was used to make them. The test body is made up of 3 lamellas with sizes 260/100 mm bonded with polyvinyl acetate adhesive - PVA glue with trade mark of Jowacoll / Jowacoll 103.05. The glue utilization used is the minimum of 160 g/m2 being unilaterally applied to the lamellas. For gluing the cladding material three quantities of glue were chosen – 100, 160, 220 g/m^2. For cladding material was chosen polyvinyl chloride - PVC mat foil by manufacturing by "Skai", Germany, 3D formable with thickness of 0,4 mm (Fig 1). The reverse side of the foils is coated with primer to ensure a safe and temperature-resistant bond.

Figure 1. 1 - Test samples series; 2 - Test sample vacumed under the rubber membrane and the matrix of bending with 100 mm radius of curvature

The test samples were made with a vacuum mebrane press equipt with a rubber mebrane of thikness of 3 mm and 600 % elasticity. The technological regime chossen for the producing them is 30 min of pressing time and the value of the vacuum applied under the membrane is -0,04 N/mm^2. After the producing the test samples are left of 24 hours of free stay. The tehnological regimes is determined that the test samples are glued and linned at once.

RESULTS

After the free stay the sereis of the bent furniture boards can be monitored two groups of defects – the first - of delamination of the core of the lammelas and second - on the surface by the cladding material of the samples. The amount of the glue plays a very important part in ensuring faultless cladding of the bent furniture boards. By the testing the adhesion by the pull-off test method, the greater the volume does not increase the adhesion strength. By the type of the cladding material – PVC foil, as its known it's a synthetic material and it's very difficult to achieve reliable adhesion with the used PVA adhesion, even it has primer applied on the back of the used foil (Fig. 2).

Figure 2. 1 - Test samples with poor adhesion between the PVC foil and the substarte;
2 – No adhesion can be seen by the ends of the samples, of the fact that the glue dries too fast by the initial vacuum

From the carried-out study, it was found that for the non-defective producing of bent furniture boards it is extremely important to consider the duration of the working cycle defining the time from the beginning of the vacuuming to reaching the defined vacuum. When the maximum vacuum is reached quickly, the test samples are being destroyed. The cracks are at the boundary between the radius of curvature and the straight parts of the template. For this also helps the high density of the material used, which makes it difficult to bend. On the other hand, the applied adhesive moistens the surfaces of the lamellas and plasticizes the material. It was found that in order to avoid this destruction the vacuuming time must be between 120 and 180 s. For a longer vacuum time, the glue partially dries and the required technological strength is not reached. This leads to the self debonding of the test samples, or the adhesion dries faster on the outer ends of the test sample and there is no adhesion observed (Fig. 3).

Figure 3. 1 - Self debonding of the test samples

The test samples made with the poplar plywood, can observed delamination of the lamellas, or cracks of the outer lamella of the plywood. Also, here affects the time of the initial vacuum – it should be between 120 and 180 s. Another way to prevent these types of delamination or cracks is to put an additional piece of bendable plywood between the test sample and the membrane, so that it distributes the pressure applied by the membrane more evenly.

By both series of test samples, from HDF lamellas and poplar plywood, can the observe a typical defect for the choosen matrix. The cracks are located in the area between the flat part of the matrix and that with a curvature of 100 mm radius. That could be explained of the small radius that was choosen and the big pressure that is loaded the outher

lamella of the bent board in that area (Fig. 4). The upper lamellas are loaded of crutical tensile stress, that exceds the strenght of the used material.
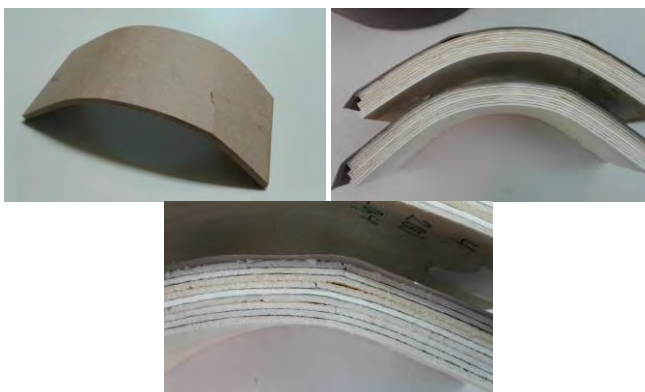
Figure 4. Cracks of the outher lamella tahat is loaded to critical tensile stress

When the used adhesive is choosen with higher consumable amount from the recomended of the manufacturer a wavy surface of the foil can monitored. That fenomen is called „orange peel", and its appereance can be explained of the physical nature of the cladding material. The PVC foil doesn't passes water to evaporated and stays traped under the foil. This leads to buckling of the foil and uneven surface. The traped plases more glue can monitored at it dries. (Fig. 5)

Figure 5. Uneven surface of the foil with bubles in the end of the sample, by the high amount of the adhesive

CONCLUSION

Based on the research, the following conclusions could be made:

- The amount of the glue plays a very important part in ensuring faultless cladding of the bent furniture boards. Higher amount of PVA glue doesn't make the joint between the substrate and PVC foil.
- For achieving more reliable adhesion between the substrate and the PVC foil, it has to be applied primer of the back surface of the foil.

- The duration of the working cycle defining the time from the beginning of the vacuuming to reaching the defined vacuum. When the maximum vacuum is reached quickly, the test samples are being destroyed.
- Another way to prevent the delamination or cracks is to put an additional piece of bendable plywood between the test sample and the membrane, so that it distributes the pressure applied by the membrane more evenly.
- Higher consumable amount from the recomended of the manufacturer a wavy surface of the foil can monitored. That fenomen is called „orange peel".

REFERENCES

1. Angelski D., Mihailov V., (2017), The influence of various types of adhesive on the adhesion strength between bonded HPL and furniture boards
2. Landrock A. H., Ebnesajjad S. (2008) Adhesives Technology Handbook. William Andrew - Technology & Engineering, 475 p. - ISBN 9780815516019
3. Kayis S., Bektas I., Kilic Ak A. (2016): Comparing The Technological Properties Of Mdf's Coated With Pvc Folios Using Wrapping And Membrane Press Methods, International Furniture Congress. Mugla
4. Zosel A. (1991) Effect of cross-linking on tack and peel strength of polymers. The Journal of Adhesion, 34: 201-209.
5. Slabeyoga G., Smidriakova M., Petrilak J., Adhesion of foils to MDF board, (2016) Annals of Warsaw University of Life Sciences – SGGW

THE INFLUENCE OF HEAT TREATMENT ON GRANULARITY OF SAND WOOD DUST

Alena Očkajová[1] – **Martin Kučerka**[1] – **Adrián Banski**[2]

Abstract

The paper deals with the granular analysis of the sand dust of heat-treated wood from red meranti, depending on the treatment temperature of 160 °C, 180 °C, 200 °C and 220 °C. The proportion of dust fractions with a particle size ≤ 0.08 mm was determined by sieving. The percentage shares of these fractions are similar for natural wood 84.17 % and temperature of treatment at 160 °C (87.18 %), 180 °C (86.23 %) and 200 °C (80.79 %). A significantly lower proportion of dust fractions with a particle size ≤ 0.08 mm occurred at a temperature of 220 °C, only 74.48 %. We assume that the main factor that caused the decrease of the dust fraction with a particle size ≤ 0.08 mm at 220 °C is the reduction of wood density.

Key words: *thermowood, sanding, wood dust, granular analysis*

INTRODUCTION

Wood is one of the most interesting natural materials that has many uses. Despite its many positive attributes, it also has certain negative properties - dimensional instability due to swelling, shrinking or attack by pests or rot. And therefore, users of this natural material are constantly striving to minimize the negative properties of wood in a variety of ways. One of them is the treatment by increased temperature, thermowood. The basis of heat, steam and water treatment is that no harmful chemicals are used to change the properties of the wood, resulting in wood, with new physicochemical properties that increase its utility properties similar to those of tropical woods (Thermowood 2016). Thermowood has two standards for treatment. Thermo-S is an increase in wood stability and Thermo-D is an increase in its durability (ThermoWood Handbook 2003). Each type of wood can be heat-treated, but each wood has its own characteristics, so the thermal treatment parameters are modified for each type of wood (or similar species) in terms of optimizing the resulting quality (Kminiak, Kubš 2016).

The advantages of thermowood include: reduction of moisture absorption, dimensional stability, biological resistance, attractive appearance of heat treated wood, application of material without surface treatment, high durability of heat treated wood, removal of resin from the material, reduction of thermal conductivity, increase of hardness of the wood surface, increase of crack resistance. Heat treated wood has a higher static load in terms of mechanical properties, but the disadvantage is that its dynamic strength values are reduced – reducing both bending and toughness, which results in the wood being more brittle.

[1] Matej Bel University, Tajovského 40, 974 01 Banská Bystrica
e-mail: alena.ockajova@umb.sk, martin.kucerka@umb.sk
[2] Technical University in Zvolen, T. G. Masaryka 24, 960 53 Zvolen
e-mail: banski@tuzvo.sk

The change of physical-mechanical properties results mainly from the change in chemical properties of wood. The high temperatures degrade some wood building polymers to form of new water-insoluble substances, as well as substances with toxic or repellent effects. Wood treated in this way is more resistant to biological pests and its hygroscopicity decreases. Strength and some other mechanical properties of the heat treated wood are reduced due to chemical changes in the anatomical structure of the wood, where cracks in the cell walls are created and wood becoming more fragile. Fragility and cracks cause a reduction in wood strength and toughness (Reinprecht, Vidholdová 2008, Kačíková, Kačík 2011, Kminiak, Gaff 2015, ThermoWood Handbook, 2003). In general, as the temperature is higher and the duration of the action longer, the reactions and the changes in wood are more intense, the deciduous species of wood with a lower proportion of lignin are thermally modified more intensively than the coniferous species of wood.

Thermowood is the subject of many researches. The aims of these researches are the changes in the physical-mechanical properties (Gunduz *et al*. 2009), the chemical properties (Reinprecht, Vidholdová 2008, Kačíková, Kačík 2011, ThermoWood Handbook 2003, Čabalová *et al*. 2016), the quality of the obtained surface (Budakci *et al*. 2013, Kvietková *et al*. 2015, Vančo *et al*. 2017, Kaplan *et al*. 2018) the colour of the wood, the woodworking (Sandak *et al*. 2017, Reinprecht, Vidholdová 2008, Král, Hrázský 2005), the workability in the context of energy consumption (Kubš, Gaff, Barcík 2016), the stability against the impact of weather (Panayot, Jivko 2008, Yildiz *et al*. 2011), the granularity of the chips (Barcík, Gašparík 2014), or sawdust (Dzurenda, Orlowski, Grzeskiewicz 2010).

The aim of the present paper is to determine the granularity of sand wood dust obtained from the sanding of heat-treated wood (red meranti) along the wood grains on a vertical belt sander with a manual pressure of samples on the sanding belt, depending on the heat treatment of samples (of 160 °C, 180 °C, 200 °C and 220 °C), focusing in particular on the percentage share of particles measuring ≤ 0.08 mm, which does not settle or sediment in the working environment, and is a source of both health and safety risks.

MATERIAL AND METHODS

Experimental samples: Red meranti (*Shorea acuminata*). The red meranti was purchased in a subcontracting company and processed in test samples measuring 20 x 100 mm with a length of approximately 700 mm. The samples were then dried to a moisture content of 8 %. The entire process was performed in the Research and Development Workshops of the Technical University in Zvolen.

Heat treatment and sample processing methods

The processed samples were heat-treated in the Arborét FLD (ČZU Praha) in the city of Kostelec nad Černými lesy. The S400/03 (LAC Ltd., Czech Republic) chamber was used for thermal treatment, Fig. 1, designed to heat the wood with ThermoWood technology, with the parameters listed in Tab. 1. Five samples were prepared for experiment.

Fig. 1 Chamber S400/03

Tab. 1 Chamber parameters S400/3

Maximal temperature (°C)	300
Volume (l)	380
External dimensions - w×h×d (mm)	1400×1850×1200
Internal dimensions - w×h×d (mm)	800×800×600
Weight(kg)	350
Fan	1
Input (kW)	6,0

The heat treatment procedure for the individual temperatures was as follows: the application of temperature sensors and a humidity sensor on the samples, the storage of samples in the chamber, the closure and locking of the chamber door, the setting of the heat treatment parameters with a computer program – target temperature, steepness [°C /hr.] for heating and cooling, heat treatment of samples, sample collection from the chamber.

The thermal treatment was realized at 160, 180, 200 and 220 °C in six phases: the 1st – increase of temperature to 40 °C, the 2nd – increase of temperature to 130 °C, drying, the 3rd – heat treatment – heating to working temperature, the 4th – heat treatment – working temperature of 3 hours, the 5th – cooling to 130 °C and humidity treatment, the 6th – cooling to 60 °C with humidity treatment at the level of 4 – 7 %.
The process is completed when the temperature reaches 60 °C.

Due to the space in which the samples were stored, they were placed in the dryer at approximately 10 °C. The samples taken from the dryer after completing the heat treatment process had a temperature of about 40 °C. The heating, conditioning and cooling phases of the wood samples are shown in Fig. 2 and the time intervals are shown in Tab. 2.
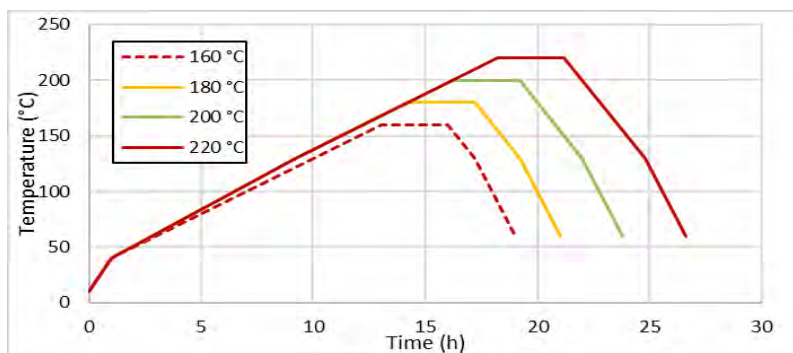
Fig. 2 Phases of heat treatment of red meranti

Tab.2 Time intervals of the thermal modification of the wood – red meranti

Working temperature (°C)	Phase (h)						$\sum$ (h)
	I.	II.	III.	IV.	V.	VI.	
160	1,0	9,0	3,0	3,0	1,2	1,8	19,0
180	1,0	8,2	5,0	3,0	2,0	1,8	21,0
200	1,0	8,2	7,0	3,0	2,8	1,8	23,8
220	1,0	8,2	9,0	3,0	3,6	1,8	26,6

Sanding machine

JET JSG-96 narrow belt sander, cutting speed of 10 m.s^{-1}, HIOLIT XO P 80 sanding belt with a grain of 80, individual pressure of wood sample on sanding belt, laboratory experiments. A sharp sanding belt was used for each heat treatment variant.

Granular analysis

Samples for the granular wood dust analysis were taken isokinetically from the suction pipe of the sander in accordance with STN 9096 (83 4610): "The manual determination of the mass concentration of solid pollutants" during the sanding of individual heat-treated wood samples.

The granularity of the wooden sand dust was found by sieving. For this purpose, a special set of superimposed sieves (2 mm, 1 mm, 0.5 mm, 0.25 mm, 0.125 mm, 0.080 mm, 0.063 mm, 0.032 mm and the bottom) was used on the vibrating stand of the sieving machine (Retsch AS 200c) with an adjustable sieving interruption frequency (20 seconds) and a sieve deflection amplitude (2mm/g), in accordance with STN 153105/STN ISO 3310-1.

The granular composition was obtained by weighing the percentages remaining on the sieves after sieving on a Radwag WPS 510/C/2 electronic weighing scale, with a capacity of 510 g and an accuracy of weighing at 0.001 g. For each variant, three sievings were performed and the results are given as their mean value.

RESULTS AND DISCUSSION

The results of the experiment are presented in the Tab. 3.

Tab.3 Granularity of sand wood dust – red meranti heat treated

Dimension of sieve mesh [mm]	Percentage of fractions of sand dust [%]				
	Meranti				
	natur	160 [°C]	180 [°C]	200 [°C]	220 [°C]
2	0.00	0.00	0.00	0.00	0.00
1	0.00	0.10	0.00	0.00	0.00
0.5	0.20	0.10	0.35	0.45	0.00
0.25	0.71	0.45	0.80	0.91	1.41
0.125	14.95	11.18	12.64	17.88	24.12
0.08	31.14	23.31	27.82	31.33	35.45
0.063	11.26	14.98	17.91	13.81	10.21
0.032	34.84	34.70	26.47	24.70	22.23
Bottom	6.93	14.19	14.03	10.94	6.59
Particles below 0.1	**84.17**	**87.18**	**86.23**	**80.79**	**74.48**

Meranti is tropical wood and is characterized as a typical deciduous scattered-porous wood with similar physical and mechanical properties as beech. Based on the results of the granular analysis it can be stated that the percentage shares on the individual sieves are characterized by the fact that 2 kinds of particles are produced (Očkajová, Beljaková, Luptáková 2008), with the highest percentage shares on sieve 0.08 mm (from 23.31 % to 35.45 %) and on the sieve 0.032 mm (from 22,23 % to 34,84 %). The percentage shares of fractions ≤ 0.08 mm is similar for natural wood (84.17 %) as well as for temperatures 160° C (87.18 %), 180 ° C (86.23 %). A certain decrease in the percentage share of particles with a dimension of ≤ 0.08 mm is at temperature of 200 °C (80.79 %), which represents a decrease of this fraction by about 4 %, a significant decrease occurs at 220 °C when this percentage share is only 74.48 %, which is about 11% less than at natural wood. At this treatment temperature, the high percentage share of particles is on sieve 0.125 mm (up to 24.12 %) compared to other temperatures of treatment where the value ranges from 11.18 to 17.88 %. For wood treatment to increase its stability to about 180 °C (Thermo-S) it can be stated that the granular composition is similar to that of natural wood. For thermal treatment up to 220 °C to increase its durability (Thermo-D), granularity varies toward larger fractions, which declare the results of particle stratification on individual sieves.

The density of meranti by (Wagenführ, Scheiber 1985) is 670 kg.m^{-3}, but according to previous research by Očkajová, Banski, Rončka (2006) the measured density for meranti was lower, only 496 kg.m^{-3} and therefore the obtained values of percentage shares of particles ≤ 0.08 mm are lower compared to beech, where this value is 87.23 % for the vibrating sander (Marková *et al.* 2016) 91.95 % for narrow-belt sander (Očkajová, Banski 2013) 94.28 % for hand-belt sander for sanding perpendicular to wood grains and 96.29 % for hand disk sander Očkajová *et al.* (2014).

By Reinprecht, Vidholdová (2008), Král, Hrázský (2005) in machining process of the heat treated wood, the problem can be in creation of more fine fraction of dust, what is caused by increasing brittleness and decreasing some mechanical properties. This assumption is confirmed by Dzurenda *et al.* (2010) during sawing and by Barcík, Gašparík (2014) during milling, although a statistically significant difference is not reported.

In the case of sanding, however, it is necessary to mention the change in physical properties of heat-treated wood, mainly the decrease in weight and density. The density of the heat-treated spruce through the Platowood method decreased by 10 %, (ThermoWood Hhandbook, 2003, www.platowood.nl), similar result is for beech (Maulis 2009). Gunduz

et al. (2009) reporting a decrease in the density of common alder at a treatment temperature of 210 °C for 12 hours by 16.12 %. According to preliminary our results (so far not published), the density of samples decreased approx. from 18 % (spruce) to 21.5 % (oak) at a temperature of 220 °C.

Based on many granular analyses of various wood sand dusts, from the longitudinal sanding in previous research, we found that the granularity of sand wood dust significantly changes with density, because when sanding wood with low density, the individual chips are easier to separate than for wood with higher density (Hammilä, Usenius 1999, Očkajová, Banski 2009). With increasing of wood density (cca 42 %) in the tested interval from 450 kg.m^{-3} ÷ 774 kg.m^{-3} (spruce 450 kg.m^{-3}, poplar 487 kg.m^{-3}, alder 527 kg.m^{-3}, pine 551 kg.m^{-3}, maple 619 kg.m^{-3}, beech 624 kg.m^{-3}, oak 774 kg.m^{-3}) for sanding process (hand belt sander GBS 100 AE), there is increased the percentage share of small fractions (particle size < 100 μm) from 4.2 % to 53.06 % (Očkajová, Banski 2009). So we assume that our granular analysis results are substantially influenced by the decreasing density of heat-treated wood.

CONCLUSION

The results of the experimental measurements can be summarized as follows:

- in sanding process of red meranti the assumption that with the increasing temperature of the wood treatment the proportion of dust fractions increases too has not been confirmed,
- the lowest value of dust fractions measuring ≤ 0.08 mm was obtained at treatment temperature of 220 °C; when this percentage share is only 74.48 %, which is about 11 % less than at natural wood,
- we assume that the main factor influencing the granular analysis of heat-treated wood in the sanding process is the decreasing density of heat-treated wood.

ACKNOWLEDGEMENT

REFERENCES

BARCÍK, Š., GAŠPARÍK, M. 2014. Effect of Tool and Milling Parameters on the Size Distribution of Splinters of Planed Native and Thermally Modified Beech Wood. In BioResources, 9(1): 1346-1360.
BUDAKCI, M., ILCE, A. C., GURLEYEN, T., UTAR, M. 2013. Determination of the Surface Roughness of Heat-Treated Wood Materials Planed by the Cutters of a Horizontal Milling Machine. In BioResources, 8(3): 3189-3199.
ČABALOVÁ, I., KAČÍK, F., ZACHAR, M., DÚBRAVSKÝ, R. 2016. Chemical changes of hardwoods at thermal loading by radiant heating. In Acta Facultatis Xylologiae. Zvolen: Technical University in Zvolen, 58(1): s. 43-50.

DZURENDA, L., ORLOWSKI, K., GRZESKIEWICZ, M. 2010. Effect of thermal modification of oak wood on sawdust granularity. In Drvna Industrija, 61(2): s. 89-94.

GUNDUZ, G., KORKUT, S., AYDEMIR, D., BEKAR, I. 2009. The density, compression strength and surface hardness of heat-treated hornbeam (Carpinus betulus L.) wood. Maderas. Ciencia y tecnología, 11(1): 61-70.

HAMMILÄ, P., USENIUS, A. 1999. Reducing the amount of noise and dust in NC-milling. In Proceedings of the 14th IWMS. Volume II. France, 355-365.

KAČÍKOVÁ, D., KAČÍK, F. 2011. Chemical and mechanical changes during thermal treatment of wood. (Chemické a mechanické zmeny dreva pri termickej úprave). TU vo Zvolene. ISBN 978-80-228-2249-7

KAPLAN, L., KVIETKOVÁ, M., SEDLECKÝ, M. 2018. Effect of the Interaction between Thermal Modification Temperature and Cutting Parameters on the Quality of Oak Wood. In BioResources, 13(1): 1251-1264; DOI: 10.15376/biores.13.1.1251-1264.

KMINIAK, R., GAFF, M. 2015. Roughness of surface created by transversal sawing of spruce, beech, and oak wood. In BioResources, 10(2): 2873-2887; DOI: 10.15376/biores.10.2.2873-2887.

KMINIAK, R., KUBŠ, J. 2016. Cutting Power during Cross-Cutting of Selected Wood Species with a Circular Saw. In BioResources, 11(4): 10528-10539; DOI: 10.15376/biores.11.4.10528-10539.

KRÁL, P., HRÁZSKÝ, J. 2005. Využití nového materiálu ThermoWood. Materiály pro stavbu 1/2005

KUBŠ, J., GAFF, M., BARCÍK, Š. 2016. Factors Affecting the Consumption of Energy during the Milling of Thermally Modified and Unmodified Beech Wood. In BioResources, 11(1): 736-747.

KVIETKOVÁ, M., GAFF, M., GAŠPARÍK, M., KAPLAN, L., BARCÍK, Š. 2015. Surface Quality of Milled Birch Wood after Thermal Treatment at Various Temperatures. In BioResources, 10(4): 6512-6521.

MARKOVÁ, I., MRAČKOVÁ, I., OČKAJOVÁ, A., LADOMERSKÝ, J. 2016. Granulometry of selected wood dust species of dust from orbital sanders. In Wood research, 61(6): 983-992. ISSN 1336-4561.

MAULIS, V. 2009. Production technology and evaluation of thermal modified wood. (Technologie a zhodnocení vybraných vlastností dřeva modifikovaného teplem). M.S. Thesis, Czech University of Life Sciences, Prague.

OČKAJOVÁ, A., BANSKI, A. 2009. Characteristic of dust from wood sanding process. In Wood machining and processing – produkt quality and waste characteristics. Monography, Warsaw: WULS – SGGW Press: 116-141.

OČKAJOVÁ, A., BANSKI, A. 2013. Granulometria drevného brúsneho prachu z úzko-pásovej brúsky. In Acta Facultatis Xylologiae. Zvolen: Technical University in Zvolen, 55(1): s. 85-90.

OČKAJOVÁ, A., BANSKI, A., RONČKA, J. 2006. Dust in Woodworking Plants and Possibilities of its Reducing. In 1st Jubilee Scientific Conference Manufacturing Engineering in Time of Information Society. Gdansk University of Technology, 255-260. ISBN 83-88579-61-4

OČKAJOVÁ, A., BELJAKOVÁ, A., LUPTÁKOVÁ, J. 2008. Selected properties of spruce dust generated from sanding operations. In Drvna industrija, 59(1): 3-10.

OČKAJOVÁ, A., STEBILA, J., RYBAKOWSKI, M., ROGOZINSKI, T., KRIŠŤÁK, Ľ., ĽUPTÁKOVÁ, J.: The granularity of dust particles when sanding wood and wood-based materials. In: Advanced Materials Research. Vol. 1001 (2014) pp 432-437. ISBN-13: 978-3-03835-198-6

PANAYOT, A., JIVKO V. G. 2008. Weathering of polymer coatings, formed on thermally modified wood. In Chip and chipless woodworking processes: Zborník prednášok, TU vo Zvolene: 363-368. ISBN 978-80-228-1913-8

REINPRECHT, L., VIDHOLDOVÁ, Z. 2008. ThermoWood - preparing, properties and applications. Thermodrevo - príprava, vlastnosti a aplikácie. TU Zvolen. ISBN 978-80-228-1920-6

SANDAK, J., GOLI, G., CETERA, P., SANDAK, A., CAVALLI, A., TODARO, L. 2017. Machinability of Minor Wooden Species before and after Modification with Thermo-Vacuum Technology. Materials 2017, 10, 121; DOI: 10.3390/ma10020121.

SEDLECKÝ, M. 2017. Surface Roughness of Medium-Density Fiberboard (MDF) and Edge-Glued Panel (EGP) After Edge Milling. In BioResources, 12(4): 8119-8133; DOI: 10.15376/biores.12.4.8119-8133.

STN ISO 9096 (83 4610): 2004. Ochrana ovzdušia. Stacionárne zdroje znečisťovania. Manuálne stanovenie hmotnostnej koncentrácie tuhých znečisťujúcich látok.

STN 1531 05/ STN ISO 3310-1: 2000. Súbor sít na laboratórne účely.

VANČO, M., MAZÁN, A., BARCÍK, Š., RAJKO, Ľ., KOLEDA, P., VYHNÁLIKOVÁ, Z., SAFIN, R. F. 2017. Impact of Selected Technological, Technical, and Material Factors on the Quality of Machined Surface at Face Milling of Thermally Modified Pine Wood. In BioResources, 12(3): 5140-5154.

WAGENFÜHR, R., SCHEIBER, CH. 1985. Holzatlas. Leipzig, VEB Fachbuchverlag Leipzig, s. 380, 428, 656.

YILDIZ, S., YILDIZ, U. C., TOMAK, E. D. 2011. The Effects of Natural Weathering on the Properties of Heat-treated Alder Wood. In BioResources, 6(3): 2504-2521.

Thermowood [online]. Špačince: Tepelne upravené vydržia večnosť, © 2016. Posledná zmena 14.6.2017 13:28 [cit. 10.4.2018].

Dostupné z: https://www.jafholz.sk/produkty/terasy/thermoborovica

ThermoWood Handbuch [online]. © 2003. [cit. 2010-04-10]. Dostupné z: https://asiakas.kotisivukone.com/files/en.thermowood.palvelee.fi/downloads/ThermoWood_Handbuch.pdf

THE EFFECT OF FULL-CELL IMPREGNATION OF PINE WOOD (*PINUS SYLVESTRIS* L.) ON THE FINE DUST CONTENT DURING SAWING ON A FRAME SAWING MACHINE

Kazimierz A. Orlowski[1] – **Daniel Chuchala**[1] – **Ladislav Dzurenda**[2]

Abstract

In this paper the results of the analysis of the effect of the impregnation treatment of pine wood on the granularity of sawdust from the sawing process on the frame sawing machine PRW 15M are presented. Granulometric analyses of chips from impregnated and unimpregnated pine wood implies that the impregnation of pine wood does not affect the size and structure of the sawdust produced. A major ≈ 95% share of the formed chips is the coarse and thick coarse fractions at a grain range of 125 µm to 2 mm. The slight difference is in the fraction of the fine fraction with a particle size of 32 - 125 µm. While the share of pine wood sawdust of unimpregnated wood is between 0.48 and 0.8%, and of the impregnated wood pine wood is 0.68 - 1.1%. This fact does not affect the efficiency of separation in fabric filters and the technological use of sawdust in the production of briquettes and pellets.

Key words: *sawdust, impregnation of wood, pine wood, sawing process, frame sawing machine*

INTRODUCTION

The increasing interest in sawdust, as a secondary raw material, in the last years, requires a proper specification of its physical properties as follows: granularity, geometric shapes and size of sawdust chips. The shape, dimensions and amount of chips depend on the form, physical and mechanical properties of the sawed wood (Beljo Lučič et al. 2009; Dzurenda et al. 2009; Dzurenda et al. 2010; Dzurenda and Orlowski 2010, 2011, 2011 a, Fujimoto et al. 2011), as well as on the shape, dimensions, and sharpness of the cutting blade, technical and technological conditions of the sawing process (Dzurenda et al. 2006; Hlásková et al. 2016; Pałubicki and Rogoziński 2016). On the contrary, Marková et al. (2018) examined granularity and size of sawdust chips not from the point of view of the further technological processes, however, they were interested in thermal parameters of beech wood dust.

Sawdust is characterized as poly-dispersion bulk material consisting of coarse and medium-coarse fractions (Hejma et al. 1981; Dzurenda 2009), i.e. bulk material with dimensions of grain over 0.3 mm, while the share of fine fractions with smaller dimensions of chips is not excluded. According to the classification parameters of bulk material described in STN 26 0070 standard, sawdust is classified as B-45UX, i.e. bulk material of fine granularity (0.5-3.5 mm), hygroscopic, low crisp and abrasive material with a tendency to crowd.

[1]Gdansk University of Technology, Narutowicza 11/12, 80-233 Gdansk, Poland
e-mail: korlowsk@pg.edu.pl, danchuch@pg.edu.pl
[2]Technical University in Zvolen, T. G. Masaryka 24, 960 53 Zvolen
e-mail: ladislav.dzurenda@tuzvo.sk

The full-cell impregnation of pine wood (*Pinus sylvestris* L.) influenced the resistance values and the accuracy of moisture content measurements (Konopka et al., 2018). For that reason, the aim of this work is to analyze the effect of the impregnation treatment of pine wood on sawdust granularity during the sawing process conducted on the frame sawing machine PRW15–M.

MATERIALS AND METHODS

Materials

The material used in the experiments was pine wood (*Pinus sylvestris* L.) impregnated and not impregnated. The wood to be used in the impregnation experiments (wood blocks $b = 50$ mm $\times H_p = 50$ mm $\times L_p = 500$ mm) was initially dried in industrial conditions until the relative moisture content was near the FSP. Next, they were full-scale impregnated in an autoclave in the industrial conditions. The impregnation process lasted 120 min, and the level of retention was 1.0 dm^3/(m^3·min). The impregnation method is based on the technique that has been described in detail by Babiński (1992), called full-cell impregnation. The blocks were placed in the impregnation solution under atmospheric pressure. The first impregnation phase lasted 25 min in a vacuum of -0.8 bar. Thereafter, a pressure of 10 bar was maintained for 55 min. After a second impregnation phase when the pressure was reduced to atmospheric, the surplus of impregnation solution was removed from the autoclave. The final impregnation step, during of which the impregnation solution is sucked out of the lumens, was carried out in a vacuum of -0.8 bar and lasted 40 min (Konopka et al. 2018). A preservative KORASIT KS2 (Kurt Obermeier Gmbh&Co KG, D) which is chracterised as a water soluble, liquid, fixative, chromate and boron free wood preservative based on copper complex compounds and a highly effective quaternary ammonium compound, was applied. Concentrate and solution of Korasit KS2 have a deep blue colour. Nevertheless, impregnated wood takes on an olive green hue. The solution can be stained with Korasit® colour pastes. The concentration of the impregnate was 3.8 %.

The other blocks in the same dimensions (58 mm $\times$ 58 mm $\times$ 500 mm) were not impregnated.

Machine tool and tools

Tests were performed on the frame sawing machine PRW15M (Fig. 1) with a hybrid dynamically balanced driving system and elliptical teeth trajectory movement (Wasielewski and Orlowski, 2002) at the Department of Manufacturing Engineering and Automation (GUT, PL). The machine settings were as follows: number of strokes of saw frame per min (n_F), 685 spm; saw frame stroke (H_F), 162 mm; number of saws in the gang (n), 5; and average cutting speed (v_c), 3.69 m·s^{-1}. The saw blades were sharp, with stellite tipped teeth: overall set (kerf width) (S_t), 2 mm; saw blade thickness (s), 0.9 mm; free length of the saw blade (L_0), 318 mm; tension stresses of saws in the gang (σ_N), 300 MPa; blade width (b), 30 mm; tooth pitch (P), 13 mm; tool side rake (γ_f), 9°; and tool side clearance (α_f), 14°. The only varying cutting parameter was feed speed, which was applied at two levels: $v_{f1} \approx 0.9$ m·min^{-1} and $v_{f2} \approx 1.72$ m·min^{-1}. This corresponds to a feed per tooth (f_z) of ~0.105 mm and ~0.2 mm, respectively. Lamellae with thicknesses of 5 ± 0.2 mm were obtained as a result of the re-sawing process. The actual value of the feed per tooth were computed on the basis of the sawing time taken from the plots of time changes of electrical power consumption (Fig.2). The mean value of feed per tooth for a sash gang saw is calculated as:

$$\bar{f}_z = \frac{1000 \cdot v_f \cdot P}{n_{RP} \cdot H_{RP}} \qquad (1)$$

where: strokes number of the frame n_{RP} = 685 1/min, stroke of the frame H_{RP} = 162 mm, P = 13 mm is a tooth pitch, and v_f in m· min^{-1} is calculated as:

$$v_f = \frac{L_p}{60 t_c} \qquad (2)$$

where: L_p is length of the sample in m, and t_c is the real cutting time taken from the plot, e.g. Fig. 2.

Figure 1. Narrow-kerf frame sawing machine (sash gang saw) PRW15–M

Sawdust collection and sieve analyses
For granulometric analyses, samples of pine sawdust (natural, not impregnated) and impregnated pine sawdust were taken isokinetically from the exhaust pipe of a frame sawing machine PRW-15 in accordance with a standard ISO 9096.
The moisture content of both types of dust samples was MC = 10%, and was determined by the weight method.
Sieve analysis was carried out on an automated vibratory screening machine Retsch AS 200 control; a set of control stainless steel sieves, diameter of sieve 200 mm, height 50 mm, diameter of sieve mesh 2 mm, 1 mm, 0.50 mm, 0.25 mm, 0.125 mm, 0.080 mm, 0.063 mm, and 0.032 mm. The residues on each sieves and bottom were weighed on a digital laboratory balance EP 200 (f. BOSCH) to an accuracy of 0.001 g. The sieving parameters were an amplitude 2 mm/(g), with an interval of 10 s, and a time of 20 min.
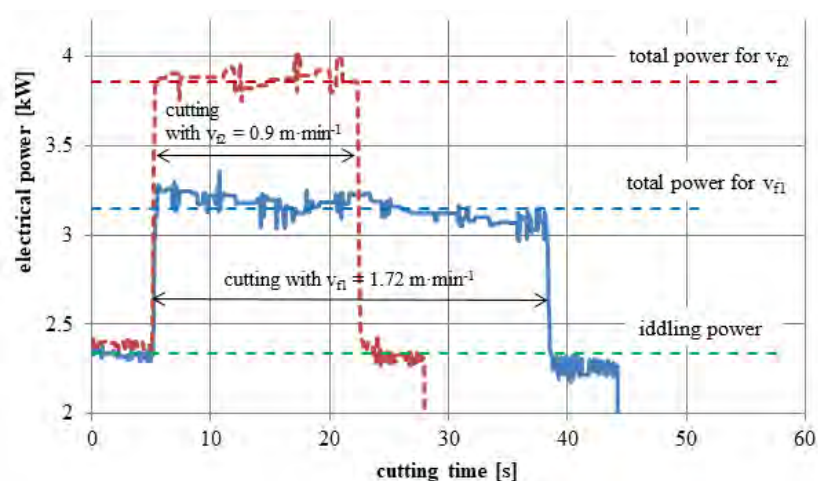
Figure 2. Time changes of electrical power consumption while sawing at two levels of feed speed v_{f1} and v_{f2} of impregnated samples

RESULTS AND ANALYSES

In Table 1 the symbols of samples, values of feed speeds v_f and feed per teeth f_z, which were used in the tests, are presented. The results of the sieve analysis - size distribution of the dry chips of untreated pine sawdust and dry impregnated pine are given in Table 2.

Table 1. Symbols of samples, feeding parameters and types of raw material

Symbol	feed speed v_f	feed per tooth f_z	kind of raw material
	m·min^{-1}	mm	
SOIM-10	0.901	0.1058	impregnated
SOIM-11	1.717	0.2052	impregnated
SONP-3	0.898	0.1055	not impregnated
SONP-4	1.719	0.2049	not impregnated

Table 2. Granulometric analysis of sawdust from unimpregnated and impregnated and pine wood

Measure of sieve mesh [mm]	Mark of fraction	Representation of fractions in dry pine wood [%]			
		pine not impregnated wood		pine impregnated wood	
		SONP-3	SONP-4	SOIM - 10	SOIM - 11
2.000	coarse	2.29	3.31	1.97	2.26
1.000		21.44	17.87	26.61	21.29
0.500	medium coarse	51.02	47.38	40.68	47.70
0.250		19.11	24.47	23.49	23.36
0,125		5.34	6.47	6.15	4.71
0.063	fine	0.77	0.47	1.08	0.68
0.032		0.03	0.01	0.02	0.00
< 0.032		0.00	0.00	0.00	0.00

The majority ≈ 95% of the chips produced are thick and the chip share of the coarse fraction in the particle size range 125 microns to 2 mm. The slight difference is in the fraction of the fine fraction with a particle size of 32 - 125 μm. While the share of pine

wood sawdust of unimpregnated wood is between 0.48 and 0.8%, whereas of the impregnated wood pine wood is 0.68 - 1.1%.

Figure 2 presents the cumulative histogram residue granularity plots of sawdust obtained during the sawing process of not impregnated and impregnated pine wood.

	0	0.032	0.063	0.125	0.25	0.5	1	2
SONP-4 (0.2)	100	99.99	99.52	93.03	68.56	21.18	3.31	0
SOIM-10 (0.1)	100	99.99	98.91	92.76	69.27	28.59	1.98	0
SOIM-11 (0.2)	100	100	99.32	94.61	71.25	23.55	2.26	0
SONP-3 (0.1)	100	99.97	99.2	93.86	74.75	23.73	2.29	0

Mesh size, mm
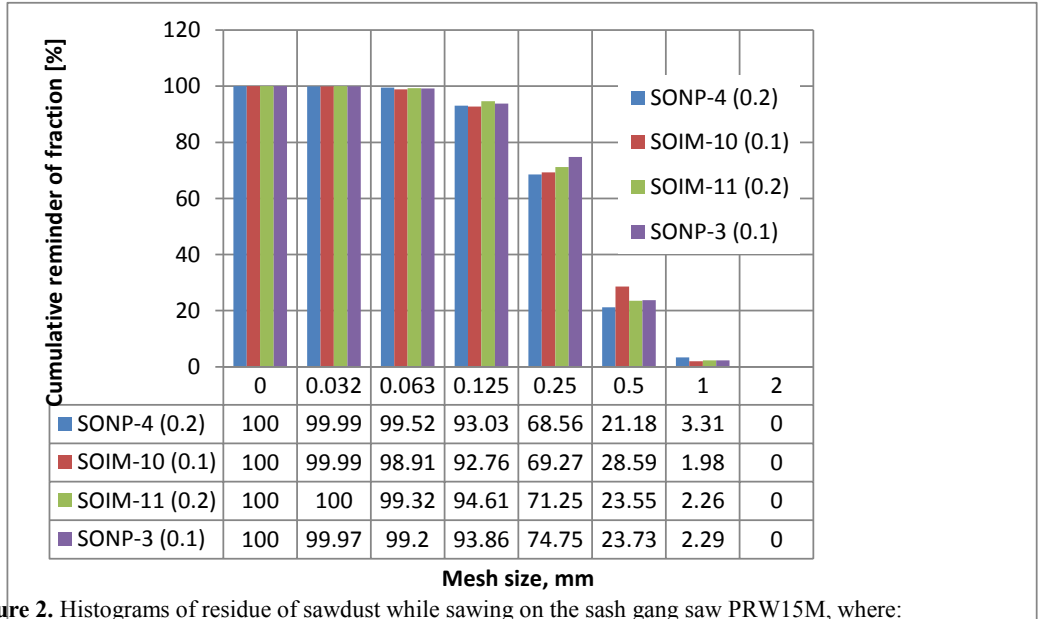
Figure 2. Histograms of residue of sawdust while sawing on the sash gang saw PRW15M, where: a) not impregnated pine, b) impregnated pine. Legend: close to the samples symbols in parentheses values of feed per tooth are provided

The obtained results show that the impregnation process practically does not affect the sawdust grain size when sawing on the frame sawing machine PRW-15M in the examined feed rate range. A slightly higher proportion of fine fraction of pine wood impregnated wood does not affect the efficiency of separation in fabric filters and the technological use of sawdust, e.g. for the production of briquettes and pellets.

CONCLUSIONS

Based on the carried out analyses, it can be concluded that:
- firstly, the sawdust of both the unimpregnated pine wood and impregnated pine wood, created in the sawing process on a frame sawing machine PRW15-M at a feed speed of v_f = 0.9-1.72 m·min^{-1}, consists of ≈ 95% of the chips with a grain size within the range from 125 μm to 2 mm;
- secondly, the slight difference is in the fraction of fine fraction with a particle size of 32 - 125 μm.
- eventually, the obtained results revealed that the impregnation process practically does not affect the sawdust granularity when sawing on the sash gang saw PRW-15M in the examined feed rate range; does not affect the efficiency of separation in fabric filters and the technological use of sawdust, e.g. for the production of briquettes and pellets.

ACKNOWLEDGMENTS

REFERENCES

BELJO LUČIČ, R., ČAVLOVIČ, A., DUKIČ, I., JUG, M., IŠTVANIČ, J., ŠKALJIČ, N., 2009. Machining propertirs of thermally modified beech-wood compared to steamed beech-wood. In: Woodworking technique. DENONA, Zagreb: 315-324.

BABIŃSKI, L. K., 1992. Impregnacja drewna metodą próżniową. Ochrona Zabytków 45/4(179): 360-368. (in Polish).

DZURENDA, L., WASIELEWSKI ,R., ORLOWSKI, K., 2006. Granulometric analysis of dry sawdust from the sawing process on the frame sawing machine PRW15M = Granulometrická analýza suchej piliny z procesu pílenia borovicového dreva na rámovej píle PRW-15M// Acta Facultatis Xylologiae Zvolen. -Vol. 48., nr 2 (2006):51-57.

DZURENDA, L., 2009. Sypká drevná hmota, vzduchotechnická doprava a odlučovanie. V-TU, Zvolen.

DZURENDA, L., ORLOWSKI, K., GRZEŚKIEWICZ, M., PAULINY, D., 2009. Sawdust size distribution analysis of thermally modified and unmodified oak wood sawed on the frame sawing machine PRW15-M// Annals of Warsaw University of Life Sciences-SGGW Land Reclamation. -., nr. Nr 68.

DZURENDA L., ORLOWSKI K., GRZEŚKIEWICZ M., 2010. Effect of thermal modification of oak wood on sawdust granularity = Utecaj termicke modifikacije na granulometrijski sastav piljevine// Drvna Industrija.Vol. 61., iss. 2.

DZURENDA, L., ORLOWSKI, K. (2010): Vplyv modifikácie dubovégo dreva technólogiou thermo-wood na zrnistosŤ piliny z procesov pilenia dreva na rámovej pile PRW 15M// W The 7th International Science Conference : Chip and Chipless Woodworking Processes 2010 : Proceedings of papers, September, 9-11. 2010, Terchová./ Zvolen: Technická Univerzita vo Zvolene, pp. 69-75

DZURENDA, L., ORŁOWSKI, K., 2011. The effect of thermal modification of ash wood on granularity and homogeneity of sawdust in the sawing process on a sash gang saw PRW 15-M in view of its technological usefulness. Drewno, Vol. 54, nr 186.

DZURENDA L., ORŁOWSKI K., 2011a. Influence of feed rate on the granularity and homogenity of oak sawdust obtained during the sawing process on the frame sawing machine PRW15M// Proceedings of the 4th International Science Conference Woodworking Techniques/ ed. Barcik S., Dvorak J. - Czech University of Life Sciences Prague, Univ Zagreb. Prague: Czech University of Life Sciences Prague, Czech Republic.

FUJIMOTO, K., TAKANO, T., OKUMURA, S., 2011. Difference in mass concentration of airborne dust during circular sawing of five wood-based materials. J Wood Sci 57: 149-154. https://doi.org/10.1007/s10086-010-1145-y

HEJMA, J. et al., 1981. Vzduchotechnika v dřevozpracovávajícím průmyslu. SNTL, Praha.

HLÁSKOVÁ, L., ROGOZINSKI, T., KOPECKÝ, Z., 2016. Influence of feed speed on the content of fine dust during cutting of two-side-laminated particleboards. Drvna Ind 67 (1): 9-15 (DOI: 10.5552/drind.2016.1417)

KONOPKA, A., BARAŃSKI, J., ORŁOWSKI, K., SZYMANOWSKI, K., 2018. The effect of full-cell impregnation of pine wood (Pinus sylvestris L.) on changes in electrical

resistance and on the accuracy of moisture content measurement using resistance meters. BioRes. 13(1): 1360-1371. (DOI: 10.15376/biores.13.1.1360-1371)

MARKOVÁ, I., LADOMERSKÝ, J., HRONCOVÁ, E., MRAČKOVÁ, E.,2018. Thermal parameters of beech wood dust. BioRes. 13(2), 3098-3109. (DOI: 10.15376/biores.13.2.3098-3109).

PAŁUBICKI, B., ROGOZIŃSKI, T., 2016. Efficiency of chips removal during CNC machining of particleboard. WOOD RESEARCH, Vol. 61, Number 5: 811-818.

WASIELEWSKI R., ORŁOWSKI K., 2002. Hybrid dynamically balanced saw frame drive. Holz als Roh- und Werkstoff 60(3):202–206.(DOI: 10.1007/s00107-002-0290-4).

KORASIT KS2 , 2017. https://www.kora-holzschutz.de/fileadmin/assets/produkte/Technische-Merkblaetter_Englisch/Korasit_KS2_TM_CLP_2017-02_EN.pdf (accessed on 23 May, 2018).

ISO 3310-1, 2007. Test sieves. Technical requirements and testing. Part 1: Test sieves of metal wire cloth. International Organization for Standardization, Geneva, Switzerland.

ISO 9096: 2017. Stationary source emissions – Manual determination of mass concentration of particulate matter.

STN 26 0070, 1995. Klasifikácia a označovanie sypkých hmôt dopravovaných na dopravných zariadeniach. (In Slovak: Clasification and symbolization of bulk material transported on conveyor equipment).

INFLUENCE OF SEQUENCE AND TIMING OF OPERATIONS ON THE PRODUCTIVITY OF DOOR ASSEMBLY

Tomasz Rogoziński – Łukasz Sankiewicz

Abstract

The use of production lines in wood industry plants results from the necessity to reduce the labour intensity involved in the technological operations. Production lines are characteristic of mass production, where similar operations are performed on different products. An example is door production. This paper presents an example of the organisation of a door assembly line. Line efficiency was also calculated for two door models based on the assembly programmes prepared as part of the project and the takt times adopted. The paper also describes the possibility of forecasting efficiency depending on changing production tasks.

Key words: *door assembly, production line, productivity*

INTRODUCTION

The mechanisation and automation of production processes in industrial plants is reflected in the creation of production lines. Depending on the character of the technological operations performed, production lines can be used for processing or assembly purposes. A production line comprises workstations set in the order in which particular technological operations are performed. Such production organisation is typical of mass production [1, 2, 3, 4].

Each workstation within a production line should be assigned identical workload and at the same time should be used to its maximum capacity. The operation of those workstations should be synchronised, which means that they should work according to a common *takt*. The takt time of a production line is a measure of its efficiency and refers to the time between the production of two consecutive units. A production line should include no parallel stations or stations performing operations from outside the scope of its work. For these reasons, a production line always constitutes a distinct whole.

Apart from workstations, the correct operation of a production line is affected by the transporting devices used. Their task is to provide efficient transport of elements between particular workstations. Additionally, a production line should make use of manipulators that are to replace completely manual operations related to gathering elements before the performance of an operation, handing elements over to workstations, removing elements in an appropriate manner, and collecting ready units from workstations. Such devices include all types of feeders, which enable the precise separation of individual elements from a large number of objects held in a container.

Poznań University of Life Sciences, Wojska Polskiego 38/42, 60-627 Poznań, Poland
e-mail: trogoz@up.poznan.pl

Due to the similar character of accessory mounting operations in different door types and models, the creation of production lines performing such tasks is particularly justified, especially that it enables the elimination of time-consuming manual activities. Thus, a decision was made to design a door fitting assembly line and to perform an initial analysis of its productivity.

DOOR ASSEMBLY LINE ANALYSIS

In order to increase the efficiency of assembly operations on door fittings produced using the principles of mass customisation, such operations on the TechnoPorta line were designed to be performed also in the line system. They will be performed within a newly-designed assembly line. The door fitting assembly line is basically made up of five universal stations — working tables (Fig. 1.). All of them use the same equipment that enables them to perform assembly operations. Up to 10 fitting operations can be performed at each station. Examples of assembly operations on doors:
• mounting of hinges,
• mounting of locks,
• mounting of door closers,
• mounting of bolts,
• mounting of automatic door bottom seals,
• mounting of seals,
• mounting of stainless steel panels,
• mounting of stainless steel strips protecting narrow door surfaces,
• mounting of glazing elements,
• mounting of any other accessories.
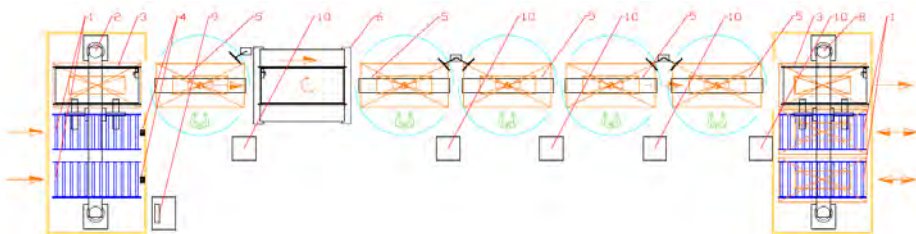
Legend:
1. Roller conveyor
2. Double station stacker with transverse vacuum gripping system.
3. Motorized belt conveyor.
4. Automatic barcode scaner/s.
5. Rotary assembly table with double high.
6. Longitudinal turntable
7. Operators monitors.
8. Double station Stacker with transverse vacuum gripping system.
9. Line control computer with manual scaner
10. Label printing system

Fig. 1. Door assembly line setup

Table 1. Timing of assembly operations for door type 1

Operations	Notes	Door type 1				
		Station	**Op No.**	**Number of accessories**	**Time/act**	**Time/Station**
Washing	Side 1	1	1	1	0:01:44	0:01:44
	Side 2	2	2	1	0:01:44	0:01:44
3-element hinge			3	3	2	0:00:52	0:01:43
3-element hinge		4	4	1	0:00:52	0:01:50
Security bolt			3	4	0:00:15	
Multipoint lock	8 screws	5	4	1	0:01:12	0:01:34
Mounting of the ID plate			5	1	0:00:22	
					Total:	**0:08:35**
					Takt time:	**0:01:50**
					Total time:	**0:09:09**

Table 2. Timing of assembly operations for door type 2

OPERATIONS	Notes	Door type 2				
		Station	**Op No**	**Number of accessories**	**Time/act**	**Time/unit**
Washing	Side 1	1	1	1	0:01:44	0:03:23
Cleaning fire seal grooves	all		2	4	0:00:07	
Fire seal 20×2	bottom		3	1	0:01:12	
Washing	Side 2	2	4	1	0:01:44	0:04:09
Fire seal 20×2	hinge + top		5	2	0:01:12	
Fire seal 10×2	lock	3	6	1	0:00:24	0:02:49
Fire seal 20×2			7	2	0:01:12	
3-element hinge		4	8	3	0:00:52	0:03:33
Security bolt			9	4	0:00:15	
Multipoint lock	8 screws	5	10	1	0:01:12	0:02:58
ID plate — registration in the IFS			11	1	0:01:23	
ID plate — mounting			12	1	0:00:22	
					Total:	**0:16:51**
					Takt time:	**0:04:09**
					Total time:	**0:20:43**

The purpose of the analysis is to determine the potential efficiency capacities of the assembly line for different types of produced doors. Using the proposed calculation method, it will be possible to predict the target efficiency of the production line depending on the quantitative proportions of doors subjected to fitting on the line. However, at first, it is necessary to develop an assembly program based on which particular operations on consecutive working tables will be performed. The assembly programme needs to take into account the equal assignment of those operations due to the logic of the technology and the time burden. Thus, the workload of particular working tables should result in a similar accessory assembly time at each station — the takt time. Examples of assembly programmes for two door models are presented in Tables 1 and 2.

Under line synchronisation conditions, in a specific takt time, the line efficiency can be calculated using the formula:

$$N = F \times k/T$$

Where:
F — nominal line work time fund,
k — line workstation use coefficient,
T – takt time.

For the takt times determined for door type 1: 1,83 min/unit and for door type 2: 4.15min/unit and the adopted value of the use coefficient: $k = 0.85$, with a nominal two-shift work time fund of $F = 4000$h/y, the following annual efficiency was calculated: $N_1 = 111475$ units and $N_2 = 57831$ units.

SUMMARY AND CONCLUSION

The analysis performed above shows that the assembly line takt time determined on a project basis affects significantly the final efficiency of the line. Thus, the correct determination of accessory assembly programmes for different door models is very important. Such correctness should be characterised by the shortest possible takt time. An accessory assembly programme should also take into account the technological order of particular activities, which is a limiting factor for takt time optimisation.

With projected or known quantitative tasks for particular door types or models and for takt times determined on a project or chronometric basis, it is possible to predict the efficiency of an assembly line and thus of the entire process.

REFERENCES

1. Stanisław Dolny and Jerzy Strumiński, *Technologiczne projektowanie zakładów mechanicznej obróbki drewna*, Part 1: *Ogólne zasady projektowania i zagadnienia technologiczne*; Part 2 *Zagadnienia wybrane*, Poznań, Ar, 1993, 1996.
2. Witold Rybarczyk and Maria Suska, *Obniżanie kosztów wytwarzania przez samofinansujące się modernizacje stanowisk pracy*, Centrum Zastosowań Ergonomii, Zielona Góra, 2004

3. Trofimov, S.P., *Projecting of woodworking enterprises* / S.P. Trofimov — In 2 parts, Part 1: *Introduction to automate system preparation of production*, Minsk, BSTU, 2005

4. Trofimov, S.P., *Projecting of woodworking enterprises* — In 2 parts, Part 2: *Technological and over-all technical preparation of production*, Minsk, BSTU, 2013

ACKNOWLEDGEMENTS

THE CONTENT OF BIOACTIVE COMPOUNDS IN CHIPS FROM THE WOOD PROCESSING LINE

Tomasz Rogoziński − Lidia Szwajkowska-Michałek − Anna Matysiak − Kinga Stuper-Szablewska

Abstract

Industrial wood waste is the effect of mechanical treatment of wood and wood products. This group of wastes includes bark, sawdust, wood chips, sawmill dust, dust and chips Analyses were conducted on four sterols: desmosterol, campesterol, stigmasterol, β-sitosterol and organic acids (malonic, citric, quinic, succinic, lactic, maleic, fumaric, oxalic) using UPLC in bark of three species of deciduous trees (oak, beech, hornbeam) and two conifers (spruce, pine). In the bark of deciduous trees these sterols were not found. Deciduous trees are poorer in organic acids than in coniferous ones. The spruce contained all the acids determined in the experiment The bark of the oak contained mainly citric acid and small amounts of fumaric and oxalic acid

Key words: *bark, sterols, organic acids, UPLC analysis, woodworking*

INTRODUCTION

Industrial wood waste is the effect of mechanical treatment of wood and wood products. This group of wastes includes bark, sawdust, wood chips, sawmill dust, dust and chips.

The amount of waste generated during machining, ranging from raw material abrasion to finished product is very high and in many cases exceeds the mass of finished product elements. That is why some of the wood waste from the wood industry companies is used for the production of board materials, and the rest is used in agriculture and horticulture and as fuel for energy purposes. Full use of this industrial raw material allows manufacturing plants to produce products with high technical advantages, used in many areas of everyday life [1]. Waste management is an important element of the wood industry. Ensuring their safety elimination or deactivation of chemical and microbiological factors is a necessary condition that must be met in order for the waste material to be used. One of the most commonly used methods is drying wood in order to obtaining semi-products and waste.

It consists in reducing the humidity to the level of hygroscopic equilibrium with ambient conditions corresponding to the environment in which the products made from this raw material will be used. An additional purpose of drying is to get rid of, among others, fungi and their spores, which can settle dead wood, leading to its degradation. The effect of high temperature also causes the deactivation of biologically active compounds of wood among them enzymes and the breakdown of high molecular weight antioxidant compounds. Literature studies show that the main residues after the wood drying process are low molecular weight compounds, such as organic acids. It also leads to complete disintegration of eg: endogenous sterols [2, 3, 4]. In the light of the few studies on this subject, it was

Poznań University of Life Sciences, Wojska Polskiego 38/42, 60-627 Poznań, Poland
e-mail: trogoz@up.poznan.pl

decided to carry out analyzes of endogenous wood sterols and the content of organic acids after the drying process in waste from the wood processing line.

MATERIAL AND METHODS

Tested material

The bark of three species of deciduous trees (oak, beech, hornbeam) and two conifers (spruce, pine) was tested in three replications. After drying, the bark was milled using a cutting mill Pulverisette 19 (Fritsch, Germany) and analyzed for the content of sterols (campesterol, desmosterol, stigmasterol, beta-sitosterol) and organic acids.

Analysis of the content of sterols

Methanol and acetonitrile were HPLC grade (Sigma-Aldrich, St. Louis, MO, USA); hydrochloric acid and natrum hydroxide were purchased from POCH S.A (Gliwice, Poland); deionized water was prepared using a Millipore Milli-Q system (Millipore, MA, USA). The standards of campesterol, desmosterol, stigmasterol, β-sitosterol were purchased from Sigma-Aldrich (St. Louis, MO, USA.).

Sterols were determined following microwave assisted basic hydrolysis. Samples of 100 mg material were placed into 17 ml culture tubes, suspended in 1 ml of methanol, treated with 0.1 ml of 2 M aqueous NaOH and sealed tightly. Then the culture tubes were placed within 250 ml plastic bottles, sealed tightly and placed inside a microwave oven (Whirpool model AVM 401/WH) operating at 2450 MHz and 900 W maximum output. Samples were irradiated (370 W) for 20 s, after c. 5 min irradiated again for an additional 20 s and extracted with pentane (HPLC grade, Sigma-Aldrich, Steinheim, Germany) (3 × 4 ml) within the culture tubes. The combined pentane extracts were evaporated to dryness in a gentle stream of a high purity nitrogen using a RapidVap Evaporator (Labconco, Kansas, MO, USA). The extracts were stored at -25ºC until analysis. Prior to analyses the samples were dissolved in 1 ml of methanol, filtered through 13mm syringe filters with a 0.22 μm pore diameter (Fluoropore Membrane Filters).

Contents of sterols were analysed using an Aquity H class UPLC system equipped with a Waters Acquity PDA detector (Waters, USA). Chromatographic separation was performed on an Acquity UPLC® BEH C18 column (100 mm × 2.1 mm, particle size 1.7 μm) (Waters, Ireland). The elution was carried out isocratically using the following mobile phase composition: A, acetonitrile 10%; B, methanol 85%; C, water 5%; at a flow rate of 0.5 mL/min.

Measurements of sterol concentrations were performed using an external standard at wavelengths λ = 210 (desmosterol, stigmasterol, β-sitosterol, campesterol). Compounds were identified based on a comparison of retention times of the examined peaks with that of the standard and by adding a specific amount of the standard to the tested sample and repeated analyses. The limit of detection was 1 mg/kg.

Analysis of the content of organic acids

The analysis of LMWOAs was performed using a Waters Acquity H-class UPLC system. Separation was achieved on an Acquity UPLC BEH C18 column (150 mm × 2.1 mm, 1.7 μm, Waters) thermostated at 35°C. The gradient elution was performed with water and acetonitrile (both containing 0.1% formic acid, pH=2) at a flow rate of 0.4 mL/min. Detection was carried out in a Waters Photodiode Array Detector (Watres Corporation, Milford, MA, USA) at λ = 280 nm as the preferred wavelength for acetic, citric, fumaric,

lactic, malic, maleic, malonic, oxalic, quinic and succinic acids. Compounds were identified by comparing of retention time of the analyzed peaks with the retention time of standards or by adding a specific amount of the standard to the analyzed samples and a repeated analysis. The LMWOAs found were quantified by comparing of the area of their peaks recorded at 280 nm with calibration curves obtained from commercial standards of each compound obtained from Sigma (St. Louis, MO, USA). The results were expressed in milligrams per gram of dry weight (mg/g).

RESULTS AND DISCUSSION

As part of this work, the concentration of the four most important sterols (desmosterol, stigmasterol, β-sitosterol, campesterol) wood bark was tested. In the bark of deciduous trees after the drying process, these sterols were not found (Table 1) with the exception of beech bark and hornbeam, where only campesterol was identified. However, they were found in bark samples from conifers. In the bark of pine and spruce, capesterol occurred at the highest concentration compared to other sterols. Beta-sitosterol occurred in the lowest concentration in the bark of conifers (at the level of 1.6 to 1.78 mg/kg) (Table 1).

Table 1. Average concentration of endogenous wood sterols (mg / kg) in the analyzed bark of deciduous and coniferous trees

Trees species	Sterols (mg/kg)			
	Campesterol	Desmosterol	Stigmasterol	Beta-sitosterol
pine	270,4	2,5	1,9	1,78
spruce	247,9	17,2	5,6	1,6
hornbeam	222,17	< LOD	< LOD	< LOD
beech	18,63	< LOD	< LOD	< LOD
oak	< LOD	< LOD	< LOD	< LOD

The concentration of endogenous wood sterols is related to the level of mycobiota pollution as observed in the tested samples. The role of sterols in plant tissues during infection with pathogens has not been sufficiently explained. Bark is dead tissue, therefore the role of sterols can not be discussed in the context of defense mechanisms in plants. During the decomposition of wood, microscopic fungi degrade reserve substances. Substances released during degradation include phytosterols contained in cell membranes and cell walls. The susceptibility of plant organisms to microbial infections is related to the stability and impermeability of cell membranes, and sterols are indispensable components of cell walls and cell membranes [5]. The sterols contained in dead cells released from plant tissues as a result of fungal action are identifiable. The higher the fungus contamination, the higher the content of free endogenous sterols due to the amount of decomposed wood cells [6].

An important component of wood with a biogenic effect are organic acids. According to Siegelman (1964) [7], these acids play an important role in the biosynthesis of phenolic compounds in trees, they are also the products of their decomposition.

Organic acids are involved in the regulation of a wide range of basic cellular processes, e.g. biochemical and physiological processes. They act as signal relays [8], as well as a modulator of transport through biological membranes [9]. It has been shown that the metabolism of organic acids in the cytosol is involved in abiotic reactions stressful [10]. Organic acids are also involved in the chemical modification of proteins, for example in acetylation or succinylation [11, 12].

Table 2. The content of organic acids in the bark of conifers and deciduous trees (mg/g)

Trees species	Malonic acid	Citric acid	Quinic acid	Succinic acid	Lactic acid	Maleic acid	Fumaric acid	Oxalic acid
pine	0,12	400,6	41,84	12,95	< LOD	< LOD	7,8	3,35
spruce	0,12	349,93	297,5	42,17	37,64	49,92	7,97	11,89
hornbeam	0,04	432,36	< LOD	< LOD	< LOD	< LOD	6,16	2,8
beech	< LD	137,18	30,9	45,21	< LOD	< LOD	6,19	3,8
oak	< LD	356,8	< LOD	< LOD	< LOD	< LOD	5,33	0,6
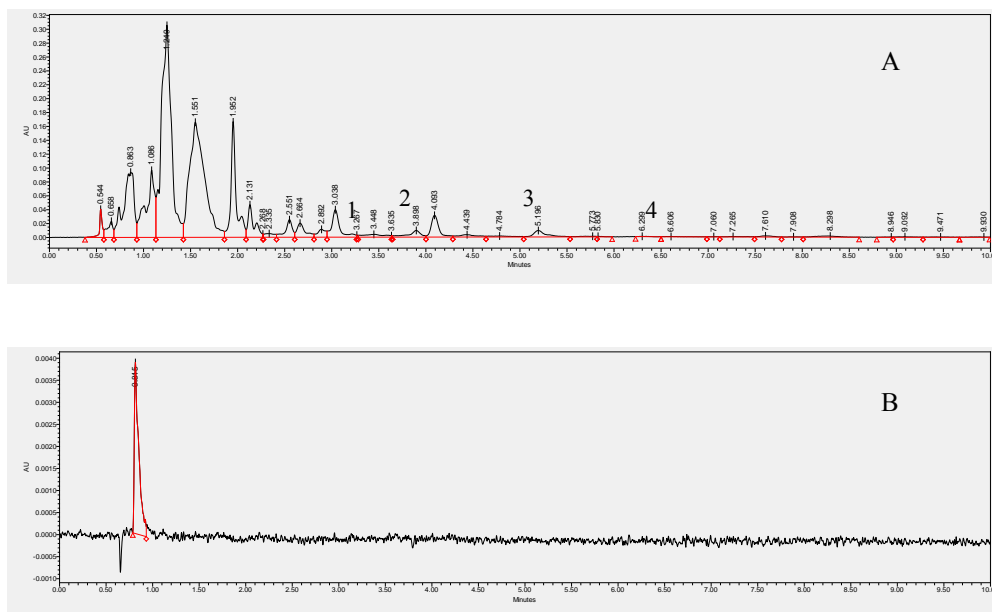
Fig. 1. An example of a spruce bark chromatogram (A) 1-campesterol, 2-desmosterol, 3-lanosterol, 4-beta-sitosterol and oak (B)
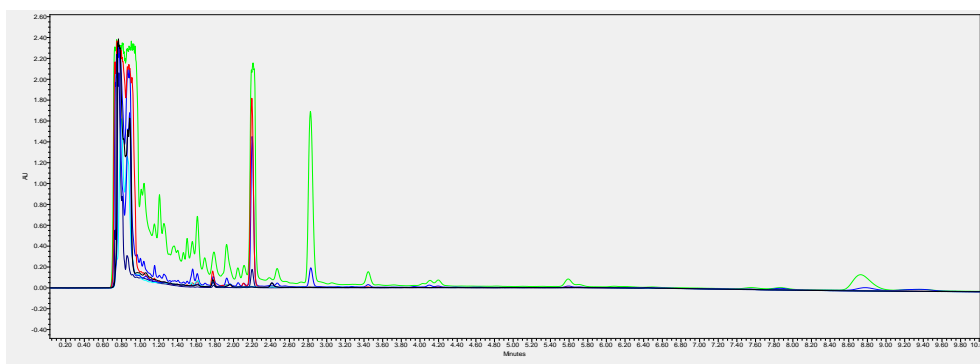
Fig. 2 Comparison of chromatograms of organic acids of all analyzed samples
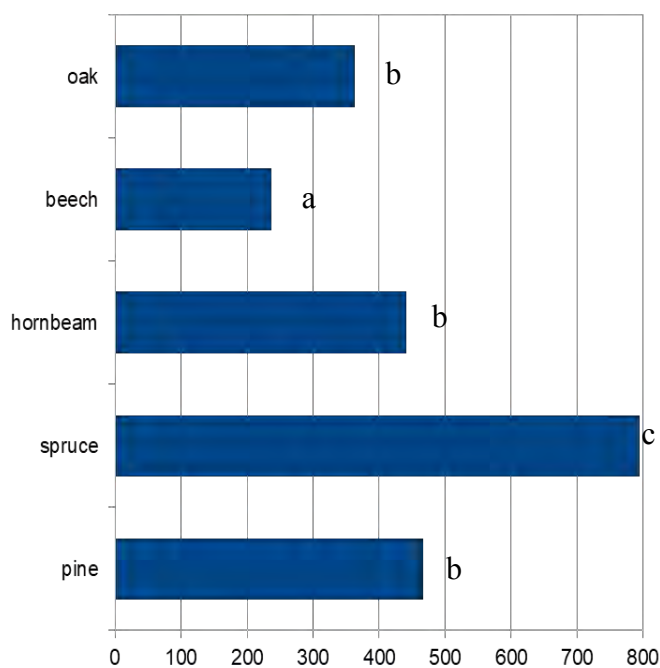
Fig. 3. Concentration of sum of organic acids [mg/g]

In the present research, the content of organic acids of oak bark, beech, hornbeam, spruce and pine was determined (Table 2, Figures 1, 2, 3). Deciduous trees are poorer in organic acids than in coniferous ones. The spruce contained all the acids determined in the experiment (malonic, lemon, quinic, amber, lactic, maleic, fumaric and oxalic), among them citric acid in the highest concentration. The bark of the oak contained mainly citric acid and small amounts of fumaric and oxalic acid (5.33 and 0.6 mg/g). The bark of hornbeam and beech proved to be slightly richer in organic acids. Beech bark, in comparison with the bark of the oak, additionally contained small amounts of malonic acid, and beech quinic and succinic acid. Previous research on this subject is limited, and knowledge about the impact of technological processes on bioactive compounds contained in it is small. Short references to organic acids in wood have been found on the basis of

literature studies. For example: Wang and Steffen [13] determined the content of organic acids in apple wood. They detected the presence of acids: amber, apple, lemon and chin. It turned out that the content of organic acids changes periodically, in spring it decreases and increases in the winter.

REFERENCES

[1] Rosik – Dulewska Cz., Podstawy gospodarki odpadami, Wydawnictwo Naukowe PWN, Warszawa 2010.

[2] Alén, R., Kotilainen, R. Zaman, A. (2002). Thermomechanical behaviour of Norway spruce (Picea abies) at 180–225 ºC. Wood Science and Technology, 36, 163–171.

[3] Nuopponen, M., Vuorinen, T., Jämsä, S. i Viitaniemi, P. (2004). Thermal modifications in softwood studied by FT-IR and UV resonance Raman spectroscopies. Journal of Wood Chemistry and Technology, 24, 13-25.

[4] Sudo, K., Shimizu, K., Sakuirai, K. (1985). Characterization of Steamed Wood Lignin from Beech Wood. Holzforschung, 39, 281-288.

[5] Piispanen R, Saranpää P. Seasonal and within-stem variations of neutral lipids in silver birch (Betula pendula) wood. Tree Physiol 2004;24:991-9. doi: 10.1093/treephys/24.9.991

[6] Stuper-Szablewska K et al. Contamination of pine and birch wood dust with microscopic fungi and determination of its sterol contents Arh Hig Rada Toksikol 2017;68:127-134

[7] Siegelman HW (1964) Physiological studies on phenolic biosynthesis. In: Harborne JB (ed) Biochemistry of phenolic compounds. Academic Press, New York, pp 437–456

[8] Finkemeier, I., König, A. C., Heard, W., Nunes-Nesi, A., Pham, P. A., Leister, D., et al. (2013). Transcriptomic analysis of the role of carboxylic acids in metabolite signaling in Arabidopsis leaves. Plant Physiol. 162, 239–253. doi: 10.1104/pp.113.214114

[9] Hedrich, R., and Marten, I. (1993). Malate-induced feedback regulation of plasma membrane anion channels could provide a CO_2 sensor to guard cells. EMBO J.12, 897–901.

[10] Dyson, B. C., Miller, M. A., Feil, R., Rattray, N., Bowsher, C., Goodacre, R., et al. (2016). FUM2, a cytosolic fumarase, is essential for acclimation to low temperature in Arabidopsis thaliana. Plant Physiol. 172, 118–127. doi: 10.1104/pp.16.00852

[11] Zhang, Z., Tan, M., Xie, Z., Dai, L., Chen, Y., and Zhao, Y. (2011). Identification of lysine succinylation as a new post-translational modification. Nat. Chem. Biol. 7, 58–63. doi: 10.1038/nchembio.495

[12] Weinert, B. T., Schölz, C., Wagner, S. A., Iesmantavicius, V., Su, D., Daniel, J. A., et al. (2013). Lysine succinylation is a frequently occurring modification in prokaryotes and eukaryotes and extensively overlaps with acetylation. Cell Rep. 29, 842–851. doi: 10.1016/j.celrep.2013.07.024

[13] Wang, S.Y. & Steffens, G.L.   Effect of paclobutrazol on accumulation of organic acids and total phenols in apple wood. J Plant Growth Regul (1987) 6: 209. https://doi.org/10.1007/BF02102549

THE EFFECT OF THE CUTTING EDGE INCLINATION ANGLE ON THE CHIPS EXIT FROM THE CUTTING ZONE DURING PLANE MILLING OF WOOD MATERIALS

Pavel Rudak[1] – **Štefan Barcík**[2] – **Mats Ekevad**[1] – **Oksana Rudak**[1] – **Michal Korčok**[2] – **Vadzim Chaveuski**[1]

Abstract

The purpose of the study, the results of which are presented in this paper, is the investigation of the regularities of chips and dust particles movement leaving the milling zone. Mathematical equations are established and the following regularities are analyzed for the plane milling process of wood materials: the effect of the cutting edge inclination angle on the chip exit angle; the influence of the cutting edge inclination angle on the speed of the chips moving along the blade and the speed of the chips exiting the cutting zone; the dependencies of the chip exit angle on the friction coefficient of the chips on the surface of the processed material and on the friction coefficient of the chips along the blade surface; the influence of the mill rotation frequency on the chip exit angle.

Key words: *milling, wood material, chipboard, chips, chip exit angle, cutting edge inclination angle*

INTRODUCTION

Woodworking CNC machines are most often used for milling of wood materials. These machines allow the workpiece to be processed from different sides during its single installation on the machine. This technology provides a high quality of processing performance and efficiency. At the same time, most enterprises deal with the problem of the efficient removal of chips and dust from the cutting zone (ROGOZIŃSKI et al. 2015; RUDAK & KUIS 2011).

Woodworking mills operate at frequencies 10000–24000 min^{-1} and feed rates of 3–40 m/min. Referring to this, wood chips and dust have a high initial speed which makes it difficult for the machine aspiration system to capture them (PAŁUBICKI & ROGOZIŃSKI 2016). The chips, not being caught by the aspiration system, can fly away for 3–5 m from the processing zone. Such chips and dust mess up the machine, workpieces, and surrounding space. When chips get into the area of infrared sensors of the CNC machine, they can cause emergency stops and product defects. Insufficient efficiency of chip removal from the cutting zone can cause an increased wear of tools.

[1]Belarusian State Technological University, Sverdlova 13A Minsk BY, 220006, Bielorusko
e-mail: puma.legno@inbox.ru, RudakPV@belstu.by, chaevskiv@gmail.com
[2]Technical University in Zvolen, T. G. Masaryka 24, 960 53 Zvolen, Slovak Republic
e-mail: barcik@tuzvo.sk, korcokmichal@gmail.com

One way to increase the efficiency of collecting waste from the cutting zone of milling woodworking machines is to use the kinetic energy of chips and dust and direct their movement towards the chip receiver (SU et al. 2002; RUDAK & KUIS 2011).

The organization of chip motion in the required direction can be carried out by the inclination of the tool blade. The inclined blade, especially the helical edges, provides a better chip flow compared to the conventional edge of mill (DARMAWAN et al. 2011).1

To improve the efficiency of their collection by the aspiration system by the use of kinetic energy of chips and dust (KVIETKOVA et al. 2015), it is necessary to understand the processes of the chip and dust exit from the cutting zone.

The purpose of the study is the investigation of the regularities of chips and dust particles movement when leaving the milling zone.

MATERIALS AND METHODS

A chip element with a mass m, located in the chip flute of the mill, was considered for the mathematical modelling of the chip exit from the cutting zone. The tool has a radius R and rotates with a cyclic frequency ω. The board wood material is milled at the depth of milling e (Fig. 1).
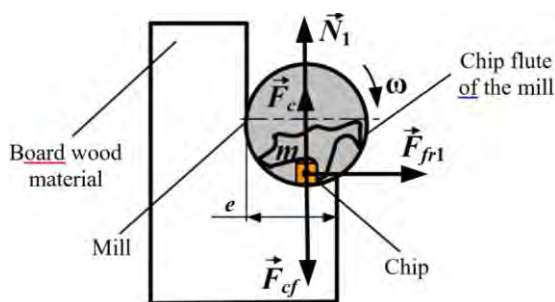
Fig. 1 A chip element, located in the chip flute of the mill

The blade has a cutting edge inclination angle λ. The chip element moves along the blade rectilinearly at the speed V_x (Figure 2, *a.*). When the mill rotates at an angle, providing the release of the chips via flute, the chips leave it at the speed V_{exit}, moving at a chip exit angle v. The velocity V_{exit} is the vector sum of the velocities of the circular motion V_ω and the velocity V_x.

The motion of a chip particle is considered in the *XYZ* coordinate system, rotating together with the mill at frequency ω. In this case, the *X*-axis is oriented parallelly to the direction of movement of the chips along the blade, and the *Y*-axis is perpendicular to the indicated direction (Fig. 2, *b.*).

Moving along the blade, the chip particle undergoes the action of the centrifugal force F_{cf}, the Coriolis force F_c, and also the reaction of the surface of the processed material N_1 (Fig. 1). The friction force F_{fr1} between the surface of the particle and the surface of the processed material, the gravitational force F_g, and the reaction force N_2 of the blade surface also affect the chip particle movement (Fig. 2, *b.*).

The equation of the equilibrium of forces acting on a chip particle was written neglecting aerodynamic, electrostatic forces and forces acting on a chip particle from other particles:

$$\overset{r}{ma} = \overset{r}{F}_g + \overset{r}{F}_c + \overset{r}{F}_{cf} + \overset{r}{F}_{fr1} + \overset{r}{F}_{fr2} + \overset{r}{N}_1 + \overset{r}{N}_2. \tag{1}$$

The auxiliary angle $\chi = 90° - \lambda$ was introduced. Projection of the forces acting on the chip particle was performed on the axes coordinate.

In the projections on the *X*-axis:

$$ma_x = -F_{fr2} + F_{fr1}\cos(\nu + \chi) - mg\sin\chi. \tag{2}$$
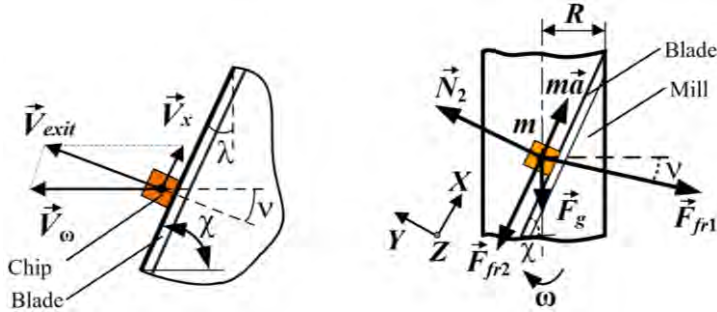
Fig. 2 The scheme of movement velocities at which the chip elements operate (a) and the scheme of forces, acting on the chips in the chip flute of the mill (b).

In the projections on the *Y*-axis:

$$0 = N_2 - mg\cos\chi - F_{fr1}\sin(\nu + \chi). \tag{3}$$

In the projections on the *Z*-axis:

$$0 = F_{cf} - F_c - N_1. \tag{4}$$

The friction force between the particle of chips and the surface of the processed material is determined by the formula:

$$F_{fr1} = \mu_1 N_1, \tag{5}$$

where μ_1 is the friction coefficient between the chip particle and the surface of the material being processed, [-]
The friction force between the chip particle and the surface of the blade is determined by the formula:

$$F_{fr2} = \mu_2 N_2, \tag{6}$$

where μ_2 is the friction coefficient between the chip particle and the blade surface, [-].

Taking equation (4) into account, the equation to determine the friction force between the chip particle and the surface of the material being processed was written down:

$$F_{fr1} = \mu_1 m\left(\omega^2 R - 2\omega V_x \cos\chi\right). \tag{7}$$

From the equation (3):

$$N_2 = \mu_1 m \left(\omega^2 R - 2\omega V_x \cos\chi \right) \sin\left(\nu + \chi \right) + mg \cos\chi. \tag{8}$$

Taking into account equations (2) and (7), and also, knowing that the acceleration $a = \dot{V}_x$ the differential equation was obtained:

$$\dot{V}_x = \mu_1 \left(\omega^2 R - 2\omega V_x \cos\chi \right) \cos\left(\nu + \chi \right) - \mu_2 \frac{N_2}{m} - g \sin\chi. \tag{9}$$

From the vector sum of the velocities (Fig. 2, *a.*):

$$\cos(\nu + \chi) = \frac{\omega R \cos\chi - V_x}{\sqrt{V_x^2 + (\omega R)^2 - 2V_x \omega R \cos\chi}}. \tag{10}$$

Equations (8)–(10) allow the process of chip exit from the cutting zone to be analyzed. To solve the equations and designing graphical dependencies, the computer program Math CAD 15 (PTC Inc., USA) was applied. The chip mass was assumed to be $m=1$g.

RESULTS AND DISCUSSION

The solution of equations (8)–(10) brought the following results. Figure 3 shows the dependence of the chip exit angle ν on the cutting edge inclination angle λ.
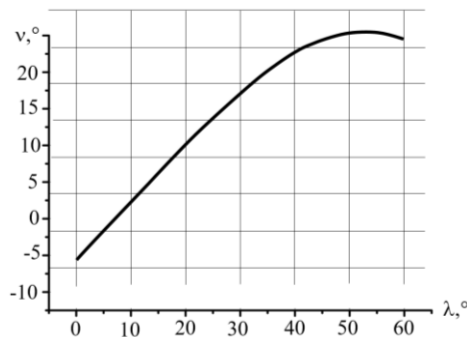
Fig. 3 Dependence of the chip exit angle ν on the cutting edge inclination angle λ (the diameter of the mill 20 mm, the frequency of rotation of the mill 24000 min^{-1}).

For values of the cutting edge inclination angle λ from 0° to 11.3°, the chips are directed downward when they exit. At $\lambda = 11.3°$ the chip exit angle $\nu = 0$ and chips leave the cutting zone, moving in a plane perpendicular to the axis of rotation of the mill. With a further increase in the angle λ, the chips leave the cutting zone being directed upwards. At an angle $\lambda = 25°$, the chip exit angle is $\nu = 10.4°$. With an increase in the angle λ greater than 55°, the angle ν begins to decrease.

Figure 4 shows the dependences of the movement speed V_x of the chips along the blade and the exit speed of the chips from the cutting zone V_{exit} on the cutting edge inclination angle λ.

In Figure 4, it is seen that increasing the angle λ causes an increase in the speed V_x of the movement of the chips along the blade.

The velocity vector V_x is directed along the blade downwards in the interval of values of the angle λ from 0 to 11.3°, which leads to an insignificant increase in the speed V_{exit}. A further increase in the angle λ and the speed V_x results in a decrease in the velocity V_{exit}.

Thus speed V_{exit} increases in the range of angle values from λ from 0° to 55°. This is completely consistent with the results of experiments for milling natural wood. The exit speed of the chips decreased when the cutting edge inclination angle increased (DARMAWAN *et al.* 2011).

Figure 5 shows the dependences of the chip exit angle ν on the friction coefficients.
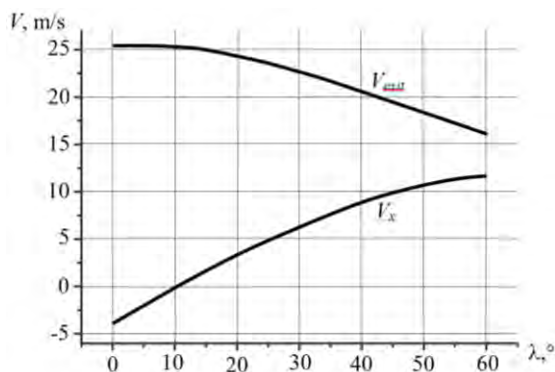
Fig. 4 Dependences of the speed Vx of the movement of the chips along the blade and the exit speed Vexit of the chips from the cutting zone from the cutting edge inclination angle λ (the diameter of the mill 20mm, the frequency of rotation of the mill 24000 min^{-1}).
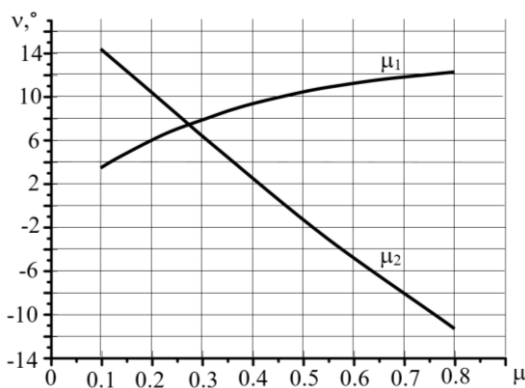
Fig. 5 Dependences of the chip exit angle ν on the friction coefficient µ1 of the chips on the surface of the processed material (at µ2 = 0.2) and on the friction coefficient µ2 of the chips along the surface of the blade (at µ1 = 0.5) (the mill diameter 20 mm, the cutting edge inclination angle λ = 25°).

It can be seen from the graphs in Figure 6 that the values of friction coefficients $µ_1$ and $µ_2$ have a significant effect on the value of the chip exit angle. This is consistent with the results of studies that showed a significant effect of the tribological characteristics of the blade on the process of wood materials cutting (VOSKRESENSKIY 1955).

Figure 6 shows the dependence of the chip exit angle ν on the frequency of rotation of the mill *n*.

At the frequency of rotation of the mill *n* = 1000 min^{-1}, the chip exit angle ν = 2.6°,

at the frequency of rotation of the mill $n = 3000$ min^{-1}, the chip exit angle $v = 9.4°$, and with a further increase of the frequency of rotation of the mill, the chip exit angle changes only slightly and remains at the level $v \approx 10°$.
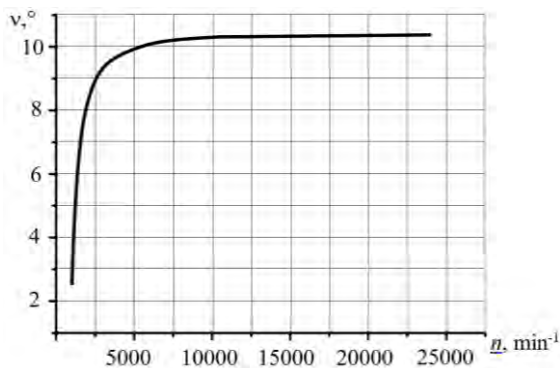
Fig. 6 Dependence of the chip exit angle v on the frequency of rotation of the mill n (the diameter of the mill 20 mm, the cutting edge inclination angle $\lambda = 25°$).

CONCLUSION

Mathematical dependencies allow us to determine the chip exit angle, the speed of the movement of the chips along the blade and the exit speed of the chips from the cutting zone take into account the values of the cutting edge inclination angle, the frequency of rotation and radius of the mill, the chip mass, the friction coefficient of the chips on the surface of the processed material and the chips along the blade surface.

The greatest influence on the value of the chip exit angle is provided by the cutting edge inclination angle. A friction coefficient of the chips along the blade surface has a great influence on the chip exit angle and, the friction coefficient of the chips on the surface of the processed material provides the same effect to a somewhat lesser extent.

The frequency of rotation of the mill when it is more than 5000 min^{-1} does not affect the chip exit angle significantly, but together with the radius of the mill, it determines the chip exit speed from the cutting zone and so the initial kinetic energy of chips and dust.

These mathematical dependencies can be used in the process of constructing wood-cutting mills and in the development of aspiration systems for wood-cutting machines.

ACKNOWLEDGEMENTS

REFERENCES CITED

BERSHADSKY A. L. 1975. Резание древесины [Wood cutting]. Minsk. Vishejshaja skola. 303 p.

DARMAWAN W., GOTTLÖBER C., OERTEL M., WAGENFÜHR A., FISCHER R. 2011. Performance of helical edge milling cutters in planing wood. European Journal of Wood and Wood Products. 69(4): 565–572. ISSN 00183768. DOI 10.1007/s00107-010-0517-8.

KVIETKOVA M., BARCIK S., ALAC P. 2015. Impact of angle geometry of tool on granulometric composition of particles during the flat milling of thermally modified beech. Wood research. 60(1): 137–146. ISSN 1336-4561.

PAŁUBICKI B., ROGOZIŃSKI T. 2016. Efficiency of chips removal during CNC machining of particleboard. Wood Research. 61(5): 811–818. ISSN 13364561.

ROGOZIŃSKI T., WILKOWSKI J., GÓRSKI J., CZARNIAK P., PODZIEWSKI P., SZYMANOWSKI K. 2015. Dust creation in CNC drilling of wood composites. BioResources. 10(2): 3657–3665. ISSN 19302126. DOI 10.15376/biores.10.2.3657-3665.

RUDAK P., KUIS D. 2010. Эффективное удаление стружки и пыли из области обработки в процессе фрезерования древесных материалов [Effective removal of chips and dust from the processing area during the milling of wood materials]. Resource- and energy-saving technologies and equipment, environmentally safe technologies: materials of Intern. Scientific-Techn. Conf., Minsk, 24–26 November 2010, Belarusian. State. Technol. Un-t, pp. 121–124. ISBN 978-985-530-036-7.

RUDAK P., KUIS D. 2011. Снижение шумовых характеристик и повышение эффективности удаления стружки из зоны резания при эксплуатации дереворежущих машин [Reducing noise characteristics and increasing the efficiency of chip removal from the cutting zone when operating wood-cutting machines]. Proceedings of BSTU. Forest and Woodworking. XIX, pp. 242–247. ISSN 1683-0377.

SU W., WANG Y. 2002. Effect of the helix angle of router bits on chip formation and energy consumption during milling of solid wood. Journal of Wood Science. 48(2): 126–131. ISSN 14350211. DOI 10.1007/BF00767289.

VOSKRESENSKIY S. 1955. Резание древесины [Wood cutting]. Moscow : Goslesbumizdat. 199 p.

FRACTURE TOUGHNESS IN MECHANICAL TESTING AND CUTTING MODELS

Gerhard Sinn[1] **− Jürgen Maierhofer**[2] **− Helga Lichtenegger**[1]

Abstract

Since the concept of a surface energy necessary to separate a material was introduced in cutting theories, these theories were successfully applied to different materials, one of them wood. While the approach is convincing it is still an open question, what is the counterpart in mechanical testing. In this experimental work fracture energy from cutting experiments were compared to fracture energies from mechanical testing.

Key words: *cutting, modeling, fracture toughness*

INTRODUCTION

The study of cutting forces is of central interest for machine and tools producer to predict power requirements and loads for their products. It would be of major advantage to predict these parameters from required process parameters, e. g. depth of cut and general wood properties like density or strength. Whereas usually it is very simple to get density data from literature, e. g. from collections like [1-3] it is often a challenge to get more detailed data on strength of wood, and also to find the full set of nine elastic parameters to model wood as an orthotropic material is often impossible. Finally data on fracture toughness of different wood species is very scarce.

This general lack of data might be one of the reasons why many wood cutting models are more or less empirical [4] [5] [6] These models are often gained directly from a specific cutting process and are therefore limited in their applications. Some of these models focus on the influence of the materials to be cut, keeping the machining parameters constant. Examples of this kind of models are the works of [7] and [6]. Eyma et al. [7] analysed a peripheral milling process with a single set of process parameters and studied the influence of wood species, characterised by their densites, shear and compression behaviour. Two models predicting the measured cutting forces from a subset of parameters were presented. The best model had an $R^2=0,73$. A more general approach is presented by Naylor et al. [6] They used a variant of single tooth cutting process with a rake angle of 0°. Studied parameters where moisture content depth of cut and direction (along or accross the grain), wood species described by density, shear tests and three point bending tests. The correlation coefficients of the statistical models ($R^2=86\%$ across and 90% along the grain) for the cutting forces are higher than the models presented by Eyma et al. [7] and cover a broader set of parameters.

[1]BOKU – University of Natural Resources and Life Sciences, Peter-Jordan-Str. 82 1190 Vienna, Austria
e-mail: gerhard.sinn@boku.ac.at, helga.lichtenegger@boku.ac.at
[2]Materials Center Leoben Forschung GmbH
e-mail: Juergen.Maierhofer@mcl.at

Other studies focus on the influence of machining parameters while keeping the wood species and its physical condition constant. An example of this kind of studies is the work of Axelsson et al. [8]. They varied the cutting orientation from a rip sawing process to a milling orientation, modified the rake angle, tool radius, cutting speed and chip thickness while cutting scots pine. Beside these paramters they also changed the temperature and the moisture content. Proposed model is nonlinear in the cutting orentation, furthermore some interaction terms of moisture content with temperature and cutting orientation are included. Porankiewicz et al. [9] proposed a new non-linear statistical cutting model based on cutting orientation, tool geometry and condition, cutting speed and wood properties like density, moisture content and temperature for scots pine. The quality of approximation reached a value of R²=0,91. The authors developed their model on new experimental data and verified it on data from the literature.

Beside these statistical models, which require a high number of parameters and therfore experiments to be verified, in the last years new analytical models based on energy criteria did get popular [10-13]. The developmet of this models were driven by the difficulty to measure the fracture toughness of soft materials with traditional methods. Williams [10] developed a model which assumes a chip produced by elastic and plastic bending, whereas Atkins [11; 12] proposed a model for the generation of a chip by shear in front of the tool. Both models have in common, that they use fracture toughness as an essential parameter, which describes the energy for new surface creation in cutting. The shear chip model was successfully applied to describe the wood cutting process. For example Beer et al. [14] did apply this model to describe the cutting of particle boards. Further modifications to the shear model from Atkins [12] were described by Orlowski et al. [15] in a review on cutting processes. The force model was translated into a power model and the simultaneous action of more than one tooth were described in order to be able to apply the theoretical model to practical applications of frame saw cutting. The circular sawing process could be also described [16; 17]. This cutting process made it necessary to consider the orthotropic nature of wood which was described in detail in [18].

While the cutting models, which use fracture toughness and shear strength as parameters are very powerful in predicting cutting forces and power consumption for different processes [19] the significance of the predicted parameters remain uncertain.

In order to get some insight into this open question, single-tooth cutting experiments were performed and fracture toughness was determined. These parameters were then compared with parameters from fracture mechanical testing.

MATERIALS

Four different wood species were used for the experiments, two softwoods and two tropical woods. The softwoods were larch (*Larix decidua* Mill.) and western red cedar (*Thuja plicata* D. Don) and the tropical woods were Jatoba (*Hymenaea courbaril* L.) and Wenge (*Milettia laurentii* De Wild). Before cutting, wood logs were cut into samples of ca. 3x8x3 cm³ and stored in a climate chamber of standard environment conditions 20 °C and 65 % relative humidity until an equilibrium moisture content was reached.

METHODS
Microtome cutting and force measurement

In order to control cutting directions as well as chip thickness in a repeatable and controllable way, a modified microtome, equipped with a single cutting tooth, was used for the cutting experiments.

Cutting forces were measured with two 3d piezoelectric force sensors from PCB® joining the specimen holder with the gear of the microtome. Cutting tool had a rake angle of 7,6° degree and a width of 1,16 mm. Experiments were analysed using the cutting force equation 1 of Atkins [12], where F_c is cutting force, w is kerf width, γ shear strain and τ_f shear strength, f_z is uncut chip thickness and R is fracture toughness. Q_{shear} is called friction correction factor and it is a factor depending on rake angle, shear angle and friction. The shear angle Φ is a result from minimization of the cutting energy and depends on chip thickness, shear strength and toughness. The parameters are calculated by an iterative process described in [12].

$$\frac{F_c}{w} = \frac{1}{Q_{shear}}(\gamma \tau f_z + R)$$
(Equation 1)

The optimization procedure fits the normalized cutting force as a function of the uncut chip thickness f_z and delivers fracture toughness R, shear strength τ_f and shear angle Φ.

Fracture mechanical testing

Wedge splitting experiments were designed to measure fracture energy and fracture toughness of wood [20; 21]. Grooves were cut on the side of the specimens to reduce the loaded area and guide the crack, since the strength of wood in fiber direction is very strong for the LR-specimens (see figure 1 for specimen shape and dimensions). Specimens were loaded in mode I, i. e. crack opening mode, and LR-crack propagation system. The first letter L indicates the anatomical direction, where loading is applied, and the second letter indicates the direction of crack propagation. Specific fracture energies G_f were evaluated from load displacement curves.

a)   b)
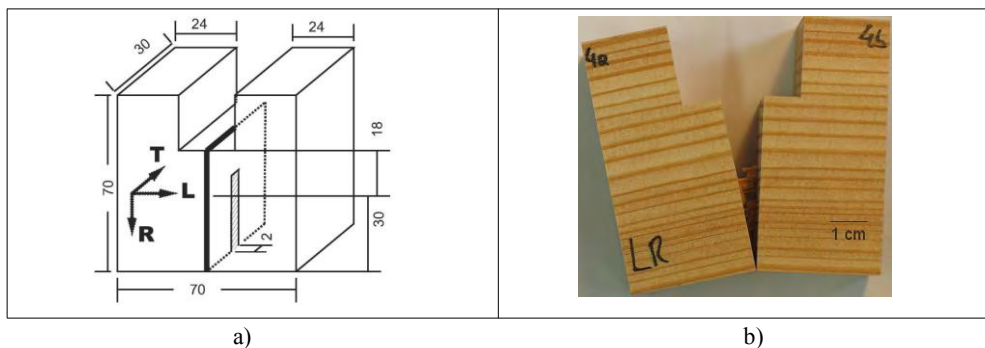
Figure 1: Wedge splitting specimen for the LR-crack propagation system with side grooves:
a) sketch and b) picture of fractured larch sample

RESULTS

Results of density measurements are summarized in table 1. The densities span a range of 368 to 937 kg/m³
The cutting forces showed linear dependence on chip thickness as predicted by the model. Fracture toughness, shear strength a swell as shear angle were evaluated according to equation 1, results are summarized in table 1:

Table 1: density and cutting parameters: fracture toughness R, shear strength τ_f and shear angle Φ from least squares fitting of equation 1.

	western red cedar	larch	Jatoba	Wenge
density, (kg/m³)	367,7±3,3	594,5±5,8	937,2±5,6	840,3±1,9
R, (J/m²)	2315	1423	1564	1808
τ, (MPa)	24,6	16,5	68,3	57,4
Φ, (°)	27,6	27,9	31,3	30,7

The results from wedge splitting experiments are shown in figure 2, only the specific fracture energy, I. e. the energy per broken area, was evaluated.
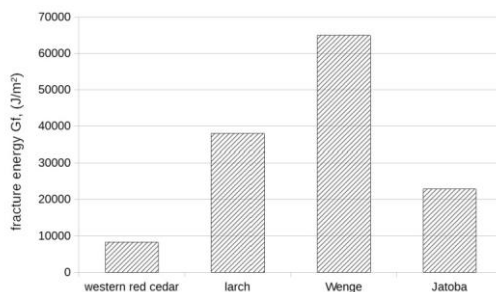
Figure 2: specific fracture energy for all investigated wood species

DISCUSSION

Analysis of data showed that shear strength from cutting correlated very well with density ($R^2=0,95$), whereas the correlation between fracture toughness from cutting with density was lower ($R=0,73$).
The correlation between energy from splitting and fracture toughness from cutting is low ($R^2=0,59$) (see fig. 3). The reason might be in the different crack growth mechanisms. In cutting the crack growth is limited to a very small region in front of the tool where loading reaches strength of the material, whereas in splitting a much larger volume is affected. Pull out of fibers on a very rough broken area was a commonly observed phenomena.
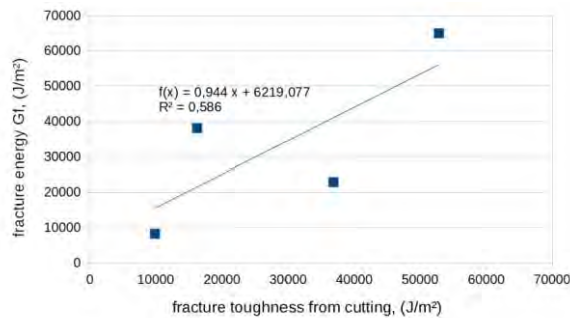
Figure 3: fracture energy G_f from splitting experiments as a function of fracture toughness R from cutting.

Due to the side grooves the fracture tests are non standard methodology for fracture testing and an additional influence of depth and size of the specimen might be expected in determining the fracture energy. Nevertheless the regression line from figure 3 has a slope of approx. 1, which shows, that the parameters follow the same trend. The non-zero axis intercept might have its origin in the different volumes involved in cutting and splitting as described before.

CONCLUSIONS

Fracture mechanical tests as well as cutting experiments were performed in order to get more insight into the parameters involved. Fracture toughness from cutting did correlate to fracture energy from splitting but the correlation coefficient found was low. Further investigations and improvements in methodology as well as theoretical models might be necessary to close the gap between fracture parameters from cutting and from independent mechanical testing. A close correlation of mechanical parameters to cutting parameters would give the possibility to predict cutting forces from mechanical testing and therefore from independent material tests.

REFERENCES

[1]   Forest Products Laboratory Madison, W., **1940**. *Wood handbook: basic information on wood as a material of construction with data for its use in design and specifications. U.S.* Government Printing Office, Washington DC, Wash..

[2]   Niemz, P., **1993**. *Physik des Holzes und der Holzwerkstoffe*. DRW-Verl., Leinfelden-Echterdingen.

[3]   Wagenführ, R. 1928., **2000**. Holzatlas. Fachbuchverl. Leipzig im Hanser-Verl., Leipzig [u.a.] ; Wien.

[4]   **Krenke, T.; Frybort, S. and Müller, U. (2014).** *Internationaler Stand zur Schnittkraftuntersuchung bei Holz - Teil 1*, Holztechnologie 55: 38-45.

[5]   **Krenke, T.; Frybort, S.; Martinez-Conde, A. and Müller, U. (2015).** *Internationaler Stand zur Schnittkraftuntersuchung bei Holz-Teil 3*, Holztechnologie 56: 43-50.

[6] **Naylor, A.; Hackney, P.; Perera, N. and Clahr, E. (2012)**. *A predictive model for the cutting force in wood machining developed using mechanical properties*, BIORESOURCES 7 : {2883-2894}.

[7] **Eyma, F.; Méausoone, P.-J. and Martin, P. (2004)**. *Strains and cutting forces involved in the solid wood rotating cutting process*, Journal of Materials Processing Technology 148: 220 - 225.

[8] **Axelsson, B. O. M.; Lundberg, Å. S. and Grönlund, J. A. (1993)**. *Studies of the main cutting force at and near a cutting edge*, Holz als Roh- und Werkstoff 51: 43-48.

[9] **Porankiewicz, B.; Axelsson, B.; Gronlund, A. and Marklund, B. (2011).** *MAIN AND NORMAL CUTTING FORCES BY MACHINING WOOD OF PINUS SYLVESTRIS*, BIORESOURCES 6: {3687-3713}.

[10] **Williams, J. G. (1998).** *Friction and plasticity effects in wedge splitting and cutting fracture tests*, Journal of Materials Science 33: 5351-5357.

[11] **Atkins, A. (2003).** *Modelling metal cutting using modern ductile fracture mechanics: quantitative explanations for some longstanding problems*, International Journal of Mechanical Sciences 45: 373 - 396.

[12] **Atkins, A. (2005).** *Toughness and cutting: a new way of simultaneously determining ductile fracture toughness and strength*, Engineering Fracture Mechanics 72: 849-860.

[13] Atkins, T. **(2009)**. *Chapter 2 - Fracture Mechanics and Friction: Muscles, Impact and New Surfaces*. In: Atkins, T. (Ed.), *The Science and Engineering of Cutting*, Butterworth-Heinemann.

[14] **Beer, P.; Sinn, G.; Gindl, M. and Tschegg, S. (2005).** *Work of fracture and of chips formation during linear cutting of particle-board*, JOURNAL OF MATERIALS PROCESSING TECHNOLOGY 159: {224-228}.

[15] **Orlowski Kazimierz, A. and Bartosz, P. (2009).** *Recent progress in research on the cutting processes of wood. A review COST Action E35 2004-2008: Wood machining - micromechanics and fracture*, Holzforschung 63: 181.

[16] **Hlásková, L.; Orlowski, K.; Kopecký, Z. and Jedinák, M. (2015)**. *Sawing Processes as a Way of Determining Fracture Toughness and Shear Yield Stresses of Wood*, BioResources 10.

[17] **Orlowski, K. and Ochrymiuk, T. (2017)**. *A newly-developed model for predicting cutting power during wood sawing with circular saw blades*, Maderas. Ciencia y tecnologia 19: 149 - 162.

[18] **Orlowski, K. A.; Ochrymiuk, T.; Sandak, J. and Sandak, A. (2017).** *Estimation of fracture toughness and shear yield stress of orthotropic materials in cutting with rotating tools*, Engineering Fracture Mechanics 178: 433 - 444.

[19] **Orlowski, K. A.; Ochrymiuk, T.; Atkins, A. and Chuchala, D. (2013).** *Application of fracture mechanics for energetic effects predictions while wood sawing*, Wood Science and Technology 47: 949-963.

[20] **STANZLTSCHEGG, S.; DM, TAN and TSCHEGG, E. (1995).** *NEW SPLITTING METHOD FOR WOOD FRACTURE CHARACTERIZATION*, WOOD SCIENCE AND TECHNOLOGY 29: {31-50}.

[21] **StanzlTschegg, S.; Tan, D. and Tschegg, E. (1996).** *Fracture resistance to the crack propagation in wood*, INTERNATIONAL JOURNAL OF FRACTURE 75: {347-356}.

3D MODELLING AND FEM ANALYSIS OF DEFORMATIONS OF A FURNITURE SKELETON WITH OSB SIDE PLATES

Nelly Staneva – Yancho Genchev – Desislava Hristodorova – Gergana Alexandrova

Abstract

3D geometric model of one-seat skeleton for upholstered furniture was created by CAD system. A linear static analysis was carried out with CAE system Autodesk Simulation Mechanical® by the method of finite elements (FEM) simulating light-service loading of the skeleton. The orthotropic material characteristics of pine solid wood (Pinus sylvestris L.) for the rails and OSB for the side plates are considered in the analysis. Two variants of corner joints in the skeleton (model A – staples and PVA; model B - staples, PVA and strengthening elements) were considered. FEA was performed with regard to laboratory determined and calculated coefficients of rotational stiffness of used staple corner joints. As results the distribution of displacements and equivalent strains in the 3D discrete model of upholstered furniture skeleton with staple corner joints are presented and analysed.

Key words: *upholstered furniture skeleton, staple joints, deformations, CAE, FEM*

INTRODUCTION

The skeleton of upholstered furniture is usually wood and/or wood-based products. Although the wood composites are commonly used in box type furniture, their utilization in the frame type furniture is not widespread. It is recommended that wood composites could be used in the production of the frame type furniture, especially in the upholstered furniture frames, but, in this case, it is important according to material type used that the additional reinforcing details and giving a decision about its place (Kasal, A., 2006).

There is limited number of references concerning the deformation behaviour of upholstered frames constructed with structure elements of OSB although OSB panels are increasingly used in the construction of upholstered furniture frames latterly.

Wang, X. (2007a) has investigated a three-seat sofa frame made entirely of 18 mm thick OSB plates. With software SAP 2000 she has created 3D linear models by beam finite elements of 3 different constructions of a sofa frame with two types of connections – rigid and semi-rigid and two types of connectors: 1) screws and metal plates; 2) staples and metal plates. Nonlinear static analysis has been performed simulating 3 loads: light-, medium- and heavy-service. Wang has established the most appropriate configuration of the sofa frame of OSB under investigated loads and has concluded that the type of connectors does not change the joint displacements remarkably.

Erdil Y. et al. (2008) have investigated the behaviour of 3-seat upholstered furniture frames constructed with ¾ inch thick OSB (EN 300, 1997) and joining elements - yellow

University of Forestry, blvd. "Kl. Ohridsky" 10, 1797 Sofia, Bugaria
e-mail: nelly_staneva@yahoo.com

birch dowels and aliphatic resin glue (PVA) using the simplified methods of structural analysis in the engineering of such frames. They have concluded that OSB may be used in construction of upholstered furniture frames to meet specific design loads.

The aim of this study was to define and analyze the displacements and strains of one-seat skeleton of upholstered furniture with staple joints and side plates of OSB by CAD/CAE using the method of finite elements (FEM).

MATERIALS AND METHODS

3D model of one-seat upholstered furniture skeleton with length 600 mm, width 680 mm and height 625 mm was created with Autodesk Inventor Pro® (Educational product) – Fig.1. The used rails are with cross section 25x50 mm.

A linear static analysis of 3D modeled skeleton was carried out with CAD/CAE system Autodesk Simulation Mechanical® by the Finite Elements Method (FEM).

Two discrete models were created - *model A* without and *model B* with strengthening details under the upper rails of the seat with a shape of triangle prism (Fig.1) and two design scenarios were performed. The generated Midplane mesh has 5130 orthotropic plate finite elements and 33616 DOF's for *model A* and 5230 orthotropic plate finite elements and 34096 DOF's for *model B*.
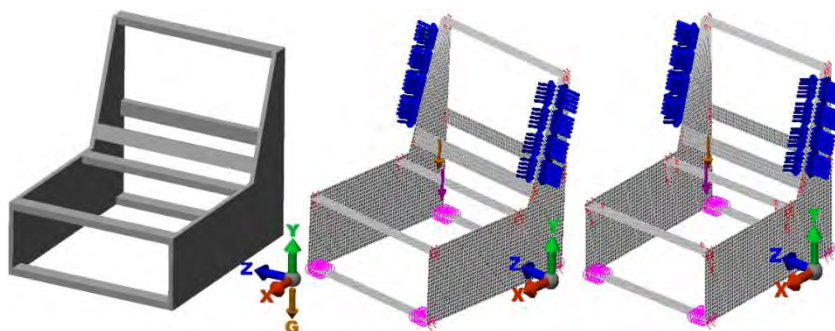
Fig. 1. 3D skeleton models *A* and *B* and loading

Orthotropic materials type was used for construction elements of the skeleton:

Scots pine (*Pinus sylvestris L.*) for rails and strengthening details with measured density 435,50 kg/m³ according to BDS EN 323:2001 and elastic characteristics: $E_z=E_L=9000.10^6$ N/m², $E_x=E_T=593.10^6$ N/m², $G_{LT}=554,5.106$ N/m², $\nu_{LT}=0,027$, $\nu_{TL}=0,41$, $\nu_{LR}=0,03$, $\nu_{RL}=0,049$.

Oriented strandboard (OSB), type EGGER OSB2 EN 300 E1 CE, designed for load-bearing structures for use in a dry environment with thickness 16 mm and technical requirements according to BDS EN 13986:2004+A1:2015 were used for side plates. The physical and mechanical characteristics of the OSB panels are: density 595.67 kg/m³, measured according to BDS EN 323:2001; modulus of elasticity in bending (major axis) – $E_x=3800.10^6$ N/m²; modulus of elasticity in bending (minor axis) – $E_y=3000.10^6$ N/m²; Poisson ratios $\nu_{12}=0,030$ according to Thomas, W. (2003) and $\nu_{21}=0,24$, calculated according to Bodig J. and B. Jayne (1982) by the equation: $\frac{\nu_{12}}{E_1}=\frac{\nu_{21}}{E_2}$.

Support boundary conditions were set: bottom front rail – no translation on *y* direction and bottom rear rail no translation on *x*-, *y*- and *z* direction.

In order to simulate semi-rigid connections between rails and side plates of the skeleton two actions were performed:

First − narrow zones were created in the place of joints in the discrete model with established via tests by FEM lower modules of elasticity of the used materials perpendicular to the common edge of the corner joint.

Second - the laboratory determined by Hrisodorova (2018) coefficients of rotational stiffness of the corner joints with 2 staples (type M1) and PVA glue, loading under compression were introduced in the nodes of the respective corner joints - case butt joints (c=766,84 N.m/rad) and end to face butt joints (c=509,99 N.m/rad).

The both discrete skeleton models were loaded with a total load of 800 N, distributed as follows (Genchev, 2018) - Fig.1:

Seat: 80% were set as a remote force, distributed between upper rails of the seat with application point of 100 mm in front of the upper rear rail, simulating upholstery base made of zig-zag springs;

Backrest: 16% were set as equal nodal forces, distributed on the edges of the two sides of the backrest simulating elastic belts.

The changed angle γ between the joint shouders at upper front rails of the seat was mesuared with the program Autodesk Simulation Mechanical®.

RESULTS AND DISCUSSION

The results for linear displacemets u, nodal rotations θ, and equivalent strains $\varepsilon_{von\ Mises}$, as well as the changed angle γ between the joint shouders at upper front rails of the seat for both *models A* and *B* are shown in Table 1, Table 2 and in Fig.2 to Fig. 5 for the skeleton and for the side plates of the skeleton respectively. The visualizations of the deformed model are shown with a scale factor 3% of model size for the skeleton and with a scale factor 5% of model size for the side plates.

In Fig.2 the distribution of resultant displacement is presented. The maximal resultant displacements of 2.5 mm for *model A* and 1.79 mm for *model B* are received in the

Table 1. Maximal displacements and strains of the skeleton

Parameters and location		model A	model B
u_x, [mm]	side plates	0.03	0.04
u_y, [mm]	front upper rail	-1.28	-0.92
	rear upper rail	-2.50	-1.79
u_z, [mm]	side plates	0.30	0.50
θ_x, [°]	rear upper rail	0.75	0.51
θ_y, [°]	side plates	1.55	0.16
θ_z, [°]	front upper rail	1.62	1.3
	rear upper rail	-1.74	-1.38
$\varepsilon_{von\ Mises}$, [m/m]	side plates	0.0072	0.0049
γ, [°]	front upper rail	89.81	89.95
	rear upper rail	89.69	89.94

Table 2. Maximal displacements in the side plates

Parameters and location		*model A*	*model B*
u_x, [mm]	front upper rail	-0.039	-0.036
	rear upper rail	0.028	0.029
	Backrest	0.026	0.043
u_y, [mm]	front upper rail	0.093	0.055
	rear upper rail	-0.107	-0.062
u_z, [mm]	Base	0.30	0.488
	rear upper rail	-0.108	-0.061
	Backrest	-0.091	-0.086
θ_x, [°]	front upper rail	-0.28	-0.07
	rear upper rail	-0.55	-0.39
θ_y, [°]	rear upper rail	-0.15	-0.15
θ_z, [°]	front upper rail	0.23	0.15
	rear upper rail	-0.15	-0.08
$\varepsilon_{von\ Mises}$, [m/m]	front upper rail	0.0074	0.0047
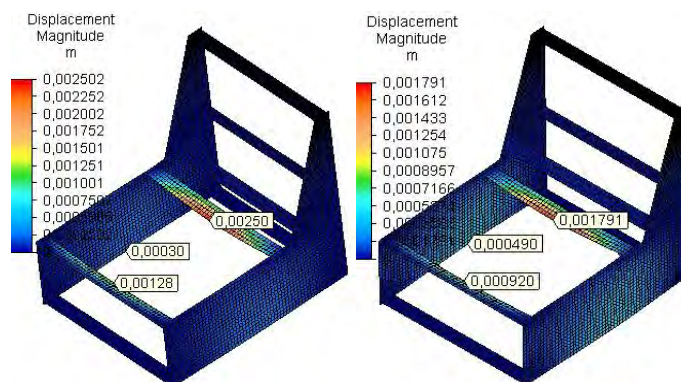
Figure 2. Distribution of resultant displacements for model A and model B

middle of the upper rail of the seat, on the inside of the rails and are determined mainly by the *y*-displacements (u_y) – Table 1. The resultant displacement is 1.4 times greater in *model A* than the same in *model B*.

In the side plates the maximum values of the resultant displacement for both models are received in the places of the base of the seat where dissolution of the side plates is observed - Fig.3. This is due to the fact that the resultant displacements are determined mainly by *z*-displacements (u_z) – Table 2. The resultant displacements in the base of the seat of *model B* are 1.6 times greater that this of *model A* because of rearrangement of displacements due to the strengthening details, but in the upper rails of the seat they are reduced approximately 1.6 times for *model B*.

The maximal resultant nodal rotations θ_{res}=1.74° for *model A* and θ_{res}=1.38° for *model B* are located in the rear upper rail for both models (Fig.4) and they are determined mainly by rotations about *z*-axis –Table1. The resultant nodal rotations of *model A* are 1.3 times greater than the same in *model B*.

Maximal values of resultant nodal rotation in the side plates are received in the contact field with the rear upper rail for both models (Fig.5). The resultant nodal rotations in the side plates of *model A* are 1.4 times greater than the same in *model B*.

Expectedly, the change in the angle *γ* between the joint shouders at upper front and upper rear rails of the seat is minor in the presence of the strengthening elements (*model B*) – Table 1.

The maximal values of equivalent starin are located in the side plates in the field of front upper rail of the seat for both models, as for *model A* they are 1.5 times greater than the same of *model B* – Table 1 and Table 2.
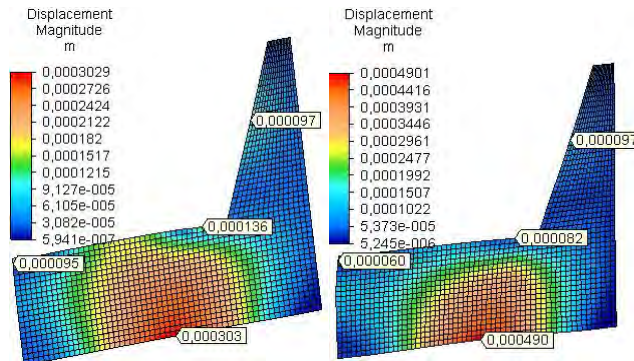
Figure 3. Resultant displacements in the side plates for model A and model B
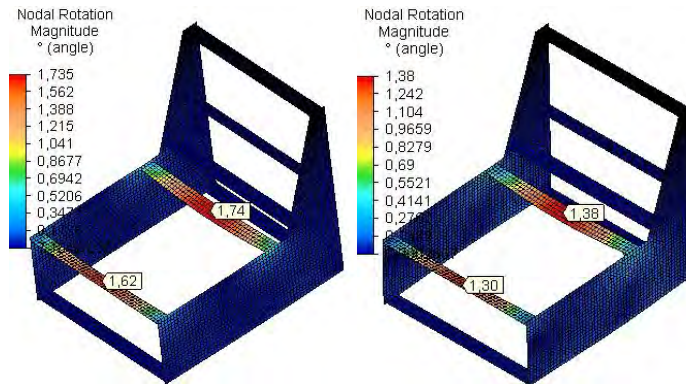
Figure 4. Distribution of resultant rotational displacements for model A and model B
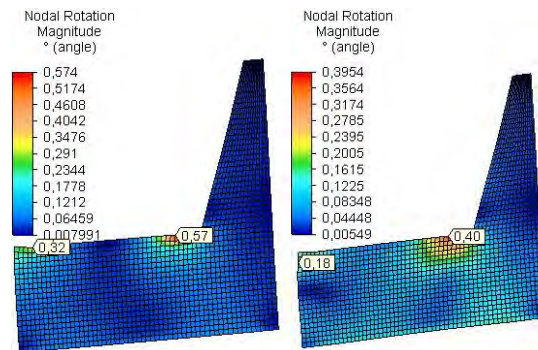
Figure 5. Resultant rotational displacements in the side plates /model A and model B/

CONCLUSIONS

From the results of this study by FEM with CAE program Autodesk Simulation Mechanical® on the deformations of one-seat upholstered furniture skeleton with staples and glue joints made of Scots pine and OSB several conclusions can be derived:

Under light-service load due to the nature of the applied force the maximum values for linear displacements and nodal rotations are received in the rear upper rail of the seat.

The strengthening with solid wood components of the upper rails to side plates joints infuences the deformability of the skeleton with side plates of OSB – the linear displacements reduce with 28.00% and nodal rotations reduce eith 21%. The strengthened skeleton with side plates of OSB has greater stiffness. The change in the angle $γ$ between the shoulders of the upper rails to side plate of the seat is also minor in the presence of strengthening elements.

The deformation behavior in side plates of OSB is considerably improved after strengthening of the upper rails to side plate joints of the seat - the linear displacements are reduced approximately with 28%, the nodal rotations - 21%.

REFERENCES

1. BODIG, J. , JAYNE, B. (1982): Mechanics of Wood and Wood Composites, Van Nostrand Reinhold Co. Inc., New York.
2. GENCHEV, YA. (2018): Special Productions and Wood Products. Production of Upholstered Furniture, Publish house – Univ. of Forestry, Sofia, in print (in Bulgarian).
3. HRISTODOROVA, D. (2018): Stiffness Coefficients in Joints by Staples of Skeleton Upholstered Furniture, Innovation in Woodworking Industry and Engineering Design (INNO), in print.
4. KASAL, A. (2006): Determination of the Strength of Various Sofa Frames with Finite Element Analysis, G.U. Journal of Science, vol.19, No.4, 191-203.
5. MARINOVA, A. (1996): Methodology of Stress and Strain Furniture Structure Analysis, Proceeding of International Science Conference "Mechanical technology of wood", Sofia, 257-267 (in Bulgarian).
6. THOMAS, W. (2003): Poisson's Ratio of an Oriented Strand Board, Wood Sci. Tehnology, Vol. 37, No.3, 259-268.
7. WANG, X. (2007a): Designing, Modelling and Testing of Joints and Attachment Systems for the Use of OSB in Upholstered Furniture Frames, PhD thesis, University Laval, Quebec, Canada.

FEA OF STRESSES OF AN UPHOLSTERED FURNITURE SKELETON WITH SIDE PLATES FROM OSB

Nelly Staneva – Desislava Hristodorova – Yancho Genchev – Yosif Zarkin

Abstract

A linear static analysis of one-seat skeleton 3D model for upholstered furniture was carried out with CAD/CAE system Autodesk Simulation Mechanical® by the method of finite elements (FEM) simulating light-service loading of the skeleton. The orthotropic material characteristics of pine solid wood (Pinus sylvestris L.) for the rails and OSB for the side plates are considered in the analysis. Two variants of corner joints in the skeleton (model A – staples and PVA; model B - staples, PVA and strengthening elements) were considered. FEA was performed with regard to laboratory determined and calculated coefficients of rotational stiffness of used staple corner joints. As results the distribution of principal stresses in the 3D model of upholstered furniture skeleton with staple corner joints are presented and analysed. It has been confirmed that the strengthening of the upper rail of the seat leads to reduction of the stresses in the skeleton and in the side plates of OSB.

Key words: *upholstered furniture skeleton, staple joints, OSB, stresses, CAE, FEM*

INTRODUCTION

The skeleton of upholstered furniture is usually wood and/or wood-based products. Although the wood composites are commonly used in box type furniture, their utilization in the frame type furniture is not widespread. There is limited number of references concerning the strength behaviour of upholstered frames constructed with structure elements of OSB although OSB panels are increasingly used in the construction of upholstered furniture frames latterly.

Wang, X. (2007a) has investigated a three-seat sofa frame made entirely of 18 mm thick OSB plates. She has created 3D linear models by beam finite elements with software SAP 2000 of 3 different constructions of a sofa frame with two types of connections – rigid and semi-rigid and two types of connectors: 1) screws and metal plates; 2) staples and metal plates. Nonlinear static analysis has been performed simulating 3 loads: light-, medium- and heavy-service. Wang has established the most appropriate configuration of the sofa frame of OSB under investigated loads and has concluded that the type of connectors does not change the joint displacements and strength remarkably.

Kasal, A. (2006) has investigated the strength properties of glued-dowel joined sofa frames constructed of solid wood and wood based composite materials by using the finite beam elements by CAE. Considering wood materials as isotropic, he has established that the OSB (18 mm thick) has lowest load bearing capacity. The failure of OSB sofa frame

University of Forestry, blvd. "Kl. Ohridsky" 10, 1797 Sofia, Bulgaria
e-mail: nelly_staneva@yahoo.com

has been the pull-out of dowels from the member with some core wood particles attached to the dowel and some splits have occurred at the edge of the butt members in the sofa frames.

Erdil Y. et al. (2008) have investigated the behaviour of 3-seat upholstered furniture frames constructed with ¾ inch thick OSB and joining elements - yellow birch dowels and aliphatic resin glue (PVA) using the simplified methods of structural analysis in the engineering of such frames. They have concluded that OSB may be used in construction of upholstered furniture frames to meet specific design loads.

More information concerning the strength characteristics of upholstered furniture joints made of OSB is available: Jivkov et al. (2003) have established the ultimate bending strength under compression of end corner joints of 18 mm thick OSB with different connectors – screws, dowels, "Confirmat"; Wang, X. et al. (2007b) and Wang, X. et al. (2007c) have investigated T-shape corner gusset-plate joints with staples and with/without PVA glue of details of 18 mm thick OSB panels under static bending, torsion and fatigue load. They have concluded that the static bending strength increases with 27% when the reinforcing elements are glued. They have established that both stapled and glued stapled joints had similar static-to-fatigue moment capacity ratios.

Data about strength characteristics of other joints of OSB for upholstered furniture in tension, shear, bending and cyclic loads are given by Erdil Y. et al. (2008) in the result of previous researches for dowel joints of different construction elements (front rail to stump, top rail to back post and back post to top rail joints of 4-inch thick OSB), Zhang, J. et al. (2001a), Zhang, J. et al. (2002) for dowel joints; Wang, X. et al. (2007d), Wang, X. et al. (2008) for metal-plate connected joints; Zang, J. et al. (2001b) for gusset-plate joints; Dai at al. (2008) for glued face-to face and end-to-face joints.

The literature study revealed a limited number of publications on skeleton strength studies of upholstered furniture with staple joints and side plates made of OSB.

The aim of this study was to define and analyze the stresses of one-seat skeleton of upholstered furniture with staple joints and side plates of OSB by CAD/CAE using the method of finite elements (FEM).

MATERIALS AND METHODS

3D model of one-seat upholstered furniture skeleton with length 600 mm, width 680 mm and height 625 mm was created with Autodesk Inventor Pro® – Fig.1. The used rails are with cross section 25x50 mm. A linear static analysis of 3D modeled skeleton was carried out with CAD/CAE system Autodesk Simulation Mechanical® by the Finite Elements Method (FEM). Two discrete models were created - *model A* without and *model B* with strengthening details under the upper rails of the seat with a shape of triangle prism and two design scenarios were performed. The generated Midplane mesh has 5130 orthotropic plate finite elements and 33616 DOF's for *model A* and 5230 orthotropic plate finite elements and 34096 DOF's for *model B*.

Orthotropic materials type was used for construction elements of the skeleton:

Scots pine (*Pinus sylvestris L.*) for rails and strengthening details with measured density 435.50 kg/m³ according to BDS EN 323:2001 and elastic characteristics: $E_z=E_L=9000.10^6$ N/m², $E_x=E_T=593.10^6$ N/m², $G_{LT}=554.5.10^6$ N/m², $\nu_{LT}=0.027$, $\nu_{TL}=0.41$, $\nu_{LR}=0.03$, $\nu_{RL}=0.049$;

Oriented strandboard (OSB), type EGGER OSB2 EN 300 E1 CE, designed for load-bearing structures for use in a dry environment with thickness 16 mm and technical requirements according to BDS EN 13986:2004+A1:2015 were used for side plates. The

physical and mechanical characteristics of the OSB panels are: density 595.67 kg/m³, measured according to BDS EN 323:2001; modulus of elasticity in bending (major axis) – E_x=3800.10⁶ N/m²; modulus of elasticity in bending (minor axis) – E_y=3000.10⁶ N/m²; bending strength (major axis) – 16.4.10⁶ N/m²; bending strength (major axis) – 8.2.10⁶ N/m²; Poisson ratios v_{12}=0.030 according to Thomas, W. (2003) and v_{21}=0.24, calculated according to Bodig et al. (1982) by the equation: $\frac{v_{12}}{E_1} = \frac{v_{21}}{E_2}$.
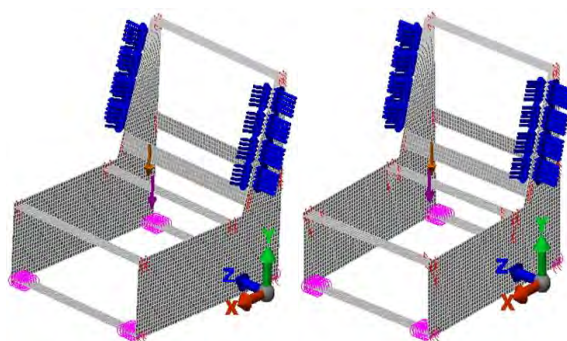
Fig. 1. 3D skeleton models *A* and *B* and loading

Support boundary conditions were set: bottom front rail – no translation on *y* direction and bottom rear rail no translation on *x*-, *y*- and *z* direction.

In order to simulate semi-rigid connections between rails and side plates of the skeleton two actions were performed: First – narrow zones were created in the place of joints in the discrete model with established via tests by FEM lower modules of elasticity of the used materials perpendicular to the common edge of the corner joint; Second - the laboratory determined by Hristodorova, 2018 coefficients of rotational stiffness of the corner joints with 2 staples and PVA glue, loading under compression were introduced in the nodes of the respective corner joints - case butt joints (*c*=766.84 N.m/rad) and end to face butt joints (*c*=509.99 N.m/rad).

The both discrete skeleton models were loaded with a total load of 800 N, distributed as follows (Fig.1): *Seat*: 80% were set as a remote force, distributed between upper rails of the seat with application point of 100 mm in front of the upper rear rail, simulating upholstery base made of zig-zag springs; *Backrest*: 16% were set as equal nodal forces, distributed on the edges of the two sides of the backrest simulating elastic belts.

RESULTS AND DISCUSSION

The results for maximum principal stresses (σ_1) – tension stresses and minimum principal stresses (σ_3) – compression stresses for both *models A* and *B* are shown in Fig.2 to Fig. 5 for the skeleton and for the side plates of the skeleton respectively. The visualizations of the deformed model are shown with a scale factor 3% of model size for the skeleton and with a scale factor 5% of model size for the side plates.

For *model A* the maximum principal stresses (tension; (+)) and the minimum principal stresses (compression (-)) have maximal values located in the upper rear rail of the seat at the bottom and on the top respectively – Fig. 2 and Fig. 3. For *model B* maximal values of the tension and compression stresses are located in the strengthening details of the upper rear rail of the seat.

The tension and compression stresses in the upper rear rail of the seat decrease in the *model B* 1.3 times and 1.2 times respectively, comparing to the same in *model A.*
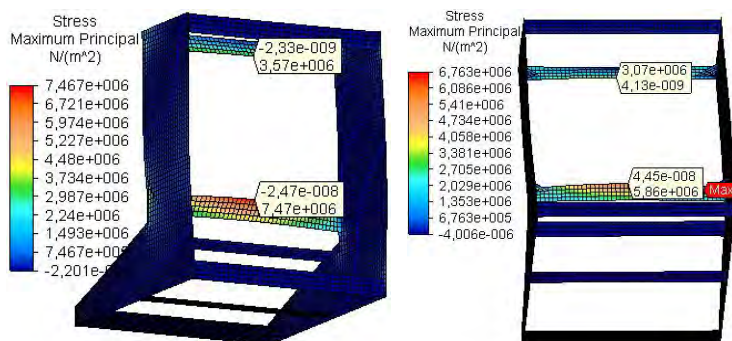
Figure 2. Distribution of maximum principal stresses for model A and model B
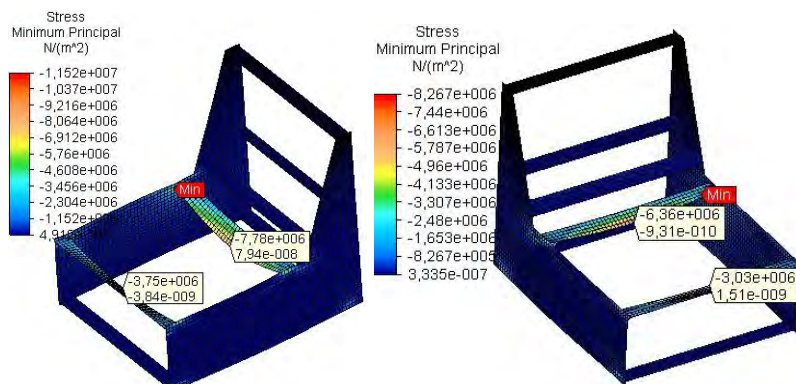
Figure 3. Distribution of minimum principal stresses for model A and model B
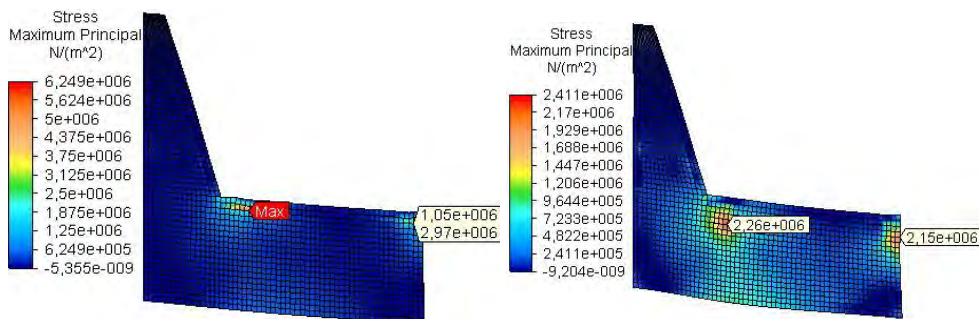
Figure 4. Distribution of maximum principal stresses in the side plates for model A and model B

In the side plates of OSB the maximal values of tension and compression stresses are located in the field of upper rear rail for both models – Fig.4 and Fig.5. It is evident that the compression stress in the field of upper rear rail in the side plates of OSB for *model A* is greater than the maximum bending stress of OSB plates $(8.2.10^6 \, \text{N/m}^2)$.

It was established a reduction of the tension stresses almost 2,6 times and reduction of the compression stresses approximately 4 times in the side plates of the skeleton for *model B* comparing to the same in *model A.*
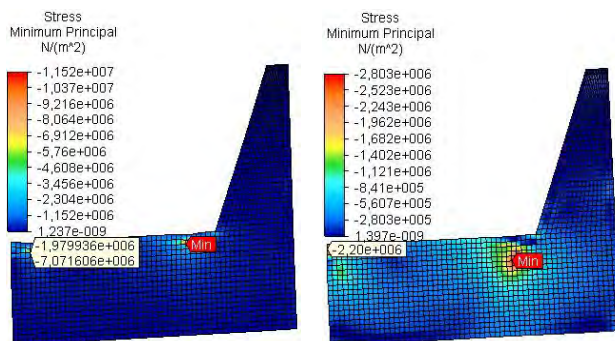
Figure 5. Distribution of minimum principal stresses in the side plates for model A and model B

CONCLUSIONS

From the results of this study by FEM with CAE program Autodesk Simulation Mechanical® on the deformations and stresses of one-seat upholstered furniture skeleton with staples and glue joints made of Scots pine and OSB several conclusions can be derived:

Under light-service load the most loading construction part of the skeleton with side plates of OSB is the rear upper rail of the seat where the maximum values of stresses are received due to the nature of the applied force.

The reinforcement of the upper rails to side plate joints with solid wood components improves the strength behaviour of the skeleton with side plates of OSB – the tension stresses are reduced with 22%, compression stresses with 18%.

The strength behaviour of the side plates is also impruved after reinforcement – tension stresses are reduced with 22%, compression stresses - more significantly with 75%.

REFERENCES

1. BODIG, J. and JAYNE, B. (1982): Mechanics of Wood and Wood Composites, Van Nostrand Reinhold Co. Inc., New York.
2. DAI, L., ZHANG, J., QUIN, F. (2008): Lateral and Tensile Resistances of Glued Face-to-face Joints in Pine Plywood and Oriented Strandboard, Forest Products J., Vol. 58, No.3, 50-54.
3. ERDIL, Y., KASAL, A., ECKELMAN, C., (2008): Theoretical Analysis and Design of Joints in a Representative Sofa Frame Constructed of Plywood and Oriented Strand Board, Forest Products J., Vol. 58, No.7/8, 62-67.
4. HRISTODOROVA, D. (2017): Stiffness Coefficients in Joints by Staples of Skeleton Upholstered Furniture, Innovation in Woodworking Industry and Engineering Design (INNO), in print.

5. KASAL, A. (2006): Determination of the Strength of Various Sofa Frames with Finite Element Analysis, G.U. Journal of Science, vol.19, No.4, 191-203.
6. MARINOVA, A. (1996): Methodology of Stress and Strain Furniture Structure Analysis, Proceeding of International Science Conference "Mechanical technology of wood", Sofia, 257-267 (in Bulgarian).
7. PĚNČÍK, J. (2014): Modelování Dřeva Pomocí Ortotropního Materiálového Modelu s Kritérii Porušení, Stavební Obzor, No.1–2, 6-7 (in Slovak).
8. THOMAS, W. (2003): Poisson's Ratio of an Oriented Strand Board, Wood Sci. Tehnology, Vol. 37, No.3, 259-268.
9. ZHANG, J., QUIN, F., TACKETT, B. (2001a): Bending Strength and Stiffness of Two-Pin Dowel Joints Constructed of Wood and Wood Composites, Forest Products J., Vol.51, No.2, 29-35.
10. ZANG, J., LYON, D., QUIN, F. AND TACKETT, B. (2001b): Bending Strength of Gusset-Plate Joints Constructed of Wood Composites. Forest Prod. J., Vol.51, No.5, 40-44.
11. ZHANG, J., ERDIL, Y., ECKELMAN, C. (2002): Torsional Strenght of Dowel Joints Constructed of Plywood and Oriented Strandboard, Forest Products J., Vol.52, No.10, 89-94.
12. WANG, X. (2007a): Designing, Modelling and Testing of Joints and Attachment Systems for the Use of OSB in Upholstered Furniture Frames, PhD thesis, University Laval, Quebec, Canada.
13. WANG, X., SALENIKOVICH, A., MOHAMMAD, M., I. ECHAVARRIA AND J. ZHANG. (2007b): Moment Capacity of Oriented Standboard Gusset-Plate Joints for Upholstered Furniture. Part 1. Static Load. Forest Products J., Vol.57, No.7/8, 39-45.
14. WANG, X., SALENIKOVICH, A., MOHAMMAD, M. AND J. ZHANG. (2007c): Moment Capacity of Oriented Strandboard Gusset-Plate Joints for Upholstered Furniture. Part 2. Fatigue Load. Forest Products J., Vol.57, No.7/8, 46-50.
15. WANG, X., MOHAMMAD, M., SALENIKOVICH, A., KNUDSON, R. AND J. ZHANG. (2007d): Static Bending Strength of Metal-Plate Joints Constructed of Oriented Strandboard for Upholstered Furniture Frames. Forest Products J., Vol.57, No.11, 52-58.
16. WANG, X., SALENIKOVICH, A., MOHAMMAD, M., (2008): Out of Plane Static Bending Resistance of Gusset-Plate and Metal-Plated Joints Constructed of Oriented Strandboard for Upholstered Furniture Frames, Forest Products J., Vol.58, No.3, 42-49.

DETERMINATION OF VARIABLITY THE REPOSE ANGLE OF THE CHIPPED WOOD

Sergei Trofimov[1] – Tomasz Rogoziński[2]

Abstract

This report presents the results of the study of the angle of repose of some types of chipped wood in a calm state and its variability in the process of dynamic effects. The results of experimental studies can be used to solve problems of transportation, bunkering and cumulative storage of some common breeds of chipped wood (sawdust, shavings, grinding dust). When studying the effect of dynamic influences (shaking) on the angle of the repose of loose material, a special laboratory test stand was used to regulate the drive of the motor's rotation speed by means of inventory. Taking into account the flow characteristics of chipped wood of different types is the basis for improving technical solutions and operating rules for equipment (for example, conveyor belts with roller bearings on the working branch).

Key words: *chipped wood; variablity of repose angle; slope angle, dynamic effects*

INTRODUCTION

In the processes of wood processing, a huge amount of chipped wood is formed, transported and used in the form of production waste and products of special purpose for technological needs. Taking into account the properties of bulk material is necessary for transportation, bunkering, cumulative storage and solving a number of other practical production tasks. One of the important characteristics of the chipped wood is the size and variability of the angle of repose of this material. This figure is affected by the fractional composition and geometry of the particles, the wood's species and moisture, the temperature of the medium, and many other factors, including the dynamic effects on the material. The basis for obtaining data on the magnitude of the angle of the repose and its variability are experimental works. The results of the study are of practical interest and can serve as a basis for improving certain types of equipment and technological processes with the presence of chipped wood.

MATERIALS AND METHODS

Experimental work was carried out on the example of several species (pine, beech, oak) and types of dry chipped wood (sawdust, shavings and grinding dust) without preliminary

[1]Belarusian State Technological University, Sverdlova str., 13-a, Minsk, 220006, Belarus
e-mail: tspx46@gmail.com
[2]Poznań University of Life Sciences, Wojska Polskiego 38/42, 60-627 Poznań, Poland
e-mail: trogoz@up.poznan.pl

sorting by fractions. Experimental material was obtained from enterprises in the form of waste generated in the technological processes of some woodworking industries.

When studying the variability of the angle of a natural repose, the type of chipped wood and the frequency of dynamic impacts (shaking) were considered in conditions of modeling the operation of a conveyor belt with roller bearings. Taking into account the specificity of the object of experimental research, for tape and some other conveyors, the amount of material in experimental portions was taken as small.

Determination of the angle of repose of chipped materials can be carried out in several ways using different equipment [1–5 and etc.]. There are information about several patents for the design of devices for performing these works. In Fig. 1 shows some examples of some simple frequently used devices.
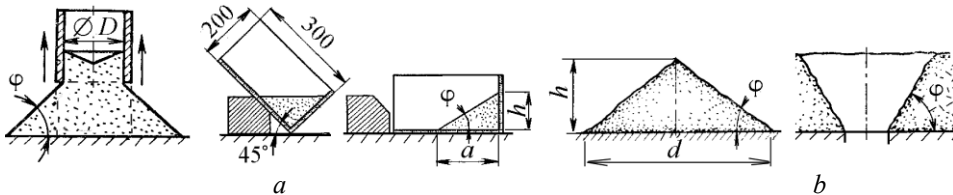
Fig. 1 Determination of the angle of repose of the cargo in a calm state
a – using a cylinder and a box; *b* – with free pouring and collapse

During the experimental work to determine the angle of repose of the chipped wood and its variability under the influence of dynamic influences on the bulk material, a specially designed laboratory test stand with an adjustable shaking frequency was used, simulating the conditions of cargo transportation with a belt conveyor with rollers on the working branch (Fig. 2). The control of the speed of shaking was done by the inventor.
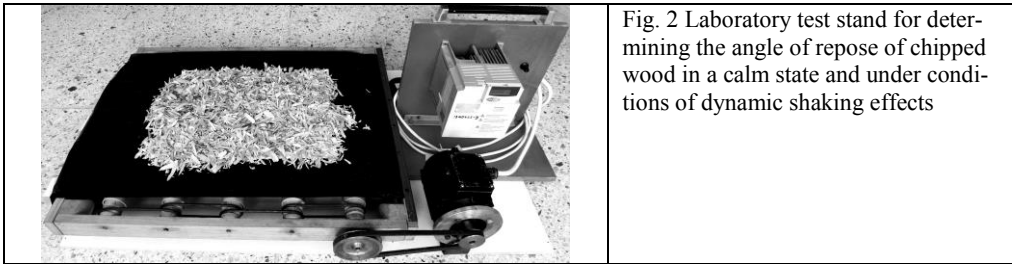
Fig. 2 Laboratory test stand for determining the angle of repose of chipped wood in a calm state and under conditions of dynamic shaking effects

The experiments began with the precipitation of chipped wood from two cylinders (Fig. 1*a*) without a horizontal horizontal flat surface of the conveyor belt. Fig. 4 illustrates the work done with two cylinder-accumulators of diameters (D = 100 and 150 mm), and Tab. 1 contains a sample of experimental results.
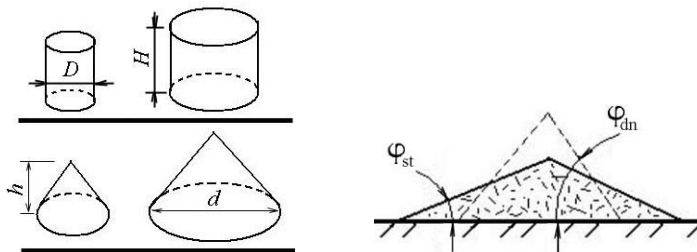
Fig. 4 Measurement of static φ_{st} and dynamic φ_{dn} the angle of chipped wood repose

Based on the measurement of the height h and the diameter d of the base of the vaulting cone (Fig. 3), the repose angle of the material in the quiescent state φ_{st} was determined and after the dynamic shaking effects φ_{dn} by the formula

$$\varphi = \operatorname{arctg}\left(h/(d/2)\right), \tag{1}$$

where: φ – the angle of repose of the chipped wood, deg .; h – height of the cone or profile of the material layer; d – the diameter of the base of the cone or the width of the base of the profile of the layer of material.

During studying the properties of chipped wood, various indicators characterizing it were determined, including the angle of the repose and the influence of a number of factors on it. Experimental studies of the influence of dynamic influences on bulk material were carried out on a specially manufactured laboratory test stand with an adjustable shaking frequency simulating the transportation of goods by a belt conveyor with roller bearings on the working branch.

The fractional composition of the chipped wood was determined using standard sieves. The sieves were arranged top-down in direction of meshes´ lessening and placed on a vibrating holder of a sieving machine AS 200c (Retsch, Germany) with an adjustable frequency and amplitude of oscillation.

A laser particle sizer "Analysette 22 Microtec Plus" (Fritsch, Germany) with measuring range 0,08–2000 μm was used in this stage of experiments. Dust sizes up to 100 μm were taken into consideration in the analysis.

An example of the results of analysis of the fractional composition of the experimental material in the form of histograms of particle size distribution is shown in Fig. 5.
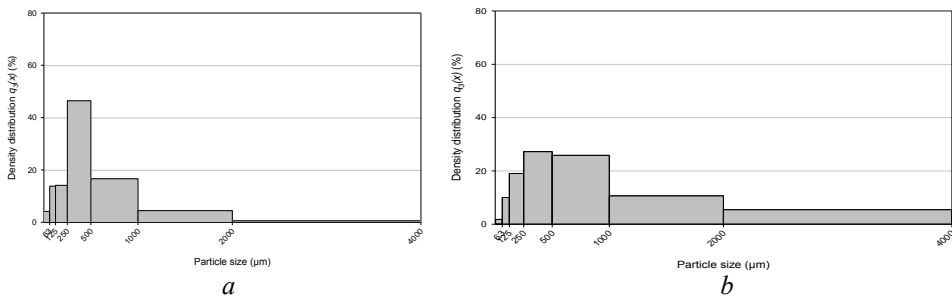
Fig. 5 Particle size distribution: a – birch dust of grinding plywood; b – pine sawdust

RESULTS AND DISCUSION

The main results of research of shaking are given in Tab. 1 and are illustrated by the graphs in Fig. 6.

The materials of Tab. 1 and Fig. 6 characterize the variability of the chipped wood repose angle, depending on the type of material and the frequency of the dynamic shaking effects. They indicate a significant decrease in the angle of the repose with an increase in the shaking frequency.

Tab. 1 Mean values of the angle of repose depending on the type and kind of wood and the shaking frequency

Kind of chipped wood	Source of chipped wood	Diameter of storage cylinder, D, mm	The average value of the angle of repose of the chipped wood, φ, deg. at a shaking frequency, n, 1/s				
			0	1	2	3	4
Shavings dry pine	Four-side planer "Powermat-500"	100	50,5	-	35,2	26,2	18,8
		150	47,4	-	33,2	25,0	18,6
Shavings dry beech	Four-side planer "Unimat-500"	100	39,2	-	35,0	25,7	19,3
		150	43,9	-	37,8	29,8	21,1
Sawdust oak, after sawing were dried	Log band saw "Wood Mizer"	100	42,2	-	39,3	29,4	22,2
		150	44,8	-	40,9	30,7	22,7
Birch dust when grinding plywood	Grinding machine "Steinemann"	100	32,0	-	27,5	21,2	16,0
		150	34,6	-	29,2	22,7	17,9
Sawdust sawing of MDF boards	Circular saw "Solco" for cutting plates	100	32,3	-	25,5	18,2	14,7
		150	35,2	-	26,3	18,6	14,2
Shavings dry pine	Four-side planer "Grigio"	100	33,9	-	25,0	19,2	15,1
		150	36,3	-	25,7	19,4	15,4
Pine sawdust, after sawing were dried	Log saw canter machine "TT5/550/320"	100	47,7	-	36,5	26,3	20,8
		150	45,4	-	32,8	25,0	20,4
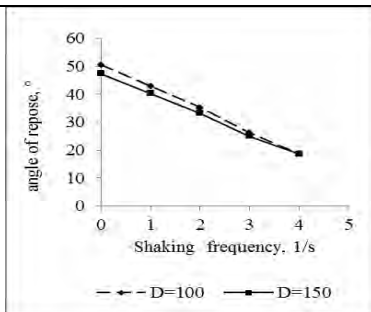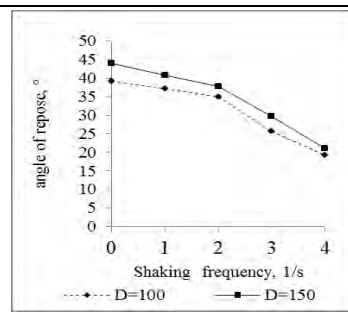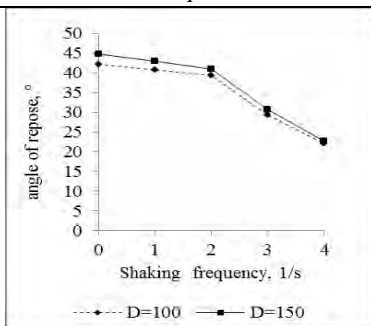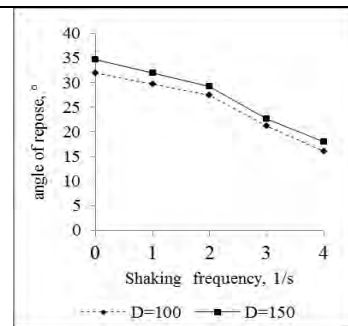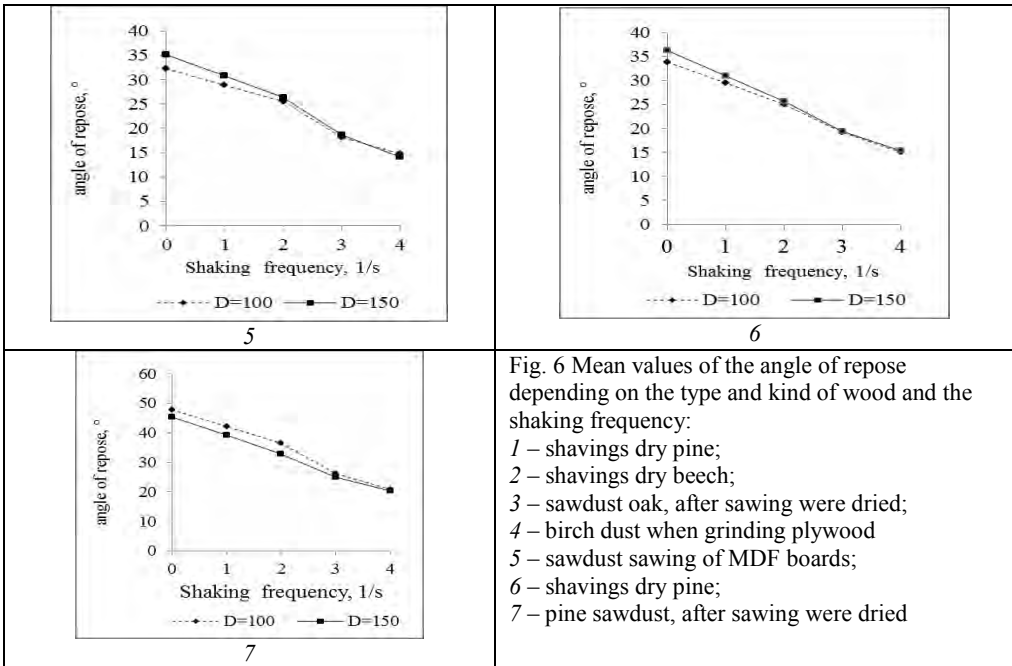
Fig. 6 Mean values of the angle of repose depending on the type and kind of wood and the shaking frequency:
1 – shavings dry pine;
2 – shavings dry beech;
3 – sawdust oak, after sawing were dried;
4 – birch dust when grinding plywood
5 – sawdust sawing of MDF boards;
6 – shavings dry pine;
7 – pine sawdust, after sawing were dried

Experiments carried out with storage cylinders of diameter *D* = 100 and 150 mm showed good convergence of the results, which confirms their sufficient reliability.

With respect to the belt conveyor, the shaking frequency of the material being conveyed depends on the speed of the tape *v* and the distance between the roller bearings *l* (Fig. 7). It can be determined by the formula

$$n = v/l, \tag{2}$$

where: *n* – the shaking frequency of the chipped material, 1/s; *v* – speed of movement of the traction body of the belt conveyor, m/s; *l* – the distance between the rollers on the working branch of the conveyor, m.

The results of calculating the frequency *n* of shaking shredded wood according to the formula 2 are shown in Fig. 7. They allow to determine the range of change of the investigated factor of dynamic impact on cargo.
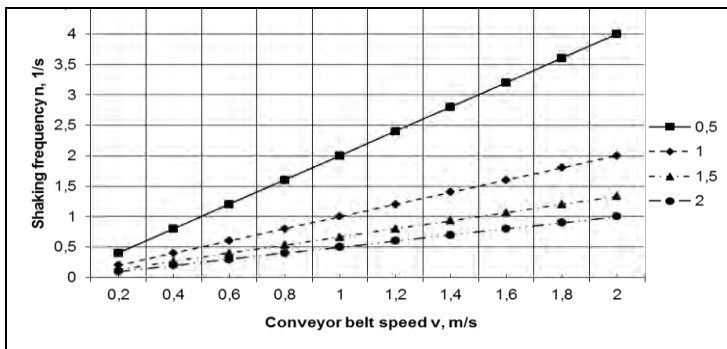
Fig. 7 Influence of conveyor belt speed *v* and distance between roller bearings *l* on shaking frequency *n*

.°The angle of natural repose of chipped wood in a quiet state is often characterized in the literature by the value φ_{st} = 35–45°. It depends on the moisture content and fractional composition of the cargo, with simplified depersonalized calculations, the value φ_{st} = 39° is usually adopted. However, in reality the magnitude of this angle can vary over a much wider range, a more accurate knowledge of it can avoid errors in design calculations and improve the energy efficiency of mechanical transport devices.

When transporting and shaking the load under the influence of dynamic forces, the angle of the repose considerably decreases over a wide range of deviation, depending on the frequency, type and characteristics of the chipped wood.

CONCLUSION

The results of the research are of practical interest for increasing the effectiveness of technical solutions in the technology of woodworking production. In particular, they make it possible to improve the rationale for constructive parameters and operational limitations on the use of certain types of technological equipment, belt, inertial and vibrational conveyors when they operate at different speeds and reposes. Based on the analysis of the data obtained, can be determined the tasks of the following studies, for example phenomena segregation and seal material.

REFERENCES

[1] Rogozinski, T. Dust creation during birch plywood production / T. Rogozinski, S. Trofimov. – Annals of Warsaw University of Life Scienes – SGGW. Forestry and Wood Technology. No 98, 2017. – p. 99–103.

[2] Rogozinski, T. A study on properties of wood dust created during windows manufacturing / C. Dembinski, A. Ockajova, Z. Potok. – Annals of Warsaw University of Life Scienes – SGGW. Forestry and Wood Technology. No 98, 2017. – p. 94–98.

[3] Bacherikov, I.V. Opredelenie ugla estestvennogo otkosa sipuchih materialov / I.V. Bacherikov, B.M. Lokshtanov // Izvestija Sankt-Peterburgskoj lesotehnicheskoj akademii. Vip. 214. – SPb.: SPbGLTA, 2016. – s. 167–177.

[4] Bacherikov, I.V. Vlijanie temperaturi i vlazhnosti na ugol estestvennogo otkosa drevesnih sipuchih materialov / I.V. Bacherikov, B.M. Lokshtanov // Izvestija Sankt-Peterburgskoj lesotehnicheskoj akademii. Vip. 217. – SPb.: SPbGLTA, 2016. – s. 158–165.

[5] Kouzov, P.A. Metodi opredelenija fiziko-mehanicheskih svojstv promishlennih pilej / P.A. Kouzuv, L.J. Skrjabina. – L.: Himija, 1983. – 143 S.

INFLUENCE OF THE CUTTING MODE ON THE SURFACE QUALITY DURING LONGITUDINAL PLANE MILLING OF ARTICLES FROM BEECH WOOD

Pavlin Vitchev – Zhivko Gochev – Valentin Atanasov

Abstract

The objectives of the current study are to investigate the influence of the cutting mode on the surface quality during longitudinal plane milling of details from beech (Fagus sylvatica L.) wood. The influence of the rotation frequency (n) and the feed rate (U) at different thickness of the cut-out layer (h) has been assessed. On the basis of the obtained results, graphical dependencies, representing the relationship between the different studied factors have been derived. In order to achieve a higher quality of the processed surfaces, practical recommendations for the optimal values of the evaluated factors have been suggested. The surface roughness of the material (surface) was measured with a roughness tester, type „Surftest SJ-210"(Mitutoyo, Japan).

Key words: *surface roughens, cutting mode, wood milling, Fagus sylvatica*

INTRODUCTION

Milling is one of the main technological processes involved in the processing of solid wood and wood-based materials, which aims to give a certain shape of the processed details and at the same time to ensure a higher surface quality (higher roughness class). It is well-known that the quality of the processed surfaces may be influenced by different factors, related to the characteristics of the processed material (Sandac et al., 2004), of the cutting tool and at last but not least, to the cutting mode during the material's processing (Keturakis, 2007; Gochev, 2014[b]). When determining the roughness of the wood surfaces, the direction of the wood fibers in which the measurements will be carried out is also important. Due to the anisotropic structure of the wood, the roughness of the surface is different and depends on the orientation of the fibers (Sandac et al., 2004). Some of the influencing factors can be controlled during processing, therefore they should be given more attention and become subject to wider and more comprehensive study in order to be managed in a more adequate way. In the recent years, a number of studies have been focused on investigating the processes related to the longitudinal plane milling and the resulted surface quality (Costes et al., 2002; Keturakis, 2007; Prakasvudhisarn et al., 2009; Rousek et al., 2010; Gonzalez-Adrados et al., 2012; Гочев, 2014[a]; Гочев, 2014[b];). Their common goal was to assess and determine the optimal parameters and conditions, assuring higher surface quality.

In relation to this, the aim of the current experimental study was to investigate the influence of following factors: the rotation speed of the cutting tool (*n*), the feed rate (*U*) and the

University of Forestry, 10 Kliment Ohridski Blvd., Sofia, Bulgaria
e-mail: p_vitchev@ltu.bg; zhivkog@ltu.bg; vatanasov_2000@ltu.bg.

thickness of the cut-out layer (*h*) on the surface roughness of samples from beech wood (*Fagus Sylvatika* L.) during longitudinal plane milling.

MATHERIALS AND METHODS

The experiments have been carried out using woodworking spindle moulder machine, type T1002S (ZMM "Stomana" GmbH, Bulgaria) (Fig. 1). The machine was equipped with a two-speed three-phase electric motor with power 3,2/4,0 kW, which through a belt drive provides the following rotating frequency of the working shaft: 3000, 4000, 5000, 6000, 8000 and 10000 min^{-1}.

Figure 1. Woodworking spindle moulder machine, type T1002S – general view

A cutting tool with an assembled construction for longitudinal plane milling (Metal World, Italy) was used. The technical characteristics of the tool are presented in Table 1, where: *D* is the diameter of the cutter head, *d* – diameter of the threaded hole, *L* – longitude of the main cutting edge, γ – hook angle, *z* – number of teeth.

Table 1. Technical characteristics of the used cutting tool

General look of the milling cutter	*D* mm	*d* mm	*L* mm	β °	γ °	*z* No	Material of the teeth
	125	30	50	47	16	4	Hard alloy (HM)

In the course of the study, the samples from beech (*Fagus sylvatica* L.) wood have been processed, with the following characteristics: density: ρ = 690 kg.m^{-3}, moisture content *W* = 12 % and elasticity module $E_{L(12\%)}$ = 13225.10^6 N.m^{-2}, have been processed according to BDS ISO 3131, BDS ISO 3130 and EN 310, respectively. The samples had the following characteristics: longitude (*l*) 1000 mm and milling width (*b*) 40 mm. The details were fed automatically by a roller feeder.

In order to investigate the complex influence of the rotation frequency (*n*) of the milling tool, the feed rate (*U*) and the thickness of the cut-out layer (*h*) (milling height) on the quality of the processed surfaces, the methodology of multifactorial planning and subsequent regression analysis have been used (Vuchko et al. 1986). The measurements were performed in accordance with a preliminary designed matrix for three factorial experiment plan of G. Box (Box et. al., 1951; Box et. al. 1999). In Table 2 the levels of the input variables in explicit and coded form are presented. The selected values are in line with the most frequently used in practice.

Table 2. Values of the variables *n*, *U* and *h*

Variables	Minimum value		Average value		Maximum value	
	expl.	coded	expl.	coded	expl.	coded
Rotation frequency $n = X_1$, min^{-1}	4000	-1	6000	0	8000	1
Feed rate $U = X_2$, m.min^{-1}	3,5	-1	7	0	10,5	1
Thickness of the cut-out layer $h = X_3$, m	1	-1	2	0	3	1

In order to assess the quality of the treated surfaces, depending on the variables, the roughness parameter R_z, μm was used. It has been determined separately for five base lengths in the longitudinal direction of the wood fibers of each part. For each base length the parameter R_z is determined by the mathematical equation:

$$R_z = \frac{\sum_{i=1}^{5} \left| y_{p_i} \right| + \sum_{i=1}^{5} \left| y_{V_i} \right|}{5}, \mu m \tag{1}$$

where:
y_{pi} is the height of the biggest roughness of the profile, μm;
y_{vi} – the depth of the greatest slot of the profile, μm.

The surface roughness of each workspace was determined using the mean average value $\overline{R}_z$ from the five measurement. The applied methodology is in accordance with BDS EN ISO 4287 and is described in details by Gochev (2005). The measurements were performed with the digital profilomer, model "Surftest SJ-210" (Mitutoyo, Japan) (Fig. 2).

Figure 2. Profilometer, model Surftest SJ-210 – general view

For the statystical analysis of the data QstatLab softwear was used.

RESULTS AND DISCUSSION

Based on the performed experiments and after statistical analysis of the data, we received the follwoing regression equation:

$$y = 35,661 + 0,946X_1 + 3,457X_2 + 0,611X_3 + 3,672X_1^2 - 1,393X_2^2 - 1,663X_3^2$$
$$- 0,135X_1X_2 + 0,738X_2X_3 + 1,390X_1X_3$$

(2)

where:
y is the expected surface quality of the processed detail, defined by the roughness parameter R_z in coded form;
X_1 – rotation frequency of the cutting tool (n) in coded form;
X_2 – feed speed (U) in coded form;
X_3 – thickness of the cut-out layer (h) in coded form.

By using the equation (2) the surface quality, depending on the changes in the rotation frequency (n), feed speed (U) and the thickness of the cut-out layer (h) can be predicted.

In Table 3, the planning matrix for the three-factorial experiment and the mean average value of the roughness parameter, determined for different factor combinations are presented. The regression coefficients are given in Table 4.

Table 3. Planning matrix for three-factorial experiments and mean average values of the roughness parameter $\overline{R}_z$ (μm)

№	$X_1 = n$ min⁻¹		$X_2 = U$ m.min⁻¹		$X_3 = h$ mm		$\overline{R}_z$ μm	№	$X_1 = n$ min⁻¹		$X_2 = U$ m.min⁻¹		$X_3 = h$ mm		$\overline{R}_z$ μm
1	-1	4000	-1	3,5	-1	1	34,98	9	-1	4000	0	7	0	2	34,57
2	-1	4000	-1	3,5	1	3	30,42	10	1	8000	0	7	0	2	46,49
3	-1	4000	1	10	-1	1	38,47	11	0	6000	-1	3,5	0	2	31,98
4	-1	4000	1	10	1	3	41,27	12	0	6000	1	10	0	2	38,95
5	1	8000	-1	3,5	-1	1	29,65	13	0	6000	0	7	-1	1	35,94
6	1	8000	-1	3,5	1	3	35,06	14	0	6000	0	7	1	3	34,45
7	1	8000	1	10	-1	1	37,01	15	0	6000	0	7	0	2	34,30
8	1	8000	1	10	1	3	40,96								

Table 4. Regression coefficients

Coefficient	Coded value	Coefficient	Coded value	Coefficient	Coded value
b_1	0,946	b_{11}	3,672	b_{12}	-0,135
b_2	3,457	b_{22}	-1,393	b_{23}	0,737
b_3	0,611	b_{33}	-1,663	b_{13}	1,390

From the values of the regression coefficients (Tabl. 4) it is visible that during milling of the samples from beech wood, the greatest influence on the surface quality has the feed speed $U = x_2$ with regression coefficient $b_2 = 3,457$, followed by the rotation frequency of the cutting tool $n = x_1$ with regression coefficient $b_1 = 0,946$. The least influence among the investigated factors has the thickness of the cut-out layer $h = x_3$, with regression coefficient $b_3 = 0,611$. The positive values of the three regression coefficients show that by increasing

the values of the investigated factors, the surface roughness of the processed surfaces will also increase.

Figure 3 is a graphical representation of the changes in the surface roughness, depending on the rotation frequency at the three different speed feeds and determined by the roughness parameter R_z. From the roughness curves it is visible that by increasing the rotation frequency of the cutting tool (n) from 4000 to 5500 min^{-1}, the roughness of the surface decreased at the three feed speeds. The best surface quality was observed at $n = 5500$ min^{-1}, and it stays stable up to $n = 6500$ min^{-1}. With the increase of the rotation frequency of the cutting tool from $n = 6500$ min^{-1} to $n = 8000$ min^{-1}, the surface roughness increases as well. At the three feed speeds, the similar tendency in the variations of the roughness curves are observed. The details, processed at feed speed $U = 3,5$ m.min^{-1} and rotation frequency of the cutting tool $n = 6000$ min^{-1} have a better surface quality when compared to the other two higher feed speeds and are classified as roughness class IX. At feed speeds $U = 7$ m.min^{-1} and $U = 10$ m.min^{-1} and rotation frequency of the cutting tool $n = 6000$ min^{-1}, the processed details fall in roughness class VIII.
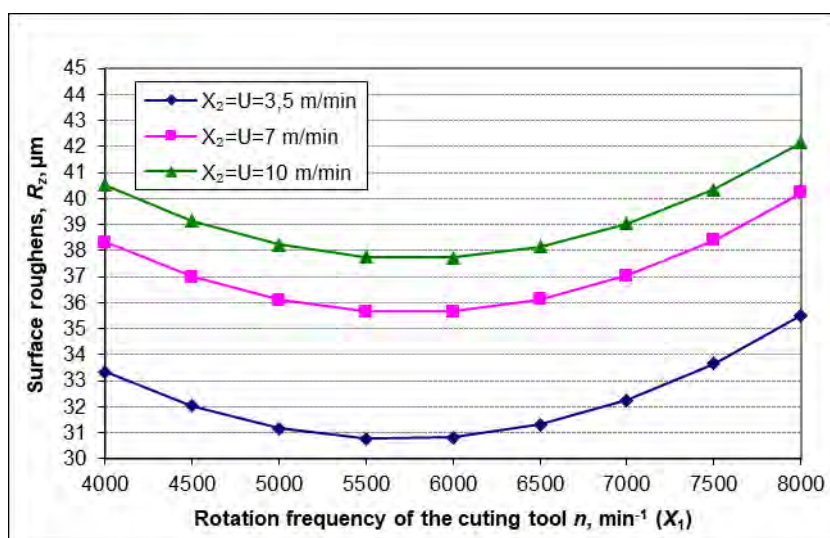
Figure 3. Changes in the surface roughness (R_z) depending on the rotation frequency of the cutting tool (n) at different feed rates (U)

The relationship between the changes in the surface quality (R_z) and the rotation frequency of the cutting tool at three different thicknesses of the cut-out layers, is presented in Figure 4. From the roughness curves it is visible that at three different thicknesses, the best surface quality was observed at rotation frequency of the cutting tool $n = 6000$ min^{-1}. The similar tendency in the variations of the roughness curves are observed at the three thicknesses of the cut-out layer. At rotation frequency of the tool from 5500 min^{-1} to 8000 min^{-1}, the increase of the thickness of the cut-out layer led to an increase of the surface roughness. At rotation frequency of $n = 7000$ min^{-1} and above, and the thickness of the cut-out layer (h) 2 and 3 mm, the surface quality is similar.

The relationship between the changes in the surface quality (R_z) and the feed rate (U), at three different thicknesses of the cut-out layers (h) is presented in Figure 5. From the graphs is clearly visible the strong influence of the feed speed (U) on the surface quality of

the processed material (R_z). The roughness curves in Fig. 5 are in good correlation with the results, presented in Fig. 4, namely that the increase of the thickness of the cut-out layer resulted in higher surface roughness. At feed rate (U) up to 5,2 m.min^{-1} and thickness of the cut-out layer (h) 1 and 2 mm, the processed details fall in roughness class IX. While the details, processed at the same feed speed but thicker h = 3, fall in class VIII.
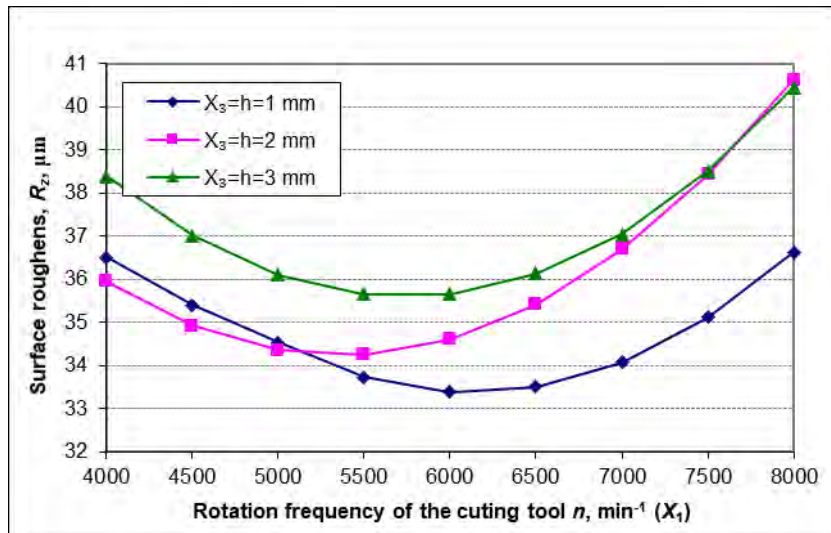
Figure 4. Changes in the surface roughness (R_z) depending on the rotation frequency of the cutting tool (n) at thee thickness cut-out layers (h)
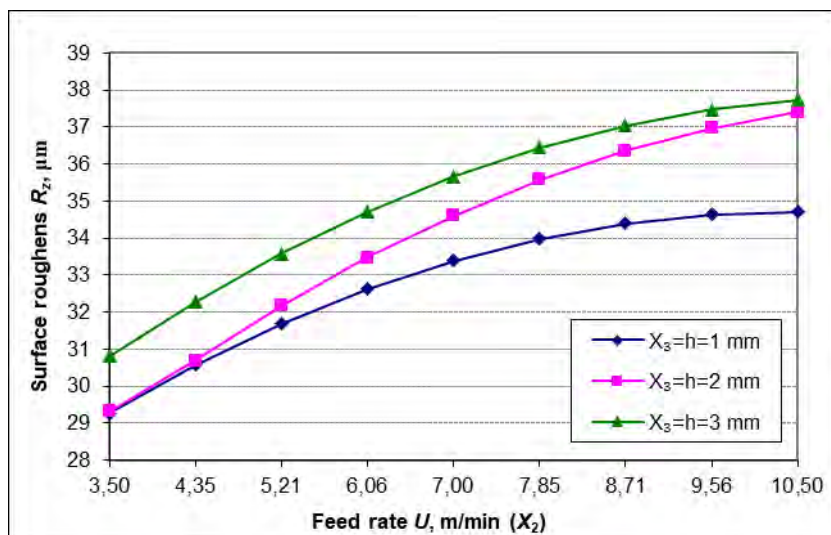
Figure 5. Changes in the surface roughness (R_z) depending on the feed speed (U) at thee thickness cut-out layers (h)

CONCLUSIONS

The current paper presents results from experimental study, investigating the surface roughness, after milling, of details from beech (*Fagus Sylvatica* L) wood, determined by the roughness parameter R_z (μm), measured along the length of the wood fibres of the samples.

Based on the obtained results, the following conclusions can be made:

- The quality of the milling surface is influenced by the mode of cutting during processing of the wooden details. Among the investigated factors, the greatest influence on the surface quality exerts the feed speed (U), followed by the rotation frequency of the cutting tool (n) and the thickness of the cut-out layer (h). By increasing the feed speed from 3,5 m.min^{-1} to 10,5 m.min^{-1} and the thickness of the cut-out layer $h = 3$ mm, the surface roughness changes significantly by 18,3 % (from 30,81 μm to 37,73 μm) (see Fig. 5).

- The optimal rotation frequency of the cutting tool is $n = 6000$ min^{-1}. This frequency, combined with the thickness of the cut-out layer $h = 2$ mm, gives the following values of the roughness parameter, measured at different feed speeds: at $U = 3,5$ m.min^{-1}, $R_z = 30,81$ μm; at $U = 7$ m.min^{-1}, $R_z = 35,66$ μm; at $U = 10,5$ m.min^{-1}, $R_z = 37,7$ μm (see Fig. 3).

ACKNOWLEDGEMENTS

REFERENCES

BDS ISO 3130 (1999): Wood – Determination of moisture content for physical and mechanical tests.

BDS ISO 3131 (1999): Wood – Determination of density for physical and mechanical tests.

BDS EN 310 (1999): Wood-based panels – Determination of modulus of elasticity in bending and of bending strength.

BDS EN ISO 4287 (2006): Geometrical product specifications (GPS) - Surface texture: Profile method – Terms, definitions and surface texture parameters.

Box G.E.P., Wilson K.B. (1951). On the experimental attainment of optimum conditions. Journal of the Royal Statistical Society, Series B13: 1–45.

Box, G.E.P., Liu P.Y.T. (1999). Statistics as a catalyst to learning by scientific method. Part I - an example, Journal of Quality Technology 31: 1–15.

Costes, J.P., Larricq, P. (2002). Towards high cutting speed in wood milling, Annals of Forest Science 59: 857–865.

Gochev Zh. (2005): Manual of cutting wood and wood cutting tools, Publishing House of University of Forestry, ISBN 954-332-007-1, Sofia, pp. 29-39 (in Bulgarian).

Gochev, Zh. (2014[a]). Examination the process of longitudinal solid wood profile milling. Part I: Performance of cutter profile, Innovation in woodworking industry and engineering design, 5(1): 40–47.

Gochev, Zh. (2014[b]). Examination the process of longitudinal solid wood profile milling. Part II: Influence of the revolution frequency and feed rate on the roughness of the treated surfaces, Innovation in woodworking industry and engineering design, 5(1): 48–54.

Gonzalez-Adrados, J.R., Garcia-Vallejo, M.C., Caceres-Esteban, M.J., Garcia de Ceca, J.L., Gonzalez-Hernandez, F., Calvo-Haro, R. (2012). Control by ATR-FTIR of surface treatment of cork stoppers and its effect on their mechanical performance, Wood Science Technology 46(1-3): 349 – 360.

Keturakis, G., Juodeikiene, I. (2007). Investigation of Milled Wood Surface Roughness. Materials science 13(1): 47–51.

Prakasvudhisarn, C., Kunnapapdeelert, S., Yenradee, P. (2009). Optimal cutting condition determination for desired surface roughness in end milling, The International Journal of Advanced Manufacturing Technology, 41: 440–451.

Rousek, M., Kopecký, Z., Svatoš, M. (2010). Problems of the quality of wood machining by milling stressing the effect of parameters of machining on the kind of wood, Annals of Warsaw University of Life Sciences – SGGW 72 No 72: 233–242.

Sandac J., Tanaka, C., Ohtani, T. (2004). Evaluation of surface smoothness by a laser displacement sensor II: comparison of lateral effect photodiode and miltielement array. Journal of Wood Science 50: 22–27.

Vuchkov I., S. Stoianov (1986): Mathematical modelling and optimizing of technological objects. Tehnika, 341 p. (in Bulgarian).

THE „SPRT" MILLING CUTTER BASED ON SELF-ROTATING BLADES

Grzegorz Wieloch[1] – Janusz Cieloszyk[2]

Abstract

Attempts to adapt new methods of machining with the use of self-rotating circular knives (SPRT) can also be noted in wood processing. Manufactured by companies such as: Lockheed Corporation, Rotary Technologies Corporation or Pokolm Frästechnik GmbH & Co. KG. and can be used in a variety of applications. Intensive tests have been carried out on the possibility of using such tools for turning wood [9,12,13,14,15]. Currently, American companies have developed tools for metal milling operations based on self-rotating disk tools. The stage of commercial applications of rotary tools began at the turn of twenty and twenty first century - around 2000. Intensification of work on SPRT tools was fostered by the need for efficient and good quality material processing. Adaptation of new rolling methods using self-rotating pulleys (SPRT) can also be noted in wood processing [10, 11, 12, 13]. So far, the use of this type of tools for turning wood has been extensively studied [12,16]. Currently, work is underway on the use of self-rotating blades of heads for leveling wood surface treatment [9,10,16], which is the subject of this report.

Key words: *milling head, SPRT tools*

INTRODUCTION

In the eighties of the twentieth century, the airline company Lockheed Corporation and, the airline company Lockheed Corporation in cooperation with tool companies Rotary Technologies Corporation has developed tools with rotary plates for milling operations. At the same time, the progress in the sciences on structural materials, and the technological capabilities of modern CNC machine tools gave the possibility to produce milling tools for industrial applications, e.g. at Rotary Technologies Corporation or Pokolm Frästechnik GmbH & Co. KG. The working principle of the SPRT tool with the self-rotating blade is illustrated in Fig.1

In recent years, together with the progress in the production of metal materials, increased interest in new

Fig1. Working principle of the SPRT tool with a self-rotating

tools for their treatment can be observed. This applies to SPRT self-rotating tools: Self Propelled Rotary Tools [2,6,8]. The interest in SPRT tools also gave an impulse for conducting tests, on the possibility of switching to this type of machining in wood

[1]University of Life Science, SGGW, Poland, e-mail:obrawiel@wp.pl
[2]West Pomeranian University of Technology in Szczecin, Poland

processing [1,4,5,6,7,9,11]. This is justified because in the woodwork the circular knives have been used for a long time, but fixed. The edges of the blades gave the opportunity to effectively extend the working time - longer cutting edge compared to flat blades [9, 10, 11].

TOOLS WITH SELF-CUTTING BLADES -SPRT

The automatic rotation of the knife during the machining process appears under the influence of friction forces that appear at the point of contact of the side surface of the tool and the surface being worked. In the case where the angle $\lambda = 0°$, the knife does not rotate during machining, but when the angle $\lambda \neq 0°$, a significant contribution to the self-revolving knife has the friction of the mobile chip on the rake face. The dependencies on the form given in the literature [3,6,7,8,9] indicate that the rotational speed of the knife v is directly proportional to the cutting speed v and the inclination of the cutting edge λ.

Thus, when the inclination of the edge λ increases, the rotation speed of the knife v_0 also increases. The working principle of the SPRT tool is shown in Fig.1. SPRT - Self-turning tools are characterized by a multiple increase in edge strength compared to fixed edges - blades. They are also characterized by a significant reduction in temperature in the area, by constant change of cutting edge position / blade rotation [2,3,11] and an increase in blade life as compared to tools with fixed blades. Also the possibility of using replaceable blades is a big advantage of this type of solution.

This is particularly evident in the tendencies of constructing tools with blade replacement blades more resistant to blunting [9,10,11,12]. The described features of these tools enable effective solving of problems related to machining, eg [1-3, 7-11]. The principle of SPRT operation is shown in Fig. 1. Research using the SPRT tool was carried out using the experience gained during the research of tools with a self-tapping blade for turning wood. A knife made of steel 45 with a rotating blade with a diameter of 20 mm was used. [Figure 2].

Fig.2. Wood turning knife with self-rotating blade

HEAD "SPRT" FOR ALIGNING FLAT SURFACES

In order to check the possibility of using a tool with self-rotating cutting inserts for milling wood planes, it was decided to use the existing milling cutter head made by Rotary Technologies and adapt it to the cutting conditions of wood.

As part of the unconventional research of cutting tools, it was decided to make a milling head with a set of four self-turning disk tools for leveling planes. Its design was inspired by solutions used in metal cutting tools.

Fig.3. Standard milling head based on self-rotating blades
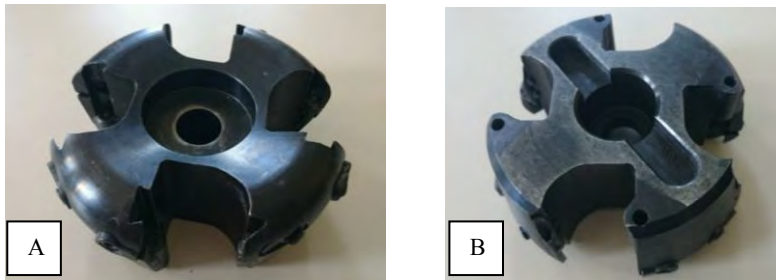
Fig.4. Head body a) top view, b) bottom view

The head body is a thick ring with four sockets to attach the blades. In the middle a hole for fixing the head on the spindle. Trapezoidal grooves leading cartridges with rotating blades are milled in each slot, which need adjustment in order to obtain the appropriate angle "λs". In addition, in the side walls there are mounting elements for the cassettes and fixing their position.

The blade of the circular knife was made in accordance with the dimensional specification of Fig.3. as rolling bearings with adjustable position of the center of the blade by twisting the tool part (blade).

Fig.5. Milling head with self-rotating

Experiments have shown that at selected angles "λs", the tool works in a smooth and stable manner [9,10,11]. The selected angular parameters of the circular knife are shown in Fig.3. SPRT tools are shown in Fig.4.

wood cutting insert

Fig.6. Construction of self-rotating SPRT tool blades
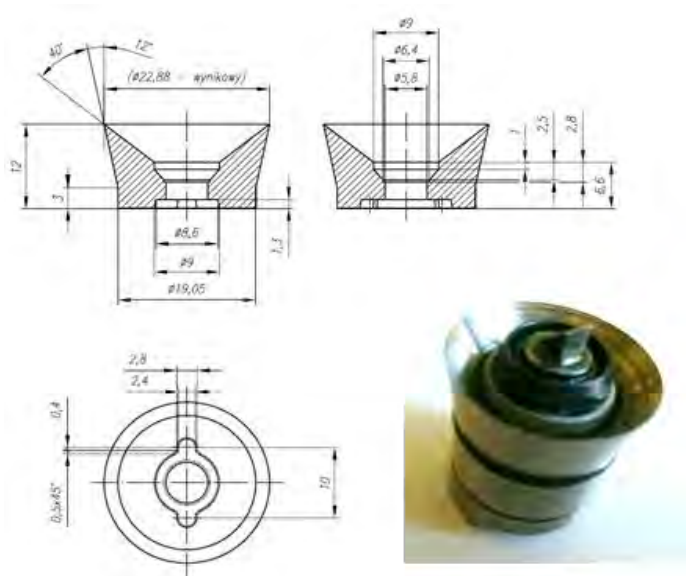
Fig.7. The dimensions of the milling head cutting insert and its
view in the toolbox

The cutting inserts are made of a tool steel with a cutting angle adapted to wood processing, i.e. 40 ° in accordance with Fig. 7. Recesses in plates took the form of a bowl which can be seen in the drawings. This resulted in a smooth chip passage through the tool insert. The insert was subjected to a cutting insert, while clamping inserts with needle bearings allowing the movement of the blades. The model of inserts is shown in Fig. 8.
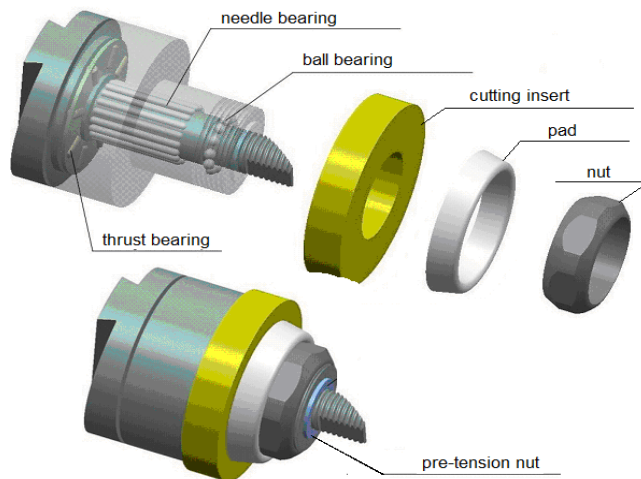
Fig. 8. Insert model used in the construction of SPRT tools

Similar to the Mitsubishi Carbide turning tool [8], the cartridge has a needle and thrust bearing, and the entire system is pre-tensioned by the nut. It presses one more ball bearing against the wall of the rotatable element on which the cutting insert is positioned (Fig.8). The milling cutter was machined into a modified milling head. For the head drive, a metal

milling machine was used on which table, the processed wood samples were fixed, as illustrated in Fig. 9.

Despite the relatively small head revolutions, very good surface alignment was achieved.
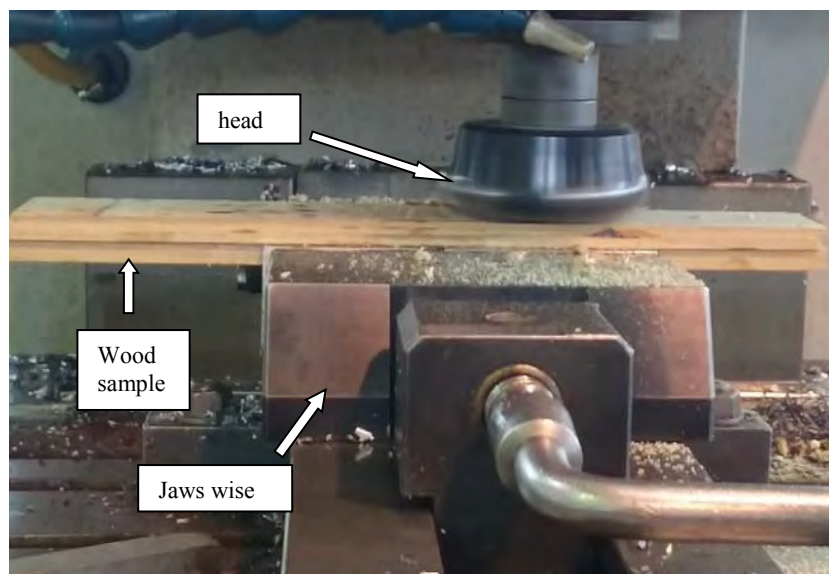
Fig.9. Stand for woodworking trials with a self - rotating blade

CONCLUSIONS

A tool with blades was designed based on the presented head. Typical inserts and body were used. Preliminary tests based on a metal milling machine were performed to obtain satisfactory results. It is planned to use a variety of cutting inserts in terms of geometry and to test their impact on the quality of machining. When machining, it depends on many factors related to the blade geometry, cutting parameters and grade and the moisture status of the wood being processed. It is planned to modify the clamping system of the blades in the cartridge to ensure better flow of chips during machining. The design and manufacturing technology of rotary tools for wood milling is much more difficult than conventional tools. The problems concern especially the bearing nodes, the selection of material for the components of the tool and the accuracy of the individual elements of the tool.

REFERENCES

[1]   CIELOSZYK, J., ZASADA, M.: *The Self-Propelled Rotary Tools-Future Conception In Metal Cutting?* The 15th DAAAM International Symposium Intelligent Manufacturing & Automation: Globalisation - Technology - Men - Nature" 3 - 6th November 2004, Vienna, Austria 2004, pp. 075-077.

[2]   CHMIELEWSKI, K., CIELOSZYK, J., ZASADA, M.:   *Narzędzia z obrotowymi płytkami skrawającymi – możliwości technologiczne i efekty stosowania,* Konferencja naukowo-techniczna TPP2006, Projektowanie Procesów technologicznych" Komisja

Budowy Maszyn PAN, Politechnika Poznańska, ISBN 978-83-903808-7-2, Poznań 2006, pp. 85-92.

[3] DESSOLY V.: *Modeling and Verification of Cutting Tool Temperatures in Rotary Tool Turning of Hardened Steel*, Georgia. Georgia Institute of Technology, April 2004

[4] DABADE, A., JOSHI, S.S., RAMAKRIHNAN N.: *Analysis of surface roughness and chip cross-sectional area while machining with self-propelled round inserts milling cutter*. Mechanical Engineering Department, Indian Institute of Technology, Vol.132, 2003.

[5] GRZESIK W.*: Podstawy skrawania materiałów konstrukcyjnych.* Warszawa WNT 2010, 527

[6] KARRI, V.*: Fundamental Studium of Rotary Tool Cutting Processes*. Ph.D. Thesis, The University of Melbourne, 1991

[7] KAUSHIKKUMAR, M., PATEL, G., SUHAS, S. Joshi, S.: *Mechanics of machining of face-milling operation performed using a self-propelled round insert milling cutter*, Journal of Materials Processing Technology Vol.171, pp 68–76, 2006.

[8] MITSUBISHI CARBIDE, *Rotary Holder*. LJ383B, Mitsubishi Materials Corporation 2000.

[9] PILC, J., ,MICIETOVA, A.: *Obrabanie kovov autorotujucimi nastrojami.* Žilina 2003.106.

[10] UDAY A., DABADE S., JOSHI S., RAMAKRISHNAN N.: *Analysis of surface roughness and chip cross-sectional area while machining with self-propelled round inserts milling cutter*, Journal of Materials Processing Technology, Vol. 132, No 1-3, pp. 305-312, 2003.

[11] VASILKO: *Teória a prax trieskového obrábania.* Presov. 2003.

[12] WIELOCH G., OSAJDA M.: *Construction of self-propelled rotary tool (SPRT) for wood turning*. Annals of Warsaw Agricultural University – SGGW, Forestry and Wood Technology, Warsow 2007, No 66, 405-408.

[13] WIELOCH G., OSAJDA M., MOSTOWSKI R: *Narzędzia do toczenia z samoobracającymi się płytkami i ich zastosowanie przy skrawaniu drewna*, Obróbka Skrawaniem, Innowacje, IOS Kraków 2008, 408–416.

[14] WIELOCH G., OSAJDA M., JAVOREK L., ZASADA M., CIELOSZYK J., CHMIELEWSKI K.: *New idea in construction and performance of turning rotary knife"*, Annals of Warsaw university of life sciences – SGGW, Forestry and wood technology No 72, 2010, 433-437.

[15] WIELOCH G., OSAJDA M., DZURENDA L.: *Wpływ kąta pochylenia głównej krawędzi skrawającej noża samoobrotowego w toczeniu drewna na wielkość powstających wiórów*. Szkoła Obróbki Skrawaniem, 2011. Nr 5, Opole.

[16] WIELOCH G., PORANKIEWICZ B., CIELOSZYK J., FABISIAK B.: *New solutions of "SPRT" tool constructions for wood surface equalizing by face milling method.* Annals of Warsaw University No 98, 2017, 143-147.

http://www.rotarytech.com/ juni 2017

CONDITION OF EDGES OF PARTICLE BOARD LAMINATED AFTER SAWS ON A PANEL SAW

Grzegorz Wieloch – Karol Szymanowski

Abstract

The purpose of the work was to examine the impact of the change of the feed speed of the saw carton in the panel saw on the quality of the edge of laminated chipboard subjected to sawing. During the test, the feed values recommended by the saw and machine tool manufacturer were applied. The tests were carried out in two sawing variants: one by one and in a package of two boards simultaneously. The quality of the machining was determined based on the evaluation of the material edge condition, i.e. the size of the nicks. A package of two plates folded with wide surfaces was treated as one thick plate with a double thickness compared to a single plate. Based on the obtained results, it was found that the size of the cracks on the lower edges is several times greater than on the upper side of the sawed slabs. This statement is valid for all considered cases of sawing.

Key words: sawing, cutting angle, machining quality, laminate, material feed

INTRODUCTION

The basic material for furniture production is chipboard and MDF. Due to its unquestionable advantages, of which it is very important to refinish them (varnishing, laminating, gluing, filling etc.). However, as a rule, refined materials have a negative effect on the durability of the tools, causing them to be exterminated more quickly. Therefore, it is important to select the machining parameters to obtain the best possible surface quality with the least tool wear. One of the parameters determining the quality of processing is the amount of feed speed at which the sawing takes place[3,9,10].

In the era of searching for the possibility of increasing the productivity of used equipment, there are attempts at simultaneous machining of several boards allowing for increased sawing efficiency. However, this may lead to a reduction in the quality of the edge of the boards, especially laminated ones. The work was aimed at explaining the expediency of such proceedings.

In the case of sawing, which aims to divide wood and boards, two working movements must be met; rotational movement of the tool and feed movement of the material or feed table on which the material is placed [3,5,8,9,13].

Previous work devoted to the issue of increasing the efficiency of cutting laminated chipboard, investigated the effect of the speed of feed on edge quality.

Warsaw University of Life Science, 02-787 Warsaw, Poland,
e-mail:obrawiel@wp.pl, karol.szymanowski@sggw.pl

Close to the research problem

Deterioration of the machining quality during milling of chipboard [7,8,9,10,11], occurs as a result of increasing: blunt cutting edge, vibrations of the tool carriage, cutting speed when using high feeds per blade. Therefore, it is important to select the machining parameters to obtain the best possible surface quality, especially laminated boards, with the least possible tool wear [5,7,8].

In the era of searching for the possibility of increasing the productivity of the equipment used, attempts are made to simultaneously process several boards allowing for increasing the efficiency of work stations. However, this can take place with a reduction in the quality of the edge of the boards, especially laminated ones. This justifies the rightness of taking up this subject in order to clarify the problems mentioned.

METHODS AND MATERIALS

The wood-based material tested was chipboard laminated on both sides with papers saturated with phenolic resins (laminated chipboard) with a thickness of 18 mm and an average density of 658 kg / m^3 [15].

The apparatus used for the assessment of quality of processing

The Mitutoyo TM-505 workshop microscope with a measuring range of 50 by 150 mm was used to evaluate the quality of processing of the test material. Optical zoom of the microscope 30 : 1.
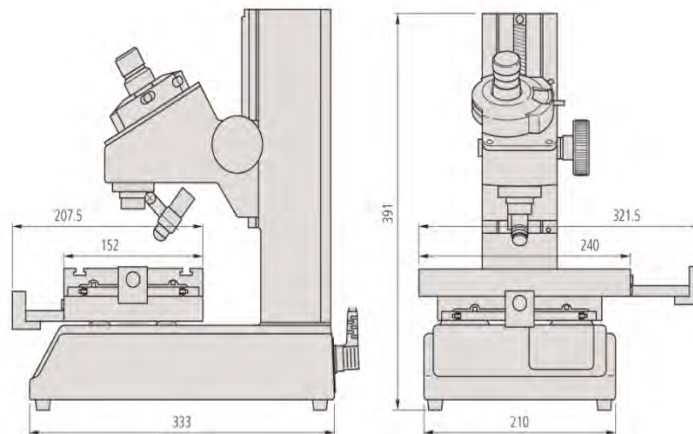
Fig.1. Mitutoyo TM 505 workshop microscope [http://www.mitutoyo.co.uk, 05.02.2017]

Machine tool and tool

The Holzma HPP 200 format saw was used for testing.

Fig.2. Holzma HPP 200 panel saw [http://www.holzma.com, 15.07.2017]

The cutting tool used was the main saw with a diameter of 310 mm with flat teeth and a undercut saw with a diameter of 200 mm with cone-flat teeth. The teeth of both saws were made of sintered carbides [4,14]. The condition of the machine corresponded to the standard PN-93/D-56216.

Tool

The cutting tools used were: the main saw 310 mm in diameter with flat teeth and the undercut saw with a diameter of 200 mm with cone-flat teeth. Both saws produced by LEUCO. The teeth of both saw blades were made of sintered carbides. The speed of the main saw spindle was 5677 rpm, while the undercut saw blade was 4371 rpm. The maximum height of the saw above the table was 60 mm. Despite the clearance for sawing three boards, the manufacturer recommends sawing with the saw being 25-40mm above the material, which means that only the sawing of a single slab would be carried out as recommended.

Fig.3. Main saw tooth [www.leuco.com, 10.01.2017]   Fig. 4. Tooth saw blade

Sawing parameters used
The value of the feed speed was calculated using the formula:

$$v_f = f_z \cdot n \cdot z_c \quad [\frac{m}{min}],$$

where: v_f - feed speed
            f_z - feed per blade
            n - spindle speed
            z_c - number of effective blades

The feed parameters were used for the test:
- minimum feed recommended by the saw manufacturer:

$$36,7\frac{m}{min} = 0,09\ mm \times 72 \times 5677\frac{obr}{min}$$

- maximum feed recommended by the saw manufacturer:

$$61,3\frac{m}{min} = 0,15\ mm \times 72 \times 5677\frac{obr}{min}$$

- maximum feed available on the Holzma HPP 200:

$$80\frac{m}{min} = 0,2\ mm \times 72 \times 5677\frac{obr}{min}$$

- comparative table example from the LEITZ catalog

$$24,5\frac{m}{min} = 0,06\ mm \times 72 \times 5677\frac{obr}{min}$$
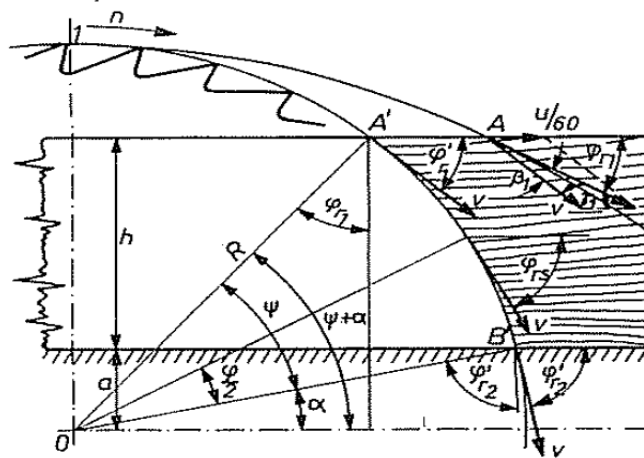
Fig.5. The sizes that characterize the saw system, the table, the saw element [2,6]

$$cos\mu = \frac{h + a}{R} \quad [°],$$

where:
h - directory wood kerf - cut height
a - distance of the element from the geometrical axis of the saw rotation
R - saw radius

- Saw tooth angle in the material when sawing a single plate:

$$cos\mu = \frac{18 + 95}{155} = 0,7290 \quad czyli\ \psi = 43°$$

- Saw tooth entry angle into the material when sawing two plate:

$$cos\mu = \frac{36 + 95}{155} = 0,8451 \quad czyli\ \psi = 32°$$

The value of the saw tooth's angle of exit from the material was calculated using the formula:

$$cos\mu = \frac{a}{R}$$

where: h – kerf

R - saw radius[°],

The value of the saw tooth angle of the material: dl

$$cos\mu = \frac{95}{155} = 0,6129 \quad \text{or} \quad \underline{\mathbf{\mu = 52°}}$$

Mesuring the quality of sawing discs

Measurements of the quality of sawing plates were made on a workshop microscope. To determine the amount of nicks in each sawing variant, the measuring section was divided into 10 parts.

Figure 7. The method of measuring the edge defects of the plate material after sawing

where: H - maximum crack size [mm]
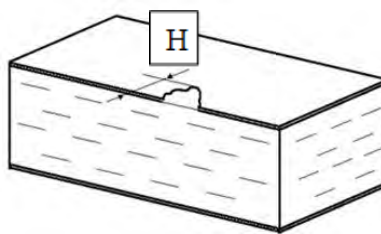
Fig.8. View of the edges of chipboard laminated with nicks

RESULTS and DISCUSSION

Tables 1-2 show the relationship between the feed speed and the state of the edges of wood-based boards after sawing with different packets of sawn slabs.

Tab.1. Nothing in the saw plate individually

feed speed [m/min]	The average value of nicks	
	the top edge of the board	the bottom edge of the board
	[mm]	
24,5	0,183	0,489
36,7	0,125	0,182
61,3	0,144	0,353
80	0,141	0,604

Fig. 9. Visualization of the results of inspection of sawing nicks indywidual plates

Tab. 2 Plates sawn in packages of 2 pieces

Feed speed [m/min]	The average value of nicks			
	The average value of nicks		the bottom edge of the board	
	[mm]			
	top edge	the bottom edge	top edge	the bottom edge
24,5	0,220	0,405	0,140	0,475
36,7	0,150	0,230	0,210	0,385
61,3	0,170	0,420	0,085	0,990
80	0,180	0,325	0,180	0,695
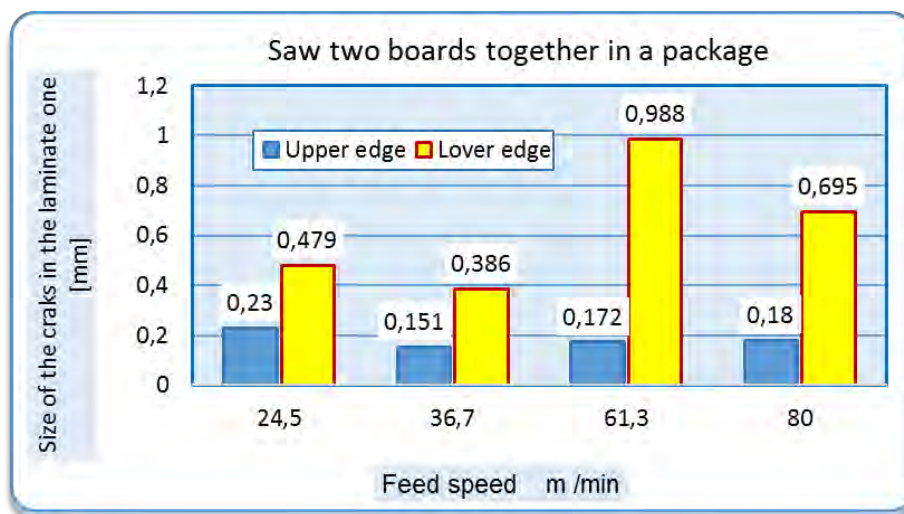
Fig. 10. The average value of nicks when sawing discs in packages of 2 plates

CONCLUSION

The best surface quality after sawing, in all variants, was obtained using the minimum feed recommended by the saw manufacturer - 36.7 m / min.

When sawing individually one laminated chipboard; significantly lower edge quality is shown by the lower edge than the upper edge, despite the use of the undercut saw.

After sawing the boards in packages of 2 pieces, the worst quality clearly differing from the rest showed the bottom edge of the bottom plate in the package. The values of chipping are several times greater than the edges on other sides of the boards. The upper edges of the boards included in the package have nicks close to each other. comparing the nicks of the plate cut individually with the bottom plate from the packet, we found similar values of chippings which would indicate the effect of sawing conditions on the final edge quality such as the angle of the tooth entry into the material and the angle of the tooth entrance into the material. The sawing speed promotes a good quality of the saw plate edges; the lower the value, the less jags it gives. The average value of nicks when sawing boards in packages of 2 plates is higher than when sawing in one plate at a time.

REFERENCES

1. BORYSIUK P., DOBROWOLSKA E., MIKLASZEWSKI S.: Opory skrawania w procesie piłowania płyt wiórowych. Przemysł Drzewny 7, s. 24 -26, 1997
2. DUCHNOWSKI K. (1997): Maszynowa obróbka, narzędzia i podstawowe obrabiarki stolarskie. Wydawnictwa Szkolne i Pedagogiczne, Warszawa
3. JEMIELNIAK K. (2004): Obróbka skrawaniem. Oficyna Wydawnicza Politechniki Warszawskiej. Warsaw.
4. KIEN W. (2002): Pilarki tarczowe formatyzujące. Meble i Technika 1, s. 32 – 38.

5. MICHALSKI E., SZCZEPANIAK J., KALIBA J.: Wpływ parametrów piłowania na jakość obróbki płyt wiórowych laminowanych i lakierowanych. Przemysł Drzewny 3, s. 17-19, 1978

6. ORLICz T**.,** (1988): Obróbka drewna narzędziami tnącymi. wydawnictwo SGGW-AR

7. PAŁUBICKI B., SINN G., RYBARCZYK W., BEER. P.: Dynamic Aspects Of Laminated Particleboard Cutting With Use Of Finite Element Method. Materiały konferencyjne The 17th International Wood Machining Seminar, 26-28 września 2005 Rosenheim, Germany, s. 94 – 101, 2005

8. PAŁUBICKI B., **(**2006): Badania nad jakością obróbki elementów meblowych z płyt wiórowych laminowanych, Doctoral Thesis. Poznań.

9. PNIEWSKI M. **(**2017): Wpływ parametrów cięcia pilarką panelową na jakość krawędzi płyt laminowanych. Dipl.Thesis. SGGW Warszawa.

10. PORANKIEWICZ B. 2000): Zużycie ostrzy narzędzi przy frezowaniu płyt wiórowych. Wydawnictwo Poznańskiego Towarzystwa Przyjaciół Nauk, Poznań,

11. PORANKIEWICZ B.)2003): Tępienie się ostrzy i jakość przedmiotu obrabianego w skrawaniu płyt wiórowych. Seria Monografie, Wydawnictwo Akademii Rolniczej, Poznań

12. PN-93/D-56216: 1993 Obrabiarki do drewna - Pilarki tarczowe do płyt jednopiłowe z przesuwnym wrzecionem - Nazewnictwo i sprawdzanie dokładności,

13. SALJE E., DRUECKHAMMER J.: Qualitaetskontrolle bei der Kanten bearbei tung. Holz als Roh- und Werkstoff 42, s. 187-192, 1984.

14. STACHOWIAK M.: Rozkrój płyt według firmy HOLZ HER. Przemysł Drzewny 6, s. 11, 2004b

15. STARECKI A. 1994): Technologia tworzyw drzewnych: T1. Wydawnictwa Szkolne i Pedagogiczne, Warszawa

http://www.gopol.pl

http://www.holzma.com,

http://www.mitutoyo.co.uk - dostęp 15 stycznia 2018

http://www.leuco.com - dostęp 10 stycznia 2018

TAGUCHI ANALYSIS OF WC-CO TOOLS LIFE IN MILLING OF WOOD-BASED MATERIALS

Jacek Wilkowski[1] **– Marek Barlak**[2] **– Zbigniew Werner**[2] **– Joanna Wachowicz**[1] **– Paweł Czarniak**[1]

Abstract

This work presented results of researches concerning influence of chosen material factors (WC grain size) and cutting parameters (spindle speed and feed per tooth) on edges durability made of WC-Co during chipboards milling. Experiment was conducted and analysed according to Taguchi method. Machining was carried out with working centre equipped with one edges milling head. Researches proved statistically relevant and useful in industrial conditions influence of feed per tooth. Regards to maximal tool life, optimal conditions were obtained for following levels of factors: WC grain size - 0,5-0,8 µm, spindle speed - 10000 rpm, feed per tooth - 0,15 mm.

Key words: *WC-Co tool material, particleboard, CNC milling, tool life, Taguchi method*

INTRODUCTION

In industry conditions Taguchi method is applied in order to estimate a significance of input factors influence on final parameters of given process such as products quality. This method is relatively common due to lower level of tests efforts in comparison to classic ways of experiments programming. Mentioned above method was used for experiment optimization by many authors (Basavarajappa et al. 2008, Davim and Reis 2003, Tsao and Hocheng 2004, 2007), during machining of wood based materials (Gaitonde et al. 2008, Wilkowski et al. 2011, 2012, 2014), too.

In stage of input factors configuration the main consideration was their significant and predictable influence on cutting edges durability during machining of wooden materials. WC grain size among numerous material factors was chosen as basic factor determining physical-mechanical properties of tungsten carbides. WC grain size and contribution of binder (cobalt) decides as well about density, hardness, fracture strength, MOR, MOE as about other parameters connected with WC-Co tool machinability (Cha et al. 2001, Rosiński et al. 2014, Schubert et al. 1998).

Plan of experimental researches takes into account fact, that edge durability depends on structure and properties of tool material and also on cutting parameters. Therefore, crucial parameter in this range is cutting speed but to some lower extent - feed per tooth, too.

[1] Warsaw University of Life Sciences - SGGW, 159 Nowoursynowska Str., 02-787 Warsaw, Poland
e-mail: jacek_wilkowski@sggw.pl
[2] National Centre for Nuclear Research Świerk - NCBJ, 7 Andrzeja Sołtana Str., 05-400 Otwock, Poland

MATERIAL AND METHODS

Durability tests were carried out in technological room of Faculty of Wood Technology SGGW in Warsaw. Raw, three layers chipboard manufactured by Pfleiderer with 18 mm thickness was subjected to machining. This is typical material used in mass production in furniture industry. Basic properties of mentioned above material was presented in Tab.1. Material for milling was divided into workpieces with dimensions 1000x400x18 mm. Machining process was conducted on working centre CNC Busellato Jet 130 with usage of one edge milling head (left rotations) Faba FTS.07L4043.01 with diameter 40 mm (Fig.1). WC-Co knifes produced by Ceratizit with dimensions 29,5x12x1,5 mm were used. Chosen properties of used for experiments tool materials were presented in Tab.2.

Tab.1. Selected mechanical and physical properties of using particleboard

Material	Density [kg/m^3]	Tensile strength [MPa]	Swelling after 24h [%]	Flexural strength MOR [MPa]	Modulus of elasticity MOE [MPa]
Particleboard 18mm thickness	648	0,41	20,5	8,68	2212

Fig.1. Milling head Faba FTS.07L4043.01

Tab.2. Properties of WC-Co materials used in experiments (according to producer)

Material symbol	Density [g/cm^3]	Hardness HV30	MOR [MPa]	WC grain size [μm]	Binder content Co [%]
UMG04	15,30	2450	3200	<0,2	2,0
SMG02	15,25	2200	3500	0,2 - 0,5	2,4
KCR08	15,20	1885	2300	0,5 - 0,8	3,2

Taguchi method is based on value of the signal-to-noise S/N (ETA) ratio as basic criterion in assessment of input factors influence on output values. As optimal values are

assumed these ones that distinguishes by maximal S/N ratio (Gaitonde et al. 2008). The S/N ratio characteristic for the bigger the better in Taguchi method can be expressed as follows:

$$\eta = -10 \log [1/n \, \Sigma(1/y^2)]$$

where η is the observe value (dB), y the experimental data, n is the number of observations (Tsao and Hocheng 2007). Three factors (WC grain size, spindle speed and feed per tooth), each on three level were showed in Tab.3. A L_9 orthogonal array was employed (Tab.4).

Tab.3. Factors and levels

Code	Factor	Levels		
		1	2	3
A	WC grain size	< 0,2 µm	0,2 - 0,5 µm	0,5 - 0,8 µm
B	Spindle speed	10 000 rpm	14 000 rpm	18 000 rpm
C	Feed per tooth	0,15 mm	0,30 mm	0,45 mm

Assumed levels of cutting factors are as high as possible (extreme values are allowable for this kind of machining with usage of analyzed machine).

Tab.4. L_9 orthogonal array

Trial	Levels of input factors		
	A	B	C
1	1	1	1
2	1	2	2
3	1	3	3
4	2	1	2
5	2	2	3
6	2	3	1
7	3	1	3
8	3	2	1
9	3	3	2

Machining was carried out according to predicted earlier scheme showed in Tab.4. Milling of grooves (width of tool diameter - 40 mm) took place in workpieces made of particleboard on depth 6 mm. In each panel was made 10 passages of tool. After each transition (feed distance - 1 m) measurement of tool wear with usage of workshop microscope was carried out. Measurement concerned clearance surface of edge. Maximal width of wear was estimated (direct indicator VB_{max}). The machining with given edge was stopped when maximal wear width was equal or bigger than 0,2 mm. Thus this value was assumed as tool wear criterion. However, feed distance up to wear criterion ($VB_{max} = 0,2$ mm) was noticed as its durability indicator.

RESULTS AND DISCUSSION

Statistical results analysis was carried out in software Statistica 13.1. The result of ANOM is represented in the response diagram as shown in Fig.2. Optimal values of factor levels due to maximal edge durability are following: WC grain size - 0,5-0,8 µm, spindle speed - 10000 rpm, feed per tooth - 0,15 mm..

Only in case of factor - feed per tooth, S/N ratio exceeded beyond range ±2*standard error, that proved about its huge influence and simultaneously usefulness in industry conditions. The rest two factors (WC grain size and spindle speed) influenced not so much on S/N ratio. Thus, theirs usefulness in industry conditions is limited.

In order to assess percentage value of indicator referred to influence of given factor (P - percentage of contribution) ANOVA analysis (Tab.5) was done. Relevant influence of feed per tooth proved indicator P on level 93,1%. Overall influence of the rest of factors was lower than 5% (Tab.5).
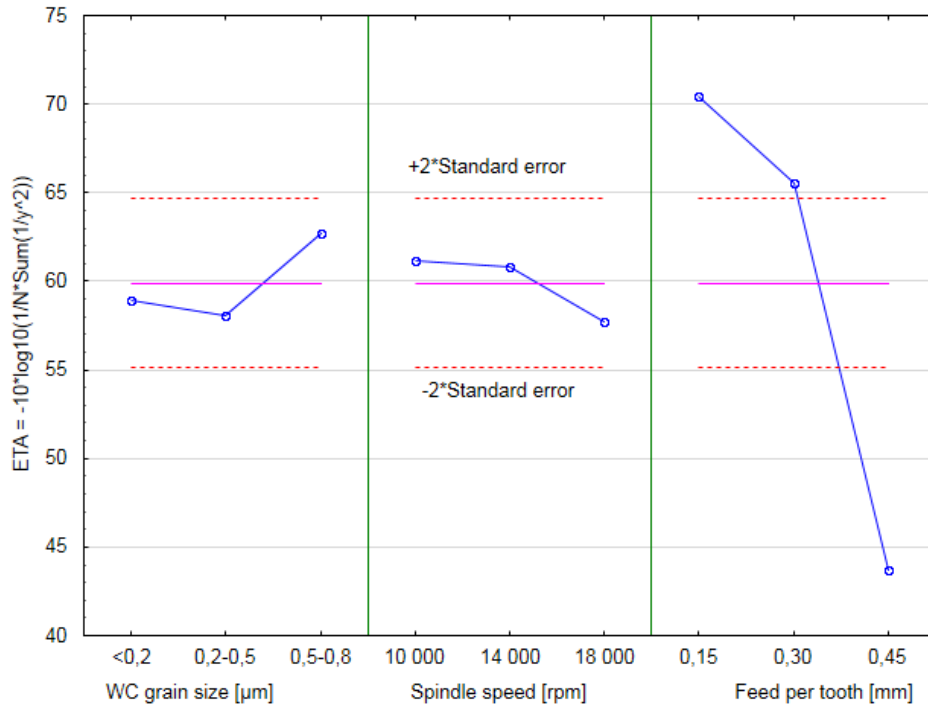
Fig.2. Response diagram of S/N (ETA) ratio for the tool life

Tab.5. ANOVA for the tool life of cutting factor

Factor	SS	d.f.	MS	F=5%	p	P (%)
A	35,99	2	18,00	1,053	0,4870	2,7
B	21,05	2	10,52	0,616	0,6189	1,6
C	1220,82	2	610,41	35,716	0,0272	93,1
Error	34,18	2	17,09			2,6
Total	1312,04	8				100,00

SS-sum of squares, d.f.-degrees of freedom, MS-mean square, P-percentage of contribution

Influence of spindle speed (P=1,6%) on edge durability seems to surprisingly low. This statement is in contrast to commonly assumed opinion that durability of edge in case of wood based materials machining depends mainly on cutting speed. Obtained in this researches results didn't confirmed this relationships. Maybe, it can follow from distinctive mechanism of WC-Co tool wearing in comparison for e.g. with high speed steel (HSS). In case of HSS dominant role in wearing process is friction. Thus, influence of cutting speed

and spindle speed is significant. In case of hard materials such as WC-Co besides abrasive mechanism of wearing, crucial contribution has fracture strength. Microscope observations revealed clear chippings of cutting edge (Fig.3). Thus, exceeding of given chip thickness and simultaneously cutting forces can decreases edge durability as result of chipping phenomena. This regularity should concern mainly the hardest WC-Co materials. This mechanism could justify optimal levels of factors keeping in mind edges durability. namely: big WC grain size – higher fracture strength, small spindle speed - higher resistance to abrasive wear and low value of feed per tooth – higher fracture strength.
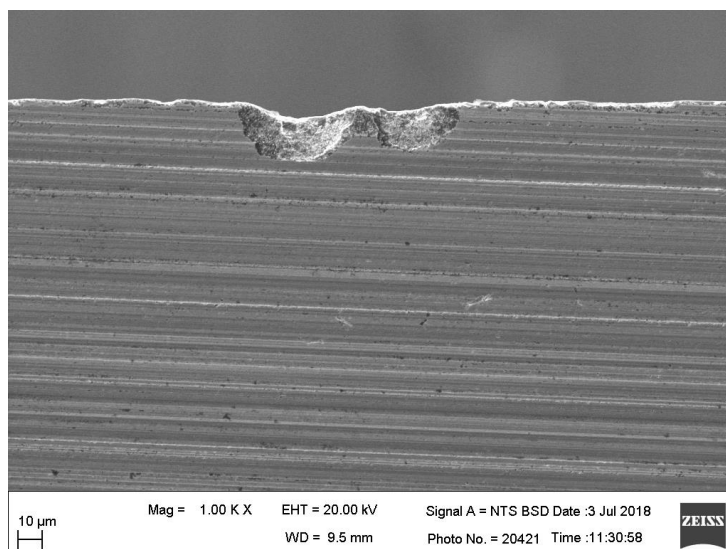
Fig.3. Chipping of WC-Co tool material (SEM image)

CONCLUSION

According to obtained results can be formulated following conclusions:
- ➢ Feed per tooth as well from statistical point of view as performance during milling of chipboards has the most important influence on tool well durability. The rest two factors (WC grain size and spindle speed) were in analysed range statistically irrelevant regards to tool durability.
- ➢ Optimal levels of factors according to edges durability were following: WC grain size - 0,5-0,8 μm, spindle speed - 10 000 rpm, feed per tooth - 0,15 mm..

ACKNOWLEDGMENTS

REFERENCES

1. Basavarajappa S., Chandramohan G., Davim J.P., 2008: Some studies on drilling of hybrid metal matrix Composites based on Taguchi techniques. *Journal of Materials Processing Technology* 196: 332-338.
2. Cha SI, Hong SH, Ha GH, Kim BK, 2001: Microstructure and mechanical properties of nanocrystalline WC-10Co cemented carbides. *Scripta Materialia* 44(8-9): 1535-1539.
3. Davim J.P., Reis P., 2003: Drilling carbon fibre reinforced plastics manufactured by autoclave – experimental and statistical study. *Materials and Design* 24: 315-324.
4. Gaitonde V.N., Karnik S.R., Davim J.P., 2008: Taguchi multiple-performance characteristics optimization in drilling of medium density fibreboard (MDF) to minimize delamination using utility concept. *Journal of Materials Processing Technology* 196: 73-78.
5. Rosiński M., Wachowicz J., Plocinski T., Truszkowski T., Michalski A., 2014: Properties of WCCo/Diamond composites produced by PPS method intended for drill bits for machining of building stones. *Ceramic Transactions*. Innovative Processing and Manufacturing of Advanced Ceramics and Composites II, 24: 181-191.
6. Tsao C.C., Hocheng H., 2004: Taguchi analysis of delamination associated with various drill bits in drilling of composite material. *International Journal of Machine Tools & Manufacture* 44: 1085-1090.
7. Tsao C.C., Hocheng H., 2007: Parametric study on thrust force of core drill. *Journal of Materials Processing Technology* 192-193: 37-40.
8. Wilkowski J., Czarniak P., Grześkiewicz M., 2011: Machinability evaluation of thermally modified wood using the Taguchi technique. COST Action FP0904 Workshop "Mechano-chemical transformations of wood during Thermo-Hydro-Mechanical (THM) processing" Bern University of Applied Sciences. February 16-18, 2011 Biel, Switzerland:109-111.
9. Wilkowski J., Borysiuk P., Czarniak P., Rousek M., 2012: Taguchi analysis of cutting power and thrust force in drilling of polyethylene bonded particleboards. *Ann. WULS–SGGW*, *For and Wood Technol.* 80: 187-191.
10. Wilkowski J., Czarniak P., Górski J., Jabłoński M., Podziewski P., Szymanowski K., 2014: Taguchi method optimization of the total power consumption during chipboard cuttig with the panel saw machine. The 9th International Science Conference "Chip and Chipless Woodworking processes" Technical University in Zvolen. September 11-13,2014, 9(1):171-174.

THE EFFECT OF THE WC-CO PROPERTIES ON THE TOOL WEAR DURING PARTICLEBOARDS MILLING

Jacek Wilkowski[1] – **Marek Barlak**[2] – **Zbigniew Werner**[2] – **Paweł Czarniak**[1]
– **Joanna Wachowicz**[1]

Abstract

This work presented influence of hardness and fracture toughness of WC-Co tool material on wearing and durability of edges during chipboards milling. Measurement of WC-Co hardness was done according to Vickers method with usage of universal device. Fracture toughness was assessed due to length of cracks with Palmquist method, created during hardness measurement. Tool life tests were carried out maintaining constant cutting parameters with working center CNC. There were observed differences in character of WC-Co edges wearing process. Results shows directly proportional influence of edge material hardness on its durability.

Key words: *WC-Co, hardness, fracture toughness, CNC milling, tool life, particleboard*

INTRODUCTION

Cemented carbides type WC-Co is widely used material designed not only for metal cutting purposes but also for machining of wood and wood based materials and plastics. The structure of them consist of wolfram carbides grains WC and metal binder in form of cobalt Co. Exemplary structure of WC-Co is showed in Fig.1. Cobalt is distinguishes by very good thermal conductivity, high melting temperature and high strength to bending. Grain size and contribution of cobalt are the main elements of WC-Co composition, having crucial influence on functionality of this material in cutting tools applications. Density and hardness of WC-Co increases together with decreasing of WC grain size. In turn, came up improvement of resistance to abrasion during wearing process and through this phenomena decreasing of fracture toughness. However, increase of cobalt contribution follows that fracture toughness is higher but simultaneously resistance to wear abrasion is lower (Cichosz 2006, Dobrzański 2002, Kupczyk 2009). These relationships determined certain level of mentioned above components of WC-Co that ensure optimal structure regards to durability of cutting tools applied in machining of given material (Rosiński et al. 2014). Surely, WC grain size and contribution of cobalt is differentiated in metal or wood based materials machining. Material and cutting parameters imposes manufacturing of tool materials according to particular applications (Dobrzański 2002). Therefore, in this work influence of WC-Co appropriable properties (hardness and fracture toughness) on theirs wearing during chipboards machining was examined.

[1] Warsaw University of Life Sciences - SGGW, 159 Nowoursynowska Str., 02-787 Warsaw, Poland
e-mail: jacek_wilkowski@sggw.pl
[2] National Centre for Nuclear Research Świerk - NCBJ, 7 Andrzeja Sołtana Str., 05-400 Otwock, Poland
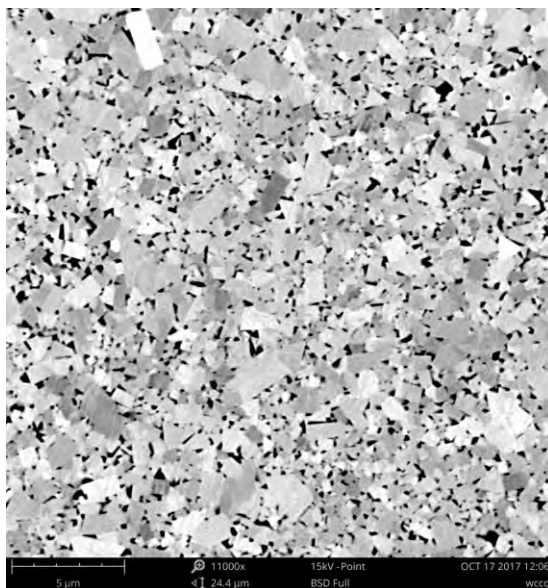
Fig.1. Microstructure of WC-Co tool material

MATERIAL AND METHODS

Knifes from WC-Co produced by Ceratizit with dimensions 29,5x12x1,5 mm were used for tool materials properties measurement (hardness, durability in milling mode). Properties of materials used in experiments according to producer data were presented in Tab.1.

For hardness and fracture toughness measurement was applied universal device Verzus 700AS produced by Innovatest. Hardness (HV30) was measured with Vickers method (PN-EN ISO 6507-1:1999) consisted on pushing in sample diamond tip with shape of pyramid with square base and vertex angle 136° with 30N and measurement of diagonal length on created in this way imprint. Measure of hardness is assumed as ratio between loading force and area of imprint. This procedure was carried out on clearance face of edge with five repetitions.

Fracture toughness (K_{Ic}) was assessed due to measurement of cracks length with Palmquist method created during Vickers hardness procedure with usage of Shetty formula (Rumman et al. 2015).

Tab.1. Chosen properties of WC-Co material (according to producer)

Material symbol	Density [g/cm³]	WC grain size [μm]	Binder content Co [%]
UMG04	15,30	<0,2	2,0
SMG02	15,25	0,2 - 0,5	2,4
KCR08	15,20	0,5 - 0,8	3,2

Three layers particleboard produced by Pfleiderer with thickness of 18 mm and density 648 kg/m³ was subjected to durability tests. Mentioned above panels are standard

construction material commonly used in furniture industry. Workpieces with dimensions 1000x400x18 mm were milled on working center CNC Busellato Jet 130 equipped with one edge milling head (left rotations) Faba FTS.07L4043.01 with diameter 40 mm.

There were made grooves (with width equal to tool diameter – 40 mm) in particleboard panels on depth 6 mm. During machining, constant cutting parameters (feed speed 2,7 m/s, spindle speed 18 000 rpm, feed per tooth 0,15 mm) were maintained. On each work piece 10 repetitions were done. After each passage (1 m of feed) measurement of tool wear with workshop microscope was carried out. The clearance surface of edge was took into account. Maximal width of wear (direct indicator VB_{max}) was estimated. Machining was stopped as soon as wear width was equal or higher than 0,2 mm. Thus, this value was assumed as tool wear criterion. Feed distance up to achieve with edge, tool wear criterion ($VB_{max} = 0,2$ mm) was its durability indicator.

RESULTS AND DISCUSSION

Visible differences in tool wear nature were observed. WC-Co denoted as UMG04 with the highest density and the WC smallest grain size was wearing mainly because of microchipping and chipping (Fig.2). However, material described as KCR08 with the lowest density and biggest grains distinguishes by high contribution of abrasive wearing what presented Fig.3.
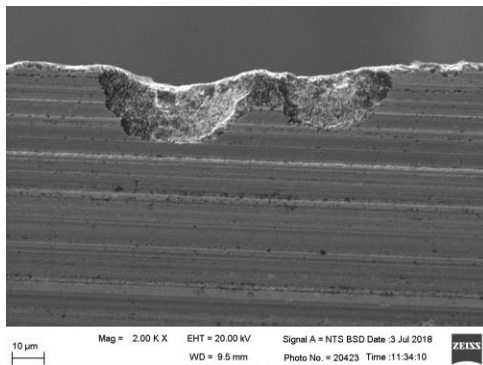
Fig.2. Chipping of UMG04 tool material (SEM image)
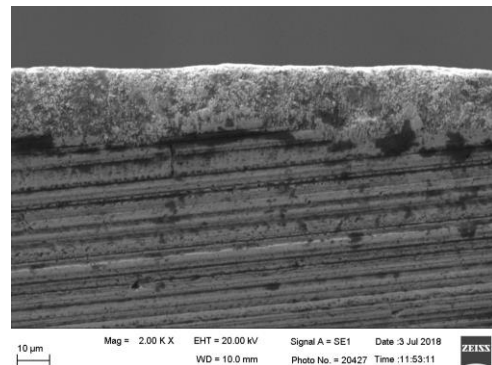
Fig.3. Abrasive wear of KCR08 tool material (SEM image)

Fig.4-6 shows measured properties of examined WC-Co materials. The highest hardness was obtained for UMG04 (HV30 = 2705), namely material with the smallest WC (<0,2 µm) grains and the lowest contribution of cobalt (2,0 wt% Co). However the lowest (HV30 = 1789) for KCR08 – the biggest WC size (0,5 - 0,8 µm) and the highest contribution of cobalt (3,2 wt% Co) (Fig.4).

The highest fracture toughness was noticed for WC-Co with symbol SMG02 (K_{Ic} = 12,16), the lowest for UMG04 (K_{Ic} = 11,32), in other words the hardest (Fig.5).

The highest durability (cutting distance for blunted tool $VB_{max} = 0,2$ mm amounted 5262 m) was received during chipboards milling with knives of the smallest WC grains and the lowest cobalt contribution. The lowest tool life was observed for KCR08 distinguishes by big WC grains and high cobalt contribution (Fig.6).
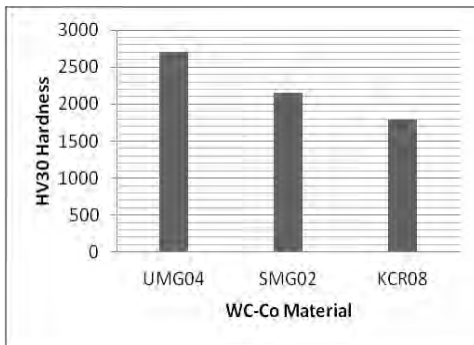
Fig.4. Hardness of examined WC-Co
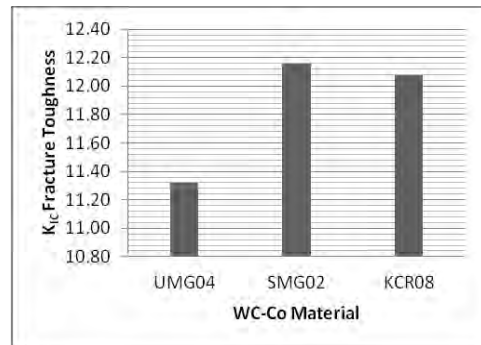
Fig.5. Fracture toughness of WC-Co edges.
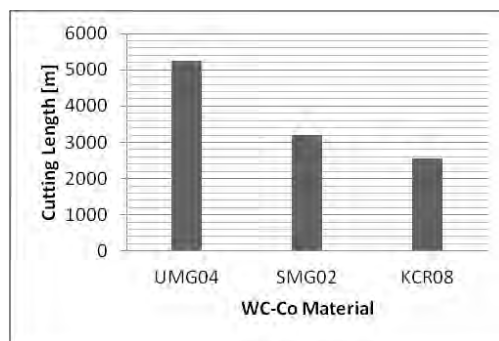
Fig.6. Tool life of examined WC-Co edges.

In Fig.7-8 were showed correlation relationships between investigated properties of tools made of WC-Co. The strongest correlations (Fig.7) were detected between hardness with tool durability expressed with cutting length (up to blunting on the level $VB_{max} = 0,2$ mm). However the weakest between hardness and fracture toughness (Fig.9). This relationship is inverted. It means that with increase of one property come up the decrease of the second one: fracture toughness and cutting length (Fig.8) or hardness and fracture toughness (Fig 9).
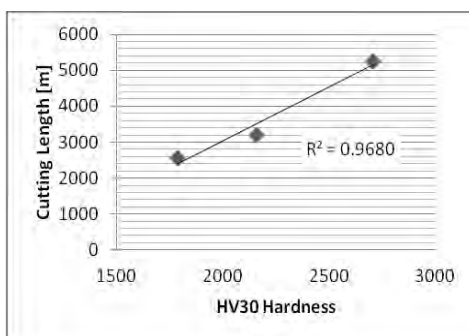
Fig.7. Relationship between tool life and hardness of WC-Co edges.
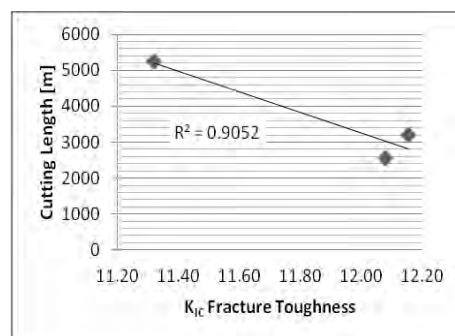
Fig.8. Relationship between durability and fracture toughness of WC-Co edges.
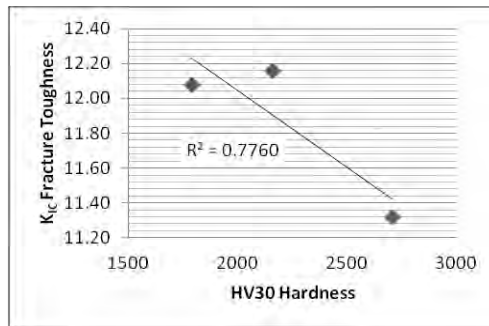
Fig.9. Dependence of fracture toughness on WC-Co edges hardness.

CONCLUSION

According to obtained results can be formulated following conclusions:

- ➤ Edges with the highest density, hardness, and the smoothest WC grains were wearing in consequence of microchipping and chipping. However, in case of these with the lowest density, hardness and the biggest WC grains took place mainly abrasive mechanism of blunting.
- ➤ WC-Co edges with the smoothest WC grains and low contribution of cobalt proved the highest hardness and durability. However increase of WC grain size and cobalt contribution caused decrease of hardness increase of fracture toughness and decrease of tool durability.

ACKNOWLEDGMENTS

REFERENCES

1. Cichosz P., 2006: Narzędzia skrawające. Wydawnictwo Naukowo-Techniczne. Warszawa.
2. Dobrzański A., 2002: Podstawy nauki o materiałach i metaloznawstwo. Materiały inżynierskie z podstawami projektowania materiałowego. Wydawnictwo Naukowo-Techniczne. Warszawa.
3. Kupczyk M.J., 2009: Wytwarzanie i eksploatacja narzędzi skrawających z powłokami przeciwzużyciowymi. Wydawnictwo Politechniki Poznańskiej, Poznań.
4. PN-EN ISO 6507- 1:1999. Metale - Pomiar twardości sposobem Vickersa.:Metoda badań.
5. Rosiński M., Wachowicz J., Plocinski T., Truszkowski T., Michalski A., 2014: Properties of WCCo/Diamond composites produced by PPS method intended for drill

bits for machining of building stones. *Ceramic Transactions*. Innovative Processing and Manufacturing of Advanced Ceramics and Composites II, 24: 181-191.

6. Rumman R., Xie Z., Hong S.J., Ghomashchi R., 2015: Effect of spark plasma sintering pressure on mechanical properties of WC-7,5wt% Nano Co. *Materials and Design* 68: 221-227.

SEKCIA / SECTION

TERMICKÁ ÚPRAVA DREVA

THERMAL TREATMENT OF WOOD

REGIMES FOR LAMINATING CURVED FURNITURE ELEMENTS WITH POLYVINYL CHLORIDE FOILS

Dimitar Angelski – Vladimir Mihailov

Abstract

The article discusses the influence of some technological factors on the laminating of curved furniture elements with polyvinyl chloride foils. High-density fiberboards (HDF) with 3 mm thickness and 850 kg/m² density have been used in the study. The specimen details were laminated at a vacuum press with polyvinyl chloride (PVC) foil. The laminating of the specimen details was made with polyvinyl acetate (PVAc) and polyurethane (PU) adhesives. The influence of the quantity of adhesive on the adhesion strength was investigated. The adhesion strength has been determined by pull-off testing method. The influence of the following technological factors was also investigated: vacuum pressure in the vacuum system, temperature of pre-heating of the foil, heating temperature, duration of pressing.

Key words: *laminating, adhesion strength, polyvinyl chloride foil, polyurethane (PU) adhesive, polyvinyl acetate (PVAc) glue*

INTRODUCTION

As it's known, the basic method of laminating (lining) curved furniture elements is by gluing. It is performed on specialized membranes and other 3D presses. The advantages of the membrane technologies are above all the complete versatility of the cladding in relation of type, dimensions and configuration of the details, the type of cladding materials and the adhesives used for this purpose. In addition, the face and the edges of the furniture elements can be lined simultaneously (by one technological cycle). A major advantage is the lack of molds and resetting when changing objects for processing.

The most preferred laminating (lining) materials are the thermoplastic foils (polyvinyl chloride - PVC, ABS - acrylonitrile butadiene styrene, polypropylene – PP), with good elasticity and plasticity, with sufficient strength and resistance to elevated temperature and considerable mechanical stresses. Polyvinylchloride (PVC) is one of the most flexible and durable laminating material. One of the main technological disadvantages in lamination with foils is that usually overlays are very thin and they do not have the strength to hide the surface irregularities of the laminated article. This defect known as "marking" negatively affects the adhesion strength of the bonding compound (Kılıç et al. 2009). In case of laminating of structural elements with foils, furniture boards with powder or fibrous surface layers are preferred. The surfaces must be of a homogeneous structure, strictly planar, dust-free, with a high grade of roughness. Specifically, the maximum deviations by thickness must be within ± 0,2 mm, local deviations from flatness - up to 0,1 ÷ 0,15 mm, and the

University of Forestry, blvd. Kliment Ohridski 10, 1797 Sofia
e-mail: d.angelski@ltu.bg

roughness is Rm ≤ 30 μm. Since the foils do not absorb water and steam, another important requirement for the panels is to possess even minimal water and steam penetration to render uptake of the glue solvents. Because most wood adhesives are aqueous, loss of water to wood is an important part of the cure. However, most adhesives generally polymerize and cross-link, and the rate of chemical reactions and of strength development are used to look at curing (Charles R. Frihart 2015).

For laminating curved furniture elements the PVC foils are mostly used with polyvinyl acetate dispersions (PVAc) and low viscous reactive polyurethane dispersions (PUs) with low polymerization temperature (50 °C) and increased open time are used. A main advantage of these adhesives has been that they can be formulated to have a wide range of properties, depending on the types and ratio of monomers (Charles R. Frihart 2015). The bonding principle of PVAc adhesives is based on the removal of the water by penetration into the wood substrate or by evaporation to the surrounding air. The forming of the bondline also requires the application of proper pressure. The final bond strength is reached after migration of the residual water away from the bondline (Dunky, M. 2003). In order to achieve minimal shrinkage of the adhesive layer during its hardening, it is recommended the adhesives to have the highest possible dry residue content (Albin et al. 1991).

Adhesion is a complex physic-chemical phenomenon for which, however, there is not a rigorous theoretical definition. Adhesion is difficult to define, and an entirely satisfactory definition has not been found (Kaelblea 1964, Landrock A. 2008, Silva et al. 2011).

In principle, laminating with membrane technologies do not differ much from those applied to the positioning of flat furniture boards on ordinary hydraulic presses. However, the pressing regimes are difficult to control and control. The problems are mainly related to the large number of factors influencing the process of cling and the restrictive conditions for its implementation. As a result of improper combination of materials and cladding modes, adhesive compounds with low adhesion strength are obtained. Adhesion strength is an important feature to measure the durability of the peel cover from the substrate. Various methods are used to determine adhesion strength. The most objective and widespread method is the pull off test. It is essentially determined the force with which the coating is removed from the pad at a tensile load perpendicular to its orientation. The bonding process is influenced both by the properties of the materials (foil, glue and furniture plate) and by the values of the main operating parameters - quantity, viscosity and temperature of the adhesive, pressure and duration of pressing, pre-stretching, etc. Only if all of these parameters are correct and well balanced in the PVC bonding process, can proper bonding results be achieved. In this regard, the aim of the present study is to determine rational ranges for the variation of basic operating parameters when facing PVC film curvilinear details.

MATERIAL AND METHODS

To determine the rational range for varying the quantity of adhesive in the laminating of curved furniture elements, a one-factor experiment was performed. The chosen range for the technology factor test is from 100 to 220 g/m². High-density fiberboards (HDF) with 3 mm thickness and 850 kg/m² density have been used in the study. The curvature details are made by folding and gluing of three layers by HDF by initial thickness and bent radius of 100 mm. From them were made test pieces to provide a 10-fold repeat of each experimental series for determining the strength of an adhesive bond between the laminate and substrate. The PVC foil (by "Hornshuch") 3D formable with thickness of 0,4 mm. The surfaces of the foil are protected by a highly light-resistant lacquer on PUR/acrylate basis. The reverse side

of the foils is coated with primer to ensure a safe and temperature-resistant bond. For bonding, is used adhesive system produced by Jowacol - D3 polyvinyl acetate (PVAc) glue (№103.05) and polyurethane (PU) adhesive dispersion (№150.50).

The test samples were laminated in a membrane press. The press mode for the test samples glued with PVA adhesive system is: vacuum pressure - 0,4 N/mm^2 and time for pressing 30 min. For the test samples wit PU adhesive dispersion was used temperature 75 °C, pressure 0,4 N/mm^2 and time for pressing 30 min. After the laminating with the PVC foil to determine the adhesion strength of the compounds is defined by a standardized pull-off method (ISO 4624:2016) with a glued stamp, was applied to the PVC film perpendicularly to the laminated board.

RESULTS AND DISCUSSION

Laminating mode. General requirements. For qualitative laminating of curved furniture elements, the parts need to be perfectly clean and smooth. Even dust and hairs are printed on the film due to high pressure. Before finishing the details, it is advisable to tempered, which leads to the improvement of the adhesion quality. The laminating case is desirably isolated from external sources of dust and air currents. It should be borne in mind that even the smallest changes in the composition and the thickness of the foil have a great effect on the regime. Changing the thickness of the foil leads to its tearing in the process. The type and composition of glue is also essential for adhesion. In order to achieve minimal compressibility of the adhesive layer when it is hardened to prevent marking of the HDF micro relief structure, it is recommended that the adhesive be as dry as possible. When PVC-free foil is coated without a membrane, at least 30% of the foil waste is realized. Therefore, if it is intended for rational use of the film, it is advisable to work with a membrane.

Determination of quantity of the adhesive for laminating curved furniture elements. The results of the one-factor experiments to determine a rational rate for the quantity of adhesive in laminating curved furniture elements are presented in Figures 1 and 2.

The adhesion strength of the tested adhesive compounds between HDF and PVC foil is relatively low. The adhesion strength of PU adhesive compounds meets the required minimum tensile strength at a glue expense over 150 g / m^2. On the basis of the results obtained, it can be assumed that the adhesive strength of the compounds increases in the range of 100 to 200 g / m^2 as the quantity of adhesive increases.
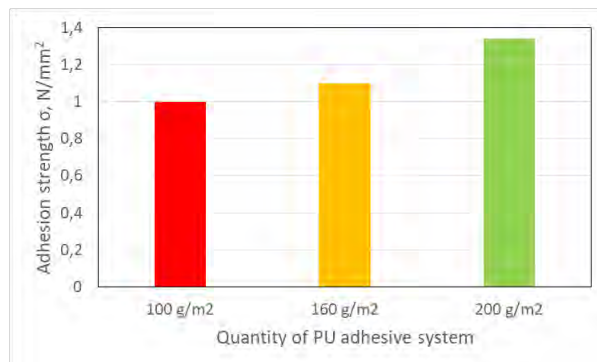
Fig. 1. Relationship between adhesion strength and the quantity of glue on laminating of curvilinear furniture parts (made of HDF) with PU adhesive

The adhesion strength of PVA adhesive compounds between HDF and PVC foil does not meet the minimum technological strength requirements. A major problem with bonding is the inability of the film to pass and adsorb water. In fact, water is adsorbed entirely into HDF. It can be argued that in the studied range the greater the quantity of glue and the presence of more water, respectively, leads to a decrease in adhesion. This problem can be limited by pre-drying of the applied glue and subsequent thermal-activation in the press equipment. However, it can be argued that the PVA dispersion used is unsuitable for laminating HDF curved structural elements with PVC foil.
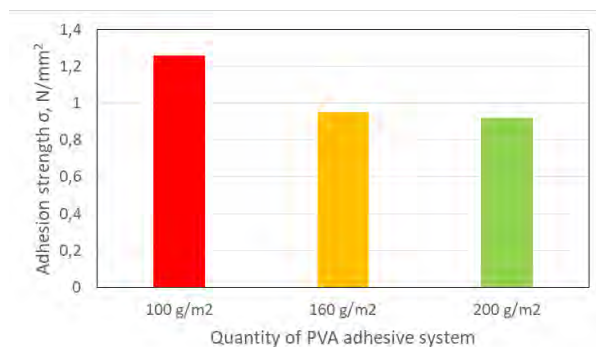
Fig. 2. Relationship between adhesion strength and the quantity of glue on laminating of curvilinear furniture parts (made of HDF) with PVA adhesive

Determination of pressure for laminating of curved furniture panels with PU adhesive. The pressure for laminating of curved furniture elements with PVC foil depends on many factors. Even the composition of the foil and the atmospheric pressure have a significant impact. Typically, the thickness of PVC cladding film is 0.35-0.5 mm. Due to the specificity of the vacuum presses, the pressure of the PVC film liner is relatively small. For laminating lining curved structural elements with a large radius of curvature at a thickness of 0,4 mm the minimum pressure is - 0,4 N / mm^2. If the thickness of the foil is greater and the radii smaller, then the working pressure is 0.5÷0.6 N/mm^2.

Temperature of heating by working with PU adhesive. The industrial use of PU adhesives for bonding PVC film to furniture components requires heating. The typical working temperature is between 65 and 125 ° C. The quality of the foil is very important, the higher the temperature the foil holds without changing its structure, the better the adhesion.

Preheating of the foil when working with PU adhesive. It mainly depends by the thickness of the foil. When working with 100 °C and with a foil thickness of 0.4 mm, it takes 55÷65 seconds to preheat the foil. It is desirable to reduce it by 4÷5 seconds. at an increase in temperature of 5 ° C. When reducing the thickness of the film, the time is reduced by 3÷4 s. For foils with a thickness of 0.4 mm and a heating temperature of 120 ° C, the preheating time of the foil is 45 seconds.

Time for pressing. The pressing time depends mainly on the type of glue used. The duration of adhesion depends on the type of adhesive, the thickness and temperature of the membrane, the chosen way to further feed the heat to the membrane. PU adhesive is pre-applied to the parts and allowed to dry for about 20-60 seconds (depending on room temperature). Once the adhesive has dried, it forms a film on the parts that are reacted in the press at 70 °C. The use of polyurethane thermosetting adhesives with a minimum cure time of 45 s is recommended for laminating of curved furniture elements.

CONCLUSION

Based on the research, the following conclusions could be made:
- The adhesion strength of the tested adhesive compounds between HDF and PVC foil is relatively low.
- The adhesion strength of PU adhesive compounds meets the required minimum tensile strength at a glue quantity over 150 g/m^2. On the basis of the results obtained, it can be assumed that the adhesive strength of the compounds increases in the range of 100 to 200 g/m^2 as the quantity of adhesive increases.
- The PVA dispersion used is unsuitable for laminating HDF curved structural elements with PVC foil. When using PVA adhesives, it is recommended to dry the applied adhesive layers in advance and to use adhesives with high concentration and viscosity.
Table 1 presents a technological regime for laminating bent HDF structural elements with PVC foil and PU adhesive.

Table 1. Cladding mode for bent HDF structural elements with PVC foil and PU adhesive

Parameters of the regime	Values of the parameters
Quantity of the adhesive	150÷200 g/m^2
Prepress technology stay	minimum 55-65 s
Temperature of heating	65÷125°C
Pressure	0,4÷0,6 N/mm^2
Pressure time	minimum 45÷60 s
Post pressure technology stay	minimum 4 h.

REFERENCES

1. Albin R, Dusil F, Feigel R, Froelich HH, Funke JH (1991) Grundlagen des Mobel- und Innenausbau, DRW - Verlag, Stuttgart: pp. 78.
2. Charles R. Frihart (2015) Introduction to Special Issue: Wood Adhesives: Past, Present, and Future. Forest Products Journal: 2015, Vol. 65, No. 1-2, pp. 4-8.
3. Dunky, M. (2003). "Adhesives in the wood industry," in: Handbook of Adhesive Technology: 2nd Edition, Revised and Expanded, A. Pizzi and K. L. Mittal (eds.), Marcel & Dekker, New York.
4. Kılıç M, Burdurlu E, Aslan S, Altun A, Tümerdem Ö (2009) The effect of surface roughness on tensile strength of the medium density fiberboard (MDF) overlaid with polyvinyl chloride (PVC). Materials and Design, 30(10):4580-4583.
5. Kaelble D.H. (1964) Theory and analysis of peel adhesion: rate-temperature dependence of viscoelastic interlayers. Journal of Colloid Science, 19: 413–424.
6. Landrock A. H., Ebnesajjad S. (2008) Adhesives Technology Handbook. William Andrew - Technology & Engineering, 475 p. - ISBN 9780815516019
7. Silva L.F.M., Ochsner A., Adams R.D (2011) Theories of Fundamental Adhesion.

ACKNOWLEDGEMENT

SPOTREBA SÝTEJ VODNEJ PARY AUTOKLÁVU APDZ 240 V PRIEBEHU TERMICKÉHO PROCESU MODIFIKÁCIE FARBY DREVA

Adrián Banski[1] – **Ján Matyašovský**[2]

Abstract

The article deals with the consumption of saturated steam autoclave APDZ 240 in the color modification process for the most unfavorable operating conditions of the autoclave: thermal adjustment wood lumber Agate white, with humidity u = 100 %, modification mode at temperature t = 137 ± 2,5 °C during period τ = 7,5 hour. The presented model of technological process of heat consumption reveals that the biggest consumption of saturated steam in volume 2136 kg/hour is at the beginning of the technological process at the heating tome τ_o ≈ 1,5 hours when the heat of condensing water vapor is used to heat the modified wood and to heat the autoclave. Subsequently, the heat of the condensing vapor in volume at 6 kg/hr is used to cover the heat loss of the autoclave. In the second phase of the process τ_2, the saturated steam is not lead into the autoclave and the heat losses of the autoclave are covered by heat from the isochoric cooling of the steam contained in the autoclave as well as by the heat from the cooling the autoclave construction material.

Key words: *wood, saturated steam, wood colour, thermal adjustment.*

ÚVOD

Drevo umiestnené do prostredia horúcej vody, sýtej vodnej pary či nasýteného vlhkého vzduchu sa nahrieva a mení svoje fyzikálne, mechanické a chemické vlastnosti. Uvedené skutočnosti sa využívajú v drevárskych technológiách varenia a parenia dreva vo výrobe dýh a preglejok, ohýbaného nábytku, či lisovaného dreva.

Termická úprava dreva – parenie reziva sa uskutočňuje v pariacich komorách, alebo v pariacich zvonoch prostredníctvom nasýteného vlhkého vzduchu pri atmosférickom tlaku a teplotách t = 80 ÷ 95 °C pre τ = 14 ÷ 48 hodín [1-4], alebo prostredníctvom sýtej pary v tlakových autoklávoch pri teplotách t = 105 ÷ 135 °C pre τ = 6 ÷ 18 hodín [5-7].

Procesy termickej úpravy dreva parením dreva sýtou vodnou parou sú okrem cielených fyzikálno-mechanických a chemických zmien dreva sú sprevádzané aj zmenou farby. Kým, v minulosti sa farebné zmeny stmavnutia v technologickom procese parenia dreva využívali na odstránenie nežiaducich farebných rozdielov medzi svetlou beľou a tmavým jadrom, či odstránenie nežiaducich farebných škvŕn vzniknutých zaparením, zahnednutím či zaplesnením, tak v ostatnom čase je problematike cielenej zmeny farby dreva jednotlivých drevín venovaná zvýšená pozornosť [3, 7, 8, 9,10].

[1]Technical University of Zvolen, T.G.Masaryka 24, 96053, Zvolen, Slovakia
[2]VIPO, a.s., Partizánske, Gen. Svobodu1069/4, 958 01 Partizánske, Slovakia
e-mail: banski@tuzvo.sk, jmatyasovsky@vipo.sk

Cieľom danej práce je stanovenie spotreby sýtej vodnej pary v priebehu procesu modifikácie farby dreva agátového reziva v autokláve APDZ 240.

MATERIÁL A METODA

Termická úprava dreva listnatých drevín sýtou vodnou parou za účelom modifikácie farby drevnej hmoty sa vykonáva v tlakových autoklávoch. Technické údaje tlakového autoklávu APDZ 240 firmy: Himmasch AD, Haskovo, Bulharsko uvádza tabuľka 1.

Tab. 1. Technické parameter tlakového autokláva APDZ 240

Parameter	Rozmer	Type autokláva		
		AP - 240	APDZ 240	AZ-240M
Vnútorný priemer autokláva	mm	2,400	2,400	2,400
Dĺžka valcovej časti autokláva	m	13	9	4.5
Vnútorný objem autokláva	m³	66	48	28
Úžitkový objem	m³	22	16	8
hmotnosť	kg	17 200	12 500	7 400
Max. prevádzkový tlak	MPa	0.45	0.45	0.45
Elektrický	kW	3	3	3

Režim najvyššiu teplotu a dobu procesu farebnej modifikácie reziva sýtou vodnou parou v tlakovom autokláve APDZ 240 pre listnaté dreviny je zobrazený na obr.1.
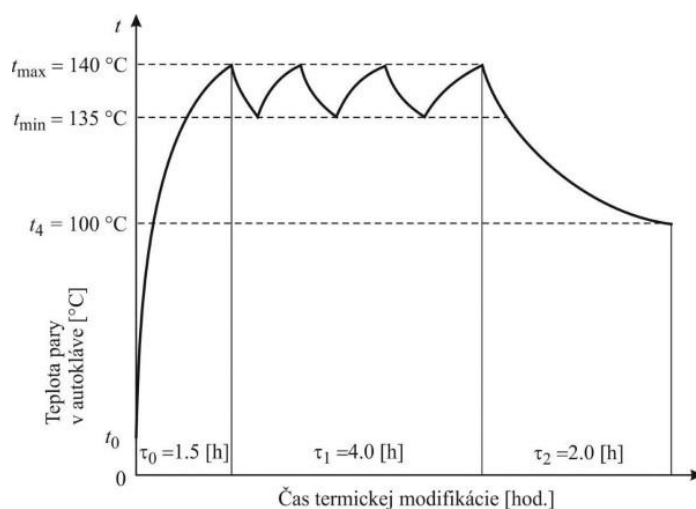
Obr. 1. Režim termickej úpravy sýtou vodnou parou za účelom modifikácie farby

Zdrojom tepla pre realizáciu technologického procesu je kondenzačné teplo vodnej pary. Jednou z alternatív stanovenia jej spotreby je bilancia spotrieb tepla technologického procesu [4, 5, 7, 10, 12]:

$$Q_{ha} = Q_{hw} + Q_{hf} + Q_{hil} + Q_{he} + Q_{hfv} + Q_{hcw} \qquad [kJ] \qquad (1)$$

kde: Q_{hw} – teplo potrebné na ohrev farebného modifikovaného dreva, kJ;

Q_{hf} – teplo potrebné na ohrev konštrukčného materiálu autoklávu, kJ;
Q_{he} – tepelná strata z povrchu tepelnej izolácie tlakového autokláva do atmosféry, kJ;
Q_{hil} – teplo potrebné na ohrev izolácie autoklávu, kJ;
Q_{hcw}– teplo extrahované kondenzátom z tlakového autoklávu, kJ;
Q_{hfv} – teplo extrahované nasýtenou parou po otvorení autoklávu, kJ;
Q_{hc} – teplo potrebné na pokrytie tepelných strát z povrchu tlakového autoklávu, kJ;

Jednotlivé spotreby tepla v technologickom procese popisujú rovnice:

Q_{hw} - teplo potrebné na ohrev farebne modifikovaného dreva s vlhkosťou $u > 30\%$:

$$Q_{hw} = V_D \left[\rho_R \left(1 + \frac{w}{100} \right) \right] \frac{c_D}{10^3} (t_4 - t_D), \qquad [kJ] \qquad (2)$$

kde: V_D – objem farebne modifikovaného dreva v tlakovom autokláve, m³;
   ρ_R – redukovaná hustota dreva, kg.m⁻³;
   u – absolútna vlhkosť farebného modifikovaného dreva,%;
   c_D – stredná hodnota špecifickej tepelnej kapacity modifikovaného dreva, kJ.kg⁻¹.K⁻¹;
   t_D – teplota dreva na začiatku termického procesu, ºC;
   t_4 – teplota nasýtenej pary a telesa autoklávu na konci technologického procesu, ºC;

Q_{hf} - Teplo potrebné na ohrev konštrukčného materiálu avtokláva:

$$Q_{hf} = m_A c_A [t_4 - t_A], \qquad [kJ] \qquad (3)$$

kde: m_A – hmotnosť telesa tlakového autoklávu, kg;
   c_A – špecifická tepelná kapacita materiálu tlakového autoklávu, kJ.kg⁻¹.K⁻¹;
   t_4 – teplota nasýtenej pary a telesa autoklávu na konci technologického procesu, ºC;
   t_A – teplota materiálu tlakového autoklávu na začiatku technologického procesu, ° C;

Q_{hil} - Teplo potrebné na ohrev izolácie avtokláva:

$$Q_{hil} = m_1 c_I \left(\frac{(t_1 + t_2)}{2} - t_{Ai} \right), \qquad [kJ] \qquad (4)$$

kde: m_1 – hmotnosť izolačného materiálu, kg
   c_1 – stredná hodnota špecifickej tepelnej kapacity izolačného materiálu kJ.kg⁻¹.K⁻¹;
   t_1 – teplota telesa autoklávu počas technologického procesu, ºC;
   t_2 – teplota na vonkajšom povrchu izolácie autoklávu počas technolog. procesu, ºC;
   t_{Ai} – teplota izolácie autoklávu pred ohrevom, ºC;
Q_{he} - Tepelná strata z povrchu tepelnej izolácie tlakového autokláva do atmosféry:

$$Q_{he} = 3,6 \cdot \alpha_k \cdot \left[\pi (D + 2 \cdot h_i) L + \pi (D + 2 \cdot h_i)^2 \right] (t_2 - t_0)(\tau_C - \tau_1), \ [kJ] \qquad (5)$$

kde: α_k – koeficient prestupu tepla povrchu autoklávu,, W.m².K⁻¹
   D – priemer tlakového autoklávu bez izolácie, m;
   h_1 – hrúbka izolačnej vrstvy telesa tlakových autokláv, m;
   L – dĺžka valcovej časti tlakového autoklávu, m;
   t_2 – teplota na vonkajšom povrchu izolácie autoklávu počas technolog. procesu, ºC;
   t_0 – teplota materiálu tlakového autoklávu na začiatku technologického procesu, ° C;
   τ_0 – čas ohrevu, h;
   τ_1 – čas 1 fázy technologického procesu, h.

Q_{hfv} - Tepelná strata tlakového autokláva odvedenou sýtou vodnou parou nachádzajúcou sa v nezaplnenom pracovnom priestore autokláva pri jeho vyprázdňovaní.

$$Q_{hfv} = \left[\frac{\pi \cdot D^2}{4} \cdot L - V_D \right] \cdot \frac{h''}{v''}, \qquad [kJ] \qquad (6)$$

kde: D – priemer tlakového autoklávu bez izolácie, m;

$\quad$ L – dĺžka valcovej časti tlakového autoklávu, m;

$\quad$ V_D – objem farebne modifikovaného dreva v tlakovom autokláve, m³;

$\quad$ h'' – entalpia nasýtenej pary v autokláve na konci technologického procesu,kJ.kg⁻¹;

$\quad$ v'' – špecifický objem sýtej pary v autokláve na konci technolog. procesu m³.kg⁻¹;

Q_{hcw} - Tepelná strata tlakového avtokláva odvedeným kondenzátu na konci technologického procesu:

$$Q_{hcw} = m_K \left(h' - h_{H2O} \right) = \frac{Q_{hw} + Q_{hf} + Q_{hil} + Q_{he}}{r} \left(h' - h_{H2O} \right), \qquad [kJ] \qquad (7)$$

kde: m_k – hmotnosť skondenzovanej sýtej pary počas technologického procesu, kg;

$\quad$ h' – entalpia kondenzátu na konci technologického procesu, kJ.kg⁻¹;

$\quad$ h_{H2O} – entalpia vody používanej na výrobu nasýtenej pary; kJ.kg⁻¹;

$\quad$ Q_{hw} – teplo potrebné na ohrev farebného modifikovaného dreva, kJ;

$\quad$ Q_{hf} – teplo potrebné na ohrev konštrukčného materiálu autoklávu;

$\quad$ Q_{hil} – teplo potrebné na ohrev izolácie autoklávu, kJ;

$\quad$ Q_{hc} – teplo potrebné na pokrytie tepelných strát z povrchu tlakového autoklávu, kJ;

$\quad$ r – kondenzačné teplo nasýtených pár použité v technologickom procese; kJ.kg⁻¹;

Proces farebnej modifikácie dreva je typickým diskontinuálnym procesom vyznačujúcim sa s nerovnomernou spotrebou tepla. Podľa prác [4, 6, 11, 13] najväčšia spotreba tepla je na začiatku technologického procesu v čase $\tau_o \approx 1,5$ hod, kedy teplo kondenzujúcej vodnej pary je využívané na ohrev modifikovaného dreva a ohrev autoklávu. Následne je teplo kondenzujúcej sýtej pary využívané na krytie tepelných strát autoklávu. V druhej fáze technologického procesu τ_2 sa sýta para do autoklávu neprivádza, tepelné straty autoklávu sú pokryté teplom z izochorického ochladzovania sýtej pary nachádzajúcej sa v autokláve a teplom z ochladzovania konštrukčného materiálu autok-lávu. Spotrebu sýtej vodnej pary počas ohrevu modifikovaného dreva a autoklávu τ_0 a I. fáze technologického procesu τ_1 popisujú rovnice (8) a (9):

$$m''_{H_2O-\tau_0} = \frac{Q_{hw} + Q_{hf} + Q_{hil} + Q_{hfv} + Q_{hcw}}{\left(h'' - h' \right) \cdot \tau_0}, \qquad [kg.h^{-1}] \qquad (8)$$

kde: Q_{hw} – teplo potrebné na ohrev farebného modifikovaného dreva, kJ;

$\quad$ Q_{hf} – teplo potrebné na ohrev konštrukčného materiálu autoklávu;

$\quad$ Q_{hil} – teplo potrebné na ohrev izolácie autoklávu, kJ;

$\quad$ Q_{hc} – teplo potrebné na pokrytie tepelných strát z povrchu tlakového autoklávu, kJ;

$\quad$ Q_{hfv} – teplo extrahované nasýtenou parou po otvorení autoklávu, kJ;

$\quad$ h'' – entalpia nasýtenej pary v autokláve na konci technologického procesu,kJ.kg⁻¹;

$\quad$ h' – entalpia kondenzátu na konci technologického procesu, kJ.kg⁻¹;

$\quad$ τ_0 – čas ohrevu, h;

$$m''_{H_2O-\tau_1} = \frac{Q_{he}}{\left(h'' - h'\right)\cdot \tau_1}, \qquad\qquad [\text{kg.h}^{-1}] \qquad\qquad (9)$$

kde: Q_{hc} – teplo potrebné na pokrytie tepelných strát z povrchu tlakového autoklávu, kJ;

   h'' – entalpia nasýtenej pary v autokláve na konci technologického procesu, kJ.kg^{-1};

   h' – entalpia kondenzátu na konci technologického procesu, kJ.kg^{-1};

   τ_1 – čas 1 fazy technologického procesu, h.

VÝSLEDKY A DISKUSIA

Bilancia spotreby sýtej vodnej pary autokláva APDZ 240 v procese farebnej modifikácie, prostredníctvom vyššie uvedeného matematického zápisu, je vykonaná pre najnepriaznivejšie podmienky prevádzky farebnej modifikácie reziva v autokláve: drevinu *Agát biely* s jednou z najvyšších hodnôt redukovanej hustoty dreva listnatých drevín ρ_r = 600 kg.m^{-3}, vlhkosť u = 100 %, projektovaný objem modifikovaného dreva V_D = 16 m^3 a režim modifikácie prevádzkovaný v autokláve APDZ 240 s najvyššou teplotou sýtej vodnej pary t = 137 ± 2,5 °C po dobu τ = 7,5 hod. Závislosť spotreby sýtej vodnej pary teploty autoklávu APDZ 240 v priebehu technologického procesu farebnej modifikácie reziva, uvádza obr. 4.
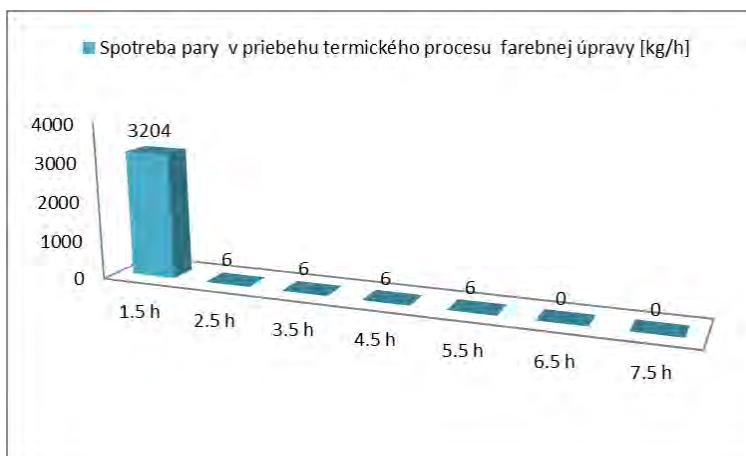
Obr. 4. Závislosť spotreby sýtej vodnej pary v priebehu technologického procesu farebnej modifikácie V = 16 m^3 agátového reziva v tlakovom autokláve APDZ 240.

Z bilancie spotreby sýtej vodnej pary autoklávom APDZ 240 plynie, že v priebehu technologického procesu sa spotrebuje m_{H2O} = 3228 kg sýtej vodnej pary o teplote t = 137 ± 2,5 °C. V čase maximálneho odberu, na počiatku technologického procesu, je hodinová spotreba sýtej pary m_{H2O} = 2136 kg.hod^{-1}.

Hodinový odber sýtej vodnej pary špecifikuje aj nevyhnutnú požiadavka na tepelný výkon parného generátora Q = 1958 kW v tepelnom systéme závodu.

Skondenzovaná vodná para je v priebehu technologickom procese termickej úpravy dreva je kontaminovaná produktmi hydrolýzy a extrakcie z termicky upravovaného dreva [15, 16, 17] a musí byť odvádzaná je na čistenie v ČOV. Uvedená skutočnosť radí termickú úpravu – modifikáciu farby dreva medzi technologické operácie s priamou spotrebou pary a nevratným kondenzátom do tepelného systému závodu.

ZÁVER

V príspevku sú prezentované výsledky analýz spotreby sýtej vodnej pary tlakového autoklávu APDZ 240 v procese termickej úpravy – modifikácie farby dreva. Z vykonanej analýzy plynie, že autokláv v priebehu technologického procesu spotrebuje m_{H2O} = 3228 kg sýtej vodnej pary o teplote t = 137 ± 2,5 °C. V čase maximálneho odberu, na počiatku technologického procesu počas ohrevu je hodinová spotreba sýtej pary m_{H2O} = 2136 kg.hod^{-1}.

Literatúra

1. KOLLMANN, F., COTE, W. A.: Principles of Wood Sciences and Technology, Vol. 1. Solid Wood, Springer Verlag: Berlin – Heidelberg - New York, 1968, 592 s.

2. SERGOVSKIJ, P. S., RASEV, A. I. 1987: Gidrotermičeskaja obrabotka i konservirovanije drevesiny. Lesnaja promyšlennost, Moskva, 1987, 360 s.

3. TREBULA, P.: Sušenie a hydrotermická úprava dreva. Zvolen: Vydavateľstvo TU Zvolen, 1996. 255 s.

4. DZURENDA, L., DELIISKI, N.: Tepelné procesy v technológiách spracovania dreva. Zvolen: Vydavateľstvo TU Zvolen, 2010. 273 s.

5. NIKOLOV, S., RAJCHEV, A., DELIISKI, N.: Proparvane na drvesinata. Sofia: Zemizdat, 1980. 222 s.

6. DELIISKI, N., DZURENDA, L., ANGELSKI, D., TUMBARKOVA, N.: An approach for computation of regimes for autoclave steaming of prisms for veneer production with a limited power of the heat generator**.** In: Acta Facultatis Xylologiae Zvolen. (2018), 60(1):101-112, doi: 10.17423/afx.2018.60.1.11

7. DZURENDA, L.: The Shades of Color of Quercus robur L. Wood Obtained through the Processes of Thermal Treatment with Saturated Water Vapor. BioResouces, (2018), 13(1): 1525 – 1533, doi: 10.1063/biores 13.1.1525-1533.

8. TOLVAJ, L., NEMETH, R., VARGA, D., MOLNAR, S.: Colour homogenisation of beech wood by steam treatment. In: Drewno. (2009), 52(181): 5-17.

9. BARCIK, Š.: GAŠPARÍK, M., RAZUMOV, E. Y.: Effect of thermal modification on the colour changes of oak wood. Wood Research. (2015), 60(3): 385-396.

10. DZURENDA, L.: Colour Modification of Robinia pseudoacacia L. during the Processes of Heat treatment with Saturated Water Steam. In: Acta Facultatis Xylologiae Zvolen. (2018). 60(1):61-70, (2018) doi: 10.17423/afx.2018.60.1.07

11. BANSKI, A: Vplyv vlhkosti dubového dreva na spotrebu tepla v procese farebnej homogenizácie sýtou vodnou parou. In: Trieskové a beztrieskové obrábanie dreva, (2016), 10(1): 235–239. ISSN 2453-904X.

12. DZURENDA, L.: Numeric Model of the Normative Consumption of Heat for the Colour Homogenisation of Wood in Pressure Autoclaves. In: AIP Conf. Proc. 1745, 020008-1–020008-7; (2016), doi: 10.1063/1.4953702.

13. DZURENDA, L.: The Effect of Moisture Content of Black Locust Wood on the Heating in the Saturated Water Steam during the Process of Colour Modification. In: MATEC Web of Conferences 168, 06004 (2018), DOI: 10.1051/matecconf/201816806004XXI.

14. BUČKO, J. 1995: Hydrolýzne procesy. Zvolen: Vydavateľstvo TU Zvolen, (1995),116 s.

15. KAČÍK, F. 2001: Tvorba a chemické zloženie hydrolyzátov v systéme drevo-voda-teplo. Zvolen: Vydavateľstvo TU Zvolen, 75 s.

16. LAUROVA, M., MAMONOVA, M., KUČEROVA, V.: Proces parciálnej hydrolýzy bukového dreva (Fagus sylvatica L.) parením a varením. [Vedecké štúdie 2/2004/A], Zvolen: TU Zvolen. (2004), 58 s.

ATTEMPTS AT APPLICATION OF POLYETHYLENE-COATED WASTE PAPER AS A RAW MATERIAL IN THE INSULATION BOARDS PRODUCTION

Piotr Borysiuk – Radosław Auriga – Michał Stępień – Izabela Jenczyk-Tołłoczko

Abstract

This study evaluates the usage of polyethylene-coated waste paper as a raw material for production of insulation boards. As part of the research, single-layer boards were made of waste paper covered on one side with polyethylene. The produced boards varied in density: 203, 311 and 397 kg/m³. Thermal conductivity, volumetric heat capacity and temperature conductivity were evaluated. The MOR values of panels covered with double-sided hardboard panels were also determined. Boards obtained from waste paper covered on one side with polyethylene were characterized by thermal properties similar to those of insulating boards or straw boards (thermal conductivity: $0.077 \div 0.122$ W/mK, volumetric heat capacity: $0.425·10^6 \div 0.692·10^6$ J/m³K, temperature conductivity: $0.180·10^{-6} \div 0.203·10^{-6}$ m²/s. After double-sided sealing with hardboards, boards can be used as insulating and structural material (MOR: $39.1 \div 92.2$ N/mm²).

Key words: *insulation boards, polyethylene coated waste paper, thermal properties, polyethylene*

INTRODUCTION

For many years, research has been conducted on the possibilities of using various types of post-consumer materials in the technology of wood-based panels (Nicewicz i in. 1997, Borysiuk i in. 2004, Pawlicki i in. 2005, Borysiuk i in. 2006, Müller i in. 2012). Particular attention in this respect is given to materials with limited application in other areas of life, and even those that are often useless waste. Such materials can undoubtedly include waste from multi-material packaging (bags, pouches, boxes for liquid food products). In their case, there are difficulties in separating individual raw materials: paper, aluminum or polyethylene. For the majority of multi-material packaging, recycling of post-consumer waste is not justified economically, technically and ecologically. Thermal recycling methods leading to energy recovery are often used in this field. It should be noted, however, that in general it is not possible to recover all the energy invested in the production of a given product. In addition, they often contain harmful substances, which combustion in itself is nuisance to the environment. According to industry data (ACE- The Alliance for Beverage Cartons and the Environment), in 2016 in the European Union, a total of 47% of beverage cartons were recycled in over 20 paper mills. This percentage

Warsaw University of Life Sciences, Nowoursynowska 159/34, 02-776 Warsaw
e-mail: piotr_borysiuk@sggw.pl, radoslaw_auriga@sggw.pl

corresponds to approximately 430000 tons of cardboard boxes. However, the total recovery rate including recycling and energy recovery was nearly 76% (https://www.tetrapak.com).

Shredded multi-material waste can be used to produce boards in chipboard technology. Tectan board is a chipboard-like material made from beverage cartons, both the scraps from production and used cartons. The drink cartons consist of various layers of paperboard, polyethylene and aluminium. In the production process of the board, the polyethylene melts and acts like a glue to keep the material together (https://materia.nl/material/tectan-board/). Another example of the possibility of recycling multi-material packaging is PolyAl roofing sheets. These are covering materials, similarly to Tectan, made of compressed multi-material waste with aluminum layer on one side (http://saahaszerowaste.com). Polyethylene coated paper can also be included in multi-material packaging. Due to the presence of plastic on the surface, this product cannot be recycled to paper. Its combustion may take place only under certain conditions.

This study presents the possibilities of re-using polyethylene coated paper as a raw material for the production of insulation boards. The big advantage of this material is in this case polyethylene, which as a thermoplastic, can be a board-binder. It is also important that this type of solution does not generate any burdens for the natural environment.

MATERIAL AND METHODS

The post-production waste paper with one side covered with polyethylene was used for the research. Paper weight with polyethylene layer was 100 g/m2. The material was in the form of long and narrow bands (Ryc. 1). During the tests, three variants of insulating boards with a thickness of 18 mm were produced, varying in terms of density: 200 kg/m^3, 300 kg/m^3 i 400 kg/m^3. Mattress were hand-formed. For the press cycle applied following settings: maximum unit pressure 1.5 MPa, pressing temperature 200°C, pressing time 15 min. The pressing time was adjusted to let temperature inside the plate exceeded 110°C (temperature at which the polyethylene begins to plasticize). The role of the binder in the plates was met by polyethylene applied on paper. After hot-press, the boards were fixed by cooling under pressure.

Ryc. 1. Paper strips coated on one side with polyethylene used in the research.

The produced panels were subjected to air conditioning in laboratory conditions for 24 hours. The following properties were determined for obtained panels:
• thermal conductivity,
• volumetric heat capacity,
• temperature conductivity.

The research was carried out using the ISOMET of Applied Precision. In the further stage of testing, boards were strengthen on both sides with 3 mm thick hardboards. For gluing components an urea-formaldehyde based resin was used. Glue recipe:
• 100 parts Silekol S-1 urea-formaldehyde resin,
• 25 parts filler - rye flour,
• 25 parts H_2O,
• 10 parts hardener - 10% aqueous solution of NH_4Cl.

The following gluing parameters were applied: glue application - 200 g/m^2 pressing temperature - 120°C; unit pressure -1.6 N/mm^2; pressing time - 5 min. During the pressing were used spacers, to prevent compression of the inner layer. For bonded boards, the bending strength was determined in accordance with the EN 310:1994 standard.

RESULTS AND DISCUSSION

The results of testing thermal properties of insulation boards are presented in Tables 1, 2 and 3. Table 4 displays the comparative values of thermal conductivity of selected materials.

Table 1. Thermal conductivity values of the insulating panels produced.

Density	Thermal conductivity			Standard deviation (SD)	Coefficient of variation (CV)
	min.	max.	mean		
[kg/m³]	[W/mK]				[%]
203	0.069	0.089	0.077	0.008	10
311	0.092	0.105	0.097	0.005	5
397	0.107	0.144	0.122	0.012	10

Table 2. Volumetric values of heat capacity of the produced insulation boards.

Density	Volumetric heat capacity			Standard deviation (SD)	Coefficient of variation (CV)
	min.	max.	mean		
[kg/m³]	[J/m³K] x10⁶				[%]
203	0.299	0.583	0.425	0.105	25
311	0.416	0.535	0.480	0.044	9
397	0.546	0.978	0.692	0.148	21

Table 3. Comparison of temperature conductivity values of the insulating panels produced.

Density	Temperature conductivity			Standard deviation (SD)	Coefficient of variation (CV)
	min.	max.	mean		
[kg/m³]	[m²/s] x10⁻⁶				[%]
203	0.153	0.239	0.186	0.031	17
311	0.176	0.225	0.203	0.019	9
397	0.147	0.195	0.180	0.018	10

Table 4. Thermal conductivity values of selected materials (based on ISO 6946:2017)

Material	Density	Thermal conductivity
	[kg/m^3]	[W/mK]
Pine (*Picea*) (cross-cut)	550	0.16
Oak (*Quercus*) (cross-cut)	800	0.22
Insulating board	300	0.06
Strawboard	300	0.08
Styrofoam	10 ÷ 40	0.045 ÷ 0.040
Mineral wool board	40 ÷ 160	0.045 ÷ 0.042

The main parameter determining the possibility of using the panels as an insulating material is their thermal conductivity coefficient (λ). It determines the heat transfer capacity of a given material. The lower it is, the better the insulation. The obtained boards were characterized, depending on the density, by thermal conductivity at the level of 0.077 ÷ 0.122 W/mK (Tab.1). The recorded values of thermal conductivity are similar to those of insulation materials such as insulating boards or strawboards (table 4). In this respect, it is also worth noting that according to EN 13986:2004, the thermal conductivity of fiberboard with a density of 250 kg/m3 should be λ = 0.05 W/(mK) and for boards with a density of 400 kg/m3 λ = 0.07 W/(mK). However, the ISO 6946:2017 standard for fibreboards with the density of 300 kg/m3 indicates the value of heat transfer coefficient λ = 0.06 W/(mK). The thermal conductivity of the tested panels decreases as the density of the panels lowers, which is related to the increase in the content of free space filled with air. It is worth adding here, that the increase in the thermal conductivity of the tested panels, along with the increase in density, is approximately linear in nature, and the differences noted are statistically significant for the 95% confidence level.

Considering the volumetric heat capacity of the tested panels, it can be generally stated that, similarly as in the case of thermal conductivity, it increases with the density increase and is in the range of $0.425 \cdot 10^6 – 0.692 \cdot 10^6$ J/m^{3}K. In general, heat capacity is the amount of heat needed to raise the material temperature by one degree. The increase in thermal capacity along with the increase in density is related to the loss of free-air-spaces. The amount of "solid" material in the board of higher density is naturally larger, and requires more energy to heat the material, according to EN 12524:2000, not less than 1700 J/kgK. In general, heat capacity (c) is calculated from the formula:

$$c = C/\rho \text{ [J/kg}\times\text{K]}$$

C – volumentric heat capaicty [J/m^{3}K],
ρ – density of the material [kg/m^3].

The average thermal capacity for plates produced under individual variants ranged from 1743 - 2094 J/kgK. It is worth of highlighting, that the differences noted in the research are statistically significant only in relation to panels with a density of 397 kg/m^3 (for a confidence level of 95%).

Unlikely to thermal conductivity and volumetric heat capacity, the temperature conductivity did not show a clear upward trend due to increase of boards density. Values for this parameter ranged from $0.180 \cdot 10^{-6}$ to $0.2 \cdot 10^{-6}$ m^2/s. Differences recorded for temperature conductivity were visible, however statistically insignificant. This type of conductivity is essential as materials with low conductivity give the impression of being "warm". That concerns wood, which temperature is $0.153 \cdot 10^{-6} ÷ 0.111 \cdot 10^{-6}$ m^2/s (for density 450 ÷ 700 kg/m^3) (Krzysik 1974).

The results of the bending strength test of the insulated boards are presented in Table 5.

Table 5. Comparison of bending strength values of the insulated boards

Density	MOR			Standard deviation (SD)	Coefficient of variation (CV)
	min.	max.	mean		
[kg/m^3]	[N/mm^2]				[%]
203	37.0	41.0	39.1	2.5	6
311	57.0	76.0	63.8	5.5	9
397	77.0	109.0	92.2	10.4	11

The uncoated insulation boards were characterized by low MOR values not exceeding 2 N/mm^2 (for panels with a density of 397 kg/m^3). It is worth noting, that according to the EN 622-4:2009 norm, insulating boards with density in the range of 230 kg/m^3 – 400 kg/m^3 should have MOR values above 0.8 N/mm^2. Double-sided coating of tested boards with a hardboard (Ryc. 2) allowed to obtain MOR values in the range of 39.1 - 92.2 N/mm^2 (Table 5). Boards manufactured in this way can therefore be used as an insulating and structural material.

Ryc. 2. Double-sided coated of tested boards with hardboard.

CONCLUSION

The insulation boards made of polyethylene coated paper were characterized by similar thermal properties to insulating materials such as insulating boards or strawboards. The boards can also be included in materials that give the impression of "warm" what creates the possibility of using them as a warming material. Double-sided sealing with hard fiberboards allows using the boards as insulating and structural material.

REFERENCES

1. Borysiuk P., Nicewicz D., Pawlicki J., 2004: Wood-based materials utilising waste thermoplastics. Vth International Symposium:„Composite Wood Materials", Zborník referátov, Zvolen, 119-124
2. Borysiuk P., Pawlicki J., Nicewicz D., 2006: New types of raw materials in technologies of wood-based materials. Materiały z konferencji COST Action E44 – E49 „Wood Resources and Panel Properties" Valencia, 277-281
3. EN 12524:2000 Building materials and products. Hygrothermal properties. Tabulated design values
4. EN 13986:2004+A1: 2015 Wood-based panels for use in construction – Characteristics, evaluation of conformity and marking
5. EN 310:1994 Wood-based panels: Determination of modulus of elasticity in bending and of bending strength
6. EN 622-4:2009 Fibreboards. Specifications. Requirements for softboards.
7. http://saahaszerowaste.com/products, access: 10.07.2018
8. https://www.tetrapak.com/pl/sustainability/recykling-w-polsce, access: 10.07.2018
9. ISO 6946:2017 Building components and building elements - Thermal resistance and thermal transmittance - Calculation methods.
10. Müller Ch., Schwarz U., Thole V., 2012: Zur Nutzung von Agrar-Reststoffen in der Holzwerkstoffindustrie. Eur. J. Wood Prod. 70(5): 587-594
11. Nicewicz D., Oniśko W., Pawlicki J., 1997: New materials in technologies of wood-based panels. XIII International Symposium „Adhesives in wood-working industry", Zborník referátov, Zvolen.
12. Pawlicki J., Nicewicz D., Borysiuk P., Zado A., 2005: Attempts at application of waste paper as supplementary raw material in the technology of particleboards. XVII International Symposium:„Adhesives In Woodworking industry", Zborník referátov, Zvolen, 205-209

ACKNOWLEDGEMENTS

COMPUTATION OF THE HEAT ENERGY AND FLUX NEEDED FOR COVERING OF THE EMISSION FROM FLAT OAK DETAILS DURING THEIR ONE SIDED HEATING BEFORE BENDING

Nencho Deliiski[1] **– Dimitar Angelski**[1] **– Neno Trichkov**[1] **– Ladislav Dzurenda**[2] **– Zhivko Gochev**[1] **– Natalia Timbarkova**[1]

Abstract

A software program has been prepared in the calculation environment of Visual Fortran for solving of own 1D non-linear mathematical model of the one sided heating process of flat wood details. The model includes a mathematical description of the specific (for 1 m^2) energy consumption, q_e, and the specific heat flux, $dq_e/d\tau$, needed for covering of the emission in the surrounding environment of the subjected to one sided heating wood details aimed at their plasticizing before bending.

Using the program, computations have been carried out for the determination of the change in the energy q_e and in the flux $dq_e/d\tau$, which are consumed by flat oak details with an initial temperature of 20 ºC, moisture content of 0.15 kg·kg^{-1}, and thicknesses of 12 mm, 16 mm, and 20 mm during their 30 min unilateral heating at temperatures of the heating metal body of 80 ºC and of the surrounding air of 20 ºC. The obtained results are graphically presented and analyzed.

Key words: *oak details, one sided heating, plasticizing, bending, heat emission, energy consumption, heat flux*

INTRODUCTION

An important component of the technologies for production of curved wood details is their plasticizing up to the stage that allows their faultless bending. The duration of the heating process and the energy consumption for one sided heating of the details aimed at their plasticizing before bending depends on many factors: wood specie, thickness and moisture content of the details, temperatures of the heating medium and of the surrounding air, desired degree of plasticizing, etc. (Chudinov 1968, Taylor 2001, Trebula and Klement 2002, Videlov 2003, Angelski 2010, Deliiski and Dzurenda 2010, Gaff and Prokein 2011).

The one sided heating of wood details is most often carried out in the specific equipment used for bending. For such heating of details with thicknesses between 10 and 25 mm, hot hydraulic presses with appropriately bent surfaces are usually used. Curved details for the back parts of chairs are produced, for example, through this method of plasticizing. These details have a relatively small thickness, a large radius R of the curvature and a

[1]Faculty of Forest Industry, University of Forestry, Kliment Ohridski Bd. 10, 1797 Sofia, Bulgaria
e-mail: deliiski@netbg.com, d.angelski@gmail.com, nenotr@abv.bg, zhivkog@yahoo.com, nataliq_manolova@abv.bg
[2]Technical university in Zvolen, T.G. Masaryka 24, 960 53 Zvolen, Slovakia
e-mail: dzurenda@tuzvo.sk

relationship of $R/h = 20 \div 25$, h is the size of the cross section of the details in the direction coinciding with the plane of bending (Kavalov and Angelski 2014).

In the specialized literature information about the energy consumption needed for the one sided heating of flat wood details was given only by the authors (Deliiski et. al. 2014b, 2016). The calculation of the energy consumption in these publications was carried out using a suggested by the authors linear model for the heat distribution in subjected to one sided heating flat wood details.

The current work presents a 1D non-linear model for the calculation of the temperature distribution along the thickness of flat wood details subjected to one sided conductive heating aimed at their plasticizing in the production of curved back parts of chairs. The aim of the work is to apply the suggested by the authors earlier (Deliiski et al. 2016) numerical approach for the computation of the specific energy consumption (in $kWh \cdot m^{-2}$) and the specific heat flux (in $kW \cdot m^{-2}$), which are needed for covering of the heat emission from the non-heated surface of the details during their heating. In this case, the approach uses the solutions of the presented in the current work non-linear 1D model.

MECHANISM OF THE HEAT DISTRIBUTION IN FLAT WOOD DETAILS SUBJECTED TO ONE SIDED CONDUCTIVE HEATING

The mechanism of the heat distribution in wood details during their one sided conductive heating can be described by the equation of the heat conduction (Deliiski 2011, 2013, Deliiski et al. 2014a, 2014b, 2016). When the width and length of the wood details exceed their thickness by at least 3 and 5 times respectively, then the calculation of the change in the temperature only along the thickness of the details in the center of their flat side during the one sided heating (i.e. along the coordinate x, which coincides with the details' thickness h_w) can be carried out with the help of the following non-linear 1D mathematical model:

$$c_w(T,u)\rho_w(\rho_b,u,u_{fsp},S_v)\frac{\partial T_w(x,\tau)}{\partial \tau} = \lambda_w(T,u,\rho_b)\frac{\partial^2 T_w(x,\tau)}{\partial x^2} + \frac{\partial \lambda_w(T,u,\rho_b)}{\partial T}\left(\frac{\partial T_w}{\partial x}\right)^2 \quad (1)$$

with an initial condition

$$T_w(x,0) = T_{w0} \qquad (2)$$

and following boundary conditions:
• from the side of the details' heating – at prescribed surface temperature, which is equal to the temperature of the metal heating body T_m (see Fig.1 below):

$$T_w(0,\tau) = T_m(\tau) , \qquad (3)$$

• from the opposite non-heated side of the details – at convective heat exchange between the details' surface and the surrounding air environment

$$\frac{dT_w(X,\tau)}{dx} = -\frac{\alpha_w(\tau)}{\lambda_{ws}(\tau)}\left[T_a(\tau) - T_s(\tau)\right] . \qquad (4)$$

For usage of eqs. (1) and (4) it is needed to have mathematical descriptions of the wood thermal conductivity cross sectional to the fibers, λ_w, of the specific heat capacity of the non-frozen wood, c_w, and of the heat transfer coefficient between the details' surface at their non-heated side and the surrounding air, α_w. For this purpose the description of λ_w and c_w given in (Deliiski 2011, 2013) and in (Deliiski and Dzurenda 2010) can be used.

The calculation of the heat transfer coefficient α_w can be carried out with the help of the following equation, which has been suggested by Chudinov (1968) for the cases of cooling or heating of horizontally situated wood plates in atmospheric conditions of free convection:

$$\alpha_w = 3.256[T_s(\tau) - T_a(\tau)]^{0.25} . \tag{5}$$

According to eq. (3), the temperature at the details surface being in contact with the heating body (i.e. the characteristic point with *x-coordinate* = 0 mm) is equal to its temperature T_m due to the extremely high coefficient of heat transfer between the body and the wood during their very close contact.

The presenting of the mathematical model (1) ÷ (5) through its discrete analogue suitable for programming in Visual Fortran corresponds to the shown in Fig. 1 setting of the coordinate system and the positioning of the nodes in the mesh, in which the 1D distribution of the temperature along the thickness of flat wood details subjected to one sided heating is calculated.
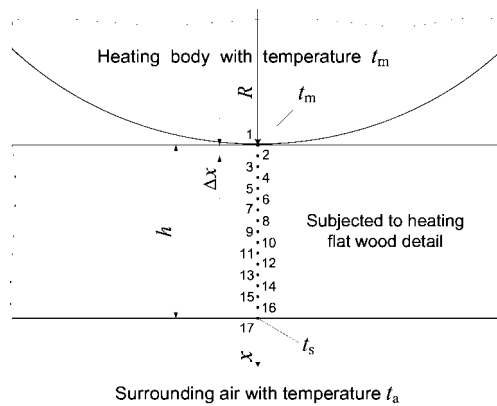
Figure 1. Positioning of the nodes of the 1D calculation mesh in a discretized detail's thickness

MODELLING OF THE SPECIFIC ENERGY CONSUMPTION AND OF THE HEAT FLUX NEEDED FOR COVERING OF THE HEAT EMISSION FROM THE NON-HEATED SIDE OF THE WOOD DETAILS

The change in the specific (for 1 m^2 of the details' surface) energy consumption q_e (in kWh·m^{-2}), which is needed for covering of the heat emission from the non-heated side of the wood details into the surrounding air environment during the time $\Delta\tau$, can be calculated according to the following equation (Deliiski 2013):

$$\Delta Q_e = \frac{\alpha_w(\tau)\Delta\tau}{3.6 \cdot 10^6}[T_{ws}(\tau) - T_a(\tau)] . \tag{6}$$

The specific energy consumption needed for the covering of the heat emission from 1 m^2 surface of the details during their unilateral heating with duration $\tau_p = N. \Delta\tau$ is equal to

$$Q_e = \sum_{i=1}^{N} \Delta Q_{ei} . \tag{7}$$

The change in the heat energy Q_e during the time $\Delta\tau$, i.e. the change in the heat flux which is needed for the covering of the heat emission from the non-heated side of 1 m^2 of

the subjected to unilateral heating wood details, $\dfrac{\mathrm{d}Q_e}{\mathrm{d}\tau}$ (in kW·m^{-2}), can be calculated according to equation

$$\frac{\mathrm{d}Q_e}{\mathrm{d}\tau} \approx \frac{3600\Delta Q_e}{\Delta\tau} \ . \tag{8}$$

RESULTS AND DISCUSSION

For the numerical solution of the above presented mathematical models aimed at usage of the suggested approach for the calculation of Q_e and $\dfrac{\mathrm{d}Q_e}{\mathrm{d}\tau}$ a software program was prepared in FORTRAN, which was input in the developed by Microsoft calculation environment of Visual Fortran Professional.

With the help of the program, as examples, computations have been made for the determination of the 1D non-stationary change of t, t_{ws}, Q_e, and $\mathrm{d}Q_e/\mathrm{d}\tau$ for non-frozen oak (*Quercus petraea* Liebl.) details with thicknesses of $h = 12$ mm, $h = 16$ mm, $h = 20$ mm, initial wood temperature of $t_{w0} = 20$ ºC, and wood moisture content of $u = 0.15$ kg·kg^{-1} during their 30 min heating at $t_m = 80$ ºC and at $t_a = 20$ ºC. All calculations have been carried out using the mathematical descriptions of c_w, λ_w, and ρ_w given in (Deliiski 2011, 2013) with the following values of the variables in these descriptions for oak wood: $u_{fsp}^{293.15} = 0.29$ kg·kg^{-1}, $\rho_b = 670$ kg·m^{-3}, and $S_v = 11.9\%$ (Videlov 2003, Deliiski and Dzurenda 2010).

The left part of Fig. 2 presents the temperatures of the heating body $t_m = 80$ ºC, which have been entered based on the input data used for the solution of the 1D model, and also the temperature change calculated by the model in 4 equidistant from one another characteristic points along the thickness of the oak detail with thickness of $h = 20$ mm during its one sided heating. The coordinates of those points are shown in the legend of the figure. The right part of Fig. 2 presets t_m and the change in the temperature of the non-heated surface, t_s, (refer to Fig. 1) of the studied oak details, depending of their thickness h.

Figure 3 presents the calculated change in λ_{ws} and in α_w, and Figure 4 – the calculated change in Q_e and in $\mathrm{d}Q_e/\mathrm{d}\tau$ during the one sided heating of the oak details with studied thicknesses at $t_m = 80$ ºC and $t_a = 20$ ºC.
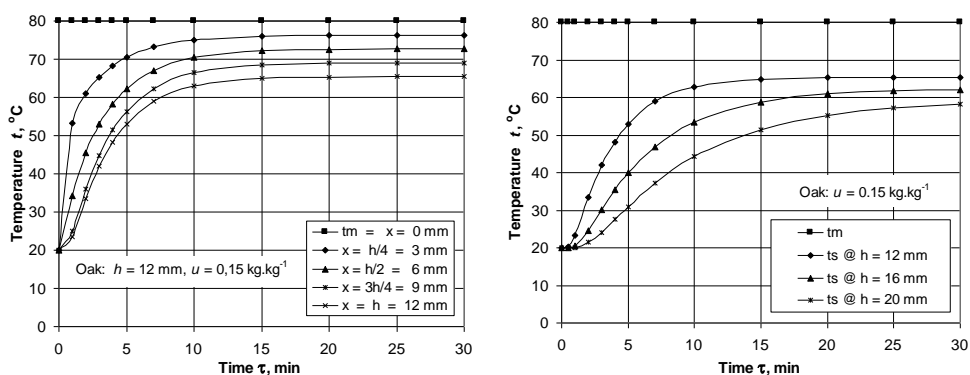
Figure 2. Change in t_w along the thickness of oak detail with $h = 12$ mm (left) and in $t_{ws} = f(h)$ (right) during the one sided heating at $t_m = 80$ ºC and $t_a = 20$ ºC

The analysis of the shown on the figures results warrants the making of the following conclusions:

1. During the unilateral heating of the details the change of all studied variables takes place according to complex curves.

2. By increasing the heating time τ, the studied variables change, as follows:

• the curves of t_w gradually approach asymptotically to their biggest values, decreasingly dependent on the remoteness of the characteristic points from the heated surface of the detail;

• the curves of t_s, λ_w, α_w, and $dQ_e/d\tau$ approach asymptotically to their biggest values, decreasingly dependent on h;

• the specific energy consumptions Q_e increases according to non-linear dependences, which change into linear after reaching of stationary distribution of t along the details' thickness.

3. The values of Q_e are decreasingly dependent on h and the slopes of the linear sections of the dependences $Q_e = f(\tau)$ are inversely proportional to h.
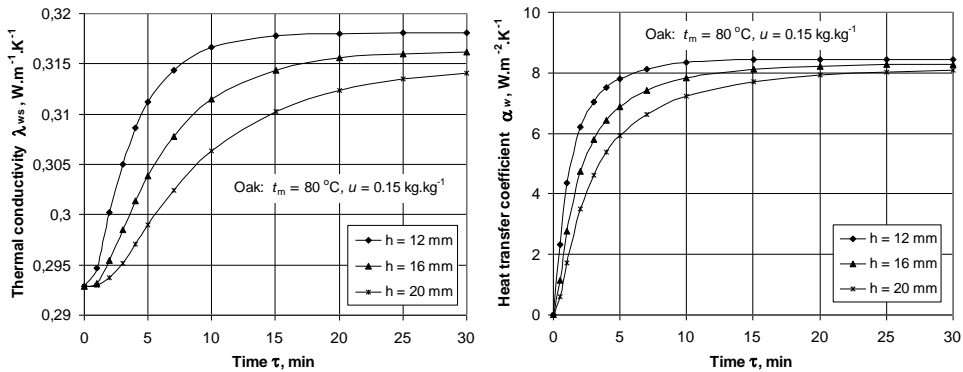
Figure 3. Change in λ_{ws} (left) and in α_w (right) of the oak details during their one sided heating at $t_m = 80\ ^oC$ and $t_a = 20\ ^oC$, depending on h
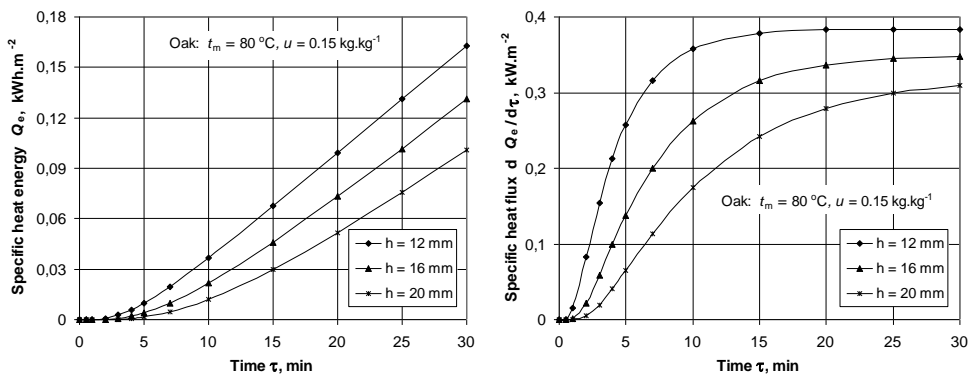
Figure 4. Change in Q_e (left) and in $dQ_e/d\tau$ (right) of the oak details during their one sided heating at $t_m = 80\ ^oC$ and $t_a = 20\ ^oC$, depending on h

After 10 min and 20 min duration of the one sided heating at t_m = 80 °C of the studied oak details, the specific energy consumption Q_e reaches the following values:
- for h = 12 mm: Q_e = 0.0366 kWh·m^{-2} and Q_e = 0.0992 kWh·m^{-2} respectively;
- for h = 16 mm: Q_e = 0.0215 kWh·m^{-2} and Q_e = 0.0733 kWh·m^{-2} respectively;
- for h = 20 mm: Q_e = 0.0119 kWh·m^{-2} and Q_e = 0.0514 kWh·m^{-2} respectively.

After 10 min and 20 min duration of the one sided heating at t_m = 80 °C of the studied oak details, the specific heat flux $dQ_e/d\tau$ reaches the following values:
- for h = 12 mm: $dQ_e/d\tau$ = 0.358 kW·m^{-2} and $dQ_e/d\tau$ = 0.383 kW·m^{-2} respectively;
- for h = 16 mm: $dQ_e/d\tau$ = 0.263 kW·m^{-2} and $dQ_e/d\tau$ = 0.337 kW·m^{-2} respectively;
- for h = 20 mm: $dQ_e/d\tau$ = 0.175 kW·m^{-2} and $dQ_e/d\tau$ = 0.279 kW·m^{-2} respectively.

CONCLUSIONS

The present paper describes the suggested by the author numerical approach for the computation of the specific energy consumption, Q_e, and the specific heat flux, $dQ_e/d\tau$, needed for covering of the emission in the surrounding environment of the subjected to one sided heating wood details aimed at their plasticizing before bending in the production of back parts of chairs. The approach is based on the integration and differentiation of the solutions of own non-linear model for the calculation of the non-stationary 1D temperature distribution along the thickness of subjected to one sided heating flat wood details.

The paper shows and analyses diagrams of a non-stationary change of Q_e and $dQ_e/d\tau$ during the one sided heating of flat oak details aimed at their plasticizing before bending for the production of back parts of chairs. All diagrams are drawn using the results calculated by the model. The change of Q_e and $dQ_e/d\tau$ for details with thicknesses of 12 mm, 16 mm and 20 mm, initial wood temperature 20 °C, and moisture content of 0.15 kg.kg^{-1} during their unilateral heating for a period of 30 min at a temperatures of the heating metal body of t_m = 80 °C and temperature of the air near the non-heated side of the details of t_a = 20 °C is calculated, visualized and analysed.

Using the scientific determined values of Q_e and $dQ_e/d\tau$, the minimum necessary power of the heating metal body can be determined depending on the desired duration of the one sided details' heating at given values for t_m, h, and R/h.

The approach that was used for the creation of the model for computation of Q_e and $dQ_e/d\tau$ could be further applied in the development of analogous models, for example, for the calculation of the change of energy consumption and of heat flux needed for covering of the emission in the surrounding environment of flat details made of various materials.

Symbols

c	= specific heat capacity (J·kg^{-1}·K^{-1})
h	= thickness (m)
Q	= specific energy consumption (kWh·m^{-2})
S	= wood shrinkage (%)
T	= temperature (°C): $t = T - 273.15$
T	= temperature (K): $T = t + 273.15$
u	= moisture content (kg·kg^{-1}): $u = W/100$
W	= moisture content (%): $W = 100u$
x	= coordinate along the thickness of the details: $0 \leq x \leq X = h$
α	= heat transfer coefficient (W·m^{-2}·K^{-1})
λ	= thermal conductivity (W·m^{-1}·K^{-1})

ρ = density (kg·m^{-3})
τ = time (s)
@   = at

Subscripts and superscripts:

a   = air (for the air temperature near the non-heated side of the wood details)
avg   = average (for the average mass temperature of the details at given moment of their one sided heating)
b   = basic (for density, based on dry mass divided by green volume)
e   = emission
fsp   = fiber saturation point of the wood
m   = medium (for the temperature of the heating metal body used for one sided heating)
s   = surface (for the non-heated surface of the wood details)
v   = volume (for the wood shrinkage)
w   = wood
0   = initial (for the average mass temperature of details at the beginning of the heating)
293.15= at 293.15 K, i.e. at 20 ºC (for the standard values of wood fiber saturation point)

REFERENCES

1. Angelski, D., 2010: Researches over the Processes of Plasticization and Bending of Furniture Wood Details. PhD Thesis, University of Forestry, Sofia, 2010 (in Bulgarian).
2. Chudinov, B. S., 1968: Theory of Thermal Treatment of Wood. Publishing Company "Nauka", Moscow, USSR (in Russian).
3. Deliiski, N., 2011: Transient Heat Conduction in Capillary Porous Bodies. In Ahsan A. (ed), Convection and conduction heat transfer. InTech Publishing House, Rieka: 149-176.
4. Deliiski, N., 2013: Modeling of the Energy Needed for Heating of Capillary Porous Bodies in Frozen and Non-frozen States. Scholars' Press, Saarbrücken, Germany, 116 p., http://www.scholars-press.com//system/covergenerator/build/1060.
5. Deliiski, N., Dzurenda, L., 2010: Modelling of the Thermal Processes in the Technologies for Wood Thermal Treatment. TU Zvolen, Slovakia (in Russian).
6. Deliiski, N., Angelski, D., Trichkov, N., 2014a: Modeling of the One Sided Heating Process of Wood Details before Bending in the Production of Stringed Music Instruments. Engineering sciences, Bulgarian Academy of Sciences, № 4: 5-15.
7. Deliiski, N., Trichkov, N., Angelski, D., Dzurenda L., 2014b: Modelling of the Energy Consumption for One Sided Heating of Wood Details Before their Bending in the Production of Stringed Music Instruments. Wood, Design & Technology, Skopje, Volume 3, No. 1: 97-105, http//www. fdme.ukim.mk/en/wood_journal/index.html.
8. Deliiski, N., Trichkov, N., Angelski, D., Dzurenda, L., 2016: Modelling and energy consumption of the unilateral heating process of flat wood details. Drvna Industrja, 66 (4): 381-391.
9. Gaff, M., Prokein, L., 2011: The Influence of Selected Factors on Coefficient of Wood Bendability. Annals of Warsaw University of Life Sciences, Forestry and Wood Technology, № 74: 78-81.

10. Kavalov, A., Angelski, D., 2014: Technology of Furniture. University of Forestry, Sofia, 390 p. (in Bulgarian).
11. Hadjiski, M., Deliiski, N., 2016: Advanced control of the Wood Thermal Treatment Processing. Cybernetics and Information Technologies, Bulgarian Academy of Sciences, 16 (2): 179–197.
12. Taylor, Z., 2001: Wood Bender's Handbook. Sterling Publ. Co., Inc., New York.
13. Trebula, P., Klement. I., 2002: Drying and Hydro-thermal Treatment of Wood. Technical University in Zvolen, Slovakia (in Slovak).
14. Videlov, H., 2003: Drying and Thermal Treatment of Wood. University of Forestry, Sofia (in Bulgarian).

ACKNOWLEDGEMENTS

WOOD COLOUR OF RING-POROUS BROAD-LEAVED TREE SPECIES RESULTING FROM THE PROCESS OF THERMAL TREATMENT WITH SATURATED WATER STEAM

Ladislav Dzurenda – Adrián Banski

Abstract

Changes in wood colour of woodturning blanks with dimensions of 32 x 55 x 600 mm of ring-porous broad-leaved tree species: European ash, black locust, sessile oak resulting from the thermal treatment with saturated water steam with the temperature of t = 137.5 ± 2.5°C for the time τ = 7.5 hours are presented in the paper. Natural wood colour of individual wood species as well as the hues resulting from the thermal treatment are in the CIE-L*a*b*colour space defined by the coordinate of lightness L* and the chromaticity coordinates a*, b*. The wood of ring-porous broad-leaved tree species darkens in the process of thermal treatment and due to changes in chromaticity coordinates of red and yellow colours it achieves brown hue. Mentioned changes in colour of thermally modified woodturning blanks by given mode are irreversible. Change in wood colour is uniform across the full extent and thus, the possibility for its use in the field of construction and carpentry, design as well as in the field of art is widened.

Key words: *wood, saturated water steam wood colour, thermal treatment*

INTRODUCTION

Timber placed in the environment of hot water, saturated water steam or saturated humid air is getting warmer and its physical, mechanical and chemical properties changes. Mentioned facts are used in the technology of steam bending and boiling during veneer and plywood, bent furniture or pressed wood manufacturing processes. *Kollmann – Gote (1968), Sergovsky – Rasev (1987), Trebula (1996), Dzurenda – Deliiski (2010).*

Thermal treatment processes of wood with saturated water steam, in addition to specific physico-mechanical changes of wood, are accompanied by chemical reactions such as partial hydrolysis and extraction leading to a colour change as well *Bučko (1995), Trebula – Bučko (1996), Dzurenda – Bučko (1998), Kačík (2001), Laurova – Mamonova – Kučerova (2004), Kačíková – Kačík (2011)*. In the past, colour modification, especially wood darkening, was used to remove undesirable differences in colour of lighter sapwood and darker heartwood, or to remove wood stains resulting from steaming or moulding. Recently, the research has been aimed at the colour change of specific wood species to more or less distinctive hues or imitation of the exotic wood species *Tolvaj – Nemet – Varga – Molnar (2009), Fan, Y.- Gao, J. - Chen, Y. (2010)*, *Dzurenda (2014,2018), Barcik – Gašparík –Razumov (2015), Baranski – Klement – Vilkovská – Konopka (2017).*

Technical University in Zvolen, T.G.Masaryka 24, 96053 Zvolen, SLOVAKIA
e-mail: dzurenda@tuzvo.sk, banski@tuzvo.sk

Using the coordinates of CIE-L*a*b*colour space is one of the ways to quantify the given optical wood property objectively. Lab colour space CIE-L*a*b* in accordance with ISO 7724 is based on the measurement of three parameters: lightness L* represents the brightest white at L* = 100 and the darkest black at L* = 0. The value of a chromaticity coordinate a* is a measure of the red-green character of the colour, with positive values (+a*) for red shades and negative values (-a*) for green. The value of a chromaticity coordinate b* gives the yellow-blue character with positive values (+b*) for yellow shades and negative (-b*) for blue.

The aim of the paper is to determine the hue of woodturning blanks with dimensions of 32 x 55 x 600 mm of ring-porous broad-leaved tree species: European ash, black locust, sessile oak in the CIE-L*a*b*colour space resulting from the mode of thermal treatment – colour modification of wood with saturated water steam with the temperature of t = 137.5 ± 2.5 °C for the time τ = 7.5 hours in the pressure autoclave APDZ 240.

MATERIAL AND METHODS

The mode of colour modification of woodturning blanks with saturated water steam in the pressure autoclave APDZ 240 for ring-porous broad-leaved tree species: European ash, black locust, sessile oak is illustrated in Fig.1.
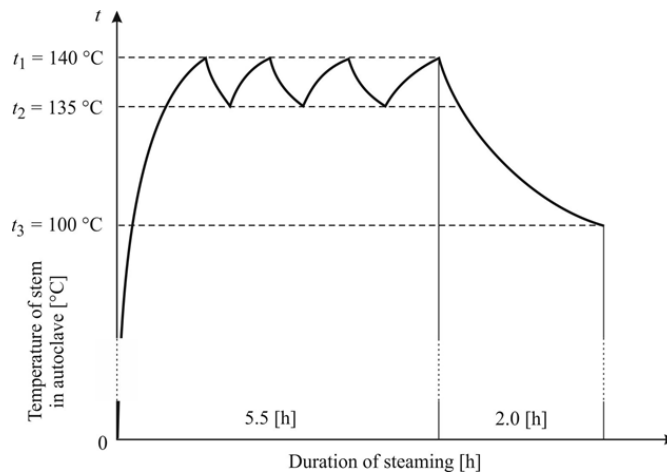
Fig.1. *Description of conditions for the process of thermal treatment of woodturning blanks of ring-porous broad-leaved tree species.*

The moisture content of woodturning blanks of the sapwood of European ash and of the heartwood of black locust, sessile oak was $W_p = 60.3 ± 3.8$ %. Some of the woodturning blanks were thermally modified in the above-mentioned mode with saturated water steam in the pressure autoclave APDZ 240 (Himmasch AD, Haskovo, Bulharsko) in the company Sundermann Ltd. Banská Štiavnica.

Thermally treated as well as untreated woodturning blanks were dried to report the moisture content of $Wp = 12 ± 0.5$% in a conventional wood drying kiln KAD 1x6 (KATRES Ltd.). Consequently, dried woodturning blank surfaces were processed using Swivel spindle milling machine FS 200.

Color Reader CR-10 (Konica Minolta, Japan) was used to assess the wood colour of woodturning blanks in the CIE-L*a*b*colour space. The light source D65 with lit area of 8mm was used.

Colour coordinates of thermally untreated woodturning blanks after drying and planing are introduced using a formula x = x ± s_x, it means using the average measured value and standard deviation.

Total colour difference ΔE is determined in accordance with the standard *ISO 11 664-4:2008* as the result of the difference in the colour coordinates of thermally untreated as well as treated woodturning blanks of individual tree species using the following formula (4):

$$\Delta E^* = \sqrt{\left(L_2^* - L_1^*\right)^2 + \left(a_2^* - a_1^*\right)^2 + \left(b_2^* - b_1^*\right)^2} \qquad (4)$$

where: L_1^*, a_1^*, b_1^* coordinate values in the CIE-L*a*b* colour space of the surface of dried, milled thermally untreated wood,
L_2^*, a_2^*, b_2^* coordinate values in the CIE-L*a*b* colour space of the surface of dried, milled thermally treated wood.

The rate of change in the wood colour and hues during the processes of thermal and hydrothermal treatment following the total colour difference ΔE* can be classified according to the chart mentioned by the authors: *Cividini et all (2007)* shown in Tab.1.

Tab. 1 *Classification of ΔE*

0.2 < ΔE*	Not visible difference
0.2 < ΔE* < 2	Small difference
2 < ΔE* < 3	Colour difference visible with low quality screen
3 < ΔE* < 6	Colour difference visible with medium quality screen
6 < ΔE* < 12	High colour difference
ΔE* > 12	Different colours

RESULTS AND DISCUSSION

Colour of the sapwood of European ash is, according to the authors: *Perelygin (1965), Makoviny (2010), Klement – Réh – Detvaj (2010)* white with light-yellow hue. The colour of sessile oak heartwood is light brown-yellowish in comparison to the wood colour of black locust heartwood that is light yellow-green and brown. According to the authors: *Babiak – Kubovský – Mamoňová (2004)* the colour of European ash wood is described with the coordinate values in the CIE-L*a*b*colour space: L* = 81.80; a* = 4.18; b* = 18.45, the coordinates of the colour of sessile oak are L* = 69.9; a* = 6.5; b* = 20.6. The colour of black locust wood is described by the coordinate values: L^* = 71.8; a^* = 5.3; b^* = 25.0. The results of our measurements are similar to the mentioned values and are shown in Tab. 1

Natural colour of the surface of dried, planed native – thermally untreated ash, oak and acacia wood and the hues of mentioned tree species after thermal treatment with saturated water steam are illustrated in Fig. 2.

Light white-yellowish colour of European ash sapwood was changed to brown with the darker hue of latewood of growth ring on tangential and radial section in the process of thermal treatment with saturated water steam – by the mode of colour modification.

Original light white-yellowish colour of heartwood of sessile oak became brown-grey in the process of thermal treatment accompanied with hydrolysis and extraction. Light yellow-green and brown colour of the heartwood of black locust changed to unique dark brown-grey hue in the process of thermal modification.

Sessile oak (Quercus robur L.)

European ash (Fraxinus excelsior L.)

Black locust (Robinia pseudoacacia L.)

Fig. 2 *The colour of the surface of dried and planed wood thermally untreated and treated with saturated water steam.*

Values of the colour coordinates in the CIE-L*a*b* colour space describing the wood colour resulting from the thermal treatment and drying of planed surface are mentioned in Tab. 2.

Tab. 2 *Values of colour coordinates in the CIE-L*a*b* colour space describing thermally untreated and treated wood with the saturated water steam*

Tree species	Woodturning blanks	Number of samples	Colour coordinates		
			L*	a*	b*
European ash	thermally untreated	178	84.6 ± 1.5	6.7± 0.6	19.8± 0.9
	thermally treated	180	65.6 ± 1.4	10.8 ± 0.5	21.7 ± 0.9
Sessile oak	thermally untreated	245	69.4 ± 2.5	8.8 ± 0.6	20.7 ± 0.8
	thermally treated	245	47.5 ± 2.1	5.9 ± 0.9	17.9 ± 1.2
Black locust	thermally untreated	183	69.2 ± 2.9	4.7 ± 0.8;	28.7 ± 2.4
	thermally treated	180	44.3 ± 1.6	8.9 ± 0.4	15.1 ± 0.9

The changes in coordinate values of ΔL^* and in chromaticity coordinates of Δa^* and Δb^*, the changes in red and yellow shades in the CIE-L*a*b*colour space of European ash, of sessile oak and black locust wood resulting from the processes of partial hydrolysis and extraction of water soluble accessory substances during the thermal treatment with saturated water steam are illustrated in Fig. 3.
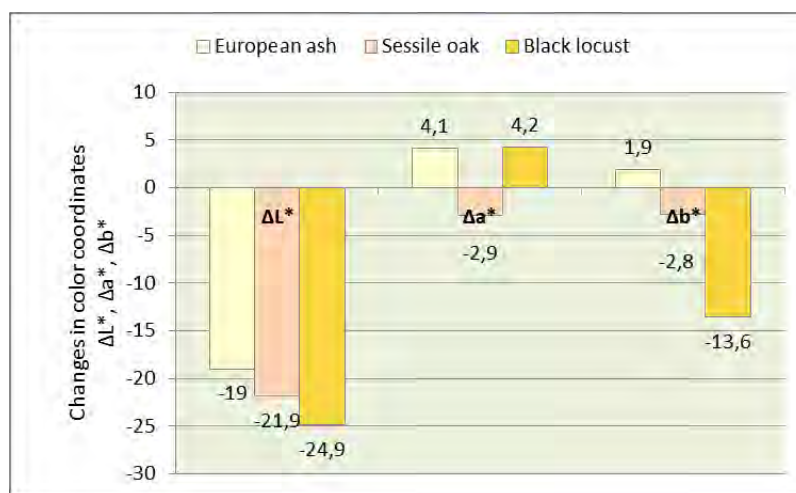
Fig.3 *The rate of change in the coordinate of lightness L* and chromaticity coordinates a* and b* in the CIE-L*a*b colour space of individual ring-porous broad-leaved tree species resulting from the process of thermal treatment with saturated water steam.*

Total colour differences ΔE^* of colour modified woodturning blanks of individual tree species achieved by the individual thermal treatment modes calculated using the formula (1) are shown in Fig. 4.
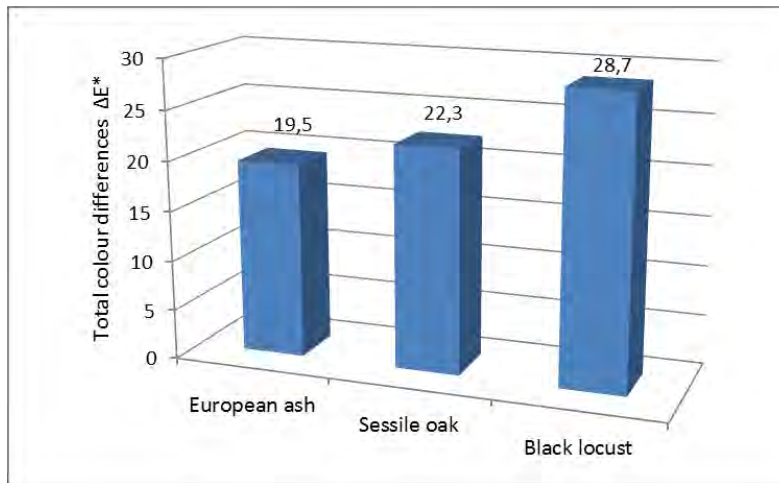
Fig.4. *Total colour differences of woodturning blanks of individual tree species resulting from the process of thermal treatment with saturated water steam*

Chromophore system of lignin-polysaccharide matrix of the heartwood of tree species: sessile oak and black locust contains, in comparison to the sapwood of European ash, more components with chromophore structure of tannin and dyestuff. Due to wide variety of ways to convert new chromophore structures in the processes of partial hydrolysis and extraction, the heartwood of sessile oak becomes darker and changes markedly to dark brown or dark brown-grey hue. On the other hand, more homogenous sapwood of European ash changes to less saturated hue of brown colour.

According to the authors: *Kollmann – Gote (1968), Trebula (1996),* colour changes in individual thermally modified tree species are, in accordance with the classification of changes in physical and mechanical properties of wood resulting from the process of thermal treatment, irreversible (permanent).

Since the total colour difference ΔE^* of thermally treated woodturning blanks of European ash, sessile oak and black locust is higher than $\Delta E^* = 12$, the colour change can be defined as significant resulting in different colour according to the classification of colours in Tab. 2 *Cividini et all (2007).*

The fact that achieved colour is uniform across the full extent of wood can be considered another positive feature of the mode of thermal treatment with saturated water steam with the temperature of $t = 137.5 \pm 2.5$ °C for the time $\tau = 7.5$ hours in the pressure autoclave APDZ 240. Following the finding, the thermally modified woodturning blanks can be used to produce lamellas for flooring, or 3D machining of solid wood without any change in wood colour between the surface and the centre of woodturning blank.

New hues of European ash, sessile oak and black locust woodturning blanks resulting from the process of thermal treatment with saturated water steam widen the possibility for the use of mentioned tree species of in the field of construction and carpentry, design as well as in the field of art.

CONCLUSION

The colours of European ash, sessile oak and black locust woodturning blanks resulting from the process of thermal treatment with saturated water steam with the

temperature of t = 137.5 ± 2.5 °C for the time τ = 7.5 hours are presented in the paper. Original light white-yellowish colour of the sapwood of European ash was changed to brown hue with the coordinates: $L^* = 65.6 \pm 1.4$; $a^* = 10.8 \pm 0.5$; $b^* = 21.7 \pm 0.9$. Light brown-yellowish colour of the heartwood of sessile oak became brown-grey with the coordinates in the CIE-L*a*b* colour space: $L^* = 47.5 \pm 2.1$; $a^* = 5.9 \pm 0.9$; $b^* = 17.9 \pm 1.2$ during the process of hydrolysis and extraction. The most significant change resulting from the mentioned mode of thermal treatment with saturated water steam occurred in black locust wood. Light yellow-green and brown colour changes to unique dark brown-grey hue with the coordinates in the CIE-$L^*a^*b^*$ colour space: $L^* = 44.3 \pm 1.6$; $a^* = 8.9 \pm 0.4$; $b^* = 15.1 \pm 1.6$.

New colours and hues of European ash, sessile oak and black locust woodturning blanks resulting from the process of thermal treatment with saturated water steam widen the possibility for the use of ring-porous tree species use in the field of construction and carpentry, design as well as in the field of art.

REFERENCES

1.   BABIAK, M., KUBOVSKÝ, I., MAMOŇOVÁ, M. 2004: Farebný priestor vybraných domácich drevín. [Color space of selected local woods] In: Interaction of wood with various Forms of Energy. Zvolen: TU Zvolen, pp. 113 – 117, ISBN 80-228-1429-6.
2.   BARAŃSKI, J., KLEMENT, I., VILKOVSKÁ, T., KONOPKA, A. 2017: High Temperature Drying Process of Beech Wood (Fagus sylvatica L.) with Different Zones of Sapwood and Red False Heartwood. In: BioResources 12(1), 1861-1870. DOI:10.15376/biores.12.1.1761-1870.
3.   BARCIK, Š., GAŠPARÍK, M., RAZUMOV, E.Y. 2015: Effect of thermal modification on the colour changes of oak wood. In: Wood Research. 60 (3):385-396, ISSN 002-6136.
4.   BUČKO, J. 1995: Hydrolýzne procesy. Zvolen:Vydavateľstvo TU Zvolen, 1995. 116 p.
5.   CIVIDINI, R., TRAVAN, L., ALLEGRETTI, O.2007: White beech: A tricky problem in drying process. In: International Scientific Conference on Hardwood processing. Quebec City, Canada.
6.   DZURENDA, L., BUČKO, J. 1998: Príčiny poklesu vlhkosti dreva mokrých bukových podvalov v prpocese parenia nasýtenou vodnou parou. [Reasons of decrease of the moisture content of wood of green beech sleepers during the steaming process with saturated water steam] In: Acta facultatis xylollogiae 40 (1): 67-75.
7.   DZURENDA, L., DELIISKI, N. 2010: Tepelné procesy v technológiách spracovania dreva. Zvolen: Vydavateľstvo TU Zvolen, 273 s.
8.   DZURENDA, L. 2014: Sfarbenie bukového dreva v procese termickej úpravy sýtou vodnou parou. In: Acta facultatis xylologiae Zvolen, 56 (1):13 – 22, ISSN 1366-3824.
9.   DZURENDA, L. 2018: The Shades of Color of *Quercus robur* L. Wood Obtained through the Processes of Thermal Treatment with Saturated Water Vapor. In: BioResouces 13(1), 1525 - 1533; doi: 10.1063/biores 13.1.1525-1533
10. FAN, Y., GAO, J., CHEN, Y. 2010. Colour responses of black locust (*Robinia pseudoacacia* L.) to solvent extraction and heat treatment. In Wood Sci Technol, 2010, 44:667–678. doi: 10.1007/s00226-009-0289-7.
11. KAČÍK, F. 2001: Tvorba a chemické zloženie hydrolyzátov v systéme drevo-voda-teplo. Zvolen: Vydavateľstvo TU Zvolen, 75 s.
12. KAČÍKOVÁ, D., KAČÍK, F. 2011: Chemické a mechanické zmeny dreva pri termickej úprave. Zvolen: Vydavateľstvo TU Zvolen, 71 s.

13. KLEMENT, I., RÉH, R., DETVAJ, J. 2010: Základné charakteristiky lesných drevín – spracovanie drevnej suroviny v odvetví spracovania dreva. Zvolen: NLC, 82 s.

14. KOLLMANN, F., COTE, W. A. 1968: Principles of Wood Sciences and Technology, Vol. 1. Solid Wood, Springer Verlag: Berlin – Heidelberg - New York, 592 s.

15. LAUROVA, M., MAMONOVA, M., KUČEROVA, V. 2004: Proces parciálnej hydrolýzy bukového dreva (Fagus sylvatica L.) parením a varením. [Vedecké štúdie 2/2004/A], Zvolen: TU Zvolen. 58 s.

16. MAKOVÍNY, I. 2010: Úžitkové vlastnosti a použitie rôznych druhov dreva. Zvolen: Technická univerzita Zvolen, 84 s.

17. PERELYGIN, L., M. 1965: Náuka o dreve. Bratislava: SVTL, 444 s.

18. SERGOVSKIJ, P. S., RASEV, A. I. 1987: Gidrotermičeskaja obrabotka i konservirovanije drevesiny. Lesnaja promyšlennost, Moskva, 360 s.

19. TOLVAJ, L., NEMETH, R., VARGA, D., MOLNAR, S., 2009: Colour homogenisation of beech wood by steam treatment. In: Drewno. 52 (181): 5-17, ISSN 1644-3985.

20. TREBULA, P., BUČKO, J. 1996: Vákuové sušenie dreva, technické, technolo-gické a ekologické aspekty. [Vedecké štúdie 5/1996/B], Zvolen: Vydavateľstvo TU Zvolen, 2001, 70 s.

21. TREBULA, P. 1996: Sušenie a hydrotermická úprava dreva. Zvolen: Vydavateľstvo TU Zvolen, 2001, 255 s.

ACKNOWLEDGEMENT

CHEMICAL CHANGES OF SELECTED HARDWOOD SPECIES IN THE PROCESS OF THERMAL MODIFICATION BY SATURATED WATER STEAM

Jarmila Geffertová – Anton Geffert – Eva Výbohová

Abstract

This paper deals with the determining and comparison of chemical changes that occur from the hydrothermal treatment of oak (Quercus robur L.) and maple (Acer platanoides L.) wood through various steaming modes. The greatest changes from monitored chemical characteristics were occurred in the content of extractives and hemicelluloses. In the most extreme steaming treatment in mode III (t_{max} 140 °C, total duration 7.5 h), the decrease in hemicellulose content was the most dramatic. The content of extractives first slightly decreased, but with increasing temperature and extended steaming period a considerable increase in their content was observed. This changes result from degradation of most labile hemicelluloses. The contents of cellulose and lignin show only minimal changes, and their slight increase and decrease in individual modes is the result of several concurrent effects. In addition to these changes the decrease in the crystallinity of cellulose due to steaming was observed.

Key words: *oak, maple, steaming, extractives, hemicellulose, FTIR spectroscopy.*

INTRODUCTION

Hydrothermal treatment of wood by steaming is a common industrial processing of wood (production of veneer, plywood, bentwood furniture and other wood processing), which is used to improving its properties. The wood after hydrothermal treatment is less sticky, less cracks, drying faster, having a more pleasant and uniform color, increased durability and strength, and better stability (Melcer *et al.* 1983, Nikolov *et al.* 1980, Sergovskij and Rasev 1987, Setnička 1989, Trebula and Klement 2005).

Steaming causes changes in structural, physical, chemical and mechanical properties of wood. The extent of these changes depends on the hydrothermal treatment conditions (temperature, pressure, duration of action and other). In general, hydrothermal action on wood under mild conditions (shorter time, temperature below 80 °C) causes only minor changes in its main components. Deeper chemical changes occur with longer treatment times and temperatures above 80 °C, while mechanical strength of wood decreases (Kačík *et al.*1989, Kačík 1997, Melcer *et al.* 1983, 1989, Solár and Melcer 1990, 1992).

Hemicelluloses are the most thermally labile of the wood polymeric components (Hill 2006). Degradation of especially non-cellulosic polysaccharides leads to the loss of holocellulose in hydrothermally treated wood (Kačík *et al.* 1990, Kačík 2001).

Technical University in Zvolen, T. G. Masaryka 24, 960 53 Zvolen
e-mail: geffertova@tuzvo.sk

Hardwoods have a higher proportion of hemicelluloses, and the hemicelluloses of hardwoods have a higher content of acetyl groups compared to softwoods. Additionally, hardwood hemicelluloses are richer in pentosans, which are more susceptible to degradation than hexosans. Therefore, hardwoods are less thermally stable than softwoods (Hill 2006).

In lignocellulosic materials, the main components form the so-called "lignin-saccharide complex". Cellulose microfibrils are covered with a heterogeneous hemicellulose polymer which is wrapped by amorphous lignin polymer (Volynets *et al*. 2017). According to Chen *et al.* (2010) during the initial phase of hydrothermal treatment lignin-free xylan is released, while lignin-bound xylan is dissolved in the later phase.

Several authors report that not only the carbohydrate but also the aromatic part of the wood (lignin) undergoes changes during the hydrothermal treatment. The depth of these changes depends primarily on the temperature and the time of action, as well as on the species of treated wood (Solár and Melcer 1992, Kačík *et al.* 1989, Kačík *et al*. 1990). The hydrothermal treatment causes also the formation of new chromophore structures in the lignin, which causes a change in the color of the treated material (Solár 1997).

The aim of this work was to determine and compare chemical changes occurring in the oak (*Quercus robur* L.) and maple (*Acer platanoides* L.) wood as a result of its modification in the different modes of steam.

MATERIAL AND METHODS

The samples of oak (*Quercus robur* L.) and maple (*Acer platanoides* L.) wood supplied from an industrial plant Sundermann Ltd. (Banská Štiavnica, Slovakia) were used to investigate chemical changes that occurred in different steaming treatments.

The samples with the dimensions 30 x 75 x 510 mm were thermally treated by the saturated steam in a pressure autoclave APDZ 240 (Dzurenda 2018). The temperature of the steam and duration of the processes are shown in Table 1.

The fraction of sawdust from 0.5 mm to 1.0 mm from completely disintegrated boards of the original wood and wood after steaming (including surface and center part) were used to monitor the chemical changes.

Table 1. Thermal treatment of wood

Steaming mode	Temperature of saturated water steam (°C)			Duration (h)	
	$t_{min\ (\tau 1)}$	$t_{max\ (\tau 1)}$	$t_{end\ (\tau 2)}$	$\tau_{1\ (steaming)}$	$\tau_{2\ (cooling)}$
I	110	115	100	4.5	1.0
II	125	130	100	5.0	1.5
III	135	140	100	5.5	2.0

Selected chemical characteristics were measured in the samples before steam treatment and after the various modes of steaming:

Ethanol-toluene solubility	ASTM D 1107-96
Polysaccharide fraction	Chlorite isolation method of Wise (Kačík and Solár 2000)
Cellulose	Kürschner-Hoffer method (Kačík and Solár 2000)
Lignin	ASTM D 1106-96

The isolated holocellulose and dioxane lignin were analyzed using ATR-FTIR spectroscopy. The measurements were carried out using a Nicolet iS10 FTIR spectrometer equipped with a Smart iTR attenuated total reflectance (ATR) sampling accessory with a diamond crystal (Thermo Fisher Scientific, Madison, WI). The resolution was set at 4 cm^{-1} for 32 scans for each steaming technique and following analysis. The wavenumber range varied from 4000 cm^{-1} to 650 cm^{-1}. Six analyses were performed per sample. OMNIC 8.0 software (Thermo Fisher Scientific, Madison, WI) was used to evaluate the spectra.

RESULTS AND DISCUSSION

The steaming conditions of maple and oak wood have influenced not only the required color change of wood (Dzurenda 2018) but also its chemical composition (Výbohová *et al.* 2018, Geffert *et al.* 2018).

When comparing the content of extractives in the original maple and oak wood (Fig. 1), it can be seen that the original oak wood contained 2.4 times more of these substances than wood of maple. After steaming in mode I there was a decrease in the content of extractives while maintaining a ratio of 2.4. By increasing the severity of the steaming conditions, the difference in the content of extractives (after steaming in mode III) in oak and maple wood increased to 4.2.

While the content of extractives under the most demanding conditions of steaming (mode III) with respect to the original wood was higher by 33% for maple wood, the increase for oak wood was 132%.
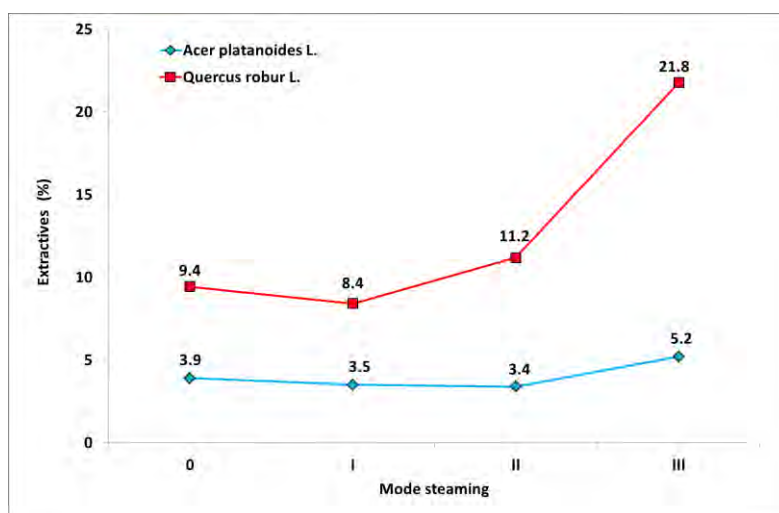
Fig. 1 Content of extractives before (0) and after steaming

With regard to the values of lignin and cellulose content by individual mode of steaming (Tab. 2) (Výbohová *et al.* 2018, Geffert *et al.* 2018), it can be stated that the increase in the content of extractives is related to the degradation of hemicelluloses and amorphous cellulose. The degradation products affected the increase in the content of extractives and thus the more intense coloring of wood samples (Fig. 2).

Table 2 Chemical characteristics

Mode		0	I	II	III
Lignin (%)	*Acer platanoides* L.	23.2	22.3	23.4	23.1
	Quercus robur L.	22.8	21.0	22.9	23.5
Cellulose (%)	*Acer platanoides* L.	45.1	46.3	45.0	45.2
	Quercus robur L.	39.1	40.0	36.7	36.9

Dzurenda (2018) in his work featured on samples oak in individual steaming modes total color differences ΔE * 3.0, 11.5 and 20.1, indicating the smallest color change in steaming mode I, a larger color shift in mode II and the largest shift in color space after mode III.

Fig. 2 Disintegrated samples of the original and steamed woods

The content of hemicelluloses in steamed wood species point to their different contents in maple and oak wood and also to the different degrading intensity (Fig. 3). The course of the change is similar.
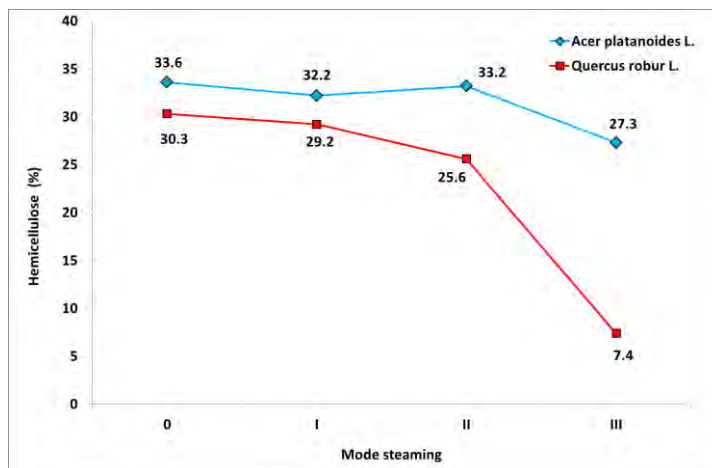
Fig. 3 Hemicellulose content before (0) and after steaming

Both wood species show the greatest decrease in hemicelluloses in mode III. While in maple wood this difference was 6.4% and represented 19% of the original wood, in oak wood the difference was 22.9%, which represented a decrease of up to 75.6%.

For both wood species, a similar course of lignin and polysaccharides ratio were also recorded (Fig. 4). Smaller changes were made again for maple wood. After steaming in mode I, the ratio decreased slightly, which may be related to the drop in content of water-soluble lignin. After two other modes, an increase of this ratio was recorded in both wood species. Although the synergistic effect of a small change of lignin and cellulose in individual steaming modes (Tab. 1) was evident, it can be clearly stated that the values of the ratio were mainly affected by the degradation of hemicelluloses.
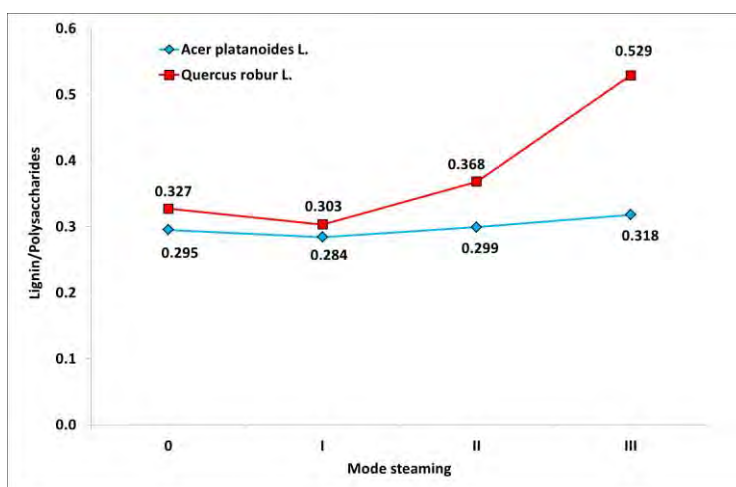
Fig. 4 Changes of lignin/polysaccharides ratio

During hydrothermal treatment of wood, various processes with different influence on the intensity of FTIR absorption bands run. On the basis of differential FTIR spectra of oak and maple wood (Fig. 5), it can be concluded, that under the most severe steaming conditions (mode III) the similar changes occurred in both examined wood species.
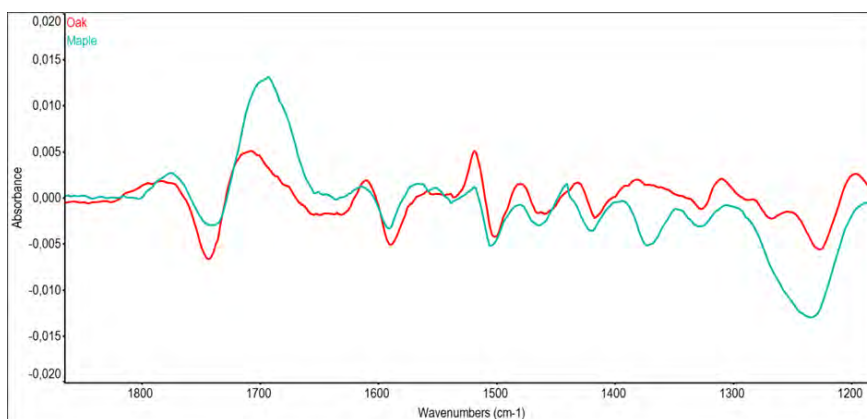
Fig. 5 Differential FTIR spectra of oak and maple wood in mode III

The decrease of intensity of absorption band at wavenumber around 1732 cm^{-1} may be caused by lignin condensation reactions, deacetylation of hemicelluloses and decomposition of aldehydes, carboxylic acids and their esters (Esteves *et al.* 2013, Özgenc *et al.* 2017, Windeissen *et al.* 2009). In the case of characteristic bands of lignin (around 1593 and 1505 cm^{-1}), the shift of peak maxima to higher wavenumber and the increase of their intensity were observed. In both cases also the intensity of absorption band between 1200 and 1300 cm^{-1} decreased. In this region absorption bands assigned to xylan and syringyl ring and C–O stretch in lignin overlapping. Considering the results of chemical analyses it can be concluded, that this decrease can be the consequence of degradation of hemicelluloses and structural changes in lignin macromolecule.

The degree of crystallinity is one of the factors, which influenced the thermal stability of cellulose (Hill 2006, Poletto *et al.* 2012). More ordered crystalline regions of cellulose exhibit low chemical reactivity, and higher thermal stability in comparison to its non-crystalline regions. In the initial stage of thermal treatment, the degradation of amorphous cellulose, and rearrangement or reorientation of quasi-crystalline regions occurred. This results in increase in cellulose crystallinity. Degradation of crystalline regions runs at increased intensity of the treatment (Bhuiyan *et al.* 2001, Kong *et al.* 2017).
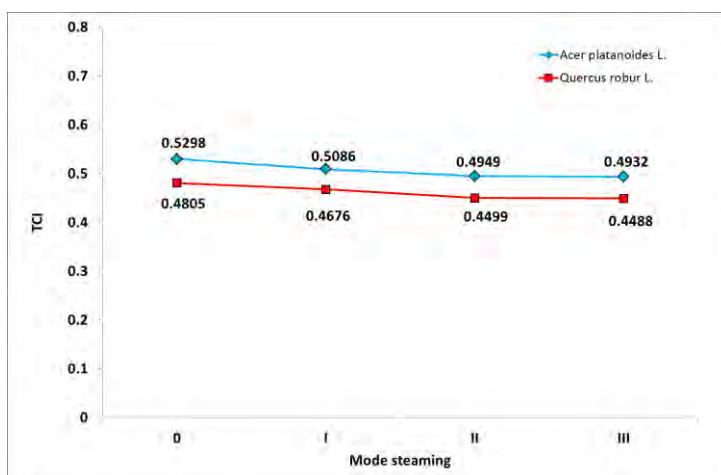
Fig. 6 Changes of the Total Crystallinity Index (TCI)

As the Figure 6 shows, the Total Crystallinity Index decreases with increased treatment severity in the case of both examined wood species. Our findings are in agreement with cited works. In our experiment, steaming times for all modes are longer, namely 5.5, 6.5, and 7.5 h. Under these conditions the degradation of microfibrillar and chain scission reactions is occurred. This reaction increased the amorphous character of cellulose, and subsequently reduced the total amount of cellulose crystalline regions.

CONCLUSION

The wood species characterized not only the content of the selected chemical characteristics but also the size of their changes during the steaming. The original maple wood contained a large amount of lignin, cellulose, hemicelluloses and a smaller proportion of extractives than oak wood.

Treatment in modes with different temperature and time of steaming resulted in minor changes monitored chemical characteristics in maple wood as the oak wood.

The largest change was determined in mode III (at the highest temperature and time of steaming) for both woods. The observed changes in the selected characteristics (a decrease in hemicellulose content and an increase in the content of extractives) were much more pronounced in oak wood than in maple wood.

The changes in the intensity of the FTIR absorption bands are the result of degradation of hemicelluloses and structural changes in lignin macromolecules and it is confirmed by the results of chemical analyses too. Degradation of crystalline regions runs at increased intensity of treatment.

ACKNOWLEDGMENTS

REFERENCES

ASTM Standard D 1106-96: 1998. Standard Test Method for Acid Insoluble Lignin in Wood.

ASTM Standard D 1107-96, Re-approved: 2001. Standard Test Method for Ethanol-Toluene Solubility of Wood.

Bhuiyan, T. R., Hirai, N., Sobue, N. 2000. Changes of crystallinity in wood cellulose by heat treatment under dried and moist conditions. In Journal of Wood Science, 2000, 46(6): 431-436. DOI: 10.1007/BF00765800.

Chen, X., Lawoko, M., Heiningen, A. 2010. Kinetics and mechanism of autohydrolysis of hardwoods. In Bioresource Technology, 2010, 101(20): 7812-7819. DOI: 10.1016/j.biortech.2010.05.006.

Dzurenda, L. 2018. The Shades of Color of *Quercus robur* L. Wood Obtained through the Processes of Thermal Treatment with saturated Water Vapor. In BioResources, 2018, 13(1): 1525-1533.

Esteves, B., Velez Marques, A., Domingos, I. Pereira, H. 2013. Chemical changes of heat treated pine and eucalypt wood monitored by FTIR. In Maderas, Cienc. Tecnol., 2013, 15(2): 245-258.

Geffertová, J., Geffert, A., Výbohová, E. 2018. The effect of UV irradiation on the colour change of the spruce wood. In Acta Facultatis Xylologiae, 2018, 60(1): 41-50. DOI: 10.17423/afx.2018.60.1.05.

Hill, C. A. S. 2006. Wood Modification: Chemical, Thermal, and Other Processes. Chichester : John Wiley & Sons, 2006. 260 pp. ISBN 978-0-470-02172-9.

Kačík, F. 1997. Vplyv teploty a vlhkosti na zmeny sacharidov [The influence of temperature and humidity on carbohydrate changes]. Zvolen : Technical University in Zvolen, 1997. 68 pp. ISBN 80-228-0608-0.

Kačík, F. 2001. Tvorba a chemické zloženie hydrolyzátov v systéme drevo – voda – teplo [Creation and chemical composition of hydrolysates in the wood - water - heat system]. Zvolen : Technical University in Zvolen, 2001. 75 pp. ISBN 80-228-1098-3.

Kačík, F., Solár, R. 2000. Analytická chémia dreva [Analytical Chemistry of Wood]. Zvolen : Technical University in Zvolen, 2000. 369 pp. ISBN 80-228-0882-0.

Kačík, F., Solár, R., Melcer, I. 1989. Štúdium hydrolyzátu po hydrotermickej úprave bukového dreva (*Fagus silvatica* L.), I. časť [Study of hydrolysate after hydrothermal treatment of beech

wood (Fagus silvatica L.), Part I]. In Zborník vedeckých prác Drevárskej fakulty [Proceedings of the Scientific Works of the Faculty of Wood Sciences and Technology], Zvolen : Technical University in Zvolen, 1989, pp. 35-45.

Kačík, F., Solár, R., Melcer, I. 1990. Štúdium hydrolyzátu po hydrotermickej úprave bukového dreva (*Fagus silvatica* L.), II. časť [Study of hydrolysate after hydrothermal treatment of beech wood (*Fagus silvatica* L.), Part II]. In Zborník vedeckých prác Drevárskej fakulty [Proceedings of the Scientific Works of the Faculty of Wood Sciences and Technology], Zvolen : Technical University in Zvolen, 1990, pp. 45-56.

Kong, L., Zhao, Z., He, Z., Yi, S. 2017. Effects of steaming treatment on crystallinity and glass transition temperature of Eucalyptuses grandis ˣ E. urophylla. In Results in Physics, 2017, 7: 914-919. DOI: 10.1016/j.rinp.2017.02.017.

Melcer, I., Melcerová, A., Solár, R., Gajdoš, E. 1983. Porovnávacia charakteristika zmien jaseňového dreva (*Fraxinus exc.* L.) po jeho hydrotermickej úprave varením a parením [Comparative characterization of changes in ash common wood (*Fraxinus exc.* L.) after its hydrothermal treatment by cooking and steaming]. In Wood Research, 1983, 28(1): 37-56.

Melcer, I., Melcerová, A., Solár, R., Kačík, F. 1989. Chemizmus hydrotermickej úpravy listnatých drevín [Chemistry of hydrothermal treatment of hardwood species]. Zvolen : University of Forestry and Wood Technology in Zvolen, 2/1989, 76 pp.

Nikolov, S., Rajčev, A., Deliiski, N. 1980. Proparvane na drevesinata [Wood steaming]. Zemizdat : Sofia, 1980. 223 pp.

Özgenc, Ö., Durmaz, S., Boyaci, I. H., Eksi-Kocak, H. 2017. Determination of chemical changes in heat-treated wood using ATR-FTIR and FT Raman spectroscopy. In Spectro-chimica Acta Part A: Molecular and Biomolecular Spectroscopy, 2017, 171: 395-400.

Poletto, M., Zattera, A. J., Forte, M. M., Santana, R. M. 2012. Thermal decomposition of wood: influence of wood components and cellulose crystallite size. In Bioresour Technol, 2012, 109(1): 148-53.

Sergovskij, P. S., Rasev, A. I., 1987: Gidrotermičeskaja obrabotka i konservirovanije drevesiny [Hydrothermal Treatment and Wood Preservation]. Lesnaja promyšlennost : Moskva,1987. 360 pp.

Setnička, F. 1989. Paření dřeva jako termodynamický proces [Wood steaming as a thermodynamic process]. In Drevo, 1989, 44(8): 223-227.

Solár, R. 1997. Zmeny lignínu v procesoch hydrotermickej úpravy dreva [Changes in lignin in hydrothermal wood treatment processes]. Zvolen : Technical University in Zvolen, 1997. 57 pp. ISBN 80-228-0599-8.

Solár, R., Melcer, I. 1990. Chemical changes of the polysaccharidic part of hydrothermally treated oak wood their reflection in its mechanical properties. In Zborník vedeckých prác Drevárskej fakulty (Proceedings of the scientific works of the Faculty of Wood Sciences and Technology], Zvolen : Technical University in Zvolen, 1990, pp. 15-26.

Solár, R., Melcer, I. 1992. Structural land chemical alterations of lignin in the proces of oak wood hydrothermal treatment. In Wood Research, 1992, 12(3): 11-23.

Trebula, P., Klement, I. 2005. Sušenie a hydrotermická úprava dreva [Drying and hydrothermal treatment of wood]. Zvolen : Technical University in Zvolen, 2005. 449 pp. ISBN 80-228-1421-0.

Volynets, B., Ein-Mozaffari, F., Dahman, Y. 2017. Biomass processing into ethanol: Pretreatment, enzymatic hydrolysis, fermentation, rheology, and mixing. In Green Processing and Synthesis, 2017, 6(1): 1-22. DOI: 10.1515/gps-2016-0017.

Výbohová, E., Geffert, A., Geffertová, J. 2018. Impact of Steaming on the Chemical Composition of Maple Wood. In Bioresources, 2018, 13(3): 5862-5874.

Windeisen, E., Bächle, H., Zimmer, B., Wegener, G. 2009. Relations between chemical changes and mechanical properties of thermally treated wood. In Holzforschung, 2009, 63: 773-778.

THE COMPARISON OF WOOD PELLETS PROPERTIES DEPENDING ON THEIR PRODUCTION PROCESS

Michal Holubčík – Nikola Kantová – Jozef Jandačka

Abstract

Pellets from biomass are more and more used. As input material can be used various types of biomass, like wood, straw, grass or different organic materials. A lot of people want to produce pellets from biomass in domestic condition. But qualities of these pellets don´t achieve quality of pellets made in manufacture. Process of production wood pellets is difficult and this process has an impact on the final properties of pellets. The article deals with the comparison of the energy and mechanical properties of experimental pellets that have been made under different conditions. Sample A was produced in domestic conditions and sample B was made in factory production. At the end of the work are displayed the results of moisture, volatiles, fixed carbon content, ash content, elemental analysis, gross calorific value, calorific value and mechanical properties.

Key words: *wood pellets, production, properties, process*

INTRODUCTION

The development of renewable energy constitutes a crucial role for the future. Dendromass and phytomass play important role in reducing fossil fuel consumption. Wood pellets and plant pellets are a form of biomass (Ďurčanský et al. 2016). Pellets are usually produced from a variety of residue feedstocks, for example: straw, sawdust, wood (agricultural and forest biomass). They are easy to store and transport (Dzurenda and Pňakovič, 2016). They are cylinders with a diameter of 6-10 mm and a length of 10-50 mm manufactured from raw wood (chips, sawdust). They are made by compression process, called pelletizing. They don't usually contain chemical additives (Nosek and Holubčík, 2016). The important parameter for fuel properties is abrasion resistance. Pellets of low abrasion resistance have low quality, because high quantities of fines are produced in the storage system. It can cause operational failures. In turn, minimal amounts of fines in the storage system indicate on a high quality of pellets (Nosek et al. 2016). In addition, water has a crucial role in the pelletizing process. Pellets, which contain the low amount of water, generally have good quality and appropriate fuel properties (Rimár et al. 2016).

Pellets from biomass are usually made in factories with pelletizing line which can produce more than 2 tons pellets per hour. These manufactories have usually perfect working automatic technology and it can work with no failures (Čarnogurská et al. 2015, Ondro et al. 2018). Pellets made by this way of production have stable quality and meet the standards and certifications. For good parameters of produced pellets is necessary also good quality of inlet raw material (Lazár et al. 2015). This all need to be paid and it is showed in

University of Zilina, Faculty of Mechanical Engineering, Univerzitna 1, 010 26 Zilina, Slovakia
e-mail: michal.holubcik@fstroj.uniza.sk

price of these pellets. People, who want to save some costs for pellets from biomass, procure domestic device for pelletizing. Main part of domestic pelletizing device is, like in pellets factories, pellet mill. It is a type of mill or machine press used to create pellets from powdered material. Pellet mills are unlike grinding mills, in that they combine small materials into a larger, homogeneous mass, rather than break large materials into smaller pieces. Biomass mass is fed to a press where it is squeezed through a die having holes of the size required (normally 6 mm diameter, sometimes 8 mm or larger). The high pressure of the press causes the temperature of the wood to increase greatly, and the lignin plasticizes slightly forming a natural "glue" that holds the pellet together as it cools (Geffertová and Geffert 2016). Pellets made in domestic pellet mills have not so quality like pellets made in large pellets factories because used pressures are much lower.

The aim of this work is comparing of different energy and mechanical properties of pellets made from the same clean spruce sawdust in domestic condition and pellets made from biomass in large scale manufactory.

PRODUCTION OF WOOD PELLETS SAMPLES

Samples of wood pellets were produced in two ways:
- Sample A is from domestic production (fig. 1),
- Sample B is from factory production (fig. 2).

Fig. 1 Domestic device for pelletizing and sample A

Fig. 2 Factory device for pelletizing and sample B

Domestic production was similar to the production of wood pellets in domestic conditions, which is mostly used by smaller woodworking companies and carpenters, who have waste sawdust and shavings. A pellet press (fig. 1) with a theoretical production of 200 kg pellets per hour was used to produce the experimental samples, but under real conditions, only about 80-100 kg pellets per hour were obtained during experimental production. The sample A (Figure 1) was made from pure sawdust on this machine. Factory production of wood pellets was carried out at a specialized facility in an external laboratory (Figure 2, illustrative photo). The production line used has a production capacity of approximately 1 000 kg pellets per hour. Sample B (fig. 2) was formed on this machine from the same input material as for sample A. The input material came from spruce sawdust from a private sawmill located in northern Slovakia. The preparation of the base material consisted in adjusting the moisture to the required parameters. As the material delivered reached a moisture content of 8.11 %, in the case of a small domestic production of wood pellets, the sawdust needed to be dampened to about 15-17 %. In the case of the production of wood pellets on the production line, the humidity was controlled by the operator to approximately 12-15 % depending on the output quality of the wood pellets.

EXPERIMENT METHODOLOGY

These parameters of wood pellets were determined:
- Gross and calorific heating value - it was determined according to ISO 1716 by using of calorimeter LECO AC 500. A sample of wood pellet with weight about 1.0 g was burned in combustion vessel filled with oxygen to a pressure 31.0 bar. Combustion vessel was immersed in 2.0 dm3 of distilled water. During burning of sample was measured temperature increase of water. The calorific value was calculated from gross calorific value, moisture and hydrogen content.
- Amount of fines (F test) - fines hinder pellets from tumbling down to the in-feed auger, thus disturbing fuel feed to the boiler. Boilers are adjusted to burn pellets, but if fines arrive in the burning chamber, the flame may get too hot as fines particles burn faster than pellets. In the worst case the ash might sinter, which means that the burner must be cleaned after it has cooled down. The amount of fines should preferably be declared for each bulk delivery, and is measured at the final point in the factory production chain. Fines should preferably be less than 1% by weight. Amount of fines was measured in Lignotester (Fig. 3), where samples were placed in stream of air for 30 s with pressure of air 30 mbar. After this was weighted amount of fines under the sieve.
- Mechanical durability (DU test) - this is a measure of how well the pellets can stand handling. Every time pellets are handled, some of them break and all of them show some wear, which will increase the amount of fines. It was determined as quality parameter according to EN 15210 by using of special device – LignoTester (Fig. 3). There 100 g of pellets sample placed in stream of air for 60 s with pressure of air 70 mbar and after this was sample weighted.
- Moisture, volatiles, fixed carbon and ash content was determined by using of thermogravimetric analyzer (TGA, fig. 4). Measured by weight loss as a function of temperature in a controlled environment in a predefined atmosphere. The device consists of a computer and a muffle furnace that allows monitoring of up to 19 samples to be analyzed simultaneously. Empty cups on the samples are placed in carousel the furnace after selecting the method of analysis. The analysis method controls the carousel, furnace, and operating weights that gradually weigh all samples were placed

on the carousel. After weighing all the crucibles, is each a crucible is gradually adjusted for the operator of device for the sample application. Individual weights of samples are measured and saved automatically. When all the crucibles are loaded begins analysis. The loss in weight of each sample was monitored and the temperature of the oven is controlled according to the chosen analytical method. The percentage weight loss of each sample is known at the end of every step of the analysis. The device is easy to use with a software program Windows that allows analytical methods that can be designed to meet the most analytic applications according to current norms. The temperature, speed of rising temperatures and atmosphere are optional for each step.
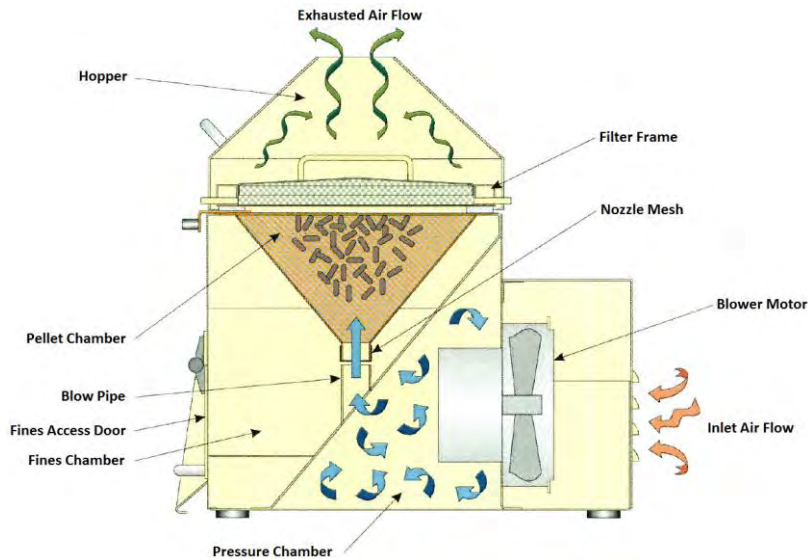
Fig. 3 LignoTester

Fig. 4 Thermogravimetric analyzer

RESULTS AND DISCUSSION

Table 1 shows the results of moisture content, gross and calorific heating value of wood pellets samples. Sample A achieved lower calorific value and gross calorific value than sample B, due to higher moisture content in sample A by other production methods.

The high calorific value difference could be also caused by lower pressure during the pelletizing and by lower compactness of sample A.

Tab. 1 The results of moisture content, gross and calorific heating value

	Moisture (%)	Gross calorific value (MJ/kg)	Calorific value (MJ/kg)
Sample A	7.33	18.7962	17.3121
Sample B	6.5	19.867	18.3626

Table 2 shows the results of amount of fines and mechanical durability of wood pellets samples. The results from the measured values showed that sample A has lower production quality than sample B. In the case of combustion in a conventional heat source for pellet burning, this causes wood pellets produced in the small pelletizer to be decomposed more rapidly during the feeding and during the combustion and thus can´t achieve the same heat output and efficiency of the heat source as the wood pellets produced in a large production line. During the operation of the heat source, this would result in higher pellet consumption and higher emissions.

Tab. 2 The results of amount of fines and mechanical durability

	F test		Amount of fines (%)	DU test		Mechanical durability (%)
	Mass before (g)	**Mass after (g)**		**Mass before (g)**	**Mass after (g)**	
Sample A	100.23	98.9	1.33	100.2	96.65	96.64
Sample B	100.89	107.86	0.03	107.87	107.34	99.51

Table 3 shows the results of moisture, volatiles, fixed carbon (FC) and ash content in wet and in dry state of wood pellets samples. Volatile and fixed carbon (FC) values are roughly identical due to the same input material - spruce sawdust. Ash content for samples A and B are also almost identical.

Tab. 3 The results of moisture, volatiles, fixed carbon (FC) and ash content in wet and in dry state

	Mosture (%)	Volatile (%)	FC (%)	Ash (%)	Volatile (%$_d$)	FC (%$_d$)	Ash (%$_d$)
Sample A	7.33	75.56	16.55	0.45	81.66	17.89	0.48
Sample B	6.5	76.45	16.41	0.48	81.91	17.58	0.51

CONCLUSION

The difference between commercial and domestic wood pellets production is quite clear from the results obtained. In domestic conditions on small pelletizing presses, high pressing pressures and temperatures can´t be achieved, as in the case of the production of wood pellets on a production line with high production. The produced wood pellets differ mainly in qualitative mechanical parameters, when domestic wood pellets are rather decaying, thereby reducing the bulk density, which is negative in their combustion. However, unless the commercial use of wood pellets is anticipated and their domestic consumption is assumed, it is important to produce wood pellets in small pellet presses.

Acknowledgements

REFERENCES

Čarnogurská, M., Lázár, M. Puškár, M., Lázárová, M., Širillová, Ľ., Václav, J., 2015. Measurement and evaluation of properties of MSW fly ash treated by plasma, Measurement. Vol. 62 (2015), p. 155-161.

Ďurčanský, P.,Holubčík, M.,Malcho, M. 2016. Effect of combustion air redistribution at performance characteristics of small heat source. AIP Conference Proceedings Vol. 1768, Article number 020029, DOI: 10.1063/1.4963051

Dzurenda, L., Pňakovič, Ľ. 2016, The influence of the combustion temperature of the non-volatile combustible wood matter of deciduous trees upon ash production and its properties, Acta Facultatis Xylologiae, 58 (1), pp. 95-104

Geffertová, J., Geffert, A., Deliiski, N., 2016. The Effect of Light on the Changes of White Office Paper. In Key Engineering materials. Selected Processes of Wood processing. ISSN 1662-9809, 2016, Vol. 688 pp 104-111.

Lázár, M., Carnogurská, M., Lengyelová, M., Korba, J. 2015. High-temperature gasification of RDF wastes and melting of fly ash obtained from the incineration of municipal wastes, Acta Polytechnica, 55 (1), pp. 1-6

Nosek, R., Holubčík, M. 2016. Energetické vlastnosti vzducho-suchého palivového dreva. Acta Facultatis Xylologiae Zvolen, 58(1): 105−112. DOI: 10.17423/afx.2016.58.1.12

Nosek, R., Holubcik, M., Jandacka, J. 2016. The impact of bark content of wood biomass on biofuel properties, BioResources, 11(1), pp. 44-53, DOI: 10.15376/biores.11.1.44-53

Ondro T., Vitázek I., Húlan T., Lawson M. K., Csáki Š., 2018, Non-isothermal kinetic analysis of the thermal decomposition of spruce wood in air atmosphere, Research in Agricultural Engineering, 64(1), 41-46

Rimár, M., Fedák, M., Korshunov, A., Kulikov, A., Mižáková, J. 2016. Determination of excess air ratio during combustion of wood chips respect to moisture content. Acta Facultatis Xylologiae 58 (2): 133-140: DOI:: 10.17423/afx.2016.58.2.14

MECHANICAL AND ENERGETIC PROPERTIES OF WOOD PELLETS DEPENDING ON BARK CONTENT

Nikola Kantová – Michal Holubčík – Jozef Jandačka

Abstract

Wood pellets are very used fuel in small heat sources in Europe. This paper deals with mechanical and energetic properties of wood pellets depending on bark content. It evaluates fine material amount and mechanical durability, moisture, volatile, fixed carbon, ash content, carbon, hydrogen, nitrogen and sulfur content, ash fusion temperature, gross calorific value and net calorific value, CO, NOx and OGC and PM concentrations of used wood pellets samples. Wood pellets samples were gradually created with 0%, 5 %, 10 % and 20 % content of bark.

Key words: *wood pellets, bark*

INTRODUCTION

Wood pellets combustion is a very used source of an energy. Poor fuel quality yields high emissions also from new boilers. Bark content in wood pellets influences also the fuel quality (Johansson et al., 2004). It has impact on following parameters: moisture content, ash content, ash fusion temperature, produced emissions and also particulate matter (PM) (Vitázek et al., 2016). High moisture in wood pellets leads to lower net caloric value and causes incomplete combustion in the combustion appliance. High content of bark results in more frequent maintenance of heat sources as bark contains more ash than barkless wood. Increased ash content also generates higher amount of particulate matter, which are very harmful emissions (Filbakk et al., 2011). Particulate matter is solid and liquid material in the atmosphere, mixture of substances consisting of carbon, dust and aerosols (Dzurenda, Pňakovič, 2016)

This paper deals with mechanical and energetic properties of wood pellets depending on bark content. It evaluates fine material amount and mechanical durability measured by using Ligno Tester, moisture, volatile, fixed carbon and ash content determined by using thermogravimetric analyses, carbon, hydrogen, nitrogen and sulfur content determined by using elemental determinator, ash fusion temperature, gross calorific value and net calorific value, CO, NO_x and OGC concentrations measured using by gas analyzer and PM concentrations measured by gravimetric method using by isokinetic automatic sampler. Wood pellets samples were gradually created with 0%, 5 %, 10 % and 20 % content of bark.

University of Zilina, Univerzitna 8215/1, 010 26 Zilina, Slovakia

e-mail: nikola.kantova@fstroj.uniza.sk

MATERIAL AND METHODS

The samples of wood pellets were produced on a specialized device in an external laboratory for pelletizing. As the input material for pelletizing was used dry spruce wood sawdust. Pellet mill was with capacity of 1000 kg.h⁻¹.

Fine material amount and mechanical durability were measured by using Ligno Tester. The Ligno Tester is operated by loading a manually weighed sample of pellets into the test chamber. After the test cycle, the pellets are manually removed and weighed to calculate the fine material amount or mechanical durability. Fines and dust are removed during the test process for a fair and accurate test.

Moisture, volatile, fixed carbon and ash content were determined by using thermogravimetric analyses. It measures weight loss as a function of temperature in a controlled environment. The instrument consists of a computer and a multiple sample furnace that allows up to 19 samples to be analyzed simultaneously. After an analysis method has been selected, empty crucibles are loaded into the furnace carousel. The analysis method controls the carousel, furnace, and balance operation. On completion of crucible tare, each crucible is presented to the operator for sample loading. The starting sample weight is measured and stored automatically. Once all the crucibles have been loaded, analysis begins (Guan et al., 2016).

The elemental determinator was used to determine carbon, hydrogen, nitrogen and sulfur. A pre-weighed and encapsulated sample is placed in the instrument's loader where the sample will be transferred to the instrument's purge chamber directly above the furnace, eliminating the atmospheric gases from the transfer process. The sample is then introduced to the primary furnace containing only pure oxygen, resulting in a rapid and complete combustion (oxidation) of the sample. Sulfur content was determined in the second module. Analysis begins as a sample is weighed into a combustion boat and placed in the furnace with pure oxygen typically regulated at 1350 °C (Eksperiandova et al., 2011).

Ash fusion temperature was determined according to STN ISO 540. Ash for testing was prepared in accordance STN ISO 1171. Ash was smashed in bowl to ensure particles less than 0.063 mm. Smashed ash was mixed with distilled water to the paste which is put to the form. Formed ash called test corpuscle must have sharp edges and is glued to templet. Deformed or damaged test corpuscle must be taken out from testing. During testing was a recorded characteristic of temperature, such as:

• Deformation temperature (DT) – test corpuscle has rounds on tip or ends because of starting melting
• Sphere temperature (ST) – test corpuscle has rounds on edges because of starting melting
• Hemisphere temperature (HT) – test corpuscle has about hemispherical shape, height is about the same like basement
• Flow temperature (FT) – ash is flowed on templet which has 1/3 height of test corpuscle at temperature in hemispherical shape

Gross calorific value was determined according to STN EN 14918 using calorimeter LECO AC 500. From gross calorific value was determined net calorific value by relation:

$$Q_i = Q_S - 2{,}453 . (M_{ar} + 9H_2) \ (MJ.kg^{-1}) \tag{1}$$

Q_S is net calorific value of fuel, M_{ar} is relative humidity of fuel and H_2 is hydrogen content of fuel.

The samples were burned in a hot water boiler with a rated output of 18 kW. This boiler was tested on an experimental device designed for the measuring of emission production.

Experimental device for testing was built from an experimental boiler, a heat consumption device, a gaseous emission analyzer, a particulate matter analyzer, measuring apparatus to which all measuring instruments are connected and a computer for the processing of measured data. During the measurements constant chimney draft 12 ± 2 Pa via a flue fan is ensured. Its speed is controlled by a frequency regulator. All pellet samples with various bark content were burned at the same operating settings of the boiler.

CO, NO_x and OGC concentrations in flue gases were measured by a flue gas analyzer ABB AO 2020 with sensor modules Uras 26 with accuracy ≤ 1 % of span and oxygen analyzer module Magnos 206 with accuracy $\pm 0.5\%$. The piping for the sampling operations must be incorporated with means for cooling, cleaning and drying flue gas samples.

Particulate matter concentrations were measured by gravimetric method by using of the isokinetic automatic sampler TECORA Isostack Basic. Gravimetric method is given by the standard ISO 9096. It is a manual, single-use method where samples are taken by a probe from flowing gas. Filtration materials are weighed before and after measurements and final mass concentration is calculated from a sample volume. Sampling probes can be placed either directly into hot flow of exhaust gases or outside the flow, where these systems must be heated. Solid particles are collected from flowing gas with the help of the probe. From them an average concentration of flowing gas particles is determined. Exhaust gases were taken from a chimney duct with the help of a three-stage separation impactor. The sampling was conducted at the same speed of exhaust gas flow as in the pipe. Hot gas was led from the pipe through cooling and drying equipment up to the sampling unit. In the cooling equipment exhaust gases were cooled and water vapour was removed from the exhaust gas sample. In the silica gel-water absorption tower residual moisture of exhaust gases was removed.

RESULTS

Table 1 shows results from Ligno Tester. There are stated fine material amount and mechanical durability.

Tab. 1 Results from Ligno Tester

	Fine material amount		Mechanical durability	
Sample	**Value**	**Unit**	**Value**	**Unit**
0 % bark content	0.91	g	97.54	%
5 % bark content	0.95	g	96.25	%
10 % bark content	1.06	g	98.44	%
20 % bark content	0.81	g	97.99	%

Results from thermogravimetric analyzer are showed in the Table 2. We can see values of moisture, volatile, fixed carbon and ash content.

Tab. 2 Results from thermogravimetric analyser

Sample	**Moisture**	**Volatile**	**Fixed carbon**	**Ash content**	**Unit**
0 % bark content	6.64	81.84	17.64	0.52	%
5 % bark content	6.81	81.21	18.01	0.77	%
10 % bark content	6.67	80.91	18.16	0.94	%
20 % bark content	7.29	79.83	18.65	1.51	%

Results from elemental determinator are stated in the Table 3, where is carbon, hydrogen, nitrogen and sulfur content.

Tab. 3 Results from elemental determinator

Sample	Carbon	Hydrogen	Nitrogen	Sulfur	Unit
0 % bark content	48.55	6.33	0.13	0.08	%
5 % bark content	49.55	6.01	0.02	0.06	%
10 % bark content	49.49	6.16	0.05	0.05	%
20 % bark content	49.59	6.14	0.06	0.03	%

Table 4 shows results of ash fusion temperature. You can see Deformation temperature (DT), Sphere temperature (ST), Hemisphere temperature (HT) and Flow temperature (FT).

Tab. 4 Results of ash fusion temperature

Sample	DT	ST	HT	FT	Unit
0 % bark content	1320	1400	1420	1475	°C
5 % bark content	1240	1260	1365	1380	°C
10 % bark content	1295	1400	1410	1415	°C
20 % bark content	1180	1200	1210	1315	°C

Gross calorific value and net calorific value are stated in the Table 5.

Tab. 5 Results of gross calorific value and net calorific value

Sample	Gross calorific value	Net calorific value	Unit
0 % bark content	18.96	17.37	MJ/kg
5 % bark content	18.78	17.20	MJ/kg
10 % bark content	18.00	17.04	MJ/kg
20 % bark content	17.01	16.91	MJ/kg

Results from measured emissions are stated in the Table 6.

Tab. 6 Results of measured emissions

Sample	CO	NO_x	OGC	PM	Unit
0 % bark content	795.84	228.55	30.01	35.54	mg/m^3
5 % bark content	1598.11	177.05	13.33	46.41	mg/m^3
10 % bark content	2718.5	149.09	89.48	48.53	mg/m^3
20 % bark content	3613.65	199.88	69.65	57.72	mg/m^3

CONCLUSION

Based on the results, we can conclude that bark content in pellets has an impact on their mechanical and energetic properties. Higher bark content in pellets increases ash content, which can adversely influence combustion process, mainly due to higher ash production during combustion and consequent necessity of more frequent boiler cleaning. But very serious shortcoming is the fact that with higher bark content, ash fusion temperature decreases. Lower ash fusion temperature can cause some problems within combustion

process, for example, to lower heat transfer intensity in heat exchangers, to cause corrosion of combustion equipment, to prevent fuel and combustion air supplies, etc. But wood bark has relatively high net calorific value. Therefore, its potential can be energetically used. Attention should be paid to its negative impact on the environment due to higher concentrations of CO, NO_x and PM as mentioned in this article.

Acknowledgements

REFERENCES

Johansson, L. S., Leckner, B., Gustavsson, L., Cooper, D., Tullin, C and Potter, A. 2004, Emission characteristics of modern and old-type residential boilers fired with wood logs and wood pellets, Atmospheric Environment, 38(25), pp. 4183-4195

Vitázek, I., Mikulová, Z., Klúčik, J.. 2016, Diagrams of the moist air extended by equilibrium moisture of dried materials, AIP Conference Proceedings, 1768,020018

Filbakk, T., Jirjis, R., Nurmi, J., Hoibo, O., 2011, The Effect of Bark Content on Quality Parameters of Scots Pine Pellets. Biomass and Bioenergy, 35, 3342-3349.

Dzurenda, L., Pňakovič, Ľ. 2016, The influence of the combustion temperature of the non-volatile combustible wood matter of deciduous trees upon ash production and its properties, Acta Facultatis Xylologiae, 58 (1), pp. 95-104

Eksperiandova, L. P., Fedorov, O. I., Stepanenko, N. A. 2011, Estimation of metrological characteristics of the element analyzer EuroVector EA-3000 and its potential in the single-reactor CHNS mode, Microchemical Journal, 99 (2), pp. 235–238

Guan, C., Gao, N., Song, Q. 2016, Pyrolysis of biomass components in a TGA and a fixed-bed reactor: Thermochemical behaviors, kinetics, and product characterization, Journal of Analytical and Applied Pyrolysis, 121, pp. 84–92

STN ISO 1171, Tuhé palivá - Stanovenie popola. 2003

STN ISO 540, Uhlie a koks. Stanovenie taviteľnosti popola. 2010

STN EN 14918, Tuhé biopalivá. Stanovenie výhrevnosti. 2009.

STN ISO 9096, Air quality. Stationary source emissions. Manual determination of mass concentration of particulate matter. 2004

KONTAMINÁCIA KONDENZÁTU PRODUKTMI HYDROLÝZY A EXTRAKCIE Z TEPELNÉHO SPRACOVANIA BUKOVÉHO A JAVOROVÉHO DREVA PRI MODIFIKÁCII FARBY DREVA

Dagmar Samešová[1] **– Ladislav Dzurenda**[1] **– Peter Jurkovič**[2]

Abstract

The paper presents the results of water contamination analysis of hydrolysis products and extractions from the thermal treatment of beech and maple timber to modify the color of wood.

From the analyzes carried out follows that the acidity of the condensate pH from 5.49 to 5.60, the content of biological oxygen demand BSK_5 = 2310 to 2390 mg $O_2.l^{-1}$, chemical oxygen demand $ChSK_{Cr}$ = 8056 mg. l^{-1}, dry mater 0.75%, ash A = 0.08 %, soluble substances RL = 6028 - 6326 mg.l^{-1} and insoluble substances NL = 969 - 1549 mg. l^{-1}.

The degree of contamination of condensed saturated steam from the thermal process of modification of the color of beech and maple wood in the sense of Government Regulation no. 269/2010 Z. is high and it is necessary to modify before it is discharged into the watercourses.

Key words: *wood, saturated steam, wood color modification, hydrolysis, extraction, pollution of the condensate*

ÚVOD

Drevo umiestnené do v prostredia horúcej vody, sýtej vodnej pary či nasýteného vlhkého vzduchu sa nahrieva a mení svoje fyzikálne, mechanické a chemické vlastnosti. Uvedené skutočnosti sa využívajú v drevárskych technológiách varenia a parenia dreva vo výrobe dýh a preglejok, ohýbaného nábytku, či lisovaného dreva *Kollmann – Gote (1968), Sergovsky – Rasev (1987), Trebula (1986)*.

Procesy termickej úpravy dreva sýtou vodnou parou, okrem cielených fyzikálno-mechanických zmien sú sprevádzané aj chemickými reakciami akými sú parciálna hydrolýza a extrakcia vyvolávajúca zmeny farby dreva. Kým v minulosti sa farebné zmeny stmavnutia termicky upravovaného dreva využívali na odstránenie nežiaducich farebných rozdielov medzi svetlou beľou a tmavým jadrom, či odstránenie nežiaducich farebných škvŕn vzniknutých zaparením, zahnednutím či zaplesnením, tak v ostatnom čase je pozornosť výskumu a vývoja zameraná na cielenú zmeny farby dreva jednotlivých drevín do menej či viac výrazných farebných odtieňov, resp. imitácie dreva domácich drevín na exotické dreviny je problematike cielenej zmeny farby dreva jednotlivých drevín venovaná

[1]Technická univerzita vo Zvolene, T.G. Masaryka 24, 96053, Zvolen, Slovensko
[2]VIPO, a.s. Partizánske, Gen. Svobodu1069/4, Slovensko
e-mail: samesova@tuzvo.sk, dzurenda@tuzvo.sk, pjurkovic@vipo.sk

zvýšená pozornosť *Tolvaj – Nemet – Varga – Molnar (2009), Dzurenda (2014,2018), Barcik – Gašparík –Razumov (2015), Baranski et all (2017).*
Vedľajším produktom termickej modifikácie dreva varením, resp. parením je voda, ktorá je v menšej, či väčšej miere kontaminovaná produktmi hydrolýzy dreva a extrakcie vodou rozpustných látok nachádzajúcich sa v dreve, akými sú: monosacharidy, organické kyseliny, základné stavebné jednotky lignínu s guajacylovou a syringylovou štruktúrou uvádzané v prácach: *Bučko (1995), Trebula – Bučko (1996), Dzurenda – Bučko (1998), Kačík (2001), Laurova – Mamonova – Kučerova (2004), Kačíková – Kačík (2011).* Kondenzát kumuluje v sebe uvedené produkty z parenia dreva a nie je ho možné vypúšťať bez predchádzajúcej úpravy. Chemické metódy založené na oxidácii patria k štandardným postupom spracovania kondenzátu. *Irmouli – Haluk, (2005).* K environmentálne prijateľným spôsobom úpravy patria metódy na báze biodegradácie v anaeróbnych, resp. aeróbnych podmienkach, ktoré boli predmetom výskumu viacerých autorov: *Ma et al. (1999), Ledig – Slavik – Broege (2003).* Hlavným problémom biologických metód je malá degradácia lignínu. Prvým predpokladom návrhu spôsobu úpravy, využitia, resp. zneškodnenia kondenzátu je analýza jeho zloženia a v prípade biologického spracovania, aj testovanie ekotoxikologických vlastností.

Cieľom danej práce je analyzovanie miery kontaminácie kondenzátu z termického procesu farebnej modifikácie bukového a javorového reziva h = 32 mm sýtou vodnou parou s teplotou t = 112 ± 2,5 °C po dobu τ = 5,5 hod v autokláve APDZ 240.

MATERIÁL A METODA

Režim farebnej modifikácie reziva h = 32 mm sýtou vodnou parou v tlakovom autokláve AZ 240 pre roztrúsenopórovité listnaté dreviny: Buk lesný a Javor mliečny je zobrazený na obr.1.
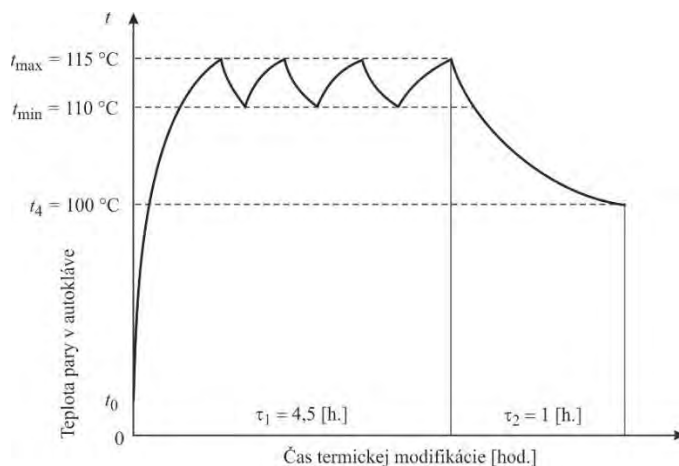
Obr. 1 *Rozpis technologických podmienok pre termický proces modifikácie reziva h = 32 mm roztrúsenopórovitých listnatých drevín.*

Sýta vodná para privedená do autoklávu v procese ohrevu dreva, strojnotechnologického zariadenia a krytia tepelných strát, kondenzuje a v priebehu termického procesu modifikácie dreva je kondenzát kontaminovaný produktmi hydrolýzy dreva a extrakcie

vodou rozpustných látok nachádzajúcich sa v dreve. Miera kontaminácie bola hodnotená na základe stanovenia nasledovných parametrov: pH, sušina, strata žíhaním, vodivosť, rozpustené látka, nerozpustené látky, chemická spotreba kyslíka, biochemická spotreba kyslíka, dusičnany, chloridy, sírany, celková tvrdosť, vápnik, horčík.

Stanovenie pH
Hodnota pH bola stanovené elektrochemicky v zmysle STN EN 12176, STN EN ISO 10523.

Stanovenie sušiny
Vzorka sa suší do konštantnej hmotnosti v sušiarni pri 105 °C ± 3 °C. (STN EN 14346).

Stanovenie straty žíhaním
Podstatou tejto metódy je spálenie vzorky a žíhanie uhlíkových zvyškov pri 550 °C do konštantnej hmotnosti. (STN 65 6063 – metóda A).

Stanovenie elektrolytickej vodivosti
Použili sme priame stanovenie elektrolytickej vodivosti vodných roztokov pomocou laboratórneho merača vodivosti. (STN EN 27888).

Stanovenie rozpustených a nerozpustených látok:
Stanovené bolo celkové množstvo všetkých látok odparením vzorky, vysušením odparku pri 105°C. Rozpustené a nerozpustené látky sa separujú filtráciou. Množstvo rozpustených látok sa následne určí stanovením sušiny filtrátu. Z rozdielu celkového množstva látok a látok rozpustených sa stanovia nerozpustené látky (Horáková, 2007, pp. 88-93)

Stanovenie chemickej spotreby kyslíka (ChSK$_{cr}$)
Princíp metódy je založený na oxidácii organických látok nachádzajúcich sa vo vzorke vody dichrómanom draselným v silne kyslom prostredí kyseliny sírovej počas dvojhodinového varu.(STN ISO 6060).

Stanovenie biochemickej spotreby kyslíka (BSK$_5$)
Stanovenie biochemickej spotreby kyslíka (BSK) slúži k nepriamemu stanoveniu organických látok, ktoré podliehajú biochemickému rozkladu pri aeróbnych podmienkach.
Vzorka skúšanej vody sa upraví a riedi rôznymi objemami riediacej vody s dostatočnou koncentráciou rozpusteného kyslíka s inokulom aeróbnych mikroorganizmov s potlačením nitrifikácie. Inkubácia sa uskutočňuje pri teplote 20 °C po dobu 5 dní v úplne naplnenej a uzavretej nádobe. Rozpustený kyslík sa stanoví na začiatku, pred jej inkubáciou a po jej ukončení. (Horáková, 2007, pp. 243-245)

Stanovenie dusičnanov
Princíp metódy spočíva v nitračnej reakcií dusičnanov s kyselinou salicylovou v prostredí kyseliny sírovej. Absorbancia sa meria spektrofotometrom pri vlnovej dĺžke 415 nm. Hmotnostná koncentrácia dusičnanov vyjadrená ako NO_3^- sa určí z kalibračnej závislosti (STN ISO 7890-3).

Stanovenie dusitanov
Metóda je založená na diazotačnej reakcií dusitanov so sulfoamidom v kyslom prostredí kyseliny fosforečnej. Absorbancia sa meria pri 540 nm a hmotnostná koncentrácia dusitanov sa vyhodnotí z kalibračnej čiary (STN EN 26777).

Stanovenie amónnych iónov

Stanovenie je založené na reakcii amoniaku a hydroxidov alkalických kovov s tetraortuťnanom sodným alebo draselným za vzniku Millonovej bázy.. Absorbancia sa meria pri 400 – 410 nm (STN 83 0530-26b).

Stanovenie síranov

Ióny SO_4^{2-} reagujú v slabo okyslenom prostredí s iónmi Ba^{2+} za vzniku veľmi málo rozpustnej zrazeniny síranu bárnatého. Zrazenina síranu bárnatého sa kvantitatívne zachytí na sklenenej frite, dokonale premyje horúcou destilovanou vodou a vysuší pri teplote 105 °C do konštantnej hmotnosti a odváži (Horáková 2007, pp 228 - 231).

Stanovenie celkovej tvrdosti, vápnika a horčíka

Stanovenie celkovej tvrdosti sa vykonalo priamou titráciou odmerným roztokom chelatónu III v amoniakálnom prostredí na eriochrómovú čerň T do jasného modrého sfarbenia. Ca^{2+} sa určilo titráciou odmerným roztokom chelatónu III. na murexid. Obsah Mg^{2+} sa vypočíta z rozdielu. (STN ISO 6059).

VÝSLEDKY A DISKUSIA

V priebehu termického procesu farebnej modifikácie dreva sa tvorí kondenzát červenohnedej až šedočiernej farby charakteristického zápachu v množstve 170 – 200 dm^3 na 1 m^3 termicky modifikovaného reziva. Teplota kondenzátu na konci cyklu termického procesu je 98 – 99 °C.

Výsledky analýz sú v tabuľke 1. Z výsledkov vyplýva vysoké zaťaženie kondenzátu organickými látkami s vysokým podielom rozpustených látok a mierne kyslou reakciou. Podiel BSK_5 voči CHSK je pod hranicou 0,5 (0,29), čo naznačuje obmedzený biochemický rozklad prítomných organických látok, tieto namerané hodnoty korešpondujú s výsledkami iných autorov MCDONALD et al., 1999, WOJTASZ-MUCHA, 2017.

Tab. 1. *Výsledky analýz kontaminácie kondenzátu z procesu termickej úpravy - farebnej modifikácie bukového a javorového dreva*

Označ. vzorky	pH	Vodivosť mS/m	BSK_5 mg O_2/l	$ChSK_{Cr}$ mg.l^{-1}	sušina %	popol %	RL mg.l^{-1}	NL mg.l^{-1}
Buk lesný	5,60	109	2 390	8 056	0,75	0,08	6 028	1 549
Javor mliečny	5,49	111	2 310	8 056	0,75	0,08	6 326	969

Tab. 2. *Výsledky analýz kontaminácie kondenzátu z procesu termickej úpravy - farebnej modifikácie bukového a javorového dreva*

Označ. vzorky	NO_3^- mg.l^{-1}	Cl^- mg.l^{-1}	SO_4^{2-} mg.l^{-1}	Celk. tvrdosť mmol.l^{-1}	Mg^+ mg.l^{-1}	Ca^+ mg.l^{-1}
Buk lesný	245,4	0	257,25	37,5	243,1	1 102,2
Javor mliečny	209,8	0	823,25	37,5	243,1	1 102,2

Stanovené koncentrácie ukazovateľov: ChSK$_{Cr}$, BSK$_5$, nerozpustené látky sú niekoľko násobne vyššie než sú limitné hodnoty znečistenia vypúšťaných odpadových vôd a osobitných vôd v zmysle Nariadenia vlády SR č. 269/2010 Z. z., ktorým sa ustanovujú požiadavky na dosiahnutie dobrého stavu vôd (tab. 3). Zaujímavým zistením je vysoká hodnota dusičnanov a vápnika, ktoré vysoko prekračujú imisné koncentrácie pre povrchové vody.

Tab. 3. *Ukazovatele prípustného znečistenia odpadových vôd pre kategóriu: 6.4 Chemického priemyslu (výroba celulózy)*

Ukazovateľ [mg.dm^{-3}]	Hodnota
BSK$_5$	50
CHSK$_{Cr}$	400
Nerozpustné látky	50

Kondenzát z procesu farebnej modifikácie pred vypustením do recipienta je nutné najprv ochladiť na teplotu 20 – 30°C a prítomné znečistenie odstrániť na prípustnú mieru znečistenia podľa platnej legislatívy.

ZÁVER

Na základe vykonaných analýz a stanovenia kyslosti kondenzátu pH = 5,49 – 5,60, obsahu BSK$_5$ = 2310 – 2390 mg O$_2$/l, ChSK$_{Cr}$ = 8056 mg.l^{-1}, sušiny 0,75 %, popola A = 0,08 %, rozpustných látok RL = 6028 – 6326 mg.l^{-1} a nerozpustných látok NL = 969 – 1549 mg.l^{-1} v kondenzáte je možné konštatovať, že miera znečistenia skondenzovanej sýtej pary z termického procesu farebnej modifikácie dreva listnatých roztrúsenopórovitých drevín: Buk lesný a Javor mliečny sa musia v zmysle Nariadenia vlády SR č. 269/2010 Z. z pred vypúšťaním do recipientu nevyhnutne upraviť. Podľa našich zistení je kondenzát nutné chemicky predčistiť a zvyškové organické znečistenie je možné odstrániť na biologickej čistiarni odpadových vôd.

LITERATÚRA

1. Barcik, Š., Gašparík, M., Razumov, E.Y. 2015: Effect of thermal modification on the colour changes of oak wood. In: Wood Research. 60 (3):385-396, ISSN 002-6136.
2. Bučko, J. 1995.: Hydrolýzne procesy. Zvolen: Vydavateľstvo TU Zvolen, 1995. 116s.
3. Dzurenda, L. – Bučko, J. 1998: Príčiny poklesu vlhkosti dreva mokrých bukových podvalov v prpocese parenia nasýtenou vodnou parou. [Reasons of decrease of the moisture content of wood of green beech sleepers during the steaming process with saturated water steam] In: Acta facultatis xylollogiae 40 (1): 67-75.
4. Dzurenda, L., Deliiski, N.: Tepelné procesy v technológiách spracovania dreva. Zvolen: Vydavateľstvo TU Zvolen, 2010. 273 s.

5. DZURENDA, L. 2014: Sfarbenie bukového dreva v procese termickej úpravy sýtou vodnou parou. In: Acta facultatis xylologiae Zvolen, 56 (1):13 – 22, ISSN 1366-3824.
6. DZURENDA, L. 2018: The Shades of Color of *Quercus robur* L. Wood Obtained through the Processes of Thermal Treatment with Saturated Water Vapor. In: BioResouces 13(1), 1525 - 1533; doi: 10.1063/biores 13.1.1525-1533
7. IRMOULI,M., HALUK, J.P. 2005.: Chemical remediation of beech condensates. In: Journal of Colloid and Interface Science, Volume 281, Issue 1,. 253-254 s.
8. HORÁKOVÁ, M.et al.: Analytika vody, druhé vydanie, Praha: VŠCHT, 2007, 335 s., ISBN 978-80-7080-520-6
9. KAČÍK, F. 2001: Tvorba a chemické zloženie hydrolyzátov v systéme drevo-voda-teplo. Zvolen: Vydavateľstvo TU Zvolen, 2001. 75 s.
10. KAČÍKOVÁ, D., KAČÍK, F. 2011: Chemické a mechanické zmeny dreva pri termickej úprave. Zvolen: Vydavateľstvo TU Zvolen, 2011. 71 s.
11. KOLLMANN, F., COTE, W. A. 1968: Principles of Wood Sciences and Technology, Vol. 1. Solid Wood, Springer Verlag: Berlin – Heidelberg - New York, 592 s.
12. LAUROVA, M., MAMONOVA, M., KUČEROVA, V. 2004: Proces parciálnej hydrolýzy bukového dreva (Fagus sylvatica L.) parením a varením. [Vedecké štúdie 2/2004/A], Zvolen: TU Zvolen. 58 s.
13. LEDIG, S. F., SLAVIK, I., BROEGE, M. 2003: Characterization and Treatment of the Condensate Generated from Steaming of Beech Timber prior to Kiln-Drying. In: 8th International IUFRO Wood Drying Conference – 2003,. 231 – 236 s.
14. MA, W.; KAMDEM, D.P.; LOCONTO, P.; PAN Y.; GAGE, D.; DAWSON-ANDOH, E.B. 1999: Characterization and Bioremedation of Birch Condensate. Wood and Fiber Science 31 (4), 370-375 s.
15. MCDONALD,A. G., GIFFORD J. S., DARE P. H., STEWARD,D., 1999, Characterisation of the condensate generated from vacuum-drying of radiata pine wood In:Holz als Roh- und Werkstoff, Volume 57, Issue 4, 251–258 s.
16. SERGOVSKIJ, P. S., RASEV, A. I. 1987: Gidrotermičeskaja obrabotka i konservirovanije drevesiny. Lesnaja promyšlennost, Moskva, 360 s.
17. TOLVAJ, L., NEMETH, R., VARGA, D., MOLNAR, S., 2009: Colour homogenisation of beech wood by steam treatment. In: Drewno. 52 (181): 5-17, ISSN 1644-3985.
18. TREBULA, P., BUČKO, J. 1996: Vákuové sušenie dreva, technické, technologické a ekologické aspekty. [Vedecké štúdie 5/1996/B], Zvolen: Vydavateľstvo TU Zvolen, 2001, 70 s.
19. TREBULA, P. 1996: Sušenie a hydrotermická úprava dreva. Zvolen: Vydavateľstvo TU Zvolen, 2001, 255 p.
20. WOJTASZ-MUCHA, J., HASANI, M., THELIANDER, H. 2017: Hydrothermal pretreatment of wood by mild steam explosion and hot water extraction, In: *Bioresource Technology*, **241**, (120)

COMPUTATION OF THE TEMPERATURE FIELD IN BEECH LOGS SUBJECTED TO DEFROSTING USING THE SOFTWARE PACKAGE ANSYS WORKBENCH 16.0

Natalia Tumbarkova – Nencho Deliiski

Abstract

An approach for the computation of the temperature field in subjected to defrosting logs with the help of software package ANSYS Workbench 16.0 has been suggested. The sequence of actions and commands for the simulation of the logs' defrosting process in the working environment of this package are given.

The first results from ANSYS' calculation of the non-stationary temperature distribution in 4 characteristic points of the longitudinal section of a beech log with a diameter of 0.24 m, length of 0.48 m, moisture content of 0.63 kg·kg⁻¹, and initial temperature –28.8 ᵒC during its 50 h defrosting at room temperature are graphically presented and analyzed. The root square mean error between the calculated and experimentally established temperature field of the studied log has been determined.

Key words: *beech logs, defrosting, ANSYS, computation, temperature field*

INTRODUCTION

The abbreviation ANSYS comes from the expression "Analysis SYStem" (https://en.wikipedia. org/wiki/Ansys). It presents a software package for the analysis based on the method of finite elements, developed by the firm "Ansys Inc." (USA). The software package ANSYS is used mainly for the solution of linear and non-linear equations from the mechanics of solid bodies, mechanics of fluids, acoustics, thermodynamics, and problems connected to the electromagnetic and piezoelectric properties of the materials and others.

When studying the processes of thermal treatment of wood materials, it is necessary to determine the change in the temperature of materials depending on the temperature of the influencing medium and on the duration of staying in this medium. Our comprehensive study shows that the software package ANSYS so far has not been used for the simulation of processes of freezing or/and defrosting of any kind of wood materials, including logs.

The aim of the present work is to suggest an approach for use of ANSYS Workbench 16.0 for the computation of the temperature filed in subjected to defrosting logs.

Department of Woodworking Machines, University of Forestry, 10 Kliment Ohridski Blvd., 1797 Sofia
e-mail: nataliq_manolova@abv.bg, deliiski@netbg.com

MATERIAL AND METHODS

Commands in ANSYS for preparation of simulations of defrosting process

The preparation of the simulation for the logs' defrosting process in the calculation environment of ANSYS consists of the following sequence of actions and commands:

a. Creation of a working file in ANSYS and input of a suitable for the aim name: **File ⇒ New**;

b. Choice of the type of the subjected to studying process – in this case unsteady thermal conductivity: **Toolbox ⇒ Transient Thermal.** This is carried out by dragging in the neighboring right window or by double clicking on the type of studied process in the right dialogue window;

c. By double clicking on the option **Engineering Data** a new window is opened, in which the type and main properties of the studied process are input. In our case we input **Wood** and after that in the tables under this input the thermo-physical characteristics of the studied process are input: **Density**, **Thermal conductivity**, and **Specific heat capacity**. The dimensions of all variables are input into the system SI. The values of the thermal conductivity and the specific heat capacity of the materials are input separately for the separate termperature ranges of the logs' freezing process.

d. After inputting of the main thermo-physical characteristics of the material, it is necessary to return to the main window by double clicking on the third position **Geometry** in the main menu. There a 3D graph of the model, which is being studied, is created (*Figure 3*). In our case this is ¼ of the longitudinal section of the log because of the circumstance that this ¼ is mirror symmetrical towards the remaining 3/4 of the same section.

e. The next step is a creation of the calculation mesh on the log using the command **Model ⇒ Mesh** in the main menu. In the window, which appeared, the type of mesh and the size of its separate components are input. In our case the change of the temperature in the longitudinal section of beech logs with a diameter of 0.24 m and length of 0.48 m is studied. That is why a rectangular mesh with a step $\Delta x = 15$ mm along the space coordinates is input. The number of knots of the mesh along the radial coordinate is equal to 9, and along the longitudinal coordinate it is equal to 17, i.e. the total amount of the knots of the used calculation mesh is equal to $N_{total} = 9 \times 17 = 153$.

f. Using the command **Setup** in the main menu, the following parameters of the studied log are input: initial temperature of the log, duration of the freezing process, time interval by which the freezing process has been monitored during experimental research (using this interval, the change in temperature in the characteristic points of the log will be calculated), dimensions (diameter and length) of the log, heat transfer coefficients in the radial α_{wr} and longitudinal α_{wp} directions of the wood fibers, and values of the temperature of the freezing air medium t_m at each moment of the process divisible by the input time interval. Input of the values of α_{wr}, α_{wp} and t_m is carried out by filling in their values in the table, which is situated in the lower right corner of the program menu of ANSYS.

g. After completing the described steps above, using the command **Solution**, the calculation of the temperature distribution in the longitudinal section of the subjected to freezing log is started. For this aim, in the opened dialogue window, the command **Solve** is selected and this way the calculation begins.

h. After the program finishes the calculations, by clicking on each of the points **Temperature** T1, T2, T3, and T4 (see Fig. 3) data are obtained about the values of the temperature in each of the 4 characteristic points of the longitudinal section of the log during the simulation of its defrosting. Taking the calculated data with the aim of its

subsequent graphical presentation in MS Excel is carried out by pressing the right button of the mouse and selecting the command **Export,** following which the type, name and place for saving the file need to be given.

Experimental research of the temperature distribution in subjected to defrosting logs

For the assessment of the solutions, which are obtained in the calculation environment of ANSYS, we needed experimentally obtained data about the change of the temperature field in logs during their defrosting. That is why we carried out such experiments. The logs subjected to experimental research were with a diameter D = 240 mm, length L = 480 mm, and moisture content u above the hygroscopic range. They were produced from a freshly felled beech trunk. Before the experiments, 4 holes with diameters of 6 mm and different lengths were drilled into each log. Sensors with long metal casings were positioned in these 4 holes for the measurement of the wood temperature during the experiments. The coordinates of the characteristic points of the logs are, as follows: Point 1: along the radius r =30 mm and along the length z = 120 mm; Point 2: with r = 60 mm and z = 120 mm; Point 3: with r = 90 mm and z = 180 mm and Point 4: with r = 120 mm and z = 240 mm (center of the log). These coordinates of the points allow to cover the impact of the heat fluxes simultaneously in the radial and longitudinal directions on the temperature distribution in logs during their freezing and subsequent defrosting (Deliiski – Tumbarkova 2016). Each log with temperature sensors in it was horizontally situated on a special stand in the open freezer at room temperature. After the closing of the freezer it was switched on at full power and the temperature of the freezing air medium in it was lowered gradually during 50 h until reaching approximately –30 ℃. After that the freezer was opened and the studieed by us 50 h defrosting process of the frozen log at room temperature started.

The automatic measurement and record of the temperature and humidity of the air processing medium and also of the temperature in the 4 points in logs during the experiments was carried out with the help of Data Logger type HygroLog NT3 produced by the Swiss firm ROTRONIC AG (http:/www.rotronic.com). On Fig. 1, as an example, the change in the temperature of the defrosting air medium, t_m and in its humidity, φ_m, and also in the temperature in the 4 characteristic points of beech log with moisture content u = 0.63 kg·kg⁻¹ and basic density ρ_b = 684 kg·m⁻³ during its 50 h defrosting, is presented.
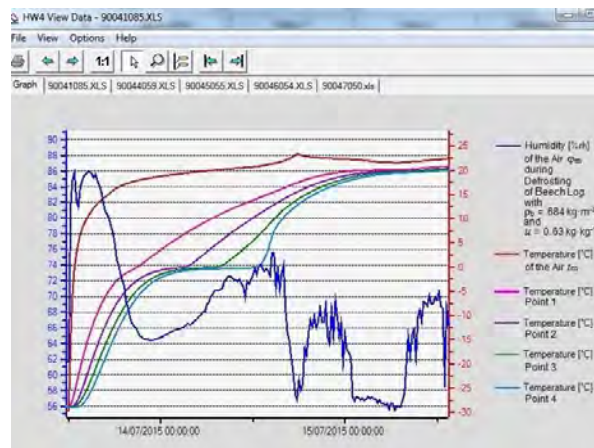
Fig. 1. Experimentally determined change in t_m, φ_m, and t in 4 points of the studied beech log during its 50 h defrosting

Determination of the values of the thermo-physical characteristics of logs needed for computations with ANSYS

On Fig. 2 the three temperature ranges are shown, at which the process of the logs' defrosting above the hygroscopic range can be defragmented. There also the thermo-physical characteristics of the wood and of the frozen water in it have been shown. The values of these characteristics are needed for the computation with ANSYS of the temperature field in subjected to defrosting logs.
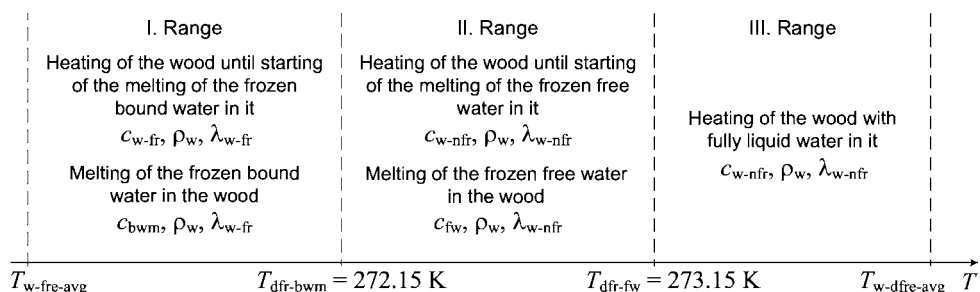
Fig. 2. Temperature ranges of the logs' defrosting process above the hygroscopic range and thermo-physical characteristics of the wood and the frozen water in it

During the first range from the average mass temperature of the log at the end ot its freezing, $T_{\text{w-fre-avg}}$, to the temperature $T_{\text{dfr-bwm}} = 272.15$ K heating of the frozen wood occurs until reaching of its state needed for starting of the melting of the frozen bound water in it. In this range also the phase transition of this water into liquid state is carried out.

During the second range from $T_{\text{dfr-bwm}}$ to $T_{\text{dfr-fw}} = 273.15$ K a further heating of the log occurs until reaching of the state needed for starting of the melting of the frozen free water in it. In this range also the phase transition of this water into liquid state is performed.

During the third range from $T_{\text{dfr-fw}}$ to the average mass temperature of the log at the end of its defrosting, $T_{\text{w-dfre-avg}}$, a heating of the log with fully liquid water in it occurs.

For the computation of the temperature field in subjected to defrosting logs using ANSYS it is needed to have average values of their thermal conductivity, λ_w, effective specific heat capacity, c_{we}, density, ρ_w, and of the heat transfer coefficients of the logs' surfaces, α_r and α_p. Such values can be obtained with the help of mathematical descriptions of the mentioned variables for the separate ranges of the logs' defrosting process. The values of λ_w, c_{we}, α_r, and α_p of the studied log have been determined using their mathematical descriptions given in (Deliiski 2011). The change of these variables during the 50 h log's defrosting has been calculated using software in Visual Fortran synchronously with the solving of an own non-linear mathematical model of the logs' defrosting process at the same initial and convective boundary conditions, as those during the experiment.

Average values of the thermal conductivities of the studied beech log

A mathematical description of the thermal conductivity, λ_w, of non-frozen and frozen wood has been suggested in (Deliiski 2013) using an experimentally obtained dissertations' data from other authors for the change of this conductivity as a function of t and u. Using the data calculated with Visual Fortran, the following average values of λ_{wr} and λ_{wp} for the separate ranges of the log's defrosting process have been determined:

- I. range: $\lambda_{wr1} = 0.646$ W·m⁻¹·K⁻¹, $\lambda_{wp1} = 1.151$ W·m⁻¹·K⁻¹;
- II. range: $\lambda_{wr2} = 0.548$ W·m⁻¹·K⁻¹, $\lambda_{wp2} = 0.975$ W·m⁻¹·K⁻¹;
- III. range: $\lambda_{wr3} = 0.559$ W·m⁻¹·K⁻¹, $\lambda_{wp3} = 0.996$ W·m⁻¹·K⁻¹.

Average values of the effective specific heat capacities of the studied beech log

The effective specific heat capacities of the logs' wood, c_{we}, during the shown on Fig. 2 three ranges of the defrosting process above the hygroscopic range are equal to:

$$c_{we1} = c_{w\text{-}fr} + c_{bwm} \quad \text{during the I. temperature range of the defrosting,} \tag{1}$$

$$c_{we2} = c_{w\text{-}nfr} + c_{fw} \quad \text{during the II. temperature range of the defrosting,} \tag{2}$$

$$c_{we3} = c_{w-nfr} \quad \text{durnig the III. temperature range of the defrosting.} \tag{3}$$

Using the mathematical descriptions of the separate specific heat capacities, which participate in the right parts of eqs. (1), (2), and (3), given in (Deliiski 2011, 2013) the following summarized expressions for c_{we1}, c_{we2}, and c_{we3} have been obtained:
- I. range: $c_{we1} = 2086 + 747 = 2833$ J·kg⁻¹·K⁻¹;
- II. range: $c_{we2} = 2684 + 61267 = 63951$ J·kg⁻¹·K⁻¹;
- III. range: $c_{we3} = 2738$ J·kg⁻¹·K⁻¹.

Average values of the heat transfer coefficients of the studied beech log

Our study has shown that for the calculation of the convective boundary conditions of the logs' defrosting process the following equations for the computation of the heat transfer coefficients of the logs are most suitable (Telegin *et al.* 2002):
- in the radial direction on the cylindrical surface of the horizontally situated logs:

$$\alpha_{wr} = 2.56 \left[T(0,z,\tau) - T_{m-fr}(\tau) \right]^{E_{dfr}} , \tag{4}$$

- in the longitudinal direction on the frontal surface of the logs:

$$\alpha_{wp} = 1.123 \left[T(r,0,\tau) - T_{m-fr}(\tau) \right]^{E_{dfr}} , \tag{5}$$

where E_{dfr} is an exponent, whose values are determined during the solving and validation of our non-linear mathematical model of the logs' defrosting process through minimization of the root square mean error (*RSME*) between the calculated by the model and experimentally obtained results about the change of the temperature fields in subjected to defrosting logs.

For the computation of the temperature field in subjected to defrosting beech log with ANSYS, calculated in Visual Fortran values of α_{wr} and α_{wp} have been used as input data. These values have been calculated with an interval of 60 s synchronously with the solving of an own mathematical model of the logs' defrosting process.

Value of the wood density of the studied beech log

The wood density of the logs, ρ_w, is determined above the hygroscopic range according to the equation (Chudinov 1966, Shubin 1990, Trebula – Klement 2002, Videlov 2003, Deliiski – Dzurenda 2010, Steinhagen 1991):

$$\rho_w = \rho_b \cdot (1 + u) . \tag{6}$$

Using eq. (6), the wood density of the studied beech log with basic density $\rho_b = 684$ kg·m⁻³ and moisture content $u = 0.63$ kg·kg⁻¹ turned out to be equal to 1115 kg·m⁻³.

Values of the temperature of the air medium near the log during its defrosting

The curvilinear change in the shown on Fig. 1 defrosting air medium temperature, T_m, with high accuracy (correlation of 0.99 and *RSME* of 1.49 °C has been approximated with the help of the software package Table Curve 2D (http://www.sigmaplot.co.uk/products/tablecurve2d/tablecurve2d.php) by the following equation:

$$T_m = \frac{a_{dfr} + c_{dfr}\tau^{0.5}}{1 + b_{dfr}\tau^{0.5}} , \tag{7}$$

whose coefficients are equal to: a_{dfr} = 297.1420433, b_{dfr} = −0.00237763, c_{dfr} = −0.70526837.

The calculated values of T_m according to eq. (7) with time step $\Delta\tau$ = 60 s have been used as input data in the boundary condition for the computation of the temperature field in subjected to defrosting beech log using ANSYS.

RESULTS AND DISCUSSION

The above described approach was used for the calculation of the non-stationary temperature field in subjected to defrosting beech log using ANSYS. On Fig. 3 the calculation mesh on ¼ of the longitudinal section of the subjected to defrosting log and also the positioning of the 4 characteristic points T1, T2, T3, and T4 in it is presented.
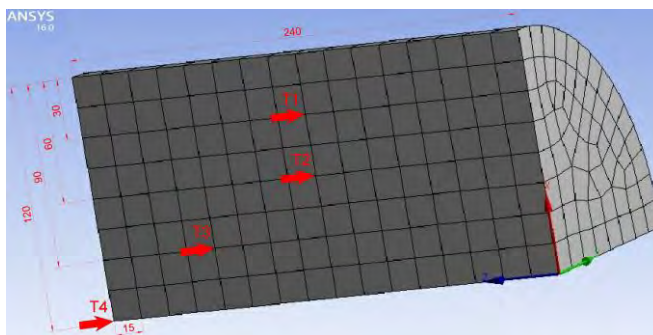
Fig. 3. Calculation mesh on ¼ of the longitudinal section of the subjected to defrosting log

Using this mesh, we have carried out some simulations in ANSYS aimed at computation of the temperature distribution in the longitudinal section of the studied beech log during its 50 h defrosting applying different combinations of the input data.

The first simulation has been made with the following combination of the input data:

  • average constant values of the thermal conductivities and of the specific heat capacities of the log, which have been determined above for the separate 3 temperature ranges of the defrosting process (refer to Fig. 2);

  • constant value of the wood density of 1115 kg·m^{-3};

  • current variable values of the heat transfer coefficients, which have been calculated with an interval of 60 s according to eqs. (4) and (5) using an exponent E_{dfr} = 0.32 in them;

  • current variable values of the defrosting air medium temperature, which has been calculated according to eq. (7) with an interval of 60 s.

The change of the temperature, which has been computed with this input data, turned out to be much slower than the experimentally determined change, which is shown on Fig. 1. Because of this, the calculated value of *RSME* was unacceptably large and equal to 15.88 °C. Our study has shown that the main reason for such a large value of *RSME* are the relatively small values of the heat transfer coefficients of the log during its defrosting, especially during the second and third temperature ranges. That is why we tried to simulate the studied defrosting process using obtained with Visual Fortran maximal values of the log's heat transfer coefficients α_{wr} = 6.62 W·m^{-2}·K^{-1} and α_{wp} = 2.98 W·m^{-2}·K^{-1} during the entire process and leaving unchanged the other input data.

On Fig. 4 the calculated in this simulation and the experimentally established temperature fields in subjected to defrosting beech log, and also the change of the log's surface temperature, t_s, and air defrosting medium temperature, t_m, are given.

The comparison to each other of the analogical curves on Fig. 4 show good enough qualitative and quantitative conformity between the calculated and experimentally determined changes in the very complicated temperature field of the log during its defrosting. This is proven by the relatively small value of *RSME*, equal of 2.64 °C.
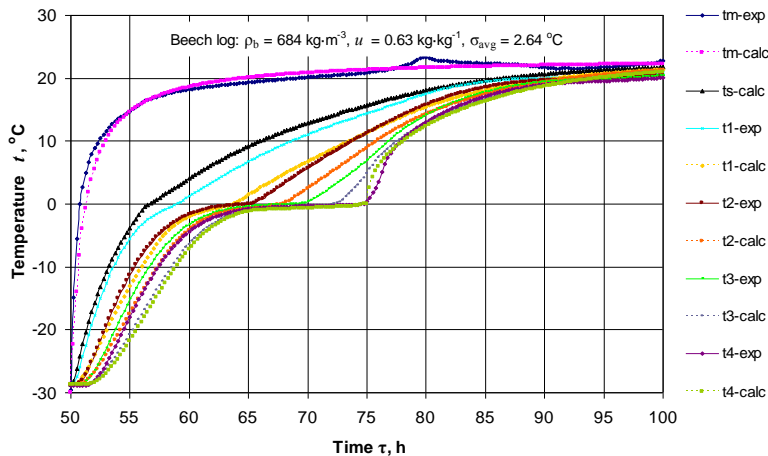
Fig. 4. Experimentally determined and calculated temperature field with average values of the log's thermo-physical characteristics and with maximal values of the log's heat transfer coefficients

CONCLUSIONS

This paper describes an approach for the computation of the temperature field in subjected to defrosting logs with the help of software package ANSYS Workbench 16.0.

The first results from ANSYS' calculation of the non-stationary temperature distribution in 4 characteristic points of the longitudinal section of frozen beech log with a diameter of 0.24 m, length of 0.48 m, initial temperature of –28.8 °C, and moisture content of 0.63 kg·kg^{-1} (above the hygroscopic range) during its 50 h defrosting at room temperature are graphically presented and analyzed.

The aim of the simulations was to assess the degree of the qualitative and quantitative compliance between the experimentally determined and calculated temperature field in the log's longitudinal section during the defrosting using ANSYS. As a criterion for the degree

of compliance between the compared temperature distributions in the log's section the average value of *RSME* total for the 4 characteristic points has been used.

During all simulations with ANSYS the average constant values of the thermal conductivities and the specific heat capacities of the log separately for each of the three temperature ranges of the defrosting process and variable values of the room air defrosting temperature, t_m, have been used. The values of t_m have been obtained after approximation of the experimentally established values of the temperature near the log from its initial value of -29.6 °C to its final value of 22.8 °C using software package Table Curve 2D.

Using this input data and also the maximal values of the heat transfer coefficient of the subjected to defrosting log, a relatively good qualitative and quantitative compliance (*RSME* = 2.64 °C) between the experimentally determined and calculated with ANSYS Workbench 16.0 temperature field in the log's longitudinal section has been obtained.

REFERENCES

1. CHUDINOV, B. S., 1966: Theoretical research of thermo physical properties and thermal treatment of wood. Dissertation, SibLTI, Krasnoyarsk, USSR (in Russian).
2. DELIISKI, N., 2011: Transient heat conduction in capillary porous bodies. In: Convection and Conduction Heat Transfer. InTech Publishing House, Rieka: 149-176.
3. DELIISKI, N., 2013: Computation of the wood thermal conductivity during defrosting of the wood. Wood research, 58 (4): 637-650.
4. DELIISKI, N., DZURENDA, L., 2010: Modelling of the thermal processes in the technologies for wood thermal treatment. TU Zvolen, Slovakia (in Russian).
5. DELIISKI, N., TUMBARKOVA, N. 2016. A methodology for experimental research of the freezing process of logs. Acta Silvatica et Lignaria Hungarica, Vol. 12, № 2: 145-156, http://dx.doi.org/10.1515/aslh-2016-0013
6. SHUBIN, G. S., 1990: Drying and thermal treatment of wood. Lesnaya promyshlennost, Moscow, URSS, 337 p., 1990 (in Russian).
7. STEINHAGEN, H. P., 1991: Heat transfer computation for a long, frozen log heated in agitated water or steam – A Practical Recipe. Holz als Roh- und Werkstoff, 49(7-8): 287-290, http://dx.doi.org/10.1007/ BF02663790
8. TELEGIN, A. S., SHVIDKIY, B. S., YAROSHENKO U. G, 2002: Heat- and mass transfer. Akademkniga, Moscow, 454 p. (in Russian).
9. TREBULA, P., KLEMENT, I., 2002: Drying and hydrothermal treatment of wood, TU in Zvolen, Slovakia (in Slovak).
10. VIDELOV, H., 2003: Drying and thermal treatment of wood, University of Forestry in Sofia, Bulgaria (in Bulgarian).
11. http://www.rotronic.com/humidity-measurement-feuchtemessung-temperaturmessung-data-loggers-datenlogger/hygrolog-hl-nt3.html
12. http://www.sigmaplot.co. uk/products/tablecurve2d/tablecurve2d.php

METROLOGICKÉ ASPEKTY MERANIA FYZIKÁLNYCH VELIČÍN

Prvé správy o mierach sa objavujú už v Sumerskej ríši. Od čias starého Egypta bola mieram a správnosti merania venovaná taká vysoká dôležitosť, že etalóny určovali a spravovali vždy najvyšší úradníci ríše. Dĺžková miera lakeť sa napríklad v niekedy stanovovala podľa dĺžky lakťa panovníka a nesprávne odmeriavanie sa nezriedka trestalo smrťou. Dodnes sú miery a metrológia pod kontrolou štátu.

Prečo je meraniu pripisovaný taký veľký význam je zrejmé na každom kroku. Len čo ráno otvoríme oči, odmeriame si **čas**. Pustíme vodu a **vodomer** odmeria, koľko sme jej minuli. Pozrieme na **teplomer** a odmeriame, aká je vonku zima/teplo. To sú prvé minúty dňa a až do večera sa neustále stretávame s mierami, meraním a meradlami a ani si to neuvedomujeme. Otázky čo chceme zmerať, čím budeme merať a čo meraním zistíme si však treba klásť, pretože od toho závisia výsledky našej činnosti.

Prvou úlohou je uvedomiť si **čo chceme merať**. Často to vieme, ale niekedy nie. Vyzerá to neuveriteľne, ale pri predaji meracích prístrojov sa to našim zákazníkom stáva. Odpoveď na otázku čo chceme zistiť príde až po analýze úlohy a stanovení charakteristík úlohy. V ďalšom kroku sa zadefinuje ako tieto charakteristiky popísať, a čo chceme odmerať aby sme ich kvantifikovali. Tento logický sled úvah, analýzu, treba vykonať, kým začneme s výberom vhodného meradla.

Ako príklad, vezmime jeden z najbežnejších parametrov, ktorý zaujíma takmer každého, a tým je **teplota**. Nuž, odmerať teplotu sa zdá ako veľmi jednoduchá úloha. Teplota je veličina, ktorá ovplyvňuje generálne väčšinu procesov na tejto Zemi a preto je jej meranie dnes už pomerne dobre zvládnuté v porovnaní s inými veličinami.
Bežne sa v praxi sa vyskytujú teploty od -200°C do 3000°C. My sa reálne pohybujeme zhruba v rozsahu povedzme od – 40°C do 1000°C. Napríklad chceme vedieť aká je teplota vzduchu v miestnosti, aká je teplota spalín v komíne a aká je teplota vody v spiatočke.

Na trhu sú k dispozícii tri základné a najpoužívanejšie druhy snímačov teploty:

- Polovodičové snímače (NTC, termistory)
- Odporové snímače (Pt100, Pt1000, Ni1000 atď.)
- Termočlánky
- Bezkontaktné teplomery, merajú v rozsahu od -20°C do 3000°C.

Z grafu je zrejmé, že si pre našu úlohu podľa meracieho rozsahu vyberieme:
  A. Na meranie teploty vody termistor alebo odporový snímač.
  B. Na meranie teploty spalín už musíme použiť Pt100 alebo termočlánok
  C. Ak nemáme na zariadení jímku ani zabudovaný snímač, musíme použiť príložný snímač teploty a lebo bezkontaktný teplomer
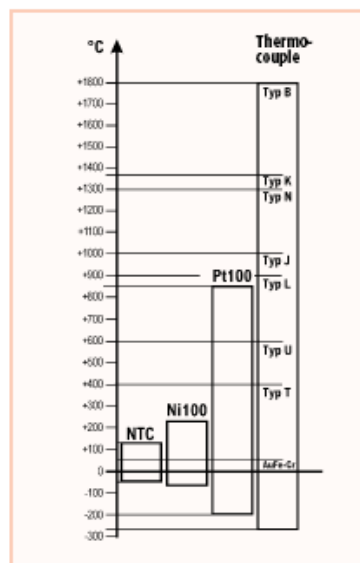
Teraz ale zvážme metrologické parametre tohto výberu. Prihliadnime teda na ich presnosť, rozlíšenie, stabilitu, objektívne aj subjektívne chyby ktorých sa môžeme dopustiť pri meraní.

Presnosti snímačov teploty:

Typ snímača	Rozsah	Max. odchýlka		
		DIN trieda B	DIN trieda A	DIN 1/5 triedyB
Odporové snímače Pt 100	pri -200°C a +200°C	±1,3°C	±0,55°C	
	pri -100°C a +100°C	±0,8°C	±0,35°C	
	pri 0°C	±0,3°C	±0,15°C	±0,06°C
	pri +300°C	±1,8°C	±0,75°C	
	pri +400°C	±2,3°C	±0,95°C	
NTC polovodičové (10K pri 25°C)	-20°C až 0°C	±0,4°C		
	0°C až 70°C	±0,1°C		
	70°C až 125°C	±0,6°C		
Termočlánky NiCr-Ni	-200°C až 1000°C	trieda 1: ±1,5°C alebo ±0,004 x meraná hodnota		
		trieda 2: ±2,5°C alebo ±0,0075 x meraná hodnota		
Dotykový snímač NiCr-Ni	-200°C až 400°C	trieda 1: ±1,5°C alebo ±0,004 x meraná hodnota		
Bezkontaktný IR teplomer 8÷14 µm	-20°C až 300°C	±1,5°C		

Pre jednotlivé merania zohľadnenie čo najlepšej presnosti znamená použitie týchto typov snímačov:
  A. Termistor NTC - je zhruba na úrovni Pt100 v triede A ale lacnejší
  B. Termočlánok typu K - Pt100 v triede B je presnejší ale pri 200 °C sa (ne)presnosťou už približuje k lacnému termočlánku typu K v triede 1
  C. Príložný aj bezkontaktný teplomer - majú presnosť porovnateľnú a na daný účel postačujúcu.

Tým je zdá sa prvý krok vyriešený. Teraz prichádza otázka, **čo s nameranou hodnotou**. Chceme ju len skontrolovať na displeji, zistiť maximum a / alebo minimum? Alebo zaznamenať sériu hodnôt v čase v nastavenom intervale, hodnoty odoslať do PC, PLC a tam s nimi ďalej pracovať?

Máme teda na výber z viacerých možností:

  a. Prístroje len so zobrazením hodnoty na displeji
  b. Prístroje so zobrazením maxima a minima
  c. Prístroje so záznamom jednotlivých hodnôt
  d. Dataloggery so záznamom aj výstupom hodnôt
  e. Modulárne univerzálne meracie ústredne s 10 až 250 vstupmi

Toto je štandardný a osvedčený postup pri výbere dobrého meracieho systému. V praxi sa ale často prijíma iný prístup, kde jediným alebo podstatným kritériom výberu je cena. Výsledkom býva nezriedka meracie zariadenie, ktoré síce meria nejakú hodnotu, avšak táto hodnota môže byť **veľmi vzdialená od skutočnosti**.

Znova použijeme príklad, tento krát pre meranie teploty a vlhkosti vzduchu. Takto vyzerá špecifikácia kvalitného snímača vlhkosti:

Merací prístroj Almemo 202 s kapacitným snímačom teploty a vlhkosti FHA636Rx

Pracovný rozsah teploty:	-50 až 100°C
Pracovný rozsah vlhkosti:	-0 až 100% r.H.
Senzor vlhkosti:	**kapacitný**
Presnosť:	**±0,8% r.H. pri nominálnej teplote**
Reprodukovateľnosť:	**0,3% RH**
Časová stabilita:	**<1%RH**
Nominálna teplota:	23°C ±2°C
Čas odozvy T63:	**15 s, bez filtra, pri rýchlosti prúdenia 1m/s**
Senzor teploty:	Pt100, 1/3 triedy B
Presnosť:	**±0,2K**
Reprodukovateľnosť:	**0,05K**
Materiál krytu snímača:	tepelne odolný plast, priemer 15mm
Hlavička snímača:	drôtená mriežka
Kábel:	dĺžka štandardne 2m, zakončený Almemo konektorom

Snímač sa pripája k meraciemu prístroju **ALMEMO 202**, ktorý má:

presnosť merania **±0,03% z nameranej hodnoty,**
teplotný drift **±0,005%/K,**

presnosť
kompenzácie
studeného spoja
termočlánku
±0,003%K

ALMEMO® Anschlusskabel
mit Sensor
(Beispiel FHAD 36 RS)

Nasleduje popis z prospektu jedného na Slovensku často používaných prístrojov:

Teplomer-vlhkomer C3121

Rozsah teplôt:	-10 až +60°C
Použitý senzor teploty:	odporový
Presnoť merania teploty:	**±0,4°C** v rozsahu -50 až +100°C,
Presnosť merania vlhkosti:	**±2,5%RV** v rozsahu 5 až 95% pri 23°C
Rozlíšenie:	0.1%

Vidíme, že presnosť merania vlhkosti je tu **viac ako štyrikrát horšia** oproti nemeckému snímaču. Údaje o type snímača, reprodukovateľnosti, časovej stabilite a časovej odozve sa vôbec neuvádzajú. Sú to pritom veľmi dôležité údaje. Reprodukovateľnosť nám pritom hovorí o rozptyle opakujúcich sa meraní v krátkom časovom odstupe. Časová stabilita zasa o tom ako sa meraná hodnota môže zmeniť povedzme za rok. Zo skúsenosti vieme, že kapacitné snímače vlhkosti s presnosťou nad 2 %RH môžu za rok merať o 1 až 4% menej. Ich reprodukovateľnosť býva horšia ako 1 % RH.

Ako posledný príklad spomenieme veľmi lacný prístroj, ktorý vyhráva verejné súťaže, žiaľ niekedy aj na univerzitách. Citujeme z prospektu tohto prístroja:

Meteostanica Hyundai WS 8236

Kľúčové vlastnosti
Elegantná meteostanica s modro podsvieteným displejom
Predpoveď počasia
Meria vnútornú a vonkajšiu teplotu aj vlhkosť
Ukazovateľ fázy mesiaca a dáta
Hodiny riadené rádiovým signálom (DCF 77)
Možnosť bezdrôtového príjmu až z troch vonkajších čidiel (1 ×
súčasťou)
Budík s možnosťou odloženia (snooze)

Parametre a špecifikácia:

Vnútorná teplota:	0 ° C až +50 °C
Vonkajšia teplota:	-40 °C až +70 °C
Vnútorná vlhkosť vzduchu:	20% až 95%
Vonkajšia vlhkosť vzduchu:	20% až 95%

Do pozornosti dávame tzv. „kľúčové vlastnosti" a o metrologických parametroch nič nehovoriacu špecifikáciu. V našom kalibračnom laboratóriu mávame aj takéto merače vlhkosti vzduchu a ich presnosť býva na úrovni ±5%RH a horšie.

Uvedené tri prístroje ukazujú rozdiely, ktoré si treba uvedomiť ale ktoré si veľa používateľov neuvedomuje. Namerané údaje sa potom nekriticky používajú v praxi napríklad pri hodnotení mikroklimatických parametrov v budovách, ale aj pri výskume **a to bez toho aby boli zohľadnené metrologické vlastnosti použitých meradiel.**

Ďalším vplyvom na správnosť merania je **subjektívna chyba**. Túto je najlepšie popísať na bezkontaktnom meraní teploty infračerveným teplomerom. Ak nezohľadníme percento vyžarovanie tepelnej energie z povrchu meraného objektu, teda jeho emisivitu, ak meriame pod uhlom väčším ako 30°, ak zvolíme nesprávnu pracovnú vlnovú dĺžku detektora, ak sa z meraného povrchu odráža tepelné a svetelné žiarenie do objektívu pyrometra, ak je v prostredí prach, dym alebo para, ak meriame cez sklo a ak nebodaj nepoznáme alebo nezohľadníme dištančný pomer prístroja, tak číslo ktoré sa zobrazí na displeji prístroja môže byť **od skutočnosti vzdialené o desiatky percent!!!** Veľa ľudí si navyše myslí, že meria teplotu telesa a nevie, že meria len povrchovú teplotu a vnútri objektu môže byť teplota celkom iná.

Z pohľadu metrológa je takýto prístup k meraniu teploty podobný snahe odčítať čas v sekundách na slnečných hodinách alebo na kostolnej veži. Žiaľ, v praxi sa s ním často stretávame.

Ak sa máme vyhnúť chybám a nepresnosti pri meraní, musíme si osvojiť kritický, metrologický prístup k meraniu a jeho vyhodnoteniu. V prvom kroku vybrať podľa parametrov zverejnených výrobcom pre daný účel **optimálny prístroj** a snímače a použiť **správu metódu merania**. Následne správne namerané údaje **vyhodnotiť** a eliminovať na minimum chybu merania.

Metrologické vlastnosti meradiel je možné si preveriť ich k**alibráciou v kalibračnom laboratóriu**.

Kalibrácia poskytne informáciu o odchýlke od pravej hodnoty, zistenej porovnaním s etalónom, čo je informácia o presnosti meradla. Kalibračný list z kalibračného laboratória obsahuje aj údaj o neistote kalibrácie. V neistote je zahrnutá okrem iných vplyvov i reprodukovateľnosť meradla.

Časovú stabilitu meradla je možné overiť opakovanou kalibráciou po dlhšej dobe. Vyzerá to náročne a zložito ale ak potrebujeme, aby namerané hodnoty boli správne, treba absolvovať popísané procedúry a zohľadňovať ich výsledky pri meraní. Taktiež sú dôležité opakované merania a ich štatistické vyhodnotenie – najmä stanovenie smerodajnej odchýlky, aby sa dala k nameranému údaju pripojiť aj štatistická informácia o jeho dôveryhodnosti.

Ak treba namerané údaje použiť v **obchodnom styku** alebo pri súdnoznaleckých výpočtoch, mať k prístrojom **kalibračný certifikát z akreditovaného kalibračného laboratória je nevyhnutné**. V rámci legislatívy je platný tzv. Zákon o metrológii, ktorý hovorí aj o tom, že každé meranie, ktoré sa vykonáva na základe akéhokoľvek zákonného predpisu alebo vyhlášky musí byť realizované iba meradlom kalibrovaným v akreditovanom kalibračnom laboratóriu.

Uvedené riziká ovplyvňujúce namerané hodnoty sú len malým zlomkom vplyvov, ktoré v praxi reálne existujú. O každom meraní, o výbere a správnom použití meracieho prístroja, o podmienkach pri konkrétnom meraní, o vyhodnotení nameraných údajov, o ich korekcii na skutočné hodnoty zistenej kalibráciou je nutné premýšľať a zohľadniť všetky podstatné vplyvy na správnosť nameranej hodnoty. Iba potom možno namerané údaje použiť a spoľahnúť sa na ich hodnovernosť.

Ing. Rudolf Košťál